DOCTORAL DISSERTATION

M. Sc., Eng. Mostafa Abotaleb

Analysis and Assessment of The Quality of Wireless Information Transmission in Shipboard Measurement and Control Systems – Collaborative Perspective

Field of science: Engineering and Technology
Discipline of science: Automation, Electronics, Electrical Engineering and Space Technology

Supervisor:
Prof. Dr. Hab. Eng. Janusz Mindykowski

Assistant Supervisor:
Ph. D., Eng. Boleslaw Dudojc

Gdynia 2025

Table of Contents

Introduction **1**

1. Wired Instrumentation in Maritime Engineering **9**
1.1. Twisted Pair Cables 9
1.1.1. Effect of Temperature on Twisted Pair Cables Dielectric Properties 10
1.1.2. Cross Linked Polyethylene (XLPE) as an Insulating Material 11
1.1.3. Salt Water and Twisted Pair Cables 11
1.2. (4-20 mA) Analogue Standard in Maritime Engineering Applications 15
1.3. Smart Sensors in Maritime Engineering Applications 17
1.3.1. HART Protocol 18
1.3.1.1. Rosemount 3051S HART Pressure Transmitter 18
1.3.1.2. Simulated Effect of Marine Environmental Conditions on HART Sensors 19
1.3.2. Foundation Fieldbus (FF) 22
1.3.2.1. Simulated FF H1 Bus Signal Modulation/Demodulation (Ideal Case) 23
1.3.2.2. Simulated FF H1 Bus Signal Modulation/Demodulation (Noisy Case - Matlab) 24
1.3.2.3. Simulated FF H1 Bus Signal Modulation/Demodulation (Noisy Case - Simulink) 27
1.3.2.4. Rosemount 3051 FF Pressure Transmitter 29
1.3.2.5. Simulation for the Application of FF in Tank Level Measurement System on a Bulk Carrier Commercial Ship (Case Study) 30

2. Wireless HART protocol in Maritime Engineering **41**
2.1. RFI and EMI in Maritime Engineering 41
2.2. Received Signal Strength Indicator (RSSI) 42
2.3. Decreased Power Supply Levels (Gateway and Field Devices) 44
2.4. Wireless HART Protocol on Various Types of Commercial Ships 45
2.5. Wireless HART Mathematical Model for Network Reinforcement 46
2.5.1. Description and Derivation of the Mathematical Model 47
2.5.2. The Network Reinforcement Rectangle (NRR) Method 51
2.5.3. NRR Example 51
2.5.4. The Minimum Required Field Device Density (MRFDD) Method 53
2.5.5. MRFDD Example 53
2.6. Wireless HART Application on Commercial Ships 75
2.6.1. Tank Level Measurement System on Bulk Carrier Ship (Planning Example) 75
2.6.2. Monitoring of Most Important Systems in Engine Room (Planning Example) 77

3. General Use Wireless Technologies (Wi-Fi) in Maritime Engineering **83**
3.1. Laboratory Stand 83
3.2. ESP-WebSerial Limited Range 89
3.2.1. Problem Characterization 90
3.3. ESP-NOW Protocol 93
3.4. Proposed Configurations for Improved Range Capabilities 94
3.5. Application of ESP32 Based Wi-Fi on Commercial Ships 97
3.5.1. Large Scale Application on a Commercial Container Ship (Planning Example) 98
3.5.2. Small Scale Application on a Ship (Fire Alarm Planning Example) 100
3.5.3. Cargo Cranes Wireless Safety and Performance System (Small Scale Total Realization) 103
3.5.3.1. Cost Analysis 106

3.5.3.2. Functionally Safe Configuration 109
3.5.3.3. Predictive Maintenance PdM Application (Hydraulic oil dynamic viscosity) 111

4. Discussion **117**
Conclusions **126**
Bibliography **130**

List of The Most Important Abbreviations

AMS	Asset Management System
AWG	American Wire Gauge
CCMP	Cipher Block Chaining Message Authentication Code Protocol
CD	Compel Data Command
CSMA/CA	Carrier Sense Multiple Access/Collision Avoidance
DART	Dynamic Arc Recognition and Termination
DART DB	DART model for Double Bottom tanks
DART TS	DART model for Top Side tanks
DDT	Distributed Data Transfer
DL	Deep Learning
DM	Differential Mode
DSSS	Direct Sequence Spread Spectrum
EMC	Electromagnetic Compatibility
EMI	Electromagnetic Interference
FAS	Fieldbus Access Sublayer
FEXT	Far-End Cross Talk
FF	Foundation Fieldbus
FHSS	Frequency Hopping Spread Spectrum
FISCO	Fieldbus Intrinsically Safe Concept
FISCO-IIB-DB	FISCO IIB model for Double bottom ballast tanks without Short Circuit Protection
FISCO-IIB-DBSC	FISCO IIB model for Double bottom ballast Tanks with Short Circuit Protection
FISCO-IIB-TS	FISCO IIB model for Top Side ballast tanks without Short Circuit Protection
FISCO-IIB-TSSC	FISCO IIB model for Top Side ballast Tanks with Short-Circuit Protection
FISCO-IIC-DB	FISCO IIC model for Double bottom ballast tanks without Short Circuit Protection
FISCO-IIC-TS	FISCO IIC model for Top Side ballast tanks without Short Circuit Protection
FMS	Fieldbus Message Specification
FNICO	Fieldbus Non-Incendive Concept
FNICO-IIB-DB	FNICO IIB model for Double bottom ballast tanks without Short Circuit Protection
FNICO-IIB-DBSC	FNICO IIB model for Double bottom ballast Tanks with Short-Circuit Protection
FNICO-IIB-TS	FNICO IIB model for Top Side ballast tanks without Short Circuit Protection
FNICO-IIB-TSSC	FNICO IIB model for Top Side ballast Tanks with Short-Circuit Protection
FNICO-IIC-DB	FNICO IIC model for Double bottom ballast tanks without Short Circuit Protection
FNICO-IIC-DBSC	FNICO IIC model for Double bottom ballast Tanks with Short-Circuit Protection
FNICO-IIC-TS	FNICO IIB model for Top Side ballast tanks without Short Circuit Protection
FNICO-IIC-TSSC	FNICO IIC model for Top Side ballast Tanks with Short-Circuit Protection
FSK	Frequency-Shift Keying
GUI	Graphical User Interface
HART	Highway Addressable Remote Transducer
HPTC	High-Power Trunk Concept
HPTC-FB-DB	HPTC model with Field Barriers for Double Bottom tanks
HPTC-FB-TS	HPTC model with Field Barriers for Top Side tanks
HPTC-SP-DB	HPTC model with Segment Protectors for Double Bottom tanks
HPTC-SP-TS	HPTC model with Segment Protectors for Top Side tanks
HSE	High-Speed Ethernet

IEC	International Electrotechnical Commission
IMO	International Maritime Organization
IR	Insulation Resistance
IS-E-DB	Intrinsically Safe Entity model for Double Bottom Tanks
IS-E-TS	Intrinsically Safe Entity model for Top Side Tanks
LAS	Link Active Scheduler
LMK	Local Master Keys
MAC	Medium Access Control
ML	Machine Learning
MRFDD	The Minimum Required Field Device Density Method
NEXT	Near-End Cross Talk
NONIS-DB	Non-Intrinsically Safe model for Double Bottom Ballast Tanks without Short-Circuit Protection
NONIS-DBSC	Non-Intrinsically Safe model for Double Bottom Ballast Tanks with Short-Circuit Protection
NONIS-TS	Non-Intrinsically Safe model for Top Side Ballast Tanks without Short-Circuit Protection
NONIS-TS-SC	Non-Intrinsically Safe model for Top Side Ballast Tanks with Short-Circuit Protection
NRR	The Network Reinforcement Rectangle Method
OSI	Open Systems Interconnection
PDIV	Partial Discharge Inception Voltage
PdM	Predictive Maintenance
PN	Probe Node
PT	Pass Token Command
RFI	Radio Frequency Interference
RSSI	Received Signal Strength Indicator
SDT	Segment Design Tool
SNIR	Signal to Interference plus Noise Ratio
SOLAS	International Convention of Safety of Life at Sea
SPM	Static Process Monitoring
STP	Shielded Twisted Pair cables
TD	Time Distribution
TDMA	Time Division Multiple Access
TSMP	Time Synchronization Mesh Protocol.
UART	Universal Asynchronous Receiver Transmitter
XLPE	Cross-Linked Polyethylene

Introduction

Shipboard measurement and control systems are mostly based on conventional analogue and on-off binary standards. 4-20 mA is the most popular analogue standard due its non-zero lower range limit in addition to its immunity to noise. In spite of the high quality as well as the high reliability and stability levels of the 4-20 mA measurement current loop, it can still be negatively affected by high levels of temperature, humidity, vibration and salinity in marine environment. The impact of such extreme conditions can be emphasized in the formation of ground loops as well as the distorted less accurate measurement readings inflected by coupled noise and common mode noise.

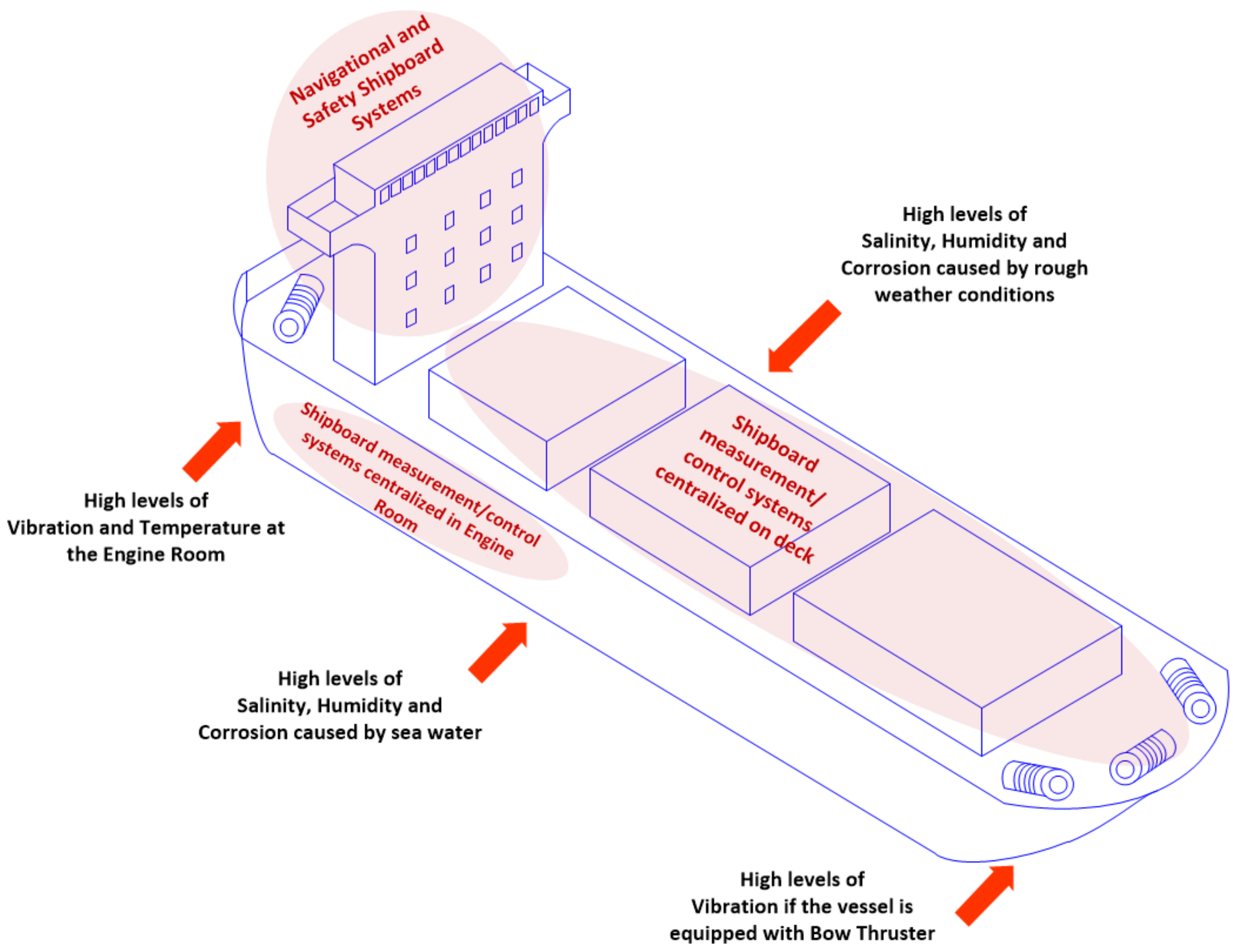

Figure 1 – Marine environmental and operational effects on shipboard systems

The major interest of shipbuilding institutions such as shipyards is to achieve the maximum possible financial profit by minimizing the ship construction expenses and maximizing the selling price. On the other hand, the major interest of ships' owners is to lower the construction cost in order to lower the overall final price of the newly delivered vessel and also to increase the price negotiation margin with the shipyard. Therefore, both of the shipbuilders and ship owners share the same goal aiming to adopt systems, technologies and building techniques which can achieve the minimum possible construction cost.

The conventional measurement/control systems based on cabling and classical analogue and binary standards, are treated as the cheapest reliable alternative to process measurement/control data at shipboard system, that's why, such systems are considered as the most popular option in shipping industry. Such an approach might be a profitable approach for the shipbuilders, as their role is limited to the construction and delivery of the ship to the shipping company, however for the ship owners such an approach is considered as a restricted approach handling the cost issue from a perspective that takes only into account the short term construction cost and neglects the long term cost associated with maintenance, troubleshooting and purchasing the required spare parts. If the major interest for the ship owner was to reduce the short term cost (related to construction and installation) at the expense of the system quality, the long term cost will increase to exceed the short term cost within a relatively short period of time after the ship's delivery.

The purpose of this doctoral study is to present a comprehensive realization for such a concept in a convincing manner supported by the conducted analysis based on simulation tools, experimental research and real time applications verifying the improved cost effectivity of adopting higher quality measurement and control systems based on the collaboration between wireless communication technologies and both of classical binary/analogue standards and smart sensing modern technologies based on bus communication protocols dedicated to execute measurement/control tasks. As the ships' owners are more concerned with minimizing the costs associated with construction, cabling and installation, it will be more reasonable to dedicate the larger part of this study to verify the enhanced quality of measurement/ control systems through adopting wireless technologies as economically efficient data transaction mediums cooperating with cabling in systems based on classical standards as well as smart sensing bus protocols.

Firstly, the study will illustrate the most concerning problems associated with cabling particularly those induced by high levels of temperature, humidity, vibration and salinity as main features of maritime environment where marine equipment and measurement/control systems are planned to exist in shipboard engineering applications (Figure 1). The effect of high temperature and relative/absolute humidity on the dielectric properties of the twisted pair cables will be demonstrated in light of some of the previous selected literature. Similarly, the negative impact of such extreme environmental features on the XLPE as one of the most popular insulation materials used as insulating material in the process of twisted pair cable production. The influence of thermal ageing and thermal variation on the properties of the XLPE material such as the insulating resistance will be briefly summarized in light of some of the selected previous literature. In conjunction with a related research investigating the effect of salt water on the twisted pair cable in traction applications, the study will relate the results of such a research to the similar expected effect in maritime engineering applications through a mathematical analysis emphasizing the deteriorating change of the twisted pair cable characteristics due to immersion in salt water for long periods of time.

Continuing the investigation of the problems associated with the cabling-based measurement/control systems in marine engineering applications, the study will spot the light on the most popular termination and interconnection techniques adopted in marine measurement/control systems based on the 4-20 mA analogue standard where measuring points are remotely separated by long distances and long cables (divided into sections interconnected through junction boxes) are required to connect between the measuring transmitter and the host controller. This section will highlight the most popular techniques used to eliminate ground loops, coupled noise and common mode noise.

As a hybrid analogue digital protocol dedicated to perform measurement/control tasks in conjunction with the 4-20 mA analogue standard, the study will provide a brief description for HART protocol. This description will be supported by an example for the most important diagnostic features rendered by the superimposed HART digital signal in a HART smart pressure transmitter such as the Rosemount 3051S pressure transmitter. In order to emphasize a more realistic approach for the deployment of HART protocol in maritime engineering applications, the study will highlight the conclusions of a research exploring the simulated effect of high levels of vibration associated with high levels of corrosion and humidity on the 4-20 mA smart HART measurement current loop. The research will also include some of the recommended techniques for earthing and grounding in order to evade the effect of ground loops.

Similarly, this doctoral dissertation will dedicate a considerable section to investigate the possible utilization of Foundation Fieldbus protocol in marine engineering applications. Unlike HART protocol, the Foundation Fieldbus protocol will be analyzed through a wider perspective including a brief description for the purely digital protocol, the proposed techniques to eliminate the expected effect of additive white Gaussian noise on the 31.25 Kbps H1 bus signal through which information is exchanged between the FF field devices, and finally a simulation-based case study exploring the various alternatives for the deployment of Foundation Fieldbus protocol in marine engineering applications such as tank level measurement system on a bulk carrier commercial ship. This case study will include the simulation of one non-intrinsically safe model for the system and five intrinsically safe models (entity model, FISCO, FNICO, HPTC and DART). Through a comparative analysis for the simulated models, the conclusions of the research will reveal the non-linear polynomial behavior of the field barriers as well as the segment protectors in the intrinsically safe HPTC model. Additionally, the conclusions will reveal the mutual dependency between some of the Foundation Fieldbus model characteristics such as the maximum allowable spur length and total number of field devices. Apart from such specific conclusions differentiating between the various types of models in the FF digital communication protocol, this case study will render an example for the expected improvement conducted on the measurement process in a shipboard tank level measurement system through the additional diagnostic techniques adopted by some of the FF transmitters such as the statistical process monitoring (SPM) in the Rosemount 3051 FF pressure transmitter.

After exploring the various possibilities of using some of the smart sensing protocols based on cabling in marine engineering applications, the dissertation will shift to the analysis of wireless technology deployment in shipboard measurement/control systems, which is the core of this study. Two wireless technologies will be analyzed. The first one is the wireless HART protocol as a technology particularly dedicated to industrial automation, and the second one will be the Wi-Fi technology as a general use cheaper technology.

Initially, a brief theoretical description will be provided for the wireless HART protocol as an upgraded version for the wired HART protocol including recommendations to avoid the expected effects of RFI and EMI maintaining high RSSI levels in different locations. Afterwards, a profound analysis will be dedicated to the planning as well as the developed reinforcement techniques which can be adopted to ensure adequate levels of robustness and reliability in wireless HART mesh networks. The doctoral study will pay a considerable attention to some of the recommended rules by the Emerson wireless HART network planning guide in order to maintain successful communication between the gateway and the field devices. The dissertation introduces a mathematical model dedicated to the implementation of such rules. Based on this mathematical model, software tools can be developed so that the user or the network planner can apply the proposed network reinforcement techniques to avoid some of the drawbacks associated with the ageing of some of the network components. In order to inflect the idea of utilizing wireless HART protocol in shipboard systems by the proposed network planning/reinforcement techniques introduced at the mathematical model, two examples dedicated to the application of wireless HART protocol will be presented at this study. The first example is dedicated to the recommended use of wireless HART level transmitters in tank level measurement system to detect the fluid levels at sea water ballast tanks on a bulk carrier ship. The second example is dedicated to the possible use of wireless HART adapters collecting groups of analogue input signals in the engine room. Both examples will formulate a perspective through which a specific perception will be granted for the exact steps needed to implement wireless HART protocol in shipboard systems.

For the Wi-Fi general use technology, this doctoral study will analyze the various alternatives of its use in shipboard systems from a point of view related to the cooperation between wireless HART, Wi-Fi and cabling as mediums for data transaction in marine measurement/control system. The analysis of such an aspect will be based on a laboratory stand performing authenticated Wi-Fi wireless data transaction from multiple sensors through the collaboration between the ESP32 controller and the Arduino Mega 2560 controller where the WebSerial remote serial monitor will automatically exchange measurement data and authentication messages between the sensors' station and the host controller. In an upgraded version for the laboratory stand, the study will propose the coexistence between the WebSerial remote serial monitor and the ESP-NOW protocol so that wider coverage areas can be obtained for the process of measurement/authentication data transaction. Based on the RSSI measurements made at some of the selected locations on a commercial container ship, the discussion will include two planning examples for the large scale as well as the small scale possible application of ESP32 based Wi-Fi in shipboard systems. Afterwards, the study will present a small scale example for the total implementation of the laboratory stand upgraded version on a container ship, where a proposed wireless safety and performance monitoring system dedicated to marine cargo cranes, will be installed aboard the container ship during its existence at the shipyard for periodic maintenance. The analysis of the proposed wireless system will spot the light on the functionally safe configuration for the system as it will operate in association with cabling as two simultaneous mediums for data transaction. Additionally, the analysis will include the use of the collected measurement data in the system performance log to develop a mathematical model dedicated to the application of the predictive maintenance PdM principal where critical changes of the cargo crane hydraulic oil dynamic viscosity will be detected at specific working hours. The analysis will highlight the economic efficiency of the system through a comparative cost analysis for two cabling options.

Eventually, the dissertation will formulate the concept of coexistence based on which wireless technology is advised to be deployed at shipboard systems, leading to enhanced quality levels of the measurement/control process without the necessity for total replacement of cabling as a data transaction medium as the wireless technology will exist as a cooperative medium not as an eliminating medium. An important result will represent the consequent outcome for the verification of the functionality of such a concept through the whole doctoral study with its elements of novelty, proposed techniques, exhibited planning examples and real time actual implementation of a wireless monitoring system on a container ship. This result will be the increased popularity of embracing the wireless technology in shipboard measurement/control systems among shipbuilders and ship owners as it will be treated as a coexistent medium rendering higher levels of reliability, stability and robustness not as a medium recommended only for minor monitoring tasks.

Objective

The development and the construction of general strategy guidelines through which the wireless technology (with its various forms) can be deployed in measurement/control marine applications as a collaborative data transaction medium coexisting with cabling at systems based on classical binary and analogue measurement/control standards as well as systems based on using smart sensors adopting more advanced communication protocols (hybrid analogue/digital and purely digital). The direct consequent outcome for the collaboration between wireless technology and cabling can be summarized in as follows:

- Higher levels of measurement reliability and stability.
- Less down time required for maintenance and troubleshooting in case of any possible failure.
- Improved cost effective implementation of the principles of functional safety and predictive maintenance.

Thesis

The dissertation is based on the following formulated theses:

- Conventional shipboard systems based on classical binary/analogue standards are subjected to considerably high levels of temperature, humidity, corrosion, salinity and vibration. The general condition of marine measurement/control systems tends to deteriorate gradually due to the influence imposed by such operational and environmental factors. Such a deterioration can be mostly manifested in ground loops formation and higher levels of capacitive coupling currents, which leads to less accuracy as well as less reliability levels. Such drawbacks can be overcome to a specific extent by the use of smart sensors based on communication protocols such as HART and Foundation Fieldbus through additional parametric as well as diagnostic information.
- In many cases, the use of wireless technology as a coexistent data transaction medium can provide the solutions for such problems. Improved security of measurement data transaction, facilitated deployment at intrinsically safe applications in explosive hazardous areas are the most important advantages for the deployment of different types of wireless technologies (solely dedicated to industrial automation and general use wireless technologies) in marine engineering measurement/control systems.
- The high density of metallic infrastructure on commercial ships can be an obstructing barrier for the radio frequency RF waves propagation. The proposed techniques in this study will offer some techniques dedicated to improve the range capabilities, avoiding the distortive influence of such metallic infrastructure through the collaboration between two protocols (WebSerial and ESP-NOW) in Wi-Fi based applications and the use of adapters and repeaters in wireless HART protocol.
- Based on the proposed techniques, wireless technologies such as Wi-Fi and wireless HART will coexist effectively with cabling based shipboard systems in order to implement important

principals such as functional safety and predictive maintenance PdM through adopting economically efficient plans.

Scope

The major goal of this doctoral study can be achieved through implementing the following subsidiary goals:

1. Indicating the negative effects induced by environmental factors on twisted pair cables (in light of previous literature) as the backbone of shipboard systems based on classical binary/analogue standards as well as protocols based on which smart sensors are built (HART and Foundation Fieldbus).
2. Identifying the effect of improper grounding techniques, vibration associated with high levels of humidity and corrosion on the 4-20 mA HART smart sensing current loop through an experimental analysis, in addition to the effect of additive white Gaussian noise on the 31. 25 kbps H1 Foundation Fieldbus signal through MATLAB/Simulink models.
3. Introducing the recommended techniques to avoid the negative effects obtained at the previous point.
4. Discussing the various options through which smart sensors (particularly FF sensors) can be deployed in shipboard systems for intrinsically safe as well as non-intrinsically safe applications through a simulation-based case study.
5. Exploring the various possibilities of deploying the wireless HART protocol on commercial ships for applications centralized on main deck as well as applications centralized in engine room.
6. Developing the required techniques for Wireless HART network reinforcement based on a proposed mathematical model developed particularly for such a purpose.
7. Constructing a laboratory stand allows for the authenticated data transaction between multiple sensors and the host controller through using Wi-Fi as a general use wireless technology in a configuration allows for the ESP32 controller to supervise such a process.
8. Improving the range capabilities of the laboratory stand through an upgraded version based on the collaboration between the WebSerial remote serial monitor and the ESP-NOW protocol.
9. Development and testing of a performance and safety wireless monitoring system dedicated to marine cargo cranes on a container ship based on the upgraded version of the laboratory stand from a perspective linked to a cost effective implementation for the principles of functional safety and predictive maintenance.

Elements of novelty

1. Highlighting the effect of associated vibration and humidity on the 4-20 mA smart HART measurement current loop.
2. Development of a new method to eliminate the effect of additive white Gaussian noise on the 31.25 kbps FF H1 bus signal through calculation of average wave energy at specific time intervals.
3. Identifying the polynomial characteristics of the field barriers and segment protectors at the HPTC intrinsically safe model.
4. Define the FF models (intrinsically safe and non-intrinsically safe) at which spur lengths were either dependent or independent on the total number of field devices of the segment.

5. Developing a mathematical model dedicated to wireless HART network reinforcement through adopting two methods of adding repeaters to the network (MRFDD and NRR), in addition to optimizing the overall number of repeaters.
6. Developing a wireless (Wi-Fi based) instrumentation network based of improved range capabilities through the collaboration between the WebSerial remote serial monitor and ESP-NOW protocol.
7. Applying the developed techniques, methods and systems at shipboard measurement/control systems:
   - Foundation Fieldbus : Tank level measurement system (sea water ballast tanks case study).
   - Wireless HART: Tank level measurement system (sea water ballast tanks planning example)
   - Wireless HART: Engine room measurement/control systems planning example.
   - ESP32 based Wi-Fi: Engine room measurement/control system planning example.
   - ESP32 based Wi-Fi: Fire Alarm system planning example.
   - ESP32 based Wi-Fi: Marine Cargo crane safety and performance monitoring system (Total realization and testing)
   - ESP32 based Wi-Fi: Cost effective implementation of functional safety.
   - ESP32 based Wi-Fi: Cost effective implementation of predictive maintenance.

Outline

This doctoral dissertation is organized as follows:

<u>Chapter1:</u> dedicated to discuss the wired instrumentation systems. The chapter will firstly highlight the most important negative effects (especially the effects imposed by extreme environmental conditions) induced on the twisted pair cables as a major component in wired instrumentation systems. Secondly, the chapter will discuss the effects induced on a smart HART 4-20 mA current loop by the simulated effect of vibration, corrosion and humidity. Thirdly, the chapter will discuss the proposed techniques to eliminate the effect of AWGN from the FF Manchester coded H1bus signal. Ultimately, the chapter will analyze the results of possible deployment of FF protocol in a shipboard system such as tank level measurement system through intrinsically safe and non-intrinsically safe simulation models.

<u>Chapter 2:</u> This chapter is dedicated to the wireless HART protocol as a wireless technology dedicated to industrial automation. Firstly, a brief theoretical background ground will be rendered for the wireless HART protocol. Secondly, the chapter will provide a description for a mathematical model dedicated to wireless HART network reinforcement in light of some of the recommended rules by the manufacturer. Thirdly, the chapter will demonstrate two network planning examples for the deployment of wireless HART protocol in tank level measurement system on a bulk carrier commercial ship, and measurement/control systems at the engine room based on the techniques proposed by the mathematical model.

<u>Chapter 3:</u> dedicated to analysis of the possible utilization of Wi-Fi as a general use wireless technology in marine engineering applications. Firstly, the chapter will introduce a laboratory stand dedicated to authenticated data transmission from multiple sensors. The laboratory stand is based on the collaboration between the Arduino controller and the ESP32 controller performing wireless communication tasks through the WebSerial remote serial monitor. Secondly, the chapter will

present an upgraded version of the laboratory stand based on using ESP-NOW protocol at wireless switches dedicated to expanding the coverage area of the Wi-Fi based wireless instrumentation network. Thirdly, the chapter will illustrate a real time realization for cargo cranes wireless performance and safety monitoring system on a container ship based on the upgraded version of the laboratory stand. The developed system will be discussed from a point of view affiliated to the economically efficient implementation of the principles of functional safety and predictive maintenance.

Discussion: This section is dedicated to formulating the main concept of this doctoral dissertation, which is the coexistence and cooperation between wired (classical + smart sensors) and wireless technologies (Wireless HART + Wi-Fi) in order to elevate the reliability, stability and accuracy levels at shipboard measurement/control systems. The formulation of such a concept will be depicted in light of the obtained results, developed and proposed techniques and the implemented wireless safety and performance monitoring system in real-time marine application.

Conclusions: this section will summarize the most important conclusions of this doctoral study in light of the formulated concept at the discussion.

1. Wired Instrumentation in Maritime Engineering

Most of shipboard measurement/control systems are based on the 4-20 mA analogue standard where instrumentation cables are used as a medium for data transaction. Other than the 4-20 mA analogue standard, modern smart sensors are also adopted by some of the shipboard systems. HART, FF and Profibus PA are examples for digital communication protocols [1] based on which such smart sensors are built. In maritime engineering applications, the quality of instrumentation cabling is a key element to ensure high reliability levels of measurement/control data processing. The cabling quality in shipboard systems is determined by the following factors:

1. The endurance level of its insulating and shielding materials.
2. The grounding technique during the installation process.
3. The degree to which cables' parameters might be negatively affected by harsh conditions in marine environment such as high levels of temperature, humidity, corrosion and vibration.
4. Cable immunity to noise and various sources of Electromagnetic Interference EMI.
5. The adopted techniques to prevent the formation of ground loops.
6. Healthy condition of cabling accessories such as junction boxes and wiring terminals.

1.1 Twisted Pair Cables

Twisted pair cables are the most widely used cables in maritime engineering measurement/control applications. They are divided into two categories. The first category is the Shielded Twisted Pair (STP) cables, and the second category is the Unshielded Twisted Pair (UTP) cables. Twisted pair cables can include a single pair or multi-pairs of wires. Twisted pair cables are usually subjected to three types of noise coupling, resistive, inductive and capacitive. The resistive coupling is usually caused by common ground loops, and it can be easily eliminated using galvanic isolators such as transformer isolators or optical isolators. Capacitive and inductive coupling are both mostly related to the phenomenon of crosstalk.

Crosstalk is defined as the induced electromagnetic coupling between wires or cables which are located within proximity to each other. This coupling can be capacitive or inductive. Crosstalk is dependent on cable type, the separation between wires or cables and the electromagnetic interference EMI level at the surroundings of the cable location. Crosstalk leads to electromagnetic compatibility EMC problems manifested in reduced reliability level of the data processed through the cable [2].

The effect of crosstalk along the cable, can be divided into Near-End Cross Talk (NEXT) and Far-End Cross Talk (FEXT). NEXT takes place when the transmitted signal through one conductor of the twisted pair, will interfere with the received signal on the other conductor at the same end. On the other hand, FEXT takes place due to interference between transmitted signal from one end with the other conductor at the receiver end. Generally cross talk can be avoided by cable shielding as well as wire twisting, as both of the two mechanisms almost eliminate the capacitive or the inductive coupling that will lead to crosstalk between wires [3]. However, the non-uniformity of wire twisting as well as improper shielding of the cables, can be possible causes for incomplete elimination of the noise induced due to crosstalk. In [4], the research highlighted the increase of the distortion induced by differential mode (DM) voltage due to the unequal pitching at wire twisting.

In [5], the research investigated the effect of the distance between the twisted pair wires and the cable shield (d) (shown in Figure1.1) on the induced coupling between the wires. The results can be summarized as follows:

- The increased levels of induced coupling with respect to the increase of the distance (d).
- The induced coupling level in case of grounding is higher than the induced coupling without grounding.
- The amplitude of the induced coupling due to differential mode disturbances is higher than the amplitude of induced coupling due to common mode coupling.
- The greater was the number of the twists, the lower was the induced coupling leading to the crosstalk.

Skin depth is defined to be the tendency of the AC current to flow at the wire outer peripheral due to circular eddy currents of a circular conductor [6,7]. AC resistance of the conductor is dependent on the skin depth, as the effective radius of the conductor will be reduced. The effect of skin depth is taken into account only when the propagating signal through the cable is an AC signal. Thus, the skin depth is taken into account with smart transducers which adopt digital communication AC signals for the delivery of measurement data [6,7].

The calculation of the twisted pair cable characteristic impedance, is dependent on the calculation of the cable conductor surface resistance, inductance, capacitance and conductance per unit length. characteristic impedance and load impedance are used to calculate the reflection coefficient which is an indication for the efficiency of the cable. The reflection coefficient is used to calculate the return loss, the power loss and the voltage standing wave ratio VSWR. The higher is the return loss, the better is the impedance match of the cable. High return loss value indicates that the power of the reflected wave is less than the power of the incident wave. The power loss indicates the amount of power lost due to the impedance mismatch in the system. The lower is the power loss, the better is the impedance matching of the system [7].

1.1.1 Effect of Temperature and Humidity on Twisted Pair Cables Dielectric Properties

Dielectric constant of any cable, is permanently affected by temperature. This was noticed over a specific temperature range. Thermal variations as well as high temperature levels lead to a significant change at the electrical, mechanical and chemical properties of the cable dielectric material. The speed of the signal processed through the cable is dependent on the dielectric constant through the cable. If the dielectric constant increased in high temperature levels, this will consequently reduce the propagation speed of the processed signal. Similarly, the thermal variation results in cyclic change of dielectric constant value of the cable material, which leads to the variation of the cable characteristic impedance [8,9].

In [10], the research analyzed the combined effect of temperature and humidity on the dielectric properties of the cable. The conclusions derived from the results have indicated that the increase of both absolute and relative humidity (at a specific temperature) will consequently induce a correspondent increase in the partial discharge inception voltage PDIV. At higher temperature levels, the PDIV decreases even at lower absolute humidity levels.

1.1.2 Cross-Linked Polyethylene (XLPE) as an insulating material

In [11], researchers have investigated the influence of temperature on the XLPE insulating material of a medium voltage cable. The analysis at the research, has highlighted the change in the dielectric properties of the XLPE material due to thermal ageing.

According to [12], during early phases of thermal ageing, there was a quite improvement in dielectric properties of XLPE material. However at later phases stages of thermal ageing, the XLPE material has shown increased levels of dielectric constant and AC leakage current.

Insulation resistance IR of the cable is a very important parameter to take into account when discussing the negative influence of high temperature levels on cabling. According to [13], the IR of the XLPE cable declines exponentially due to the effect of thermal ageing.

1.1.3 Salt Water and Twisted Pair Cable

Researchers in [14] have investigated the induced impact of salt water on the characteristics of twisted pair cable through a model simulating three samples of cables utilized for communication purposes in the railway industry. The model is based on analyzing such an effect for three types of two pairs (four wires) shielded cables. The experimental approach of the research depended on the idea of applying input signals to the cable (immersed in salt water) through a signal generator, then collecting the values of the measured output voltage signal at the cable far end over a period of time of 28 days. The conclusions of the research highlighted the degradation of cables' characteristics caused by the immersion in salt water for such a long period of time. This degradation was particularly manifested at the rapid increase of the following capacitances (for one cable type) (Figure 1.1):

- C_{pair1} and C_{pair2} has increased 46.9% and 47.4%, respectively of their initial values on the first day.
- C_{mutual} has increased 75% of its initial value on the first day.
- $C_{shield1}$ has increased 80% of its initial value on the first day.
- $C_{shield2}$ has increased 74.5% of its initial value on the first day.

$$C_{mutual} = C_7 + C_8 + C_9 + C_{10} \tag{1.1}$$

$$C_{shield1} = C_2 + C_3 \tag{1.2}$$

$$C_{shield2} = C_4 + C_5 \tag{1.3}$$

The increase in both capacitances $C_{shield1}$, $C_{shield2}$ and C_{mutual}, will lead to the increase of the induced current due to capacitive coupling, which will lead to the increase of crosstalk. The increase of the capacitance C_{pair}, will consequently lead to the decrease of the characteristic impedance, which will cause an impedance mismatch leading to more reflections and power loss. Through using curve fitting tools [14], the degradation curve for each of these capacitances, has been estimated as an exponential relation with respect to the time (t) in days:

$$C_{mutual} = 0.7868 + 1.663\,(1 - e^{-t/54.705}) \quad (1.4)$$
$$C_{shield1} = 1.771 + 0.01537\,(1 - e^{-t/59.347}) \quad (1.5)$$
$$C_{shield2} = 1.460 + 1.821(1 - e^{-t/28.377}) \quad (1.6)$$
$$C_{pair} = 502.2 + 221.9\,(1 - e^{-t/9.416}) \quad (1.7)$$

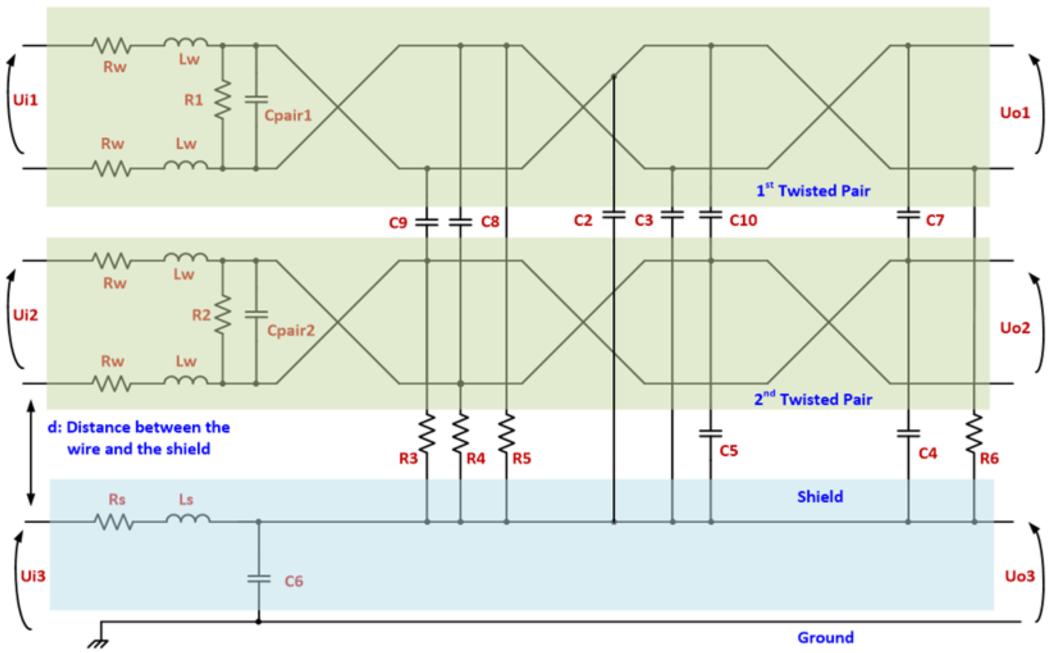

Figure 1.1 Resistances, inductances and capacitances of a double twisted pair shielded cable

Based on the highlighted conclusions from [14], the increase of the different capacitance values at a shielded twisted pair cable immersed in salt water, can be considered as a reflection for the increased dielectric permittivity between the wires and also between the wire and the shield. Assuming that k_s is the coefficient by which the capacitance C_{pair} has increased from C_{pair1} to C_{pair28}, equation (1.8) will be used to calculate C_{pair28}.

$$C_{pair28} = k_s C_{pair1} \quad (1.8)$$
$$\epsilon_0 \epsilon_{r28} A / d = k_s \epsilon_0 \epsilon_{r0} A / d \quad (1.9)$$
$$\textit{Since: } \epsilon_0 A / d = \textit{Constant and not dependent on the effect of salt water} \quad (1.10)$$
$$\textit{Then: } \epsilon_{r28} = k_s \epsilon_{r0} \quad (1.11)$$

According to equation (1.11), the dielectric permittivity between the two wires of the shielded twisted pair, will consequently increase from ϵ_{r0} to ϵ_{r28} by a coefficient of k_s due to immersion in salt water for 28 days. Assuming a lossless approximation to calculate the characteristic impedance Z_0 of the shielded twisted pair cable, it will be calculated as follows:

$$Z_0 = \sqrt{\frac{L}{C}} \quad (1.12)$$

Where L is the cable inductance in H/m and C is the cable capacitance in F/m. The research in [14] has depicted also the increase of the inductance L_w. However, such an increase of L_w can be neglected in comparison with the increase of C_{pair} , $C_{shield1}$, $C_{shield2}$ and C_{mutual} , as the cable inductance L_w has only increased from 14.5 µH on the first day to 14.6 µH on the 28th day of immersion in salt water, which is an increase of almost 0.7%. The increase of the dielectric permittivity between the wires, will induce a consequent increase of the capacitance per unit length C used to calculate the characteristic impedance Z_0.

$$Z_{01} = \sqrt{\frac{L}{C1}} \tag{1.13}$$

$$Z_{028} = \sqrt{\frac{L}{C28}} \tag{1.14}$$

$$\frac{Z_{01}}{Z_{028}} = \sqrt{k_s} = \sqrt{1.47} = 1.2 \tag{1.15}$$

Where Z_{01} and Z_{028} are the characteristic impedances calculated on the first and the 28th days of immersion in salt water, respectively. According to the results obtained at [14], k_s is equal to 1.47 with respect to the increase of C_{pair} from 49 pF/m to 72 pF/m. Therefore, the characteristic impedance calculated on the 28th day of immersion in salt water will be less than the characteristic impedance calculated on the first day of immersion in salt water. Calculating the relation between the reflection coefficients Γ_1 and Γ_{28}, the result will be as follows:

$$\frac{\Gamma_1}{\Gamma_{28}} = \frac{Z_L - Z_{01}}{Z_L + Z_{01}} \times \frac{Z_L - Z_{028}}{Z_L + Z_{028}} \tag{1.16}$$

$$\frac{\Gamma_1}{\Gamma_{28}} = \frac{Z_L - Z_{01}}{Z_L + Z_{01}} \times \frac{Z_L + 0.83Z_{01}}{Z_L - 0.83Z_{01}} \tag{1.17}$$

$$\textit{Since } Z_L - Z_{01} < Z_L - 0.83Z_{01} \textit{ and } Z_L + Z_{01} < Z_L + 0.83Z_{01} \tag{1.18}$$

$$\frac{\Gamma_1}{\Gamma_{28}} < 1 \tag{1.19}$$

As depicted at equation (1.19), the reflection coefficient of the shielded twisted pair cable will increase due to the immersion in salt water for 28 days, which will lead to a correspondent decrease at the cable return loss (equation 1.20) as well as a correspondent increase of the cable power loss (equation 1.21)

$$\text{Return Loss} = -20 \ \log_{10} \Gamma \tag{1.20}$$

$$\text{Power Loss} = -10 \ \log_{10}(1 - \Gamma^2) \tag{1.21}$$

The current induced due to the capacitive coupling is proportional to the capacitance between the cable wires and the shield. The results obtained in [14] demonstrated the increase of the capacitance $C_{shield1}$ from 0.15 nF/m to 0.27 nF/m by a coefficient k_{sh} equal to 1.8. It is assumed that the rate of voltage change with respect to time will be equal from the first day to the 28th day of cable immersion in water. If the cable is used for processing an analogue DC signal such as the 4-20 mA current signal, the voltage V will be equivalent to the DC voltage V_{DC} added to the noise AC voltage V_{noise}. Therefore, the rate of voltage change with respect to time will be equal to $\frac{dV_{noise}}{dt}$

$$I_{c1} = C_{shield1,1} \frac{dV}{dt} \tag{1.22}$$

$$I_{c28} = C_{shield1,28} \frac{dV}{dt} \tag{1.23}$$

$$V = V_{DC} + V_{noise} \tag{1.24}$$

$$\frac{dV}{dt} = \frac{dV_{noise}}{dt} \tag{1.25}$$

$$\frac{I_{c1}}{I_{c28}} = \frac{C_{shield1,1}}{k_{sh} C_{shield1,1}} \tag{1.26}$$

$$I_{c28} = k_{sh} I_{c1} = 1.8\ I_{c1} \tag{1.27}$$

The uniqueness of this research lies in its convergence with the hypothesis of the analysis conducted in this doctoral study. This convergence can be emphasized in the following points:

1- Analyzing the negative effect of salt water on twisted pair cables as an example for harsh environmental conditions in the railway industry, is a similar approach to investigating the impeding influence of seawater on instrumentation cables used in marine engineering applications. This impeding influence is clearly present at a shipboard monitoring systems such as tank level measurement system, especially when measuring the level of sea water in ballast sea water tanks (top side and double bottom tanks) where the measurement process is basically dependent on immersing a pressure switch from the top of the tank to be mounted at the bottom of the tank along with a combined instrumentation cable of a length up to 30 meters as was explained in [1]. For a single twisted pair cable of 30 meters immersed in sea water ballast tank all the time for several years, if the results obtained at [14] was applied in such a case, the time t in equations (1.28) and (1.30) is supposed to approach infinity. As $C_{shield1}$ increases, the current induced due to capacitive coupling will increase. In case the immersed pressure transmitters are HART pressure transmitters, the increased capacitive coupling current will induce its negative impact on the FSK digital signal superimposed to the 4-20 mA DC signal. Similarly, In case the immersed pressure transmitters are FF pressure transmitters, the increased, the increased capacitive coupling current will induce its negative impact on the H1 bus 31.250 kbps H1 digital signal.

$$\lim_{t \to \infty} C_{shield1} = 1.771 + 1.537 = 3.237 \text{ nF For 10 meters} \tag{1.28}$$

$$C_{shield1} = 3.237 \times 3 = 9.711 \text{ nF For 30 meters} \tag{1.29}$$

$$\lim_{t \to \infty} C_{pair} = 502.2 + 221.9 = 724.1 \text{ pF For 10 meters} \tag{1.30}$$

$$C_{pair} = 724.1 \times 3 = 2172.3 \text{ pF For 30 meters} \tag{1.31}$$

2- The idea of relying on a twisted pair Shielded Cable of two pairs, is the same idea that was adopted by the authors in [15] while conducting a comparative cost analysis between the cost of using cabling and Wi-Fi as mediums of data transaction in maritime measurement/control systems. The authors in [15] raised the attention to the most commonly adopted cabling option by shipbuilders and ship owners when planning for cabling installations at maritime measurement/control systems where sensors are remotely separated by considerably long distances. They tend to use a shielded cable of a single pair in order to achieve the maximum possible financial gain. The authors in [15] has strongly advised against adopting such an option for cabling due to the absence of spare wires in case the used pair has suffered some sort of a failure or malfunction. The main reason that motivated the authors [15] to urge for depending on using cables of two pairs (one connected and the other is kept as a backup for the used pair), is the extreme difficulties associated with the process of cables replacement in maritime engineering applications, particularly for cables extended at the locations such as void spaces, passage ways or on deck. Cables which are extended on deck, are usually passing through metallic pipes extending along the main deck of the ship. An example for such difficulties can be emphasized in the attempt to replace an old cable in an old pipe with extremely deteriorated condition due to factors such as humidity, salt water and high levels of corrosion. Therefore, it is highly recommended to consider the option of using cables with two pairs of wires (main pair used and remaining pair kept as a backup for the main pair in a 50% spare capacity configuration)

1.2 4-20 mA Analogue Standard in Maritime Engineering Applications

In [1], the researchers discussed the 4-20 mA analogue standard from a perspective related to digital communication protocols coexisting with the 4-20 mA current loop in maritime measurement and control systems. The research categorized such protocols into links undertakes administrative serial communication tasks in systems based on 4-20 mA analogue standard for collecting measurement/control data (Ethernet, RS232, RS424 and Modbus), and digital communication protocols collaborating with 4-20 mA carrying out measurement and control tasks (HART, FF, Profibus PA). The research also introduced the basics of the 4-20 mA analogue standard from the point of view of the minimum necessary requirement to implement an operational 4-20 mA measurement/control current loop such as maximum/minimum load resistance in conjunction with minimum/maximum supply voltage [16,17]. Additionally, the analysis in [1] has spotted the light on the shortened service lifetime of the 4-20 mA current loop used to measure the sea water level in sea water ballast tanks on commercial ships in comparison with other tanks. The research also highlighted the adopted technique to connect the 4-20 mA analogue pressure transmitters used by tank level measurement system to the host controller through junction boxes (Figure 1.2) located at the closest point to the tank, where signal conditioning and isolation is recommended to take place in order to avoid any negative influence induced by ground loops or noise [1].

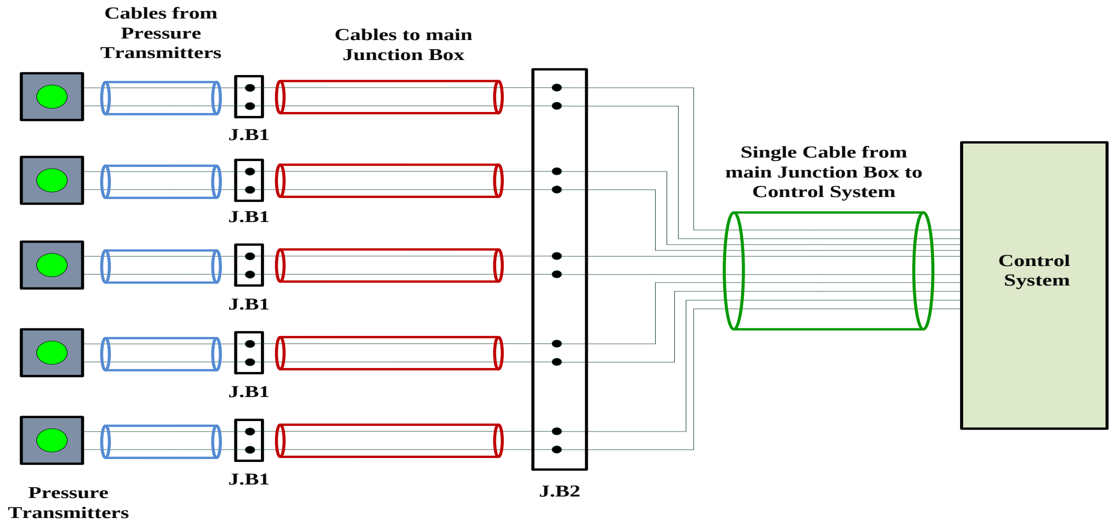

Figure 1.2 Connection diagram between 4–20 mA pressure transmitters and I/O modules in control system in a shipboard tank level measurement system

In [18], the research included a Simulink model (Figure 1.3) dedicated to the simulation of tank level measurement process on a commercial ship through using pressure transmitters mounted at the bottom of the tank (double bottom ballast water tanks), or pressure transmitters immersed inside the tank (top side ballast water tanks). Simulation has taken into account the negative effect induced on the 4-20 mA current loop by ground loops, common mode noise and coupled noise. The Simulink model has highlighted the deployment of signal isolators/conditioners (transformer and optocoupler insulation) to eliminate ground loops. Similarly, the analysis in [18] has also depicted the importance of using instrumentation amplifiers and low pass filters to eliminate common mode noise and coupled noise signals, respectively (Figure 1.4).

$$K = I_{4\text{-}20}/I_{opt} \tag{1.32}$$

$$V_{amp} = I_{opt}\, R_{amp} \tag{1.33}$$

$$I_{C4\text{-}20} = V_{amp}/R_L \tag{1.34}$$

$$V_o = (V_1 - V_2)\,\frac{R_2}{R_1} \tag{1.35}$$

$$f_c = 1/2\pi R_f C \tag{1.36}$$

$$\text{Quantized Output} = \text{round}\left(\frac{2^n\, V_{of}}{V_{max}}\right) \tag{1.37}$$

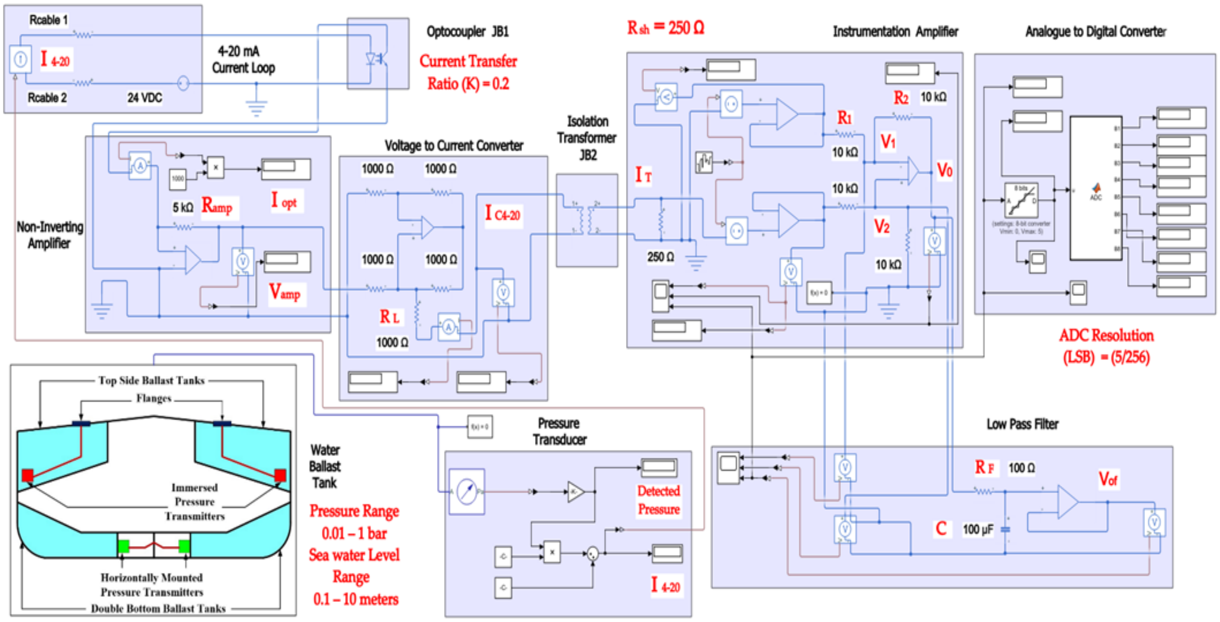

Figure 1.3. Simulink Simscape model used to simulate 4–20 mA pressure measurement current loop as a part of automation system.

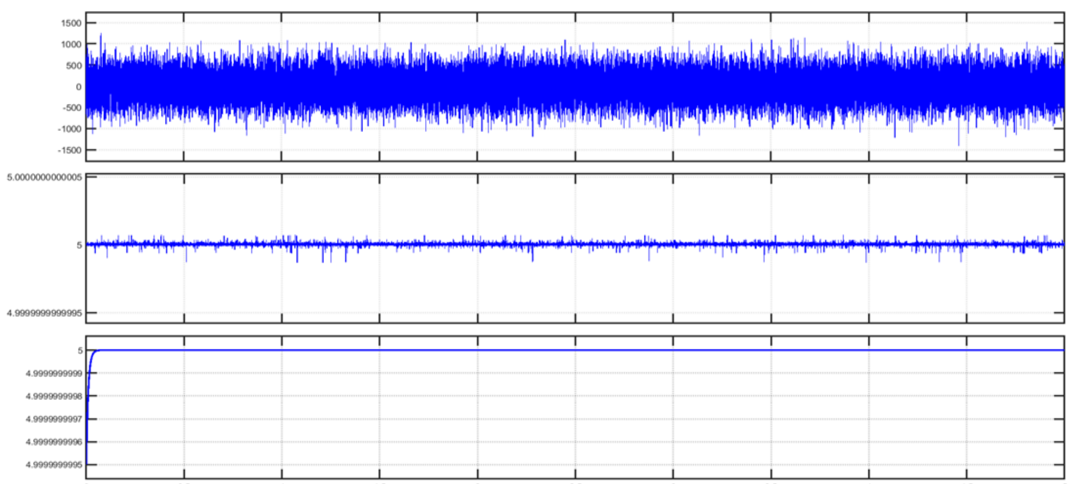

Figure 1.4. Illustration of 5 VDC voltage signal corresponding to 20 mA analogue current (1 bar of detected pressure). Upper figure illustrates voltage signal highly distorted by common mode noise at difference amplifier input. Middle figure illustrates the output voltage signal of instrumentation amplifier slightly distorted by coupled noise, while the lower figure illustrates output voltage after low-pass filtering.

1.3 Smart Sensors in Maritime Engineering Applications

Smart sensors are devices which are capable of providing reliable accurate measurement values, relying on its composition of transducers and microprocessors/microcontrollers. The transducers detect the variable which is supposed to be measured, then complex mathematical and statistical processing will be applied on the measured values by the microprocessors/microcontrollers for the purpose of noise elimination and performance prediction. Through an integrated user interface, calibration and diagnostic parameters in smart sensors can be accessed locally or remotely

1.3.1 HART Protocol

HART (Highway Addressable Remote Transducer) protocol is a hybrid technology device which depends on superimposition of a digital signal over the regular 4-20 mA analogue signal. The superimposed signal is a FSK (Frequency-Shift Keying) digitally modulated sinusoidal signal in which ones are represented by 1200 Hz, and zeroes by 2200 Hz sinusoidal waveforms. The average current of superimposed FSK signal is equal to zero. The superimposed FSK signal includes additional diagnostic information [19] to improve the reliability of measurement 4-20 mA current loop [1, 20-23].

HART protocol can operate in two modes, Poll/Response mode and Burst/Broadcast Mode. In Poll/Response mode, master polls the smart devices, and then one of the selected devices will start sending all the required information, Poll/Response mode is usually used with multidrop [1, 24] communication. Burst mode is a broadcasting mode in which device is continuously transmitting its information to the master with a rate of 3.7 times/s. Burst/Broadcast Mode can only be used with point to point communication. Load resistance in an entire HART network should be between 230 Ω and 1100 Ω. Load resistance of devices included in HART network can be calculated only at 20 mA loop current. Load resistance outside this range can increase signal attenuation and distortion, and reduce the critical transmission frequency. HART protocol is a master/slave protocol. Communication takes place between master and field devices through the exchange of three types of HART commands (Universal Commands, Common Practice Commands and Device Specific Commands) [1, 20-23].

HART message structure consists of preamble, start character, address field, expansion field, command byte, byte count, status field, data field and checksum. Each of these fields consists of a single byte or multiple bytes. Each byte is transmitted as an 11-bit UART character including a start bit, eight data bits, a parity bit and a stop bit. The HART message address field has two formats: short format and long format. Long format was firstly adopted by HART 5 version. The hamming distance of the HART protocol is equal to four; therefore, it can detect up to three corrupted bits of data at one telegram. However, some higher-level communication errors may take place during transmission, and they will be detected by the status bytes at the field device side [18,21,25,26].

1.3.1.1 Rosemount 3051S HART Pressure Transmitter

An increased reliability level can be rendered to the 4–20 mA analogue standard through using HART smart pressure transmitters such as Rosemount 3051S [8]. Improved reliability levels are provided by features such as baseline estimation and loop characterization. The baseline indicates the relation between the output current of the transmitter and the terminal voltage. Deviation of the baseline is a very important parameter based on which changes such as corrosion, water leak inside the transmitter or instability of power supply can be detected to maintain loop integrity. Such a property is turned off by default, but once the transmitter is installed, the user should start loop characterization. For proper characterization, an adequate amount of power is required. The transmitter will check the power level, and if it was within the proper limits, it will generate an output current of 4 mA and 20 mA successively, and the correspondent terminal voltage for these current values will be recorded to estimate the baseline. A value should be assigned to the terminal voltage deviation limit parameter (default value is 1.5 V) through AMS (asset management system) device manager. If the terminal voltage deviation of the baseline will exceed this limit, an alert will be automatically generated. Loop characterization also provides an estimation of the loop resistance and loop power supply voltage, based on the baseline calculations and the comparison between the previously and recently calculated baselines to detect changes in their values that might be caused by ageing of the power supply or any physical changes in the loop condition [18,27].

At any measurement/control system, the 4-20 mA current signal from the pressure transmitter is converted into 1-5 VDC at the analogue input card through a shunt resistance, as it is much more easier to process a voltage signal than processing an analogue signal. If a HART transmitter is to be tested at the benchtop, the internal resistance of the power supply used to power up the current loop, is usually less than the value that can interpret a 4-20 mA signal into 1-5 VDC. therefore a resistance of minimum 230 ohms (considering that power supply maximum resistance is 20 ohms at 1200 Hz) and standardly of 250 ohms, will be inserted in the loop to ensure its functionality [27].

In Rosemount 3051S HART pressure transmitter, Namur NE 43 is the standard that identifies the alarm and saturation levels of the 4-20 mA control signal. If the output current signal of the sensor reached either the low level saturation limit of 3.6 mA or the high level saturation limit of 21 mA and remained on such a state for at least 4 seconds [27].

Pressure transducer time constant is the time required for the sensor output to reach a value that represents 63.2% of the pressure value at a single step pressure change. For example, if the pressure applied to a pressure transmitter was 10 bars, then suddenly the pressure dropped to 0 bars, the time constant in such a case will be equal to the time it takes to change its output current to a value correspondent to a pressure of 6.32 bar. The transducer response time is equal to the time constant added to the dead time, which represents the interval between the time at which the applied pressure started actually dropping and the time at which the transducer will start responding to such a pressure drop [27].

Damping is a feature by which the operator can eliminate the noise caused by initial fast pressure fluctuations which leads to chattering, which is identified as small and rapid variations of the transmitter output reading. Chattering can be avoided by increasing the dead time which will consequently increase the overall response time of the transmitter. In Rosemount 3051S HART pressure transmitter, damping can be adjusted by field communicator or by AMS device manager from 0 to 60 seconds [27].

1.3.1.2 Simulated Effect of Marine Environmental Conditions on HART Sensors

In [1], an experimental research was conducted on a smart 4-20 mA measurement current loop. The major goals of such a research were:

- The verification of the sensitivity of a HART transmitter to various sources of noise in comparison with a classical 4-20 mA transmitter.
- Exploring the effect of the techniques used for connecting the twisted pair cable shield as well as the techniques adopted for the grounding of various power sources, which are factors that can lead to the formation of ground loops and consequently inflect a negative influence on the measurement process.

- Demonstrating the influence of the possible of physical connection between the shield terminal and the twisted pair cable wire terminal due to conditions such as low insulation in junction boxes caused by humidity, corrosion and vibration.

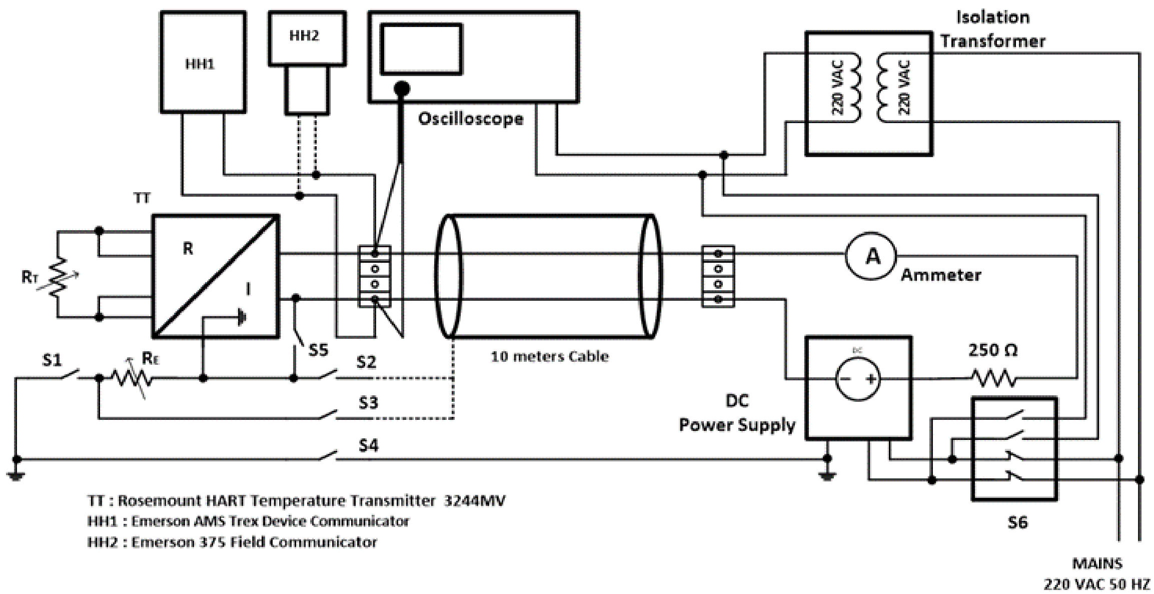

Figure 1.5 – Initial Connection of 4-20 mA measurement loop at the laboratory stand.

Brief description for the constructed laboratory stand (Figure 1.5) can be summarized as follows:

- The 4-20 mA smart current loop consists of a HART smart temperature transmitter (3244MV), 10 meters long of shielded twisted pair cable, DC power supply of 24 VDC, 250 Ω resistance and an ammeter to measure the current flowing in the loop.
- Two types of HART hand held communicators were connected across the transmitter terminals.
- The resistor R_E is connected between the grounding point of the transmitter and the earth.
- Switches S2 and S3 are used to connect the shield to various grounding points.
- Switch S4 connects the earth point to the grounding point of the DC power supply.
- Switch S5 is used to simulate a fault condition where the shield can be connected to one of the two wires outgoing from the transmitter.
- Resistance R_T is connected to the HART temperature transmitter for simulating a change in resistance corresponding to the temperature change. Rresistance R_T was adjusted to simulate a random measured temperature of 44.35℃ which is converted to a loop current of 15.61 mA (measured as 15.55 mA by hand held communicators). Table 1.1 summarizes the results of the experimental analysis.

Table 1.1- Most important results obtained during testing the simulated simultaneous effect of vibration and humidity on the 4-20 mA HART smart current loop, in addition to verification of most recommended grounding techniques to avoid ground loops

Configuration	Purpose	Results
• S1, S2 and S5 are closed. • Resistance R_E is set to 0 Ω	Simulation of a situation that might occur due to humidified terminal strip or junction box	• No effect on the current value in the 4-20 mA measurement loop after closing these switches.

		• The HART communication signal has suffered some slight distortion.
• S1,and S5 are closed. • Resistance R_E is set to 0 Ω • Switch S2 or S3 started to close and open with a frequency of approximately 3 Hz	Simulation of a situation that might occur if humidified terminal strips or junction boxes would have endured some sort of vibration	• The current value of the loop will jump from 15.61 mA to a value of 21.57 mA and sometimes up to 23.5 mA (if the smart transmitter was configured to generate a high range value alarm), or it will suddenly decline from 15.61 mA to a value of 3.78 mA (if the smart transmitter was configured to generate a low range value alarm). • Many overshoots and undershoots in HART communication signal and it will eventually lead to HART communication failure if it continued for longer periods of time.
• S4 and S1 closed. • S2, S3 and S5 open	Simulate a situation where grounding point of the DC power supply is united with the grounding point of the transmitter	• HART communication signal will suffer more distortion (Overshoots and Undershoots) than the case when both grounding points of the DC power supply and the transmitter were isolated from each other.
• S1,and S5 are closed. • Resistance R_E is gradually increased from 0 Ω to (700-800) Ω • Switch S2 started to close and open with a frequency of approximately 3 Hz	Simulating a situation at which the resistance between the cable shield and the grounding point (R_E) is increased to the level that eliminate the effect of vibration in humidified junction boxes	• For $R_E <$ (700-800) Ω, the current value of the loop will jump from 15.61 mA to a value of 21.57 mA and sometimes up to 23.5 mA (if the smart transmitter was configured to generate a high range value alarm), or it will suddenly decline from 15.61 mA to a value of 3.78 mA (if the smart transmitter was configured to generate a low range value alarm). • For $R_E >$ (700-800) Ω, there was no negative effect neither on the HART communication signal nor on the current value.
• S1,and S5 are closed. • Resistance R_E is set to 0 Ω • Switch S2 or S3 started to close and open with a frequency of approximately 3 Hz • S6 closed with the poles from isolation transformer	Illustrating the effect of using isolation transformers to eliminate the overshoots and undershoots at HART communication signal and also maintain stability of 4-20 mA current.	• No negative effect was detected

The most important conclusions derived from this experimental research:

- HART protocol is more sensitive than the 4-20 mA analog standard to the effect of vibration associated with low insulation levels at termination points or junction boxes. This can provide a means of early detection for the deteriorated conditions of junction boxes or termination points due to factors such as corrosion and humidity.

- In order to avoid ground loops, it is highly recommended to separate between the grounding point of the 4-20 mA current loop power supply and the grounding point of the 4-20 mA transmitter.
- In order to avoid the negative influence of rapid ageing time as well as high levels of humidity in marine engineering applications, it is highly recommended to supply the 4-20 mA through a 24 VDC power supply which is fed with 220 VAC by the secondary winding terminals of an isolation transformer, the primary winding of which is connected to the 220 VAC from the mains.

1.3.2 Foundation Fieldbus (FF)

The Foundation Fieldbus (FF) protocol is a digital communication protocol adopted by many smart transmitters. Foundation Fieldbus IEC 61158 is a fieldbus protocol based on the idea of using a single twisted pair of wires for the connection of multiple field devices. The role of field devices in FF is extended beyond the regular role of measuring process variables, to the role of performing automation and control tasks independently of the authority of the master controller. Field devices perform data transaction tasks through using the feature of distributed data transfer (DDT) functions. Foundation Fieldbus has also the capability of providing reliable measurement and control operations in explosive hazardous application areas depending on intrinsically safe models such as the entity model, FISCO model, FNICO model, HPTC model and DART model. Foundation Fieldbus is very similar to Profibus PA; however, Profibus PA is more popular in Europe while Foundation Fieldbus is more popular in Asia and America [1,18,28-31].

The Foundation Fieldbus signal is a Manchester-coded rectangular signal from the theoretical point of view; however, it practically takes the form of a trapezoidal waveform with rising and falling edges due to multiple factors such as the time delay imposed by modulation/demodulation electronic circuitry. The practical processing of a 31.250 Kbps Foundation Fieldbus Manchester-coded signal on the H1 bus was discussed in detail in [32], including modulation/demodulation techniques in noiseless as well as noisy conditions. The H1 bus is dedicated to the connection of all field devices along the same field bus; however, the HSE bus (high-speed Ethernet) is dedicated to performing communication tasks between host controllers with a bit rate of 1–2.5 Mbps.[18]

The Foundation Fieldbus FF adopts a distributed communication system in which LAS (Link active scheduler) plays an important role in controlling the communication process. For the purpose of redundancy, a single network may have two link masters, and in case one failed as the LAS, the other one will replace it. Communication between the LAS and field devices is divided into scheduled and unscheduled communication [1,18,28-31].

Unscheduled communication is used for the transaction of diagnostic data and field device parameters. It takes place during breaks between scheduled communication intervals. Scheduled communication can be divided into two categories: the first one is related to control and measurement variables, while the second one is related to system management. In the first category, any field device publishes its process data periodically to the entire fieldbus buffer directly upon receiving a compel data command (CD) from the LAS. In the second category, each field device will receive independent schedules (time distributions (TD)) for data transaction. As an OSI model, Foundation Fieldbus is divided into three layers, which are the user application layer, communication stack and physical layer. The communication stack performs only the roles of data link layer and application layer. A Foundation Fieldbus management system consists of two layers: the first one is the application layer, which is included in the communication stack, and the second one is the user application layer, which consists of function blocks and device description. The application layer included in the communication stack consists of fieldbus message specification (FMS) and a Fieldbus access sublayer (FAS) [1,18,28-31].

Field devices can be easily connected to the bus during operation through using the probe node (PN) command [10,12] issued by the LAS to detect the newly connected field devices to the bus. The field device will be automatically assigned an address directly after it responds to the PN command with the probe response (PR) command. Afterwards, the LAS cyclically issues a pass token (PT) command in order to check if the field device is still functional or not through acknowledging the device response to the transmitted PT. If the device fails to respond for several times to the PT command, it will be automatically excluded from the field devices' live list [18,29,31].

Each FF segment should have at least two terminators. The power supply unit is provided with a built-in terminator, and the other terminator can be separately connected to the end of the bus, or the last connection unit might be provided with a built-in terminator similarly to the power supply, a Foundation Fieldbus terminator consists of a 100 Ω resistor connected in series with a 1 μF capacitor. It is used as a current shunt for the control network, reducing the impact of reflections, noise and jitter. If more than two terminators are connected to the FF trunk, this will lead to high levels of distortion for the Manchester communication signal [18].

1.3.2.1 Simulated FF H1 Bus Signal Modulation/Demodulation (Ideal Case)

According to [32], the Simulink model in Figure 1.6 is dedicated to the simulation of the process of modulation/demodulation of Manchester coded FF bus signal with a bit rate of 31.25 kbps. The model is based on three pulse generators :

1- The first pulse generator will generate a 8 bits binary byte sequence with a frequency of 31.25 kbps that will be modulated using Manchester coding.
2- The second pulse generator generates a bit stream of (high to low) transitions with a frequency of 2·(31.25) kbps.
3- The third pulse generator generates a bit stream of (low to high) transitions with a frequency of 2·(31.25) kbps.

Manchester coding is carried out through the replacement of each binary bit of (1) from the first pulse generator with a high-low transition from the second pulse generator, while each binary bit of (0) from the first pulse generator is replaced with a low-high transition from the 3rd pulse generator. Through switching process at switch no.2, the output FF Manchester coded 31.25 kbps signal will be produced with a base current of 10 mA, increased to 19 mA (10 mA + 9 mA) for ones, and decreased to 1 mA (10 mA - 9 mA) for zeros. The demodulation process is based on firstly elimination of the DC bias current, then applying the de-biased signal as the first input signal to a XNOR gate, to which the output of the first pulse generator is applied as a second input signal (Figure 1.6 and Figure 1.7).

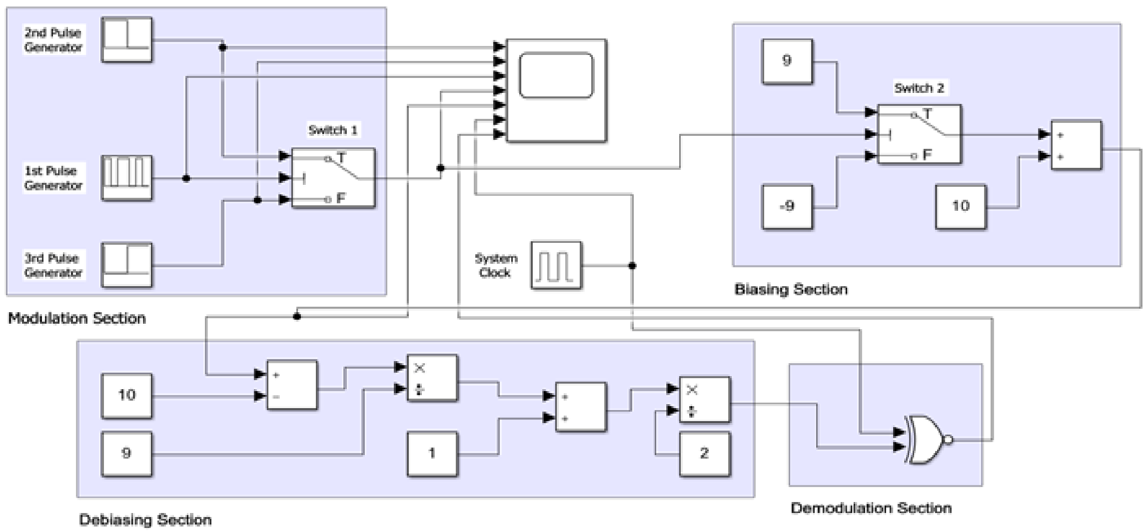

Figure 1.6 - Simulink Model used to simulate modulation/demodulation of Foundation Fieldbus Manchester coded Signal in the ideal condition [32].

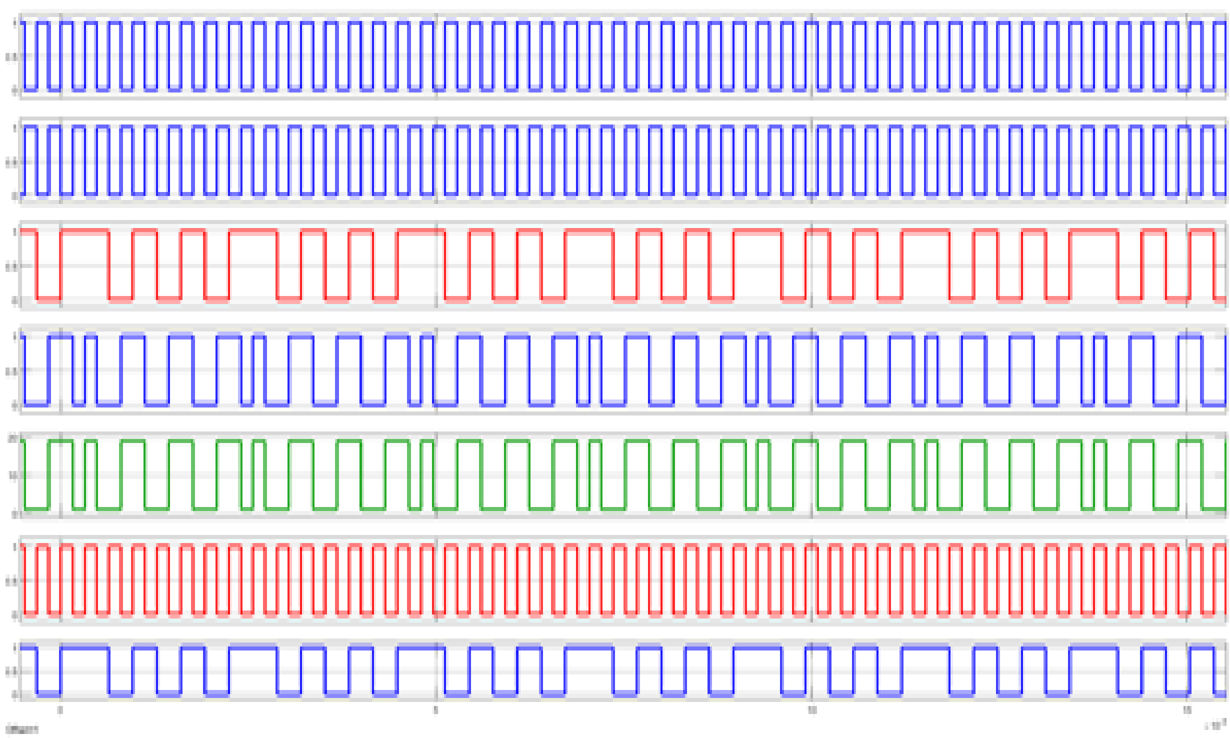

Figure 1.7- Waveforms obtained from Simulink model in Figure 1.6. 1st and 2nd waveforms are pulse trains replacing the ones and zeros in the binary code respectively. 3rd waveform represents the binary bit stream. 4th and 5th waveforms are the output signals of modulation and biasing sections respectively. 6th wave form is the system clock signal. 7th waveform is the recovered binary code bit stream at the output of the demodulation section [32].

1.3.2.2 Simulated FF H1 Bus Signal Modulation/Demodulation (Noisy Case - Matlab)

In order to simulate the modulation / demodulation process of a FF data frame (Figure 1.8) in non-ideal noisy practical conditions, the research in [32] has introduced a MATLAB code dedicated to such a purpose. The basic idea adopted by the MATLAB code is that a noisy FF Manchester coded

FF bus signal can be demodulated through a technique based on the averaging of the noisy modulated signal over specific time spans, which is equivalent to calculating the average energy of the received signal at these time intervals. the transmitted bit stream can be recovered through identifying the intervals with maximum or minimum energy levels over the wave period. The most important features of the model can be summarized as follows:

1. MATLAB code generates a noiseless 31.25 kbps Manchester coded FF signal, which takes the shape of a trapezoidal waveform similar to practical operational conditions.
2. Additive White Gaussian Noise AWGN will be added to the generated 31.25 kbps Manchester coded FF trapezoidal signal to simulate the effect of noise (Figure 1.9).
3. The sampling frequency adopted by the MATLAB model is 10 MHz (greater than 31.25 kbps) which allows for better detection of waveform changes in the Manchester coded signal as the period between samples is much less than the period of the Manchester coded signal.
4. The demodulation index is a value resulting from the division between the sampling frequency and the Manchester coded signal frequency (fs/fm), which is equal to 320 samples.
5. In order to recover the binary bit stream of the FF data frame, another train of samples is generated with a period between the samples equal to 32 microseconds, which is equal to the demodulation index multiplied by the period between the samples generated by the main sampling frequency of 10 MHz.
6. The distorted Foundation Fieldbus Manchester coded signal can be demodulated to its original binary code by averaging the signal in specific periods of time during which changes in the trapezoidal waveform are taking place.
7. A Manchester coded trapezoidal signal takes different forms according to the value of the modulated binary bit and also according to the value of the bit that precedes it. Generally, the FF Manchester coded trapezoidal waveform of 32 microseconds time interval can be divided equally into four divisions of 8 microseconds (32/4) periods, during which four types of change can be detected (rising edge, falling edge, high logic value and low logic value). Therefore, the Manchester noisy signal is averaged in each division over 8 microseconds and compared to the averaged other divisions at the same 32 microseconds cycle.
8. After the Manchester noisy signal portions of trapezoidal wave are averaged every 8 microseconds and compared to each other every 32 microseconds within the same cycle, the locations of the maximum and minimum values of the averaged signal portions can be detected. In other words, there can be only four averaged values corresponding to the four types of change in the waveform between the samples generated every 32 microseconds (Figure 1.10, upper part).
9. The binary modulated bit can be restored by detecting the location of the maximum and minimum values among these four averaged fixed values. If the maximum detected averaged value preceded the minimum detected averaged value, the demodulated binary bit will be one. However, if the minimum detected averaged value preceded the maximum detected averaged value, the demodulated binary bit will be zero.
10. In order to detect Non-Data positive and negative bits, the four fixed averaged values can be averaged to a single fixed value (Figure 1.10, middle part). The minimum 4 detected values along the data frame will indicate the location of Non-Data negative N- bits based on which the Non-Data positive N+ bits can also be detected.

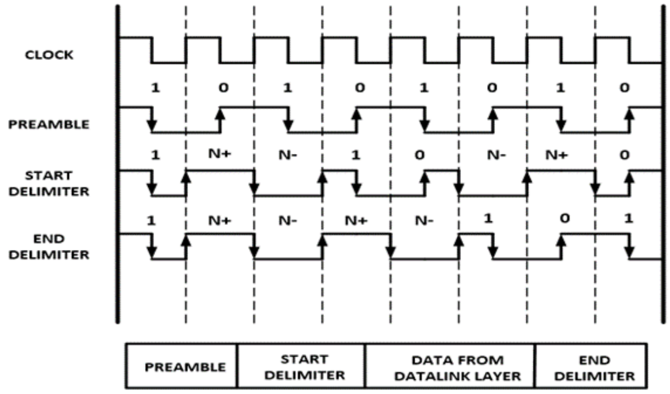

Figure 1.8- Foundation Fieldbus Data Frame [1].

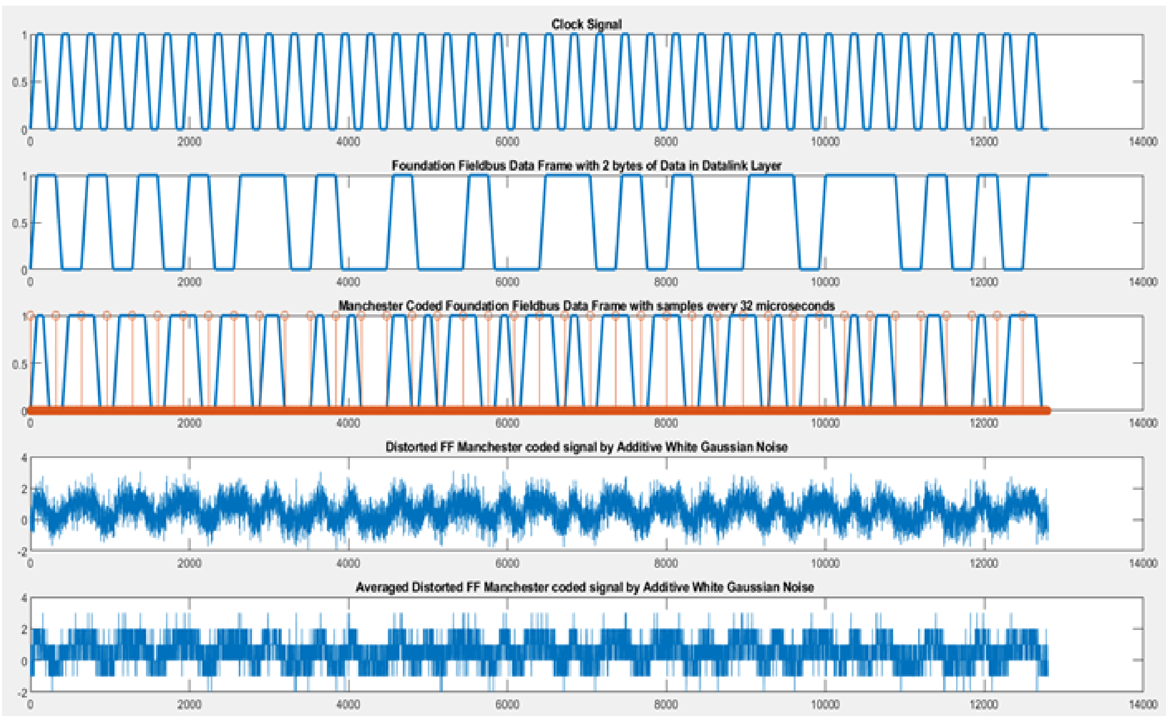

Figure 1.9- MATLAB model waveforms of clock signal, Foundation Field bus Data Frame Binary bits stream with samples every 32 microseconds, FF Manchester coded signal, Distorted FF Manchester coded signal and averaging process of this distorted signal [32].

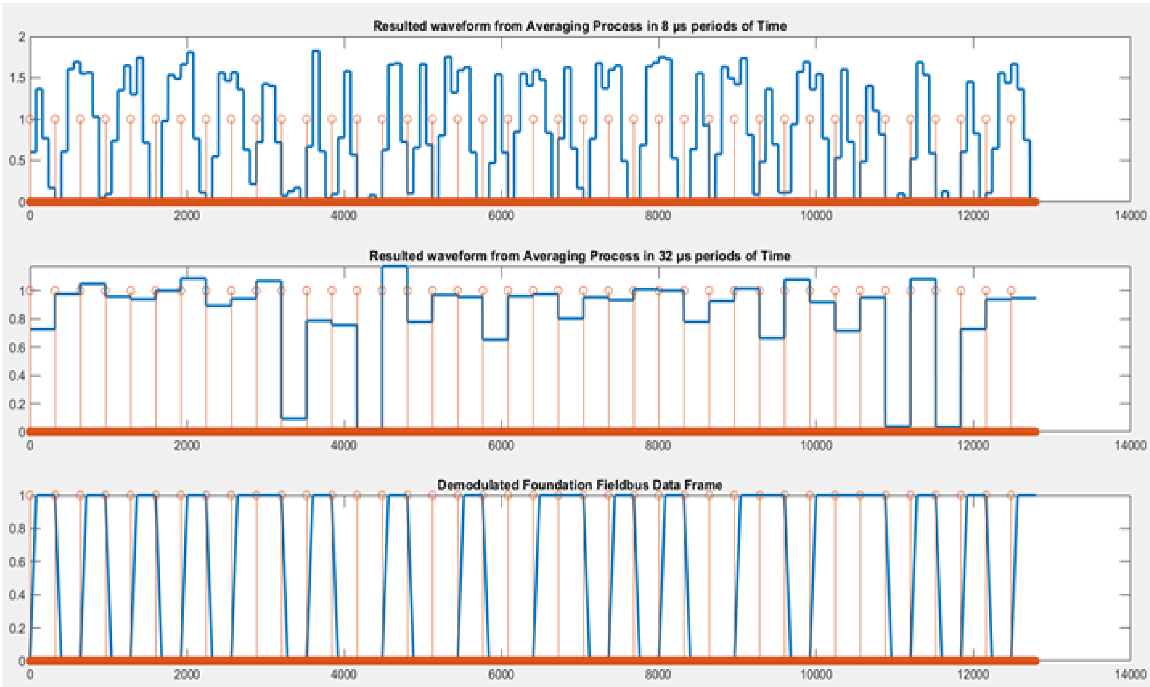

Figure 1.10 MATLAB model waveforms of Averaging Process in 8 µs periods of Time (Used to detect zeros and ones of the modulated signal), Averaging Process in 32 µs periods of Time (Used to detect Non-Data positive N+ and Non-Data negative N- bits) and demodulated FF data frame [32].

1.3.2.3 Simulated FF H1 Bus Signal Modulation/Demodulation (Noisy Case - Simulink)

The research in [32] has additionally introduced a Simulink model (Figure 1.11) dedicated to the simulation of the modulation/demodulation process of the FF Manchester coded 31.25 kbps noisy signal. The model is based on generating two pulse trains with trapezoidal waveform according to equations (1.38) and (1.39). The trapezoidal signal generated by equation (1.38) is used to modulate the binary bits of ones, while The trapezoidal signal generated by equation (1.39) is used to modulate the binary bits of zeros. Prior to the demodulation process, the model adopted the use of Kalman filter (Figure 1.12) to eliminate the effect of Additive White Gaussian Noise AWGN, in order to facilitate the demodulation process so that the original binary bits can be easily and correctly recovered (Figure 1.13).

$$Y_1=\arcsin(\sin 2\pi ft+2)+\arccos(\sin 2\pi ft+2) \tag{1.38}$$
$$Y_0=\arcsin(\sin 2\pi ft+3/2)+\arccos(\sin 2\pi ft+3/2) \tag{1.39}$$

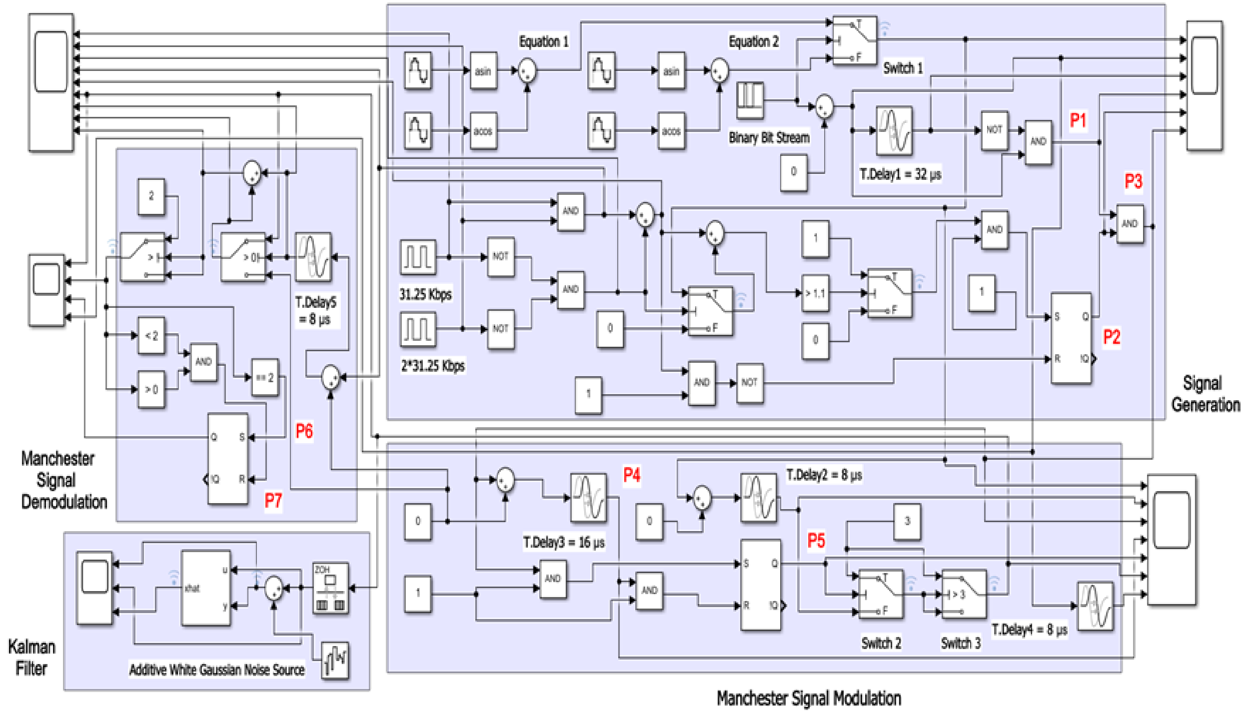

Figure 1.11 - Simulink Model used to simulate modulation/demodulation of Foundation Fieldbus Manchester coded Signal in noisy operational condition [32]

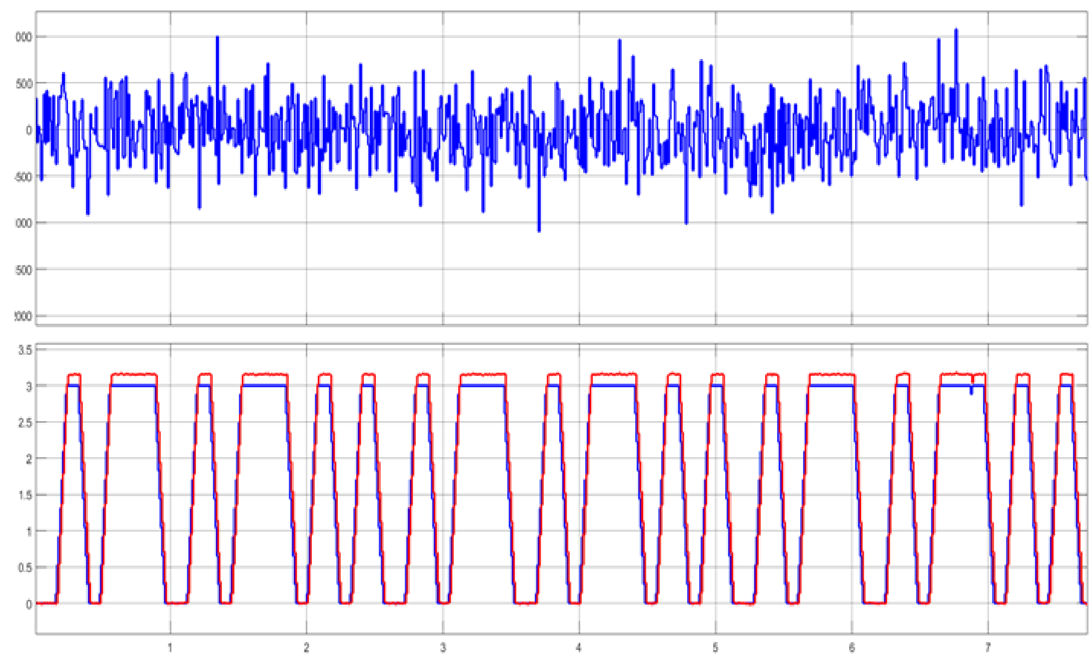

Figure 1.12 - Upper waveform illustrates the distortion induced to the FF Manchester coded signal by the additive white Gaussian source at the Kalman filter section. The lower plot illustrates the modulated FF Manchester coded signal without the effect of noise and the output filtered FF Manchester signal in blue and red colors respectively [32].

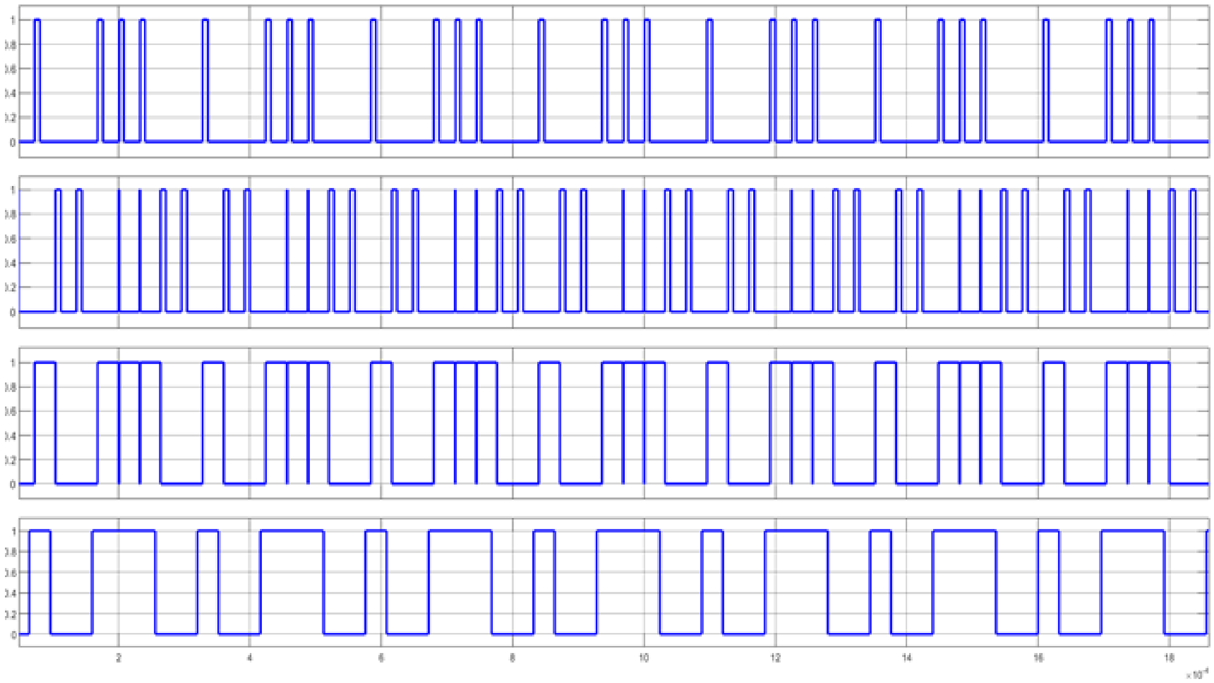

Figure 1.13 - Waveforms generated from demodulation section. From top to bottom, Set and reset signals for the SR latch flip-flop at points P6 and P7 respectively in addition to the demodulated binary bit stream of the FF data frame compared to the original binary bit stream at the last waveform.

1.3.2.4 Rosemount 3051 FF Pressure Transmitter

For the purpose of emphasizing the enhancement provided by the FF protocol on the measurement process, a brief introduction will be presented for a statistical tool (statistical process monitoring block SPM) adopted by the Rosemount 3051 FF Pressure Transmitter similar to the loop characterization tool adopted by the Rosemount 3051S HART Pressure Transmitter. The importance of such mathematical tools is to eliminate the effect of any expected noise signals through the creation of a pattern for the collected samples of measurement data.

The SPM [18,33] can be considered one of the most important function blocks at Foundation Fieldbus smart transmitters. Its task is to construct a noise signature of the transmitter primary variable with both mean and standard deviation values. SPM enables the transmitter to detect any sudden changes that may be related to some physical disturbances, such as propagation or vibration (swaying or pitching on a ship, for instance), which are not reflecting an actual real-time measured value. In a Rosemount 3051 FF smart pressure transmitter, the SPM block consists of three modules [18,33], which are:

- Statistical calculation module: The measured pressure values are applied to high-pass filter to detect any slow changes, such as set point modifications, and eliminate them while constructing the input signal noise signature. The mean value is calculated for the unfiltered signal, and the standard deviation will be calculated over the filtered signal.
- Learning module: responsible for establishing the process baseline values based on mean and standard deviation values calculated by the previous module.
- Decision module: it compares the measured value with the baseline, to decide if an alert/alarm should be activated or such a measured value should be ignored.

1.3.2.5 Simulation for The Application of FF in Tank Level Measurement System on a Bulk Carrier Commercial Ship

As an example for the deployment of the FF protocol into a conventional marine measurement/control system based on the 4-20 mA classical analogue standard, the research in [18] simulated the alternative of utilizing FF pressure transmitters for the purpose of fluid level measurement in tank level measurement system on a bulk carrier commercial ship. The research analysis included the simulation of only one non-intrinsically safe model and five intrinsically models (Entity Model, FISCO, FNICO, HPT and DART [18]). Each of these models includes a single or multiple sub-models according to the available options for adopting a specific model such as short circuit protection and power rating of the available segment power supply.

The pressure transmitters used at these models are the Rosemount 5400 non-contact radar transmitters to replace the classical 4-20 mA immersed pressure transmitters at the top side water ballast tanks, and the FF Rosemount 3051 pressure transmitters to replace the horizontally mounted 4-20 mA pressure transmitters at the double bottom tanks. The simulation of these models was carried out through using the Emerson Segment Design Tool and the Pepperl+Fuchs Segment Checker [18]. Table 1.2 briefly describes the most important specifications of each model and its sub-models

Detailed schematics for the connection diagram at each of the segments as well as an illustration for the layout of the field devices and connection units on the ship for each of the sub-models, are both included in [18] (Table 1 and Figure 7 [18]).

Table 1.2 – Most important characteristics for the FF models (intrinsically safe and non-intrinsically safe). SC: with short circuit protection. DB: Double Bottom tanks. TS: Top Side tanks. SP: Segment Protectors. FB: Field Barriers. IS: intrinsically safe. E: entity model. Ic: connection unit current. Isc: short circuit current

Model	Description	Sub-Models
1. Non-Intrinsically Safe Model (Safe Area Application)	A non-intrinsically safe Foundation Fieldbus solution can be implemented with short-circuit protection or without short-circuit protection depending on the connection units used to connect field devices.	• NON-IS-DB • NON-IS-DBSC. • Maximum capacity of power supply: 500 mA. • "Ic" for connection unit without short-circuit protection: 4 mA. • "Ic "+ "Isc" for connection unit with short-circuit protection: (5 + 55) mA.
2. Intrinsically Safe Entity Model	• It takes into account the characteristics of the field bus cable (resistance, inductance and capacitance). • more restrictive ignition curves (inductive curves) will be adopted during ignition tests [30] (pp. 114–129) [18,34,35]	• IS-E-DB • IS-E-TS • Maximum capacity of power supply: 80 mA. • "Ic" for connection unit without short-circuit protection: 7 mA.

	• The maximum available power along the field bus is decreased with respect to the increased field bus cable length. • The Foundation Fieldbus entity model allows for 2–3 field devices per segment depending on the available power provided by the power supply. • Isolated power supply: MTL5995 [36] • Intrinsically safe barrier: MTL5053 [36]	
3. FISCO (Fieldbus Intrinsically Safe Concept) Model	• It allows for a larger number of field devices per segment than intrinsically safe entity model. • It neglects cable reactance when performing intrinsically safe calculations. • Experimental analysis proved that the value of cable reactance has no negative influence on ignition test results [37,38] • IIB gas group (Ethylene) Power Supply: 265 mA – 13.1 VDC • IIC gas group (Hydrogen) Power Supply: 120 mA – 12.4 VDC	• FISCO-IIB-DB • FISCO-IIC-DB • FISCO-IIB-DBSC • FISCO-IIB-TS • FISCO-IIC-TS • FISCO-IIB-TSSC • "Ic" for connection unit without short-circuit protection: 0 mA. • "Ic "+ "Isc" for connection unit with short-circuit protection: (5 + 55) mA.
4. FNICO (Fieldbus Non-Incendive Concept) Model	• The major difference between the FNICO and FISCO models is that the FNICO model adopts a lower safety factor than the FISCO model in intrinsic safety calculations [18,34,35,39,40]. • It is only applicable in Zone 2/Division 2 hazardous areas. • IIB gas group (Ethylene) Power Supply: 320 mA – 13.1 VDC • IIC gas group (Hydrogen) Power Supply: 180 mA – 12.4 VDC	• FNICO-IIB-DB • FNICO-IIC-DB • FNICO-IIB-DBSC • FNICO-IIC-DBSC • FNICO-IIB-TS • FNICO-IIC-TS • FNICO-IIB-TSSC • FNICO-IIC-TSSC • "Ic" for connection unit without short-circuit protection: 0 mA. • "Ic "+ "Isc" for connection unit with short-circuit protection: (5 + 55) mA.
5. HPTC (High-Power Trunk Concept) Model	• It does not impose any limitations on the maximum available power at the Fieldbus trunk cable. • It allows for longer cable lengths and a higher number of field devices per segment.	• HPTC-SP-DB • HPTC-FB-DB • HPTC-SP-TS • HPTC-FB-TS

	• It allows for an output voltage up to 30 VDC and a maximum current up to 500 mA. • Within an hazardous area, this unlimited energy will be distributed using energy-limiting wiring interfaces till it is delivered to the field device. • It does not require power supply conditioners particularly dedicated to the model. • Standard non-intrinsically safe lower price power supplies can be used in the HPTC network. • Energy-limiting wiring interfaces include field barriers and segment protectors with short-circuit protection as well as galvanically isolated outputs [30] (pp. 114–129) [18,34,35,41]. • HPTC allows for a maximum number of four field barriers. Each of these barriers allows for up to four field devices. Therefore, HPTC allows for up to 16 field devices per segment.	
6. DART (Dynamic Arc Recognition and Termination) Model	• The latest intrinsically safe fieldbus segment design system. • It limits the H1 bus energy only during the first 5–10 microseconds of spark formation, which leads to extinguishing the spark before it will become incendive [18,42,43]. • It allows only for dedicated power supplies with a maximum current of 360 mA.	DART-DB DART-TS

For the non-intrinsically safe model, entity model, FISCO, FNICO and DART, voltage drop at any field device in the segment can be calculated by equation (1.40) [18].

$$V_d = V_{supply} - V_{H1} - V_c - V_{spur} \tag{1.40}$$

V_d : Voltage drop at the field device
V_{H1}: The voltage drop on the H1 bus main trunk cable from the power supply to the device
V_c : The voltage drop on the connection unit to which the field device spur is connected.
V_{spur}: The voltage drop on the spur cable. It is dependent of spur length and field device current connected to the spur.

For the non-intrinsically safe model, entity model, FISCO, FNICO, DART and HPTC (only when segment protectors are used) models, the total current consumption in a FF segment (I_{seg}) is the sum of current consumed by the host (I_{host}) and the current consumed by the H1 bus (I_{H1}) as indicated in equation (1.41). The segment power supply should be able to withstand the sum of both currents. The maximum capacity of the segment power supply is dependent on the FF model adopted by the segment [18].

$$I_{seg} = I_{host} + I_{H1} \tag{1.41}$$

$$I_{H1} = \begin{cases} I_d & \text{Field devices are connected directly to the H1 bus} \\ I_d + I_c & \text{Field devices are connected to the H1 bus through connection units without short circuit protection} \\ I_d + I_c + I_{sc} & \text{Field devices are connected to the H1 bus through connection units with short circuit protection} \end{cases} \tag{1.42}$$

I_d : Total current consumed by field devices connected to the FF segment
I_c: Total current consumed by the connection units.
I_{sc}: The short circuit protection current, in case the field devices were connected to connection units with short circuit protection. the short-circuit current (I_{sc}) is calculated only once (near the segment terminator) at the last connection unit with short-circuit protection connected to the bus.

In HPTC, segment protectors maintain constant voltage at a specific field device connected to a specific segment protector regardless of the voltage drop on the spur, while field barriers maintain constant output voltage all along the segment at the output port dedicated to a specific field device regardless of the total voltage drop on the H1 bus main trunk cable. Segment protectors are used with Zone2/Div2 applications; however, field barriers are used with Zone1/Div2 applications [18]. Therefore, the voltage available at field barrier output terminals connected for field devices is less than the voltage available at segment protector output terminals for field devices. Equations (1.43) to (1.46) characterize the terminal voltage at the field devices connected to field barriers and segment protectors

$$V_{dHPkn} = V_{oHPkn} - V_{sHPkn} \tag{1.43}$$

$$V_{oHPkn} = V_{iHPk} - K_{vHPkn} \tag{1.44}$$

$$V_{iHPk} = V_{supply} - \sum_{j=1}^{k} V_{H1j} \tag{1,45}$$

$k \in \{1,2,\ldots,K\}$ and $n \in \{1,2,\ldots,N\}$

$$K_{vHPkn} = \begin{cases} f\,(I_{dHPkn}, V_{sHPkn}) \text{ For Segment Protectors} \\ f\,(I_{dHPkn}, \sum_{j=1}^{k} V_{H1j}) \text{ For Field Barriers} \end{cases} \qquad (1.46)$$

K: Total number of connection units (field barriers or segment protectors), k = 1:K
N: Number of output ports for field devices at each of the connection units k, n = 1:N
V_{dHPkn} : The voltage level at a field device (n) connected to the connection unit (k).
V_{oHPkn} : The output voltage form the connection unit at the port connected to the device.
V_{sHPkn} : The voltage drop on the spur to which the device is connected.
V_{iHPk} : The input voltage to the (k) connection unit.
K_{vHPkn} : The coefficient by which the input voltage (V_{iHPk}) is reduced.
I_{dHPkn} : The current of the field device (n) connected to connection unit (k)

For segment protectors in HPTC, when increasing the spur length to which the field device is connected, the segment protector will increase the voltage at the output terminals to compensate the increased voltage drop on the spur. The output voltage of the segment protector is decreased from the segment protector input voltage by a reduction coefficient, which is a function of the current consumed by the field device and the voltage drop on the spur. The value of the reduction coefficient for a specific field device will decrease when increasing the spur length [18].

For field barriers HPTC, the value of the reduction coefficient will be a function of the field device current and the sum of the voltage drops on the H1 bus main trunk cable from the power supply to the field barrier to which the field device is connected.
The current consumed by each field barrier (I_{FB}) in HPTC segment, is dependent of the following variants (Equation 1.47):

1. The total current of field devices connected to the field barrier (I_{dT}).
2. The H1 bus main trunk overall cable length (L_T).
3. Number of field barriers included in the segment (N_{FB}) and current consumed by each of them (I_{dTS}).
4. Length of H1 bus main trunk cable sections between field barriers (L_{FB}).

$$I_{FB} = f\,(I_{dT},\ I_{dTS}, N_{FB},\ L_{FB},\ L_T) \qquad (1.47)$$

Simple HPTC segments (Figure 1.14) were constructed using Emerson Segment Design Tool to derive the relation between the first two variants (I_{dT} and L_T) and the current consumed by the field barrier (I_{FB}). Four of these segments are dedicated to Rosemount 3051 transmitters (Figure 1.14-a), while the other four segments are dedicated to Rosemount 5400 transmitters (Figure 1.14-b). In each of these segments, the current consumed by field barriers was calculated with respect to the change in the distance (A) between the field barrier and the power supply from 10 m to 1895 m, with increments of 10 m. These calculations were carried out when one, two, three or four transmitters are connected to the field barrier. Curve fitting tool in MATLAB was used to derive the fourth degree polynomial relation between I_{dT} and L_T in equation (1.48). Table 1.3 identifies the values of coefficients k_1, k_2, k_3, k_4 and k_5 for each of the models in figure 1.14. Figures 1.15

and 1.16 demonstrate the curves between I_{dT} and L_T (for each of the models in figure 1.14) obtained through plotting the simulation results at the Emerson segment design tool, in addition to the verification curves obtained through plotting the results of calculating I_{dT} with the knowledge of L_T using equation (1.48) [18].

$$I_{FB} = k_1 L_T^4 + k_2 L_T^3 + k_3 L_T^2 + k_4 L_T + k_5 \tag{1.48}$$

Table 1.3 - Table indicating values of the coefficients for the polynomial equation (1.48) defining the relation between the current consumed by the field barrier and H1 trunk cable length in each of the models illustrated in Figure 6a,b. Coefficients k1 in mA/m^4, k2 in mA/m^3, k3 in mA/m^2, k4 in mA/m and k5 in mA.

Model	Coefficients	Model	Coefficients
One Transmitter Rosemount 3051 I_{dT} = 18 mA	$k_1 = 4.739 \times 10^{-15}$ k_2=-2.006 $\times 10^{-11}$ k_3 =1.928 $\times 10^{-7}$ k_4 =-0.0005017 k_5 = 84.28	One Transmitter Rosemount 5400 I_{dT} = 21 mA	$k_1 = 1.537 \times 10^{-15}$ k_2=-1.202 $\times 10^{-11}$ k_3 =2.368 $\times 10^{-7}$ k_4 =-0.0004866 k_5 = 86.4
Two Transmitters Rosemount 3051 I_{dT} = 36 mA	$k_1 = 8.651 \times 10^{-15}$ k_2=-1.425 $\times 10^{-11}$ k_3 =4.713 $\times 10^{-7}$ k_4 =0.0004212 k_5 = 94.51	Two Transmitters Rosemount 5400 I_{dT} = 42 mA	$k_1 = 1.503 \times 10^{-14}$ k_2=-7.597 $\times 10^{-13}$ k_3 =1.045 $\times 10^{-6}$ k_4 =-0.002513 k_5 = 97.99
Three Transmitter Rosemount 3051 I_{dT} = 54 mA	$k_1 = 2.741 \times 10^{-14}$ k_2=2.596 $\times 10^{-11}$ k_3 =8.163 $\times 10^{-7}$ k_4 =0.001693 k_5 = 105.9	Three Transmitters Rosemount 5400 I_{dT} = 63 mA	$k_1 = 7.238 \times 10^{-14}$ k_2=-2.006 $\times 10^{-11}$ k_3 =1.928 $\times 10^{-7}$ k_4 =-0.0005017 k_5 = 111.345
Four Transmitter Rosemount 3051 I_{dT} = 72 mA	$k_1 = 1.723 \times 10^{-13}$ k_2=-1.098 $\times 10^{-10}$ k_3 =1.282 $\times 10^{-6}$ k_4 =0.00359 k_5 = 115.7	Four Transmitters Rosemount 5400 I_{dT} = 84 mA	$k_1 = 5.108 \times 10^{-13}$ k_2=-6.964 $\times 10^{-10}$ k_3 =2.04 $\times 10^{-6}$ k_4 =-0.004815 k_5 = 122.4

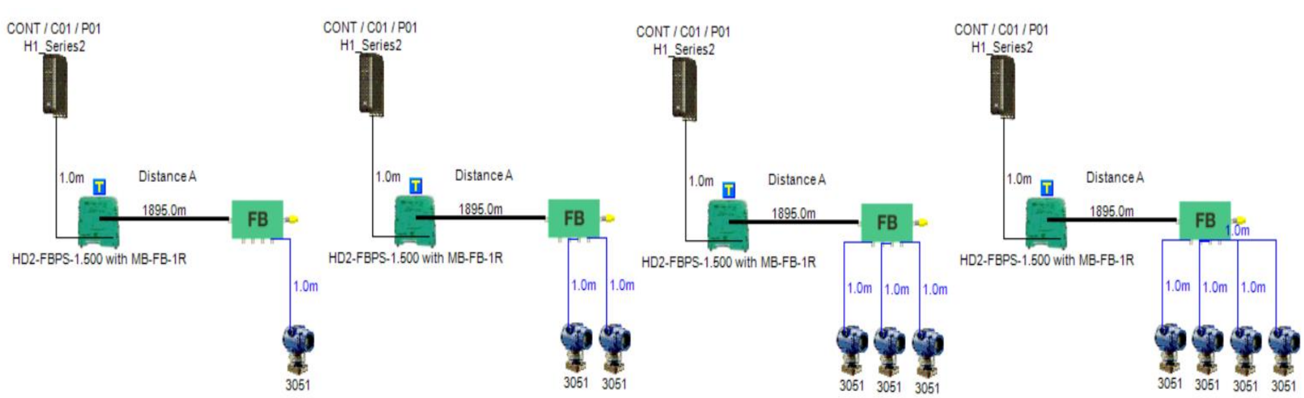

(a)

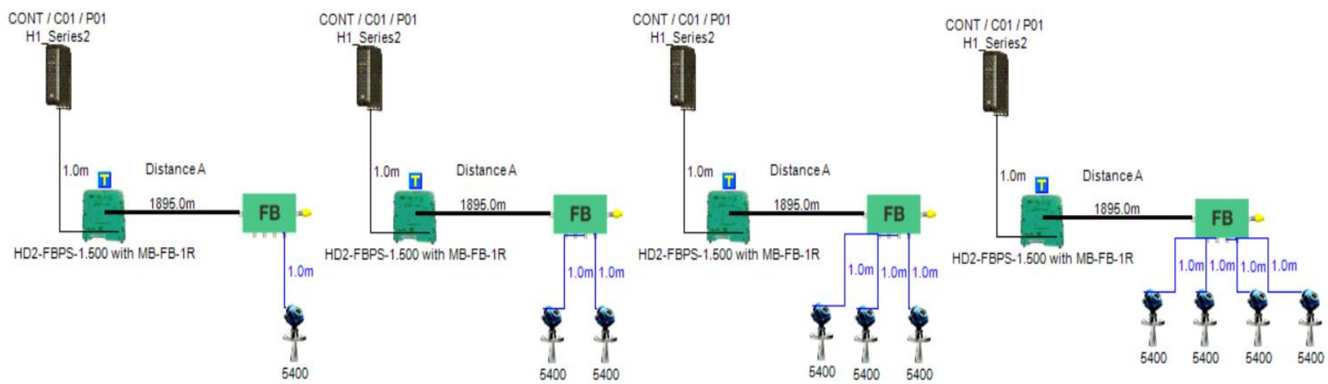

(b)

Figure 1.14 - Test segments (a and b) dedicated to deriving the relation between main FF trunk cable length and current consumed by field barriers. (a) Test segments using Rosemount 3051 Pressure Transmitters; (b) Test segments using Rosemount 5400 Radar Transmitters.

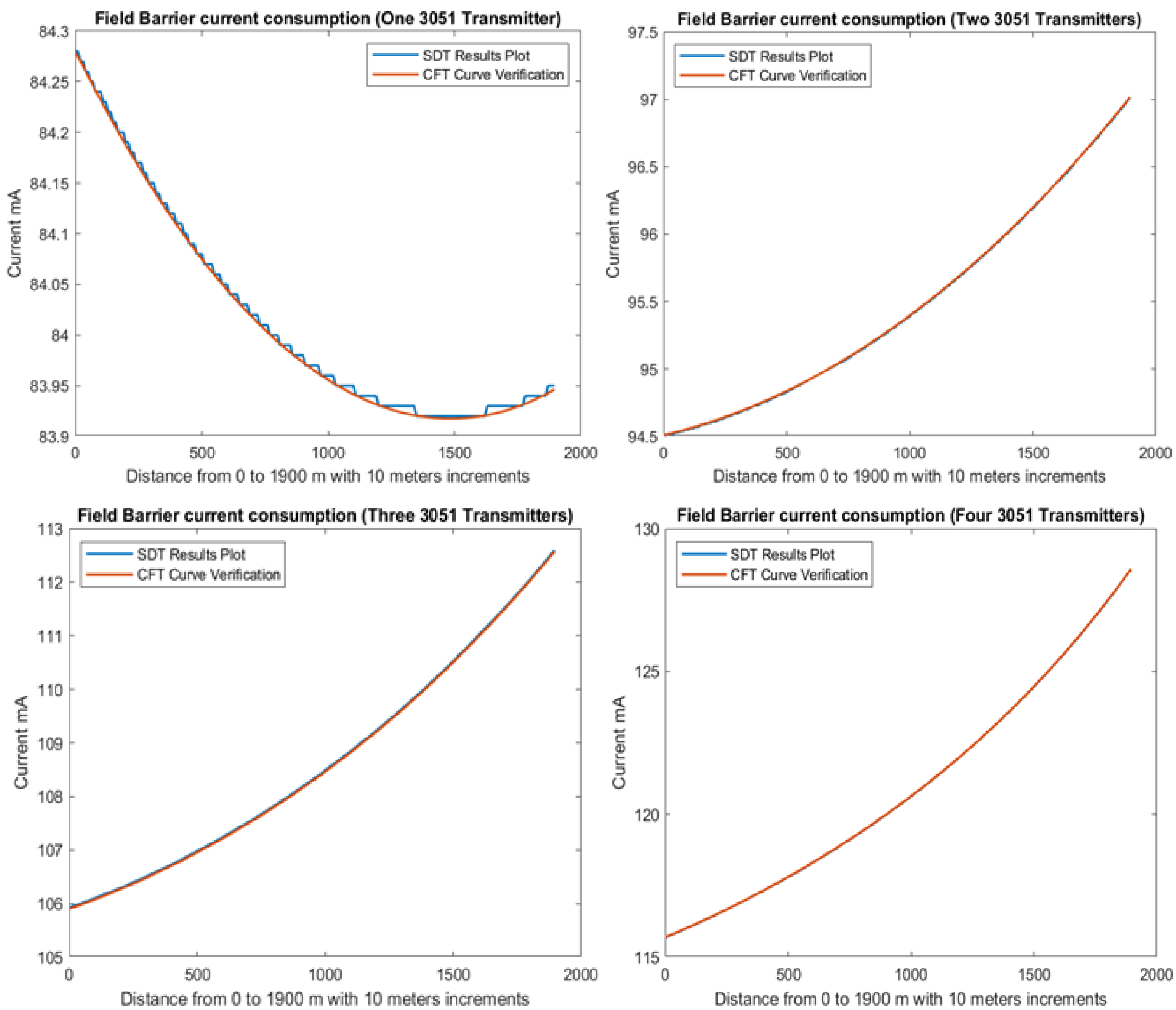

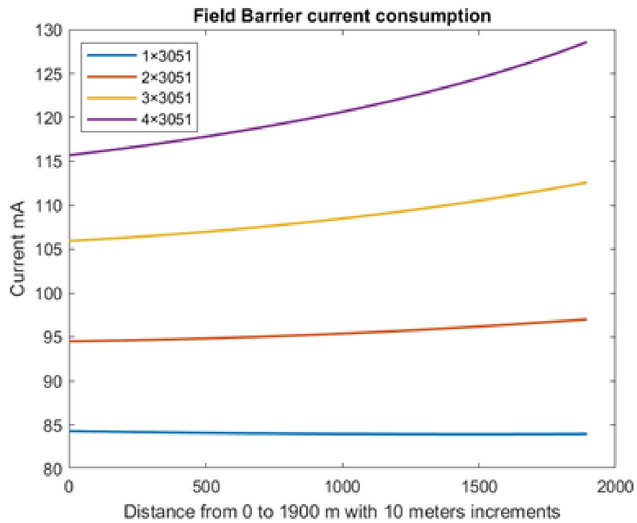

Figure 1.15 - Illustration of current consumed by field barrier with respect to FF H1 trunk cable length when for four models in which one, two, three or four 3051 transmitters were connected to the field barriers in the models in Figure 1.14-a.

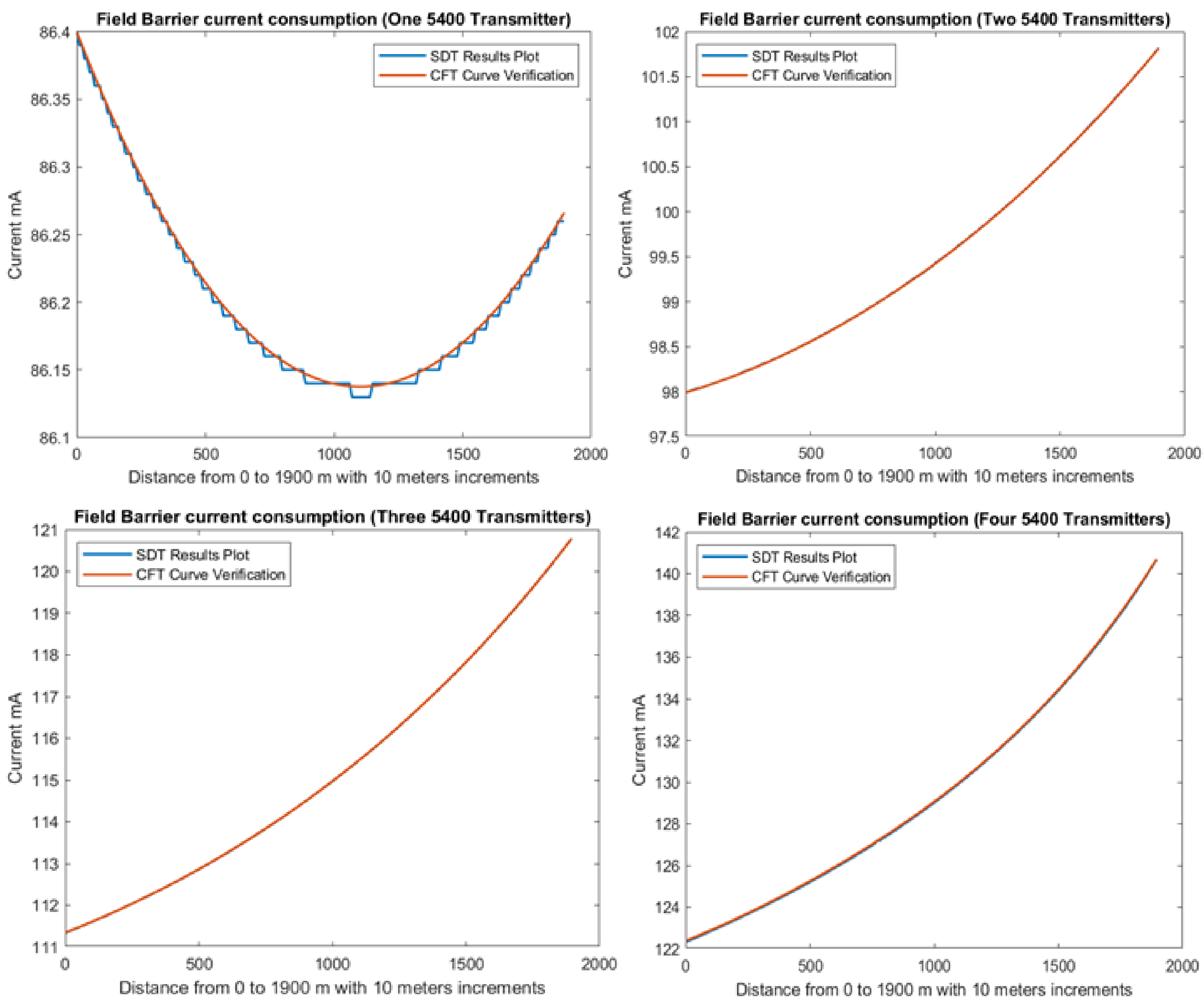

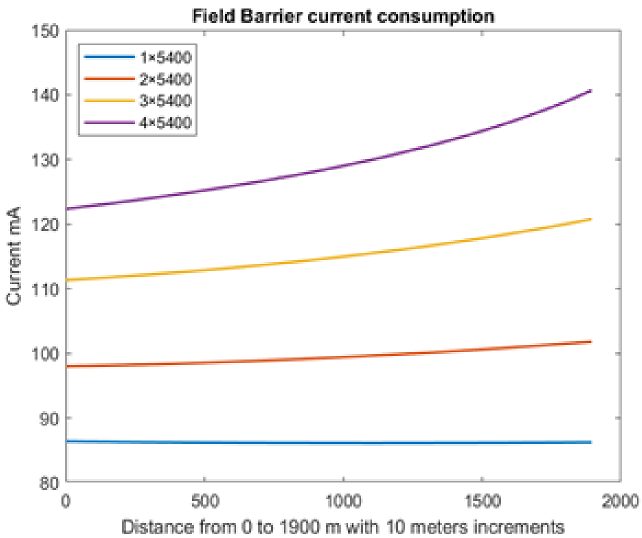

Figure 1.16- Illustration of current consumed by field barrier with respect to FF H1 trunk cable length when for four models in which one, two, three or four 5400 transmitters were connected to the field barriers in the models in Figure 1.14-b. (Last plot for both 3051 and 5400 transmitters.)

Additionally, the research in [18] has rendered a comparative analysis for:

1- Total required number of segments to implement a FF solution for each sub-model (Figure 1.17)
2- Voltage level at the furthest field device in each of the simulated segments (Figure 1.18).
3- Overall lengths for each of the simulated segments (Figure 1.19).
4- Percentage of the overall lengths for each of the simulated segments to the maximum allowable segment length (1900 m) (Figure 1.20).

The most important conclusions derived from this analysis can be summarized as follows:

1- For FF intrinsically safe models, the entity model requires the highest number of segments.
2- Using FF connection units with short-circuit protection imposes an additional current that the segment power supply should be able to withstand in case of short-circuit occurrence.
3- Short-circuit current in FF segments with short-circuit protection units is calculated only once for the last connection unit in the segment.
4- Maximum allowable spur length in the segment is dependent on the number of field devices in the segment for non-intrinsically safe, HPTC and DART models.
5- Maximum allowable spur length in the segment is independent of the number of field devices in the segment for entity, FISCO and FNICO models.
6- Applying short-circuit protection reduces the maximum number of allowable field devices per segment, as the power supply should be able to withstand the short-circuit current in case it takes place. Short-circuit current is calculated only once for the last connection unit at the field bus.
7- For similar segments (sharing the same layout and connection diagram), current flow in the H1 bus cable as well as voltage drop on the same H1 bus cable, where the HPTC model (with field barriers) is adopted, is higher than the current flow and voltage drop in the H1 bus cable of the same length where other FF models will be adopted. This can be attributed to the non-linear (polynomial) characteristics of current consumed by field barriers in the HPTC model with respect to bus cable length. The current flowing in the H1 bus trunk

cable where field barriers are used will be more than the current flowing in H1 bus trunk cable where regular connection units are used. Consequently, this results in higher voltage drops on H1 bus cable sections in comparison with all other FF models for similar segments in which the value of the current flowing in the H1 bus cable is independent of the H1 bus cable length and only dependent on total number of field devices connected to the bus and their currents. Similarly, and due to the same explanation, the highest total current consumption for a segment was observed at the HPTC model.

8- The non-linear behavior of both of current consumption and output voltage in HPTC connection units (segment protectors and field barriers) is a clear demonstration of the technique adopted by the HPTC model to distribute the overall energy consumed in the segment on each of the connection units included in the segment. This demonstration is particularly depicted in the dependence of the current consumed by a specific field barrier on the current consumed by other field barriers in the segment, whether they preceded or followed that specific field barrier. Moreover, the current consumed by that specific field barrier is also dependent on the lengths of the H1 bus main trunk cable sections before the field barrier as well as after the field barrier.

9- The research has presented a more precise specification for the maximum allowable spur length for each of the FF models as illustrated in Table 1.4.

Table 1.4 - Illustration of maximum allowable spur lengths in different FF models according to simulation results obtained from Emerson Segment Design Tool.

FF Model	Maximum Allowable Spur Length
Non-intrinsically safe	(1–10 field devices) (120 m) (11–12 field devices) (90 m) (Field devices > 12) (60 m)
HPTC	(1–11 field devices) (120 m) (12–13 field devices) (90 m) (Field devices > 13) (60 m)
DART	(1–10 field devices) (120 m) (11 devices) (90 m) (Field devices ≥ 13) (60 m)
Entity	120 m
FISCO	60 m
FNICO	60 m

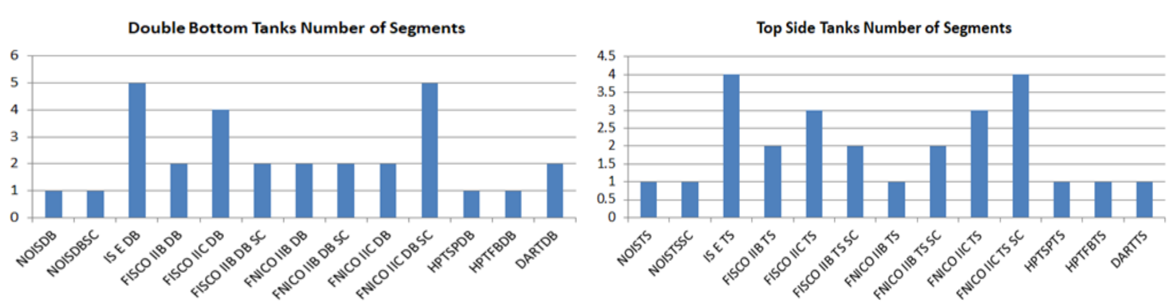

Figure 1.17 – Total number of segments for each of the simulated FF models at top side and double bottom tanks

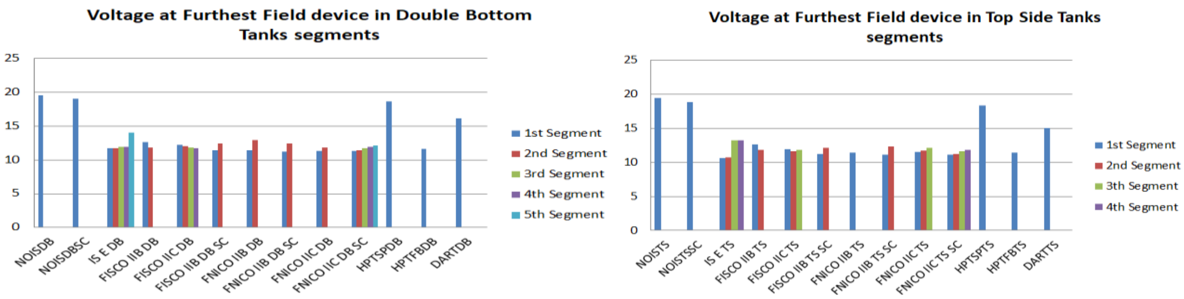

Figure 1.18 – Voltage at the furthest field device for each of the simulated FF models at top side and double bottom tanks

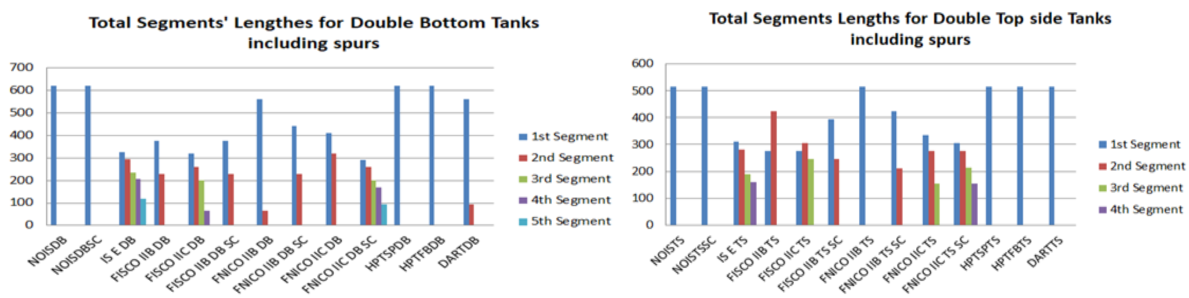

Figure 1.19 – Total segments' lengths for each of the simulated FF models at top side and double bottom tanks

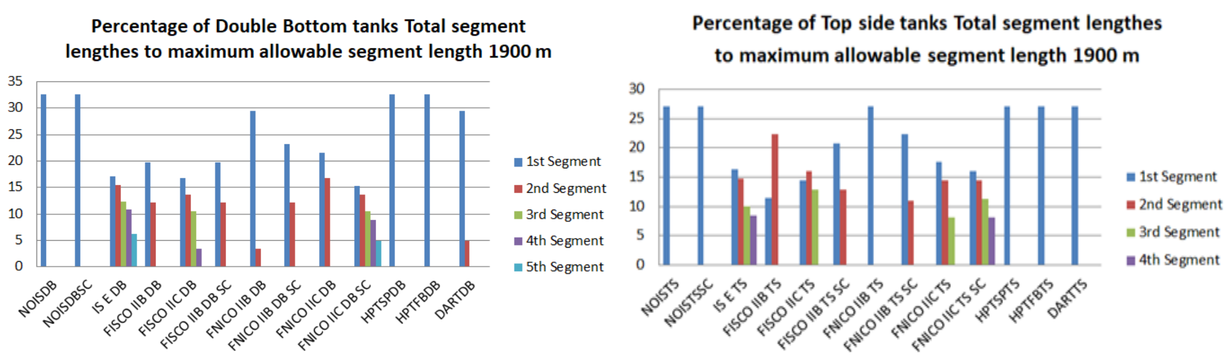

Figure 1.20 – Percentage of total segments' lengths to maximum allowable segment lengths for each of the simulated FF models at top side and double bottom tanks

2. Wireless HART protocol in Maritime Engineering

Wireless HART was firstly presented at HART 7.1 as an extension for HART protocol. It was approved as a standard which specifies a wireless communication network by the International Electrotechnical Commission (IEC 62591) in 2010. Wireless HART network is a mesh network in which various types of devices are included such as network managers, network security devices, access points, adapters, routers and handheld devices. As an extension for wired HART protocol, wireless HART shares the same application layer with wired HART where three types of HART commands are used (Universal commands, common practice commands and device specific commands) [18,44-47].

Wireless HART relies on time division multiple access (TDMA) for the purpose of scheduling communication with field devices. Based on TDMA, communication tasks are performed during 10 ms time slots. A single time slot can be dedicated to communication with a single device or multiple devices. If a time slot is dedicated to communication with multiple field devices, it will be called a shared time slot. Synchronization between devices in a wireless HART network is required so that a successful TDMA can be maintained. Synchronization is maintained by using time synchronization mesh protocol (TSMP). In TSMP, transmission is accomplished when a single packet is transmitted, and an acknowledgement is generated that this packet was completely received without any errors. TSMP performs the role of transport layer, network layer and data link layer [18,45,48,49,50].

Direct sequence spread spectrum (DSSS) [18,45,48,49,51,52] is used to reduce the overall signal interference by increasing the transmitted signal bandwidth. Only using DSSS will provide resistivity to the signal interference to a particular limit; however, using both the frequency-hopping spread spectrum (FHSS) [18,52] and DSSS leads to better interference rejection (FHSS) and higher coding gain (DSSS) [18,50]. FHSS depends on changing the frequency of the carrier signal with respect to time. The order of changing the carrier frequency should be known by both of the transmitter and the receiver [18,45,48,49,51,52].

In a wireless HART network, the data link sublayer is represented by the MAC protocol. The MAC protocol provides the mechanism that determines which user or device is allowed to access the medium when there is competition for it [18,48,49,50,54]. The MAC function [18,55] is called by the device when the device is about to transmit a message. The MAC function reads the device tables in order to check if the device is allowed to start transmission within the current time slot or not. The wireless HART network adopts TDMA for dedicated time slots while CSMA/CA (carrier sense multiple access with collision avoidance) [18,55,56] is adopted for shared time slots. CSMA/CA provides the mechanism of reducing the probability of collision between transmitted data using the exponential back-off algorithm [18,55,56].

2.1 RFI and EMI in Maritime Engineering

The RF waves propagation can be negatively influenced by various sources of RFI and EMI. Therefore, such sources should be considered carefully upon any planned deployment of wireless technologies such as wireless HART in shipboard systems. Brief description is rendered at the following points briefly for the expected sources of RFI and EMI on commercial ships.

- The INMARSAT system at the L-band (1-2 GHz), the C-band (4-8 GHz) and Ku-band (12-18 GHz) frequencies [44,57] in addition to the S-band radars operating at the (3 GHz) frequency band [58], are marine navigational equipment with operating frequency bands located in a close proximity to the ISM frequency band of 2.4 GHz. The possible negative influence induced by such a proximity in the frequency, can be manifested in decreased levels of SNIR (Signal-to-Interference-plus-Noise Ratio) and degraded throughputs. In [44,59], the research has verified such a negative effect, analyzing a similar proximity at the operating frequency band between the S-Radar and the LTE macro and small cells uplinks in the 3.5 GHz band.

- According to [44,60], Low levels of SINR might also be resulted from narrowband RFI in 802.11 networks. Therefore, a wireless HART network might similarly endure the same negative influence, as it shares various features with the 802.11 standards. There are three important types of RFI that should be avoided; narrowband RFI [44,61], all-band RFI and RFI due to adverse weather conditions (strongly present in the marine environment).

- The possible influence of electromagnetic interference (EMI), should be also taken into account when discussing the different possibilities of implementing wireless HART networks in marine engineering applications. According to [44,64], high EMI levels were observed at the frequency range of 1880-1890 MHz, which is a very close frequency range to the operational frequency of wireless HART protocol of 2.4 GHz.

- Additionally, the authors in [44,65] have highlighted the increased effect of EMI on automation systems adopting different protocols for wired and wireless instrumentation. Therefore, the research in [44,65] has recommended using similar wired and wireless protocols at the same automation field. For example, if the majority of field devices mounted at the field were HART transducers, wireless HART should be the protocol for possible planned usage of wireless transmitters in order to avoid high levels of EMI.

2.2 Received Signal Strength Indicator (RSSI)

Robust communication in a wireless HART network can be ensured at RSSI range of (-60 dB to -30 dB). Through the analysis of the obtained RSSI levels in a small wireless HART network (consisting of a wireless HART pressure transmitter, a wireless HART temperature transmitter and a wireless HART binary switch), it turned out that more uniform distances between the wireless HART field devices lead to better fairly distributed RSSI levels at each of these field devices. On the other hand, less uniform spacings between the field devices lead to very high RSSI levels at specific devices located in proximity to each other and extremely low RSSI levels at the distant field devices (Figure 2.1) [44,66,67]. Such a conclusion can be validated on commercial ships if wireless HART transmitters are supposed to be used at sea water ballast tanks where the sensors mounting locations are almost uniformly distributed [1,44].

According to [44,62,63], decreased RSSI levels in the 2.4 GHz frequency band can be caused by high levels of heavy rain, relative humidity and high temperatures. As it shares the same ISM frequency band, the wireless HART network can possibly suffer from such a consequence, particularly if the wireless HART network was dedicated to a maritime engineering application where heavy rain, high levels of relative humidity and high temperatures are common extreme features at the marine environment [44].

HART Tag	Node state	Active neighbors	Neighbors	Service denied	Reliability	Missed updates	Path stability	RSSI	Joins	Join Time
Przetwornik Temperatury	●	bramka Przetwornik cisnienia	2	●	99.9 %	2	100.0 %	-5 db	1	06/15/22 15:16:02
Przetwornik binarny	●	bramka Przetwornik cisnienia	2	●	100.0 %	0	100.0 %	-55 db	1	06/15/22 14:46:39
Przetwornik cisnienia	●	bramka Przetwornik Temperatury Przetwornik binarny	3	●	99.8 %	3	100.0 %	-5 db	1	06/15/22 14:47:33

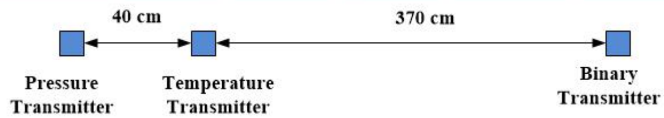

HART Tag	Node state	Active neighbors	Neighbors	Service denied	Reliability	Missed updates	Path stability	RSSI	Joins	Join Time
Przetwornik Temperatury	●	bramka Przetwornik cisnienia	2	●	99.9 %	2	100.0 %	-23 db	1	06/15/22 15:16:02
Przetwornik binarny	●	bramka Przetwornik cisnienia	2	●	100.0 %	0	100.0 %	-46 db	1	06/15/22 14:46:39
Przetwornik cisnienia	●	bramka Przetwornik Temperatury Przetwornik binarny	3	●	99.9 %	3	100.0 %	-23 db	1	06/15/22 14:47:33

HART Tag	Node state	Active neighbors	Neighbors	Service denied	Reliability	Missed updates	Path stability	RSSI	Joins	Join Time
Przetwornik Temperatury	●	bramka Przetwornik cisnienia	2	●	99.9 %	2	100.0 %	-41 db	1	06/15/22 15:16:02
Przetwornik binarny	●	bramka Przetwornik cisnienia	2	●	100.0 %	0	100.0 %	-48 db	1	06/15/22 14:46:39
Przetwornik cisnienia	●	bramka Przetwornik Temperatury Przetwornik binarny	3	●	99.9 %	5	100.0 %	-41 db	1	06/15/22 14:47:33

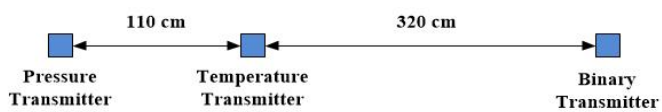

HART Tag	Node state	Active neighbors	Neighbors	Service denied	Reliability	Missed updates	Path stability	RSSI	Joins	Join Time
Przetwornik Temperatury		bramka Przetwornik binarny	2		99.4 %	42	100.0 %	-45 db	1	06/14/22 11:12:26
Przetwornik binarny		bramka Przetwornik Temperatury Przetwornik cisnienia	3		100.0 %	1	100.0 %	-45 db	1	06/14/22 11:12:11
Przetwornik cisnienia		bramka Przetwornik binarny	2		99.5 %	35	100.0 %	-45 db	1	06/14/22 11:14:11

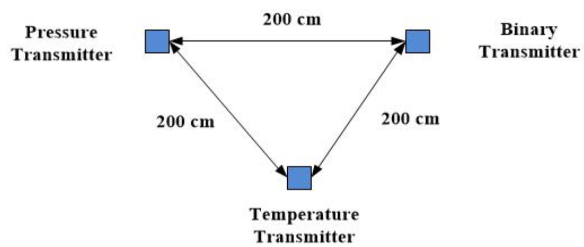

Figure 2.1 – Different cases of spacing between field devices and their correspondent effect on RSSI levels. (Przetwornik Temperatury), (Przetwornik binarny) and (Przetwornik cisnienia) are the Polish translation for the English terms; (Temperature Transducer), (Binary Transducer) and (Pressure Transducer), respectively.

2.3 Decreased Power Supply Levels (Gateway and Field Devices)

In maritime engineering facilities such as commercial ships, power failures or instability of generation units are more common failures than land based engineering applications. Wireless gateway is the only element in wireless HART network supplied by wired power source other than field devices which are powered by 7.2 VDC batteries. Accordingly, the DC voltage range in which both wireless HART gateway and the field devices (Figure 2.2) will still be properly functional (even if it was supplied with a voltage level less than its rated voltage) is an important factor when analyzing implementation of wireless HART protocol on commercial ships [44]. The results of testing the effects of the possible power supply reduction at both of the gateway and the field devices can be summarized in Table 2.1 according to [44].

Table 2.1- Status of field devices and the gateway at different levels of decreased supply voltage through the battery (for the field devices) and through the mains (for the gateway)

Equipment	Supply Voltage Range	Status
Emerson 1420 Wireless HART Gateway	12.5 – 24 VDC	Operational
Emerson 1420 Wireless HART Gateway	Less than 12.5 VDC	Not Operational
Field device	Less than 3 VDC	Not Operational
Field device	3 – 5.5 VDC	Operational • Only tertiary and quaternary variables are detected by the gateway (terminal voltage and device temperature). • Error indicated as the primary and secondary variables are not detected (set point and measured quantity)

Field device	5.5 – 7.2 VDC	Operational • All variables are detected by the gateway

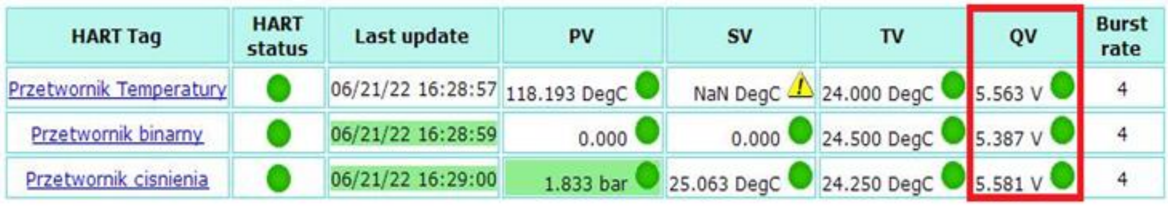

HART Tag	HART status	Last update	PV	SV	TV	QV	Burst rate
Przetwornik Temperatury		06/21/22 16:28:57	118.193 DegC	NaN DegC	24.000 DegC	5.563 V	4
Przetwornik binarny		06/21/22 16:28:59	0.000	0.000	24.500 DegC	5.387 V	4
Przetwornik cisnienia		06/21/22 16:29:00	1.833 bar	25.063 DegC	24.250 DegC	5.581 V	4

Figure 2.2 – Successful HART communication with decreased supply voltage of 12.5 VDC at the gateway and 5.5 VDC at field devices.

2.4 Wireless HART Protocol on Various Types of Commercial Ships

Container ships, tankers and bulk carriers are three among the most popular types of commercial ships. The possibility of implementing the wireless HART protocol on each of these three types was thoroughly discussed in [44]. The expected negative influence on the RF waves propagation (reduced RSSI levels) by the increased density of metallic objects and infrastructural obstacles on ships, was the basic criteria that was taken into account analyzing such an issue. Table (2.2) illustrates a summary for the comparison between container ships, tankers and bulk carriers from such a perspective.

Table 2.2- Illustration for the various possibilities of wireless technology deployment as a medium for data transaction at shipboard systems on different types of most popular commercial ships

No.	Ship Type	Specifications
1	Container	• Too many metallic obstructions of multi-horizontal as wells as multi-vertical levels (of height up to 20 meters) loaded containers. • Harsh loading/discharging operational conditions (lashing and stowing). • High possibility of damageing any wireless devices mounted on the main deck due to the excessive density of metallic objects. • Using wireless HART transmitters is recommended only in engine room. • Cargo cranes and shore cranes are major obstacles for the RF waves propagation .
2	Tanker	• Very low density of infrastructural metallic obstructions which are limited to piping and pumping equipment at a maximum height of 4-5 meters • Easy to mount any wireless HART transmitter on deck. • Smoother loading/discharging operations than both container and bulk carrier ships, which leads to higher effective range of Wireless HART equipment. • Using wireless HART protocol can be on deck or inside the engine room.
3	Bulk Carrier	• More metallic infrastructural obstructions than the tanker ships and less metallic infrastructural obstructions than the container ships. • Operational conditions smoother than container ships and more difficult than tanker ships.

		• Wireless HART field devices are possible to be mounted on deck, however the process of mounting and selecting the field device exact position, is more difficult than the tanker ships. • Probability of possible damage for the on deck field devices is higher than the tanker ships and lower than the container ships. • Cargo cranes and shore cranes, cargo holds hatch covers are major obstacles for the RF waves propagation

2.5 Wireless HART Mathematical Model for Network Reinforcement

According to the Emerson Implementation guide of wireless HART network, four important rules were introduced to ensure enhanced levels of reliability and stability at the wireless HART network. These four rules are the rule of minimum five, the rule of minimum three, the rule of percentage and the rule of maximum distance. The necessary description for these rules was rendered in [44,68]. These four rules are applied after the segmentation process for each single gateway. The segmentation process is the division of the field at which the wireless HART field devices will be installed according to the capacity of the gateway. There are two main goals for the application of the previously mentioned rules.

- The first goal: ensuring as many field devices as possible located inside the effective range of the gateway.
- The second goal: ensuring as many neighbor field devices as possible for each field device.

The Emerson Wireless HART network implementation guide has introduced such rules [44,68] in the form of recommendations for the designers without providing the precise specific technique to apply such rules. On the other hand, the guide has assumed three specific values for the effective range of the field devices according to the expected density of the infrastructural obstacles inside the field. Such an assumption did not clearly distinguish between the effective range of the gateway and the effective range of the field device. Naturally, the gateway will definitely have a wider effective range than the field devices due to power supply considerations, as the gateway is directly supplied through the mains and the field devices are powered through batteries, which will, naturally, have power rating levels less than the power rating of a power supply fed by the mains. Moreover, the ageing factor plays an important role at the identification process of the field device effective range as it is expected for the field device effective range to decline at longer service times of its battery.

Taking such notions into account, it would be very valuable to consider the idea of implementing a mathematical model, the purpose of which is to reinforce the wireless HART network through identifying precisely the specific steps that network designer should take on in order to achieve both of the aforementioned goals.

The mathematical model will be based on the following hypotheses:

1. The effective range of the field device is much more less than the effective range of the gateway.
2. The wireless HART network is not at the designing phase. It is already implemented and the field devices as well as the gateway are already mounted.

3. The wireless HART network includes only one gateway mounted almost at the center of the field at which the field devices are installed.

2.5.1 Description and derivation of the mathematical model

1. The field will be divided into four sections, the northeastern section, the northwestern section, the southeastern section and the southwestern section.
2. The field devices including the gateway are indexed from 1 to n, where (1) refers to the gateway, while (n) refers to the furthest field device from the gateway.
3. The matrix $xy_{2\times \mathrm{n}}$ will be constructed to include the (x) and (y) Cartesian coordinates of each field device.
4. The matrix $\Delta xy_{4\times \mathrm{n}}$ will be constructed to include the maximum possible relocation distances for each field device in the directions of negative (x), positive (x), negative (y) and positive (y).
5. The matrix $d_{\mathrm{n}\times \mathrm{n}}$ is constructed to include the mutual distances between all the field devices in the network including the gateway.
6. The matrix $d_{\mathrm{n}\times \mathrm{n}}$ will be reduced to (C) matrix using the same technique used to reduce a square matrix (n×n) to a $C_{\mathrm{n}/2\times \mathrm{n}-1}$ matrix for even values of n, or to a $C_{\mathrm{n}-1/2\times \mathrm{n}}$ matrix for odd values of n (the technique was thoroughly explained in [15]).
7. Similarly to the C matrix, the matrices V and R will be constructed to indicate the in range and out of range field devices respectively. The $R_{\mathrm{i,j}}$ element will be (1) if $d_{\mathrm{i,j}} > r_{\mathrm{f}}$, otherwise $R_{\mathrm{i,j}} = 0$. The $V_{\mathrm{i,j}}$ element will be (1) if $d_{\mathrm{i,j}} < r_{\mathrm{f}}$, otherwise $V_{\mathrm{i,j}} = 0$.
8. The $L_j'(i)$ array is constructed for each field device (i), indicating the indices (j)s of the field devices out of range from the field device (i).
9. The mathematical model is based on the idea that increasing the number of field devices located inside the effective range of the gateway, is a goal of higher priority than increasing the neighbor devices for each field device.
10. Accordingly, the mathematical model will start with indicating the array $L_j'(1)$ which includes the indices (j)s of the field devices located at positions out of the gateway effective range.
11. The array $L_j'(1)$ will consist of 4 sub-vectors $L_j'^{NE}(1)$, $L_j'^{NW}(1)$, $L_j'^{SE}(1)$, $L_j'^{SW}(1)$. Each of these vectors will include the indices (j)s correspondent to each of the four field divisions, the northeastern, the northwestern, the southeastern and the southwestern.
12. The vector $M_1'(1)$ will include the number of elements referring to the number of field devices out of the gateway effective range in each of the field four divisions, sorted from the division with the maximum number of field devices to the division with the minimum number of field devices out of the gateway effective range.
13. The first element of the vector $M_1'(1)$, will indicate the direction to which the gateway will be relocated based on its margins of mobility.
14. Similarly, the field devices located at the field division indicated by the first element of $M_1'(1)$ will be relocated to approach the gateway diagonally according to the $\Delta xy_{4\times \mathrm{n}}$ margins of mobility for each of them.
15. The vector $L_1'(1)$ will be recalculated to check if the number of field devices out of the gateway effective range has increased, decreased or remained the same. If it has decreased or remained the same, the relocation step of the gateway will be approved as its final position, otherwise, the gateway will be relocated with increments of h_x and h_y to the maximum point beyond which the number of field devices out of range from the gateway will start to increase.

16. After the relocation procedure) of the gateway and the field devices at the field quarter with the maximum number of out of range field devices (through moving them towards each other), the points of minimum x, minimum y, maximum x and maximum y will be indicated for the field devices at the relocated quarter.
17. Four straight lines are drawn, (x = minimum x) , (x = maximum x), (y = minimum y) and (y = maximum y). The four lines will form a rectangle. The length and the width of the rectangle will be divided on the diameter of the wireless repeater circle of range, which will indicate the number of repeaters that will be installed inside that rectangle (NRR method). If the distance between any of the installed repeaters and any of the field devices d_{rf} was less than d_{rf}^{min}, then that repeater will be omitted from the reinforcing rectangle.
18. The distance between the gateway and the nearest repeater at the first quarter will be calculated. If such a distance will turn out to be greater than the sum of the radius of the gateway range circle plus the radius of the repeater range circle, additional repeaters will be installed on the line connecting between the nearest repeater and the gateway, particularly at the points of intersection between that line and both circles of range for the repeater and the gateway.
19. The number of the needed repeaters to ensure reliable communication between the gateway and the group of field devices located at the first quarter, can be calculated by equations (2.38, 2.61, 2.84, 2.107). The divisions on r_{rp} at the equation is to have an adequate intersectional area between each two repeaters circle of range. If additional intersectional area will be required due to some infrastructural barriers, the division will be on an value less than r_{rp} such as $0.3\ r_{rp}$ or $0.5\ r_{rp}$.
20. The relocation of the gateway and the field devices of the first quarter (with maximum number of field devices outside the gateway effective range) is treated as the first round of wireless HART network reinforcement process.
21. The second round is dedicated to the relocation process of the group of field devices (with the 2nd maximum number of field devices outside the gateway effective range) located at the second field quarter. This group of field devices is represented by the second element of the array $M_1'(1)$ (Table 2.3).
22. Since that the gateway have already been relocated at the first round, it will not be possible to relocate it again at the next 2nd, 3rd or 4th rounds, which means that the relocation process at the rounds following to the first round will be applied only on the field devices.
23. In order to relocate the field devices efficiently at the second, the third and the fourth rounds, a decision making process will take place to identify the direction to which the field devices will be relocated (Tables 2.4, 2.5 and 2.6). For each of these groups of field devices, there are 3 possibilities for movement; either towards the gateway, or towards the first neighbor group of field devices or towards the second neighbor group of field devices. The determinants of such a decision making process are the matrices (d) and (V), which are being reconstructed all the time during the implementation of such a mathematical model along with the matrix R. The coordinates of the field devices at the second group will be modified by the movement towards the first group of field devices, then matrices (d) and (V) will be reconstructed. Similarly, the matrices (d) and (V) will be reconstructed when the coordinates of the field devices at the second group will be moved towards the second neighbor group of field devices once and also towards the gateway once. This procedure will be repeated at the third and fourth relocation rounds.
24. The values $\sum d_{2nd}$, $\sum d_{3rd}$ and $\sum d_{4th}$ will be identified as the minimum three values of three arrays containing the following four elements:

- The values of the average sum of all mutual distances between all the field devices (repeaters are not taken into account) directly after finishing the previous round of relocation $\sum d^1, \sum d^2$ and $\sum d^3$.
- The values of the average sum of all mutual distances between all the field devices (repeaters are not taken into account) after relocation of the field devices of the current group towards the gateway $\sum d_g^2, \sum d_g^3$ and $\sum d_g^4$.
- The values of the average sum of all mutual distances between all the field devices (repeaters are not taken into account) after relocation of the field devices of the current group towards the first group of neighbor devices $\sum d_1^2, \sum d_1^3$ and $\sum d_1^4$.
- The values of the average sum of all mutual distances between all the field devices (repeaters are not taken into account) after relocation of the field devices of the current group towards the second group of neighbor devices $\sum d_2^2, \sum d_2^3$ and $\sum d_2^4$.

25. The values $N_1^2(V), N_1^3(V)$ and $N_1^4(V)$ will be identified as the minimum three values of three arrays containing the following four elements:
    - The total number of ones at the V matrix referring to the total number of pairs of the out of range devices (repeaters are not taken into account) directly after finishing the previous round of relocation $N_1(V^1), N_1(V^2)$ and $N_1(V^3)$.
    - The total number of ones at the V matrix referring to the total number of pairs of the out of range devices (repeaters are not taken into account) after relocation of the field devices of the current group towards the gateway $N_1(V_g^2), N_1(V_g^3)$ and $N_1(V_g^4)$.
    - The total number of ones at the V matrix referring to the total number of pairs of the out of range devices(repeaters are not taken into account) after relocation of the field devices of the current group towards the first group of neighbor devices $N_1(V_{d1}^2), N_1(V_{d1}^3)$ and $N_1(V_{d1}^4)$.
    - The total number of ones at the V matrix referring to the total number of pairs of the out of range devices (repeaters are not taken into account) after relocation of the field devices of the current group towards the second group of neighbor devices $N_1(V_{d2}^2), N_1(V_{d2}^3)$ and $N_1(V_{d2}^4)$.

26. After finishing the four relocation rounds for the field devices outside the gateway effective range in the four groups located at the four field quarters, the following will be easily observed:
    - The increased number of field devices with intersectional area between their circles of effective range and the circle of the gateway effective range.
    - The increased number of neighbors for each field device due to the installed repeaters and the effective mechanism of relocation.
27. After finishing the four rounds of relocation of the field devices, the number of neighbors for each field device will be checked (the gateway will be excluded as a neighbor device). At this stage the added repeaters will be taken into account. The indices of the repeaters will start from (n+1) to (n+nr) where (nr) is the total number of the added repeaters after four rounds of devices relocation.
28. As the field device with the index (n) is the furthest field device from the gateway (field devices are indexed from (1) to (n) according to the proximity to the gateway), it will be the first device for which the number of neighbor devices will be checked.
29. The array $K_J''(n)$ will include the indices of the field devices located inside the effective range of the device (n). These indices will be sorted from the device with the minimum distance to the field device (n), to the device with the maximum distance to the field device (n). If the field device (n) has neighbor devices less than the minimum required number of neighbor devices

NB_{min}, it will be necessary to install additional repeaters. The number of the required additional repeaters can be obtained by equation (2.145). The first required additional repeater as a neighbor device will be located at the middle of the distance between the two points of the intersection between the straight line from the field device (n) to the out of range field device and the effective range circles of the device (n) and the out of range device, respectively (only if the distance between the two intersection points will be less the diameter of the repeater effective range circle), otherwise the repeater will be located closer to the field device (n). This procedure will be repeated till the field device (n) will have a number of neighbor devices equal to NB_{min}.

30. After indicating the positions of all the required repeaters for the field device (n). The same procedure will be repeated for the field devices (n-1) to (2).
31. After indicating the positions of the required repeaters for field devices from (n) to (2), the overall number of repeaters will increase from (nr) to (nr'). This overall number of repeaters includes the repeaters that were added to the network during the relocation process of the devices out of the gateway effective range in addition to the repeaters installed during the process of increasing the neighbor devices for each field device.
32. It would be worthy to stress on the fact that the first priority for this mathematical model is to increase the field devices located inside the effective range of the gateway directly by relocating the field devices, or indirectly through adding third party devices such as repeaters. The second priority of the mathematical model is to increase the neighbor devices for each field device.
33. Naturally, not all the added repeaters will be essential to increase the reliability level of the wireless HART network, that's why, there should be an optimization technique to rectify the overall number of the added repeaters to an optimal value.
34. The optimization matrix W is constructed to include the elements of $K_J''(i,p)$, which refers to the sorting index of the repeater p in the array $K_J''(i)$. In other words, $K_J''(i)$ is an array the includes the indices j of the devices which are located inside the effective range of the field device (i)(except the gateway) sorted from the device with the minimum distance to the device with the maximum distance to (i). These devices can be original field devices or the recently added repeaters. The element $K_J''(i,p)$ will indicate if the repeater p is the first or the second or the third etc., element inside the array $K_J''(i)$.
35. After the process of indicating the locations of the required repeaters to increase the neighbor devices for each field device, each of the arrays $K_J''(i)$ for all the field devices (i) from (2) to (n), should have a number of elements that doesn't exceed NB_{min}. However, that might not be the case if there were additional repeaters in the network which are not needed.
36. Accordingly, the matrix W will include the sorting indices of each repeater (p) from (1) to (nr') in all the arrays $K_J''(i)$ for all the field devices i from (2) to (n). From the matrix W, it will be easy to form arrays $W_{\mathrm{i},RP}$ for each repeater including the sorting indices of the repeater with respect to each device (i). $W'_{\mathrm{i},RP}$ will exclude the (0) valued elements from $W_{\mathrm{i},RP}$. $W''_{\mathrm{i},RP}$ is the resulting array from the intersection between $W'_{\mathrm{i},RP}$ and {1,2,..., NB_{min}}. If the intersection set is an empty set, this means that the corresponding repeater (RP) should be eliminated from the added repeaters list, as it is not required as an essential neighbor device of a sorting index from 1 to $NB_{min}$for any of the field devices in the network.

2.5.2 The Network Reinforcement Rectangle (NRR) Method

As previously explained the mathematical model is mainly based on creating a rectangle between the points on minimum x, maximum x, minimum y and maximum y at each quarter where the field device outside the gateway effective range are located. According to the area of the resulted rectangle and the area of the repeater range circle, a specific number of repeaters will be installed inside each of these rectangles, taking into account that any of these repeaters will be excluded if was separated with any of the field devices by a distance less than the minimum permissible distance between a repeater and a field device.

2.5.3 NRR Example

In order to provide a comprehensive realization for the discussed mathematical model when the NRR method is adopted, Figure (2.3) illustrates an example for the process of field devices relocation in order to increase the reliability level in a wireless HART network. The field at which the devices are installed, was equally divided into 4 sections or quarters.

- Each section includes a specific number of field devices, some of them are located inside the effective range of the gateway, while the rest are located outside the effective range of the gateway (Figures 2.3-a & 2.3-b).
- The northwestern section includes the highest number of field devices located outside the effective range of the gateway (7 field devices).
- As the first priority of the proposed mathematical model is to increase the amount of field devices located inside the effective range of the gateway, the field devices out of the effective range of the gateway will be relocated towards the southeastern direction, while the gateway will be relocated towards the northwestern direction (Figure 2.3-c).
- Afterwards, a network reinforcement rectangle will be drawn between the points of minimum (x), minimum (y), maximum (x) and maximum (y) of the Cartesian coordinates of the field devices outside the effective range of the gateway located at the northwestern quarter of the field (Figure 2.3-d).
- The added repeaters will be installed at the coordinates obtained by the division of the rectangle length and width on the diameter of the range circle of the repeater with repeaters of positions with distances less than the minimum permissible proximity with field devices are excluded (Figure 2.3-d).
- By relocating both of the gateway and the field devices out of the gateway effective range (northwestern quarter) towards each other and by installing additional repeaters to reinforce the northwestern division of the field, this will be the end of the first round.
- The second round will start by the relocation of the field devices at the second quarter of the field which includes the second maximum number of field devices located outside the effective range of the gateway. At the illustrated example, the southwestern quarter is the quarter which includes the second maximum number of field devices located outside the effective range of the gateway (6 field devices).
- Since the gateway has already been relocated towards the northwestern quarter, the relocation process at the second round will be only for the field devices at the southwestern quarter.
- There are three possibilities of relocation for the out of range field devices inside the southwestern division. The first possibility is to be relocated towards the gateway, while the second and the third possibilities is to be relocated towards the northwestern and the

southeastern divisions, respectively. The decision of relocation towards one of the three mentioned directions is taken through the application of the steps at the decision making table for the second round. These steps are based on moving the out of range devices in each direction, then recalculation of the (d) matrix and the sum of all distances inside the (d) matrix, in addition to the recalculation of the sum of ones at the in-range matrix (V).

- For simplicity purposes, it was assumed that the comparison at the decision making process during the movement of the out of range field devices in the three directions, has verified that the best relocation option for the out of range field devices at the southwestern division, is to move them towards the northwestern quarter (Figure 2.3-e).
- Similarly to the first round, the network reinforcement rectangle method will be applied again through installation of additional repeaters inside the rectangle formed by the coordinates of minimum x, minimum y, maximum x, and maximum y of the field devices outside the gateway effective range at the southeastern quarter (Figure 2.3-f).
- Through adopting the same techniques as the first and the second rounds, the relocation process at the third and fourth rounds will be assumed to result in the movement of the out of range field devices towards the gateway and installing additional repeaters inside the rectangular of minimum x, minimum y, maximum x and maximum y (Figures 2.3-g , 2.3-h, 2.3-i & 2.3-j).

After finishing the four rounds of field devices relocation and network reinforcement through adding repeaters at specific location, the next stage to increase the reliability and stability level of the wireless HART network, will be the inspection of the number of the neighbor devices for each of the field devices (gateway is excluded from such a process). The wireless HART network planning guide has recommended at the rule of minimum three that each field device should have at least minimum three neighbor devices [44,68]. As previously explained, the technique adopted to add neighbor devices is based on finding the intersection points between the line from the field device to the nearest out of range device and the range circles of the considered field device and that nearest device, then to the second nearest device and the next to it till the requirement of minimum neighbor devices is achieved. At (Figure 2.3-k), the dotted lines refer to the cancellation of adding neighbor repeaters on that lines due to the fact that the resulted proximity with other field devices will be less than the minimum permissible distance between the repeater and the field device, that's why, the neighbor repeater was installed at the fourth line connecting between the considered field device and the fourth nearest out of range field device.

A special case is illustrated at (Figure 2.3-l), as the obtained rectangle formed by the coordinates of minimum x, minimum y, maximum x and maximum y is rather smaller than expected, which will lead to a less number of added repeaters, which will not achieve the first priority purpose of establishing the connection between the out of range field devices and the gateway. Therefore, another reinforcement technique will be applied at this section of the network. This technique is based on finding the intersection points between the line from the nearest repeater to the gateway and the circles of range of both of the gateway and the nearest repeater. The obtained line between this two intersection points represents the shortest distance between the circle of range of the nearest repeater and the gateway range circle. Accordingly, repeaters will be added to the network on that line. The required number of repeaters can be obtained throw applying the equations (2.47) to (2.58) and similar equations at the 2^{nd}, 3^{rd} and 4^{th} rounds equation section.

2.5.4 The Minimum Required Field Device Density (MRFDD) Method

Another approach to install the repeaters inside the field, is to divide the whole field into square cells with a dimension indicating the degree of sensitivity according to which the repeaters will be added to the network at the center of these square cells only if there was not any of the network field devices located inside such cells. Each square cell can have a dimension from $1.5r_{rp}$ (correspondent to the highest degree of sensitivity) to $1.9r_{rp}$ (correspondent to the lowest degree of sensitivity).After dividing the whole field into such square cells, each cell will be checked if there is at least one field device included inside it or not. If not, a repeater will be installed at the center of the square cell. After the repeaters are installed in the empty square cells, the procedure of adding neighbor devices and optimization of total number of repeaters will be similar as was previously explained elaborately.

2.5.5 MRFDD Example

Similarly to the application of the NRR method to install additional repeaters at the wireless HART network, The MRFDD method is assumed to applied at the same network with the same field devices:

- The wireless HART network will be divided into square cells of a dimension of $1.5r_{rp}$.
- After relocation of the gateway as well as all the field devices at the four quarters, each of the resulted square cells will be checked if it includes a field device inside it or not.
- The square cells without a field device included inside them are colored with the yellow color (Figure 2.3-m).
- Repeaters will be installed at the centers of the empty square cells (Figure 2.3-n).
- Neighbor devices for each field device will be checked and repeaters will be added as neighbors if needed (Figure 2.3-o).
- The total number of repeaters will be optimized (Figure 2.3-p).

$$d_{\mathrm{n\times n}} = \begin{bmatrix} d_{1,1} & d_{1,2} & d_{1,3} & d_{1,4} & d_{1,5} & \dots\dots\dots & \dots\dots\dots & d_{1,n} \\ d_{2,1} & d_{2,2} & d_{2,3} & d_{2,4} & d_{2,5} & \dots\dots\dots & \dots\dots\dots & d_{2,n} \\ d_{3,1} & d_{3,2} & d_{3,3} & d_{3,4} & d_{3,5} & \dots\dots\dots & \dots\dots\dots & d_{3,n} \\ d_{4,1} & d_{4,2} & d_{4,3} & d_{4,4} & d_{4,5} & \dots\dots\dots & \dots\dots\dots & d_{4,n} \\ d_{5,1} & d_{5,2} & d_{5,3} & d_{5,4} & d_{5,5} & \dots\dots\dots & \dots\dots\dots & d_{5,n} \\ \vdots & \vdots & \vdots & \vdots & \vdots & \vdots & \vdots & \vdots \\ \vdots & \vdots & \vdots & \vdots & \vdots & \vdots & \vdots & \vdots \\ d_{n,1} & d_{n,2} & d_{n,3} & d_{n,4} & d_{n,5} & \dots & d_{n,n-1} & d_{n,n} \end{bmatrix} \tag{2.1}$$

$$d_{\mathrm{n\times n}} = \begin{bmatrix} 0 & 0 & 0 & 0 & 0 & \dots\dots\dots & \dots\dots\dots & 0 \\ d_{2,1} & 0 & 0 & 0 & 0 & \dots\dots\dots & \dots\dots\dots & 0 \\ d_{3,1} & d_{3,2} & 0 & 0 & 0 & \dots\dots\dots & \dots\dots\dots & 0 \\ d_{4,1} & d_{4,2} & d_{4,3} & 0 & 0 & \dots\dots\dots & \dots\dots\dots & 0 \\ d_{5,1} & d_{5,2} & d_{5,3} & d_{5,4} & 0 & \dots\dots\dots & \dots\dots\dots & 0 \\ \vdots & \vdots & \vdots & \vdots & \vdots & \vdots & \vdots & \vdots \\ \vdots & \vdots & \vdots & \vdots & \vdots & \vdots & \vdots & \vdots \\ d_{n,1} & d_{n,2} & d_{n,3} & d_{n,4} & d_{n,5} & \dots & d_{n,n-1} & 0 \end{bmatrix} \tag{2.2}$$

$$\frac{C_{\mathrm{n/2\times n-1}}}{n\ even} = \begin{bmatrix} C_{1,1} & C_{1,2} & C_{1,3} & C_{1,4} & C_{1,5} & \dots\dots\dots & \dots\dots\dots & C_{1,n-1} \\ C_{2,1} & C_{2,2} & C_{2,3} & C_{2,4} & C_{2,5} & \dots\dots\dots & \dots\dots\dots & C_{2,n-1} \\ C_{3,1} & C_{3,2} & C_{3,3} & C_{3,4} & C_{3,5} & \dots\dots\dots & \dots\dots\dots & C_{3,n-1} \\ \vdots & \vdots & \vdots & \vdots & \vdots & \vdots & \vdots & \vdots \\ C_{\frac{n}{2},1} & C_{\frac{n}{2},2} & C_{\frac{n}{2},3} & C_{\frac{n}{2},4} & C_{\frac{n}{2},5} & \dots & C_{\frac{n}{2},n-2} & C_{\frac{n}{2},n-1} \end{bmatrix} \tag{2.3}$$

$$\frac{C_{\mathrm{n/2\times n-1}}}{n\ even} = \begin{bmatrix} d_{2,1} & d_{3,2} & d_{4,3} & d_{5,4} & d_{6,5} & \dots\dots\dots & \dots\dots\dots & \dots\dots\dots & \dots\dots\dots & d_{n,n-1} \\ d_{3,1} & d_{4,2} & d_{5,3} & d_{6,4} & d_{7,5} & \dots\dots\dots & \dots\dots\dots & \dots\dots\dots & d_{n,n-2} & d_{4,1} \\ d_{5,2} & d_{6,3} & d_{7,4} & d_{8,5} & d_{9,6} & \dots\dots\dots & d_{n,n-3} & d_{5,1} & d_{6,2} & d_{7,3} \\ \vdots & \vdots & \vdots & \vdots & \vdots & \vdots & \vdots & \vdots & \vdots & \vdots \\ \dots\dots\dots & \dots\dots\dots & \dots\dots\dots & \dots\dots\dots & \dots\dots\dots & d_{n-1,2} & d_{n,3} & d_{n-1,1} & d_{n,2} & d_{n,1} \end{bmatrix} \tag{2.4}$$

$$\frac{R_{\mathrm{n/2\times n-1}}}{n\ even} = \begin{bmatrix} R_{2,1} & R_{3,2} & R_{4,3} & R_{5,4} & R_{6,5} & \dots\dots\dots & \dots\dots\dots & \dots\dots\dots & \dots\dots\dots & R_{n,n-1} \\ R_{3,1} & R_{4,2} & R_{5,3} & R_{6,4} & R_{7,5} & \dots\dots\dots & \dots\dots\dots & \dots\dots\dots & R_{n,n-2} & R_{4,1} \\ R_{5,2} & R_{6,3} & R_{7,4} & R_{8,5} & R_{9,6} & \dots\dots\dots & R_{n,n-3} & R_{5,1} & R_{6,2} & R_{7,3} \\ \vdots & \vdots & \vdots & \vdots & \vdots & \vdots & \vdots & \vdots & \vdots & \vdots \\ \dots\dots\dots & \dots\dots\dots & \dots\dots\dots & \dots\dots\dots & \dots\dots\dots & R_{n-1,2} & R_{n,3} & R_{n-1,1} & R_{n,2} & R_{n,1} \end{bmatrix} \tag{2.5}$$

$$\frac{C_{\mathrm{n-1/2\times n}}}{n\ odd} = \begin{bmatrix} C_{1,1} & C_{1,2} & C_{1,3} & C_{1,4} & C_{1,5} & \dots\dots\dots & \dots\dots\dots & C_{1,n} \\ C_{2,1} & C_{2,2} & C_{2,3} & C_{2,4} & C_{2,5} & \dots\dots\dots & \dots\dots\dots & C_{2,n} \\ C_{3,1} & C_{3,2} & C_{3,3} & C_{3,4} & C_{3,5} & \dots\dots\dots & \dots\dots\dots & C_{3,n} \\ \vdots & \vdots & \vdots & \vdots & \vdots & \vdots & \vdots & \vdots \\ C_{\frac{n-1}{2},1} & C_{\frac{n-1}{2},2} & C_{\frac{n-1}{2},3} & C_{\frac{n-1}{2},4} & C_{\frac{n-1}{2},5} & \dots & C_{\frac{n-1}{2},n-1} & C_{\frac{n-1}{2},n} \end{bmatrix} \tag{2.6}$$

$$\frac{C_{\mathrm{n-1/2\times n}}}{n\ odd} = \begin{bmatrix} d_{2,1} & d_{3,2} & d_{4,3} & d_{5,4} & d_{6,5} & \dots\dots\dots & \dots\dots\dots & \dots\dots\dots & d_{n,n-1} & d_{3,1} \\ d_{4,2} & d_{5,3} & d_{6,4} & d_{7,5} & d_{8,6} & \dots\dots\dots & d_{n,n-2} & d_{4,1} & d_{5,2} & d_{6,3} \\ d_{7,4} & d_{6,3} & \dots\dots\dots & d_{n,n-3} & d_{5,1} & d_{6,2} & d_{7,3} & d_{8,4} & d_{9,5} & d_{10,6} \\ \vdots & \vdots & \vdots & \vdots & \vdots & \vdots & \vdots & \vdots & \vdots & \vdots \\ \dots\dots\dots & \dots\dots\dots & \dots\dots\dots & \dots\dots\dots & \dots\dots\dots & d_{n-1,2} & d_{n,3} & d_{n-1,1} & d_{n,2} & d_{n,1} \end{bmatrix} \tag{2.7}$$

$$\frac{R_{\mathrm{n-1/2\times n}}}{n\ odd} = \begin{bmatrix} R_{2,1} & R_{3,2} & R_{4,3} & R_{5,4} & R_{6,5} & \dots\dots\dots & \dots\dots\dots & \dots\dots\dots & R_{n,n-1} & R_{3,1} \\ R_{4,2} & R_{5,3} & R_{6,4} & R_{7,5} & R_{8,6} & \dots\dots\dots & R_{n,n-2} & R_{4,1} & R_{5,2} & R_{6,3} \\ R_{7,4} & R_{6,3} & \dots\dots\dots & R_{n,n-3} & R_{5,1} & R_{6,2} & R_{7,3} & R_{8,4} & R_{9,5} & R_{10,6} \\ \vdots & \vdots & \vdots & \vdots & \vdots & \vdots & \vdots & \vdots & \vdots & \vdots \\ \dots\dots\dots & \dots\dots\dots & \dots\dots\dots & \dots\dots\dots & \dots\dots\dots & R_{n-1,2} & R_{n,3} & R_{n-1,1} & R_{n,2} & R_{n,1} \end{bmatrix} \tag{2.8}$$

$$\frac{V_{n-1/2 \times n}}{n\ odd} = \begin{bmatrix} V_{2,1} & V_{3,2} & V_{4,3} & V_{5,4} & V_{6,5} & \dots\dots\dots & \dots\dots\dots & \dots\dots\dots & V_{n,n-1} & V_{3,1} \\ V_{4,2} & V_{5,3} & V_{6,4} & V_{7,5} & V_{8,6} & \dots\dots\dots & V_{n,n-2} & V_{4,1} & V_{5,2} & V_{6,3} \\ V_{7,4} & V_{6,3} & \dots\dots\dots & V_{n,n-3} & V_{5,1} & V_{6,2} & V_{7,3} & V_{8,4} & V_{9,5} & V_{10,6} \\ \vdots & \vdots & \vdots & \vdots & \vdots & \vdots & \vdots & \vdots & \vdots & \vdots \\ \dots\dots\dots & \dots\dots\dots & \dots\dots\dots & \dots\dots\dots & \dots\dots\dots & V_{n-1,2} & V_{n,3} & V_{n-1,1} & V_{n,2} & V_{n,1} \end{bmatrix} \tag{2.9}$$

$$xy_{2 \times n} = \begin{bmatrix} x_1 & x_2 & x_3 & x_4 & x_5 & \dots\dots\dots & \dots\dots\dots & \dots\dots\dots & \dots\dots\dots & x_n \\ y_1 & y_2 & y_3 & y_4 & y_5 & \dots\dots\dots & \dots\dots\dots & \dots\dots\dots & \dots\dots\dots & y_n \end{bmatrix} \tag{2.10}$$

$$\Delta xy_{4 \times n} = \begin{bmatrix} x_{1-} & x_{2-} & x_{3-} & x_{4-} & x_{5-} & \dots\dots\dots & \dots\dots\dots & \dots\dots\dots & \dots\dots\dots & x_{n-} \\ x_{1+} & x_{2+} & x_{3+} & x_{4+} & x_{5+} & \dots\dots\dots & \dots\dots\dots & \dots\dots\dots & \dots\dots\dots & x_{n+} \\ y_{1-} & y_{2-} & y_{3-} & y_{4-} & y_{5-} & \dots\dots\dots & \dots\dots\dots & \dots\dots\dots & \dots\dots\dots & y_{n-} \\ y_{1+} & y_{2+} & y_{3+} & y_{4+} & y_{5+} & \dots\dots\dots & \dots\dots\dots & \dots\dots\dots & \dots\dots\dots & y_{n+} \end{bmatrix} \tag{2.11}$$

$$d_{i,j} = \sqrt{(|x_i - x_j|)^2 + (|y_i - y_j|)^2} \tag{2.12}$$

$$S_i = [S_1, S_2, S_3, S_4, \dots\dots\dots\dots\dots\dots\dots,\ S_n] \tag{2.13}$$

$$S_m(NE) = [S_m\ , where\ m \epsilon \{1,2,3, \dots\dots\dots, n\}\ , x_m > \left(\frac{x_f}{2}\right) \&\ y_m > (\frac{y_f}{2})] \tag{2.14}$$

$$S_m(NE) = S_m^{in}(NE)\ \cup\ S_m^{out}(NE) \tag{2.15}$$

$$S_m(NW) = [S_m\ , where\ m \epsilon \{1,2,3, \dots\dots\dots, n\}\ , x_m < \left(\frac{x_f}{2}\right) \&\ y_m > (\frac{y_f}{2})] \tag{2.16}$$

$$S_m(NW) = S_m^{in}(NW)\ \cup\ S_m^{out}(NW) \tag{2.17}$$

$$S_m(SE) = [S_m\ , where\ m \epsilon \{1,2,3, \dots\dots\dots, n\}\ , x_m > \left(\frac{x_f}{2}\right) \&\ y_m < (\frac{y_f}{2})] \tag{2.18}$$

$$S_m(SE) = S_m^{in}(SE)\ \cup\ S_m^{out}(SE) \tag{2.19}$$

$$S_m(SW) = [S_m\ , where\ m \epsilon \{1,2,3, \dots\dots\dots, n\}\ , x_m < \left(\frac{x_f}{2}\right) \&\ y_m < (\frac{y_f}{2})] \tag{2.20}$$

$$S_m(SW) = S_m^{in}(SW)\ \cup\ S_m^{out}(SW) \tag{2.21}$$

$$K_j(i) = [K_1(i), K_2(i), K_3(i), K_4(i), \dots\dots\dots\dots\dots\dots\dots,\ K_n(i)]\ Where\ i\ \neq j \tag{2.22}$$

$$L_j(i) = [L_1(i), L_2(i), L_3(i), L_4(i), \dots\dots\dots\dots\dots\dots\dots,\ L_n(i)]\ Where\ i\ \neq j \tag{2.23}$$

$$If\ d_{i,j} > r_f\ ,\ R_{i,j} = 0\ \ \&\ If\ d_{i,j} < r_f\ ,\ R_{i,j} = 1$$
$$If\ d_{i,j} < r_f\ ,\ V_{i,j} = 1\ \ \&\ If\ d_{i,j} > r_f\ ,\ V_{i,j} = 0$$

$$For\ a\ specific\ i = 1{:}n,\ If\ d_{i,j} > r_f\ or\ d_{j,i} > r_f\ ,\ K_j(i) = 0\ \&\ L_j(i) = \mathrm{j} \tag{2.24}$$

$$For\ a\ specific\ i = 1{:}n,\ If\ d_{i,j} < r_f\ or\ d_{j,i} < r_f,\ K_j(i) = \mathrm{j}\ \&\ L_j(i) = 0 \tag{2.25}$$

$$For\ the\ gateway,\ L_j(1) = [L_2(1), L_3(1), L_4(1), \dots\dots\dots\dots\dots\dots\dots,\ L_n(1)]\ Where\ i\ \neq j \tag{2.26}$$

$$\begin{gathered} For\ the\ gateway,\ L_j{}'(1) = [L_{n1}(1), \dots\dots\dots\dots\dots\dots\dots\dots,\ L_{n11}(1)] \\ Where\ j\ \neq 1\ \&\ L_j(1)\ \neq 0\ \ \&\ \{n1, n11\} \subset \{1,2,3, \dots\dots, n\} \end{gathered} \tag{2.27}$$

$$For\ the\ gateway,\ L_j{}''(1) = [L_2(1), L_3(1), L_4(1), \dots\dots\dots\dots\dots\dots\dots,\ L_n(1)]\ Where\ j\ \neq 1\ \&\ L_j(i)\ \neq 0 \tag{2.28}$$

$$\begin{gathered} For\ the\ gateway,\ L_j{}'^{NE}(1) = [L_{n2}(1), \dots\dots\dots\dots\dots\dots\dots,\ L_{n22}(1)] \\ Where\ j\ \neq 1\ \&\ L_j(1)\ \neq 0\ \&\ S_j\ \epsilon\ S_m(NE)\ \&\ \{n2, n22\} \subset \{1,2,3, \dots\dots, n\} \end{gathered} \tag{2.29}$$

$$For\ the\ gateway,\ L_j{}'^{NW}(1) = [L_{n3}(1), \dots \dots \dots \dots \dots \dots,\ L_{n33}(1)] \tag{2.30}$$
$$Where\ j\ \neq 1\ \&\ L_j(1)\ \neq 0\ \&\ S_j\ \epsilon\ S_m(NW)\ \&\ \{n3, n33\} \subset \{1,2,3, \dots \dots, n\}$$

$$For\ the\ gateway,\ L_j{}'^{SE}(1) = [L_{n4}(1), \dots \dots \dots \dots \dots \dots,\ L_{n44}(1)] \tag{2.31}$$
$$Where\ j\ \neq 1\ \&\ L_j(1)\ \neq 0\ \&\ S_j\ \epsilon\ S_m(SE)\ \&\ \{n4, n44\} \subset \{1,2,3, \dots \dots, n\}$$

$$For\ the\ gateway,\ L_j{}'^{SW}(1) = [L_{n5}(1), \dots \dots \dots \dots \dots \dots,\ L_{n55}(1)] \tag{2.32}$$
$$Where\ j\ \neq 1\ \&\ L_j(1)\ \neq 0\ \&\ S_j\ \epsilon\ S_m(SW)\ \&\ \{n5, n55\} \subset \{1,2,3, \dots \dots, n\}$$

$$M_1 = [N\left(L_j{}'^{NE}(1)\right),\ N\left(L_j{}'^{NW}(1)\right),\ N\left(L_j{}'^{SE}(1)\right),\ N\left(L_j{}'^{SW}(1)\right)] \tag{2.33}$$

$$M_1{}' = [max(M_1), \dots \dots, \dots \dots,\ min(M_1)] \tag{2.34}$$

$$If\ M_1{}'(1) = \begin{cases} N\left(L_j{}'^{NE}(1)\right) \longrightarrow (x_1^1 = x_1 + h_x x_{1+}), (y_1^1 = y_1 + h_y y_{1+}) \\ N\left(L_j{}'^{NW}(1)\right) \longrightarrow (x_1^1 = x_1 + h_x x_{1-}), (y_1^1 = y_1 + h_y y_{1+}) \\ N\left(L_j{}'^{SE}(1)\right) \longrightarrow (x_1^1 = x_1 + h_x x_{1+}), (y_1^1 = y_1 + h_y y_{1-}) \\ N\left(L_j{}'^{SW}(1)\right) \longrightarrow (x_1^1 = x_1 + h_x x_{1-}), (y_1^1 = y_1 + h_y y_{1-}) \end{cases} \tag{2.35}$$

$$Where\ h_x = 0{:}\,1\ and\ h_y = 0{:}\,1$$

<u>The First Round</u>

<u>Case 1: Northeastern field quarter with maximum number of field devices out of the gateway effective range</u>

$$If\ M_1{}'(1) = N\left(L_j{}'^{NE}(1)\right) \longrightarrow (x_m^1 = x_m + x_{m-}), (y_m^1 = y_m + y_{m-})\ for\ each\ S_m\ \epsilon\ S_m^{out}(NE) \tag{2.36}$$
$$A_{out}^1(NE) = \left(x_m^{1\,max}(NE) - x_m^{1\,min}(NE)\right) \times \left(y_m^{1\,max}(NE) - y_m^{1\,min}(NE)\right) \tag{2.37}$$

$$No.of\ required\ repeaters\ N_{rp}(NE) = \left|\frac{A_{out}^1(NE)}{\pi\,(r_{rp})^2}\right| \tag{2.38}$$

$$R_{xNE} = \left|\frac{x_m^{1\,max}(NE) - x_m^{1\,min}(NE)}{2r_{rp}}\right| \tag{2.39}$$

$$R_{yNE} = \left|\frac{y_m^{1\,max}(NE) - y_m^{1\,min}(NE)}{2r_{rp}}\right| \tag{2.40}$$

$$No.of\ required\ repeaters\ N_{rp}(NE) = R_{xNE} \times R_{yNE} \tag{2.41}$$

$$x_r^{nx}(NE) = x_m^{1\,min}(NE) + r_{rp}(2n_x - 1)\ where\ n_x\ \epsilon\ \{1,2,3 \dots \dots,\ R_{xNE}\} \tag{2.42}$$

$$y_r^{ny}(NE) = y_m^{1\,min}(NE) + r_{rp}\left(2n_y - 1\right)\ where\ n_y\ \epsilon\ \left\{1,2,3 \dots \dots,\ R_{yNE}\right\} \tag{2.43}$$

$$xy_{\mathrm{rNE}(R_{xNE} \times R_{yNE})} = \begin{bmatrix} (x_{r1}^{NE},\ y_{r1}^{NE}) & (x_{r1}^{NE},\ y_{r2}^{NE}) & (x_{r1}^{NE},\ y_{r3}^{NE}) & \dots & (x_{r1}^{NE},\ y_{rR_{yNE}}^{NE}) \\ (x_{r2}^{NE},\ y_{r1}^{NE}) & (x_{r2}^{NE},\ y_{r2}^{NE}) & (x_{r2}^{NE},\ y_{r3}^{NE}) & \dots & (x_{r2}^{NE},\ y_{rR_{yNE}}^{NE}) \\ \vdots & \vdots & \vdots & \dots & \vdots \\ \vdots & \vdots & \vdots & \dots & \vdots \\ (x_{rR_{xNE}}^{NE},\ y_{r1}^{NE}) & (x_{rR_{xNE}}^{NE},\ y_{r2}^{NE}) & \dots & \dots & (x_{rR_{xNE}}^{NE},\ y_{rR_{yNE}}^{NE}) \end{bmatrix} \tag{2.44}$$

$xy^{i}_{r\mathrm{NE}(R_{xNE}\times R_{yNE})} =$

$$\begin{bmatrix} \sqrt{(|x_i - x^{NE}_{r1}|)^2 + (|y_i - y^{NE}_{r1}|)^2} & \sqrt{(|x_i - x^{NE}_{r1}|)^2 + (|y_i - y^{NE}_{r2}|)^2} & \dots & \sqrt{(|x_i - x^{NE}_{r1}|)^2 + (\left|y_i - y^{NE}_{rR_{yNE}}\right|)^2} \\ \sqrt{(|x_i - x^{NE}_{r2}|)^2 + (|y_i - y^{NE}_{r1}|)^2} & \sqrt{(|x_i - x^{NE}_{r2}|)^2 + (|y_i - y^{NE}_{r2}|)^2} & \dots & \sqrt{(|x_i - x^{NE}_{r2}|)^2 + (\left|y_i - y^{NE}_{rR_{yNE}}\right|)^2} \\ \vdots & \vdots & \dots & \vdots \\ \vdots & \vdots & \dots & \vdots \\ \sqrt{(\left|x_i - x^{NE}_{rR_{xNE}}\right|)^2 + (|y_i - y^{NE}_{r1}|)^2} & \sqrt{(\left|x_i - x^{NE}_{rR_{xNE}}\right|)^2 + (|y_i - y^{NE}_{r2}|)^2} & \dots & \sqrt{(\left|x_i - x^{NE}_{rR_{xNE}}\right|)^2 + (\left|y_i - y^{NE}_{rR_{yNE}}\right|)^2} \end{bmatrix}$$

$$where\ S_i \in S^{out}_m(NE) \tag{2.45}$$

$$For\ a\ repeater\ coordinates\ of\ \left(x^{nx}_r(NE), y^{ny}_r(NE)\right), if\ d_{rf} < d^{min}_{rf}\ , the\ point\ will\ be\ excluded \tag{2.46}$$

$$d^{\min 1}_{r,1}(NE) = \sqrt{(|x^{NE}_{r1} - x^1_1|)^2 + (|y^{NE}_{r1} - y^1_1|)^2} \tag{2.47}$$

$$if\ d^{\min 1}_{r,1}(NE) > r_{rp} + r_1 \tag{2.48}$$

$$N_{rp,g}(NE) = \left|\frac{d^{\min 1}_{r,1}(NE) - r_{rp} - r_1}{r_{rp}}\right| + 1 \tag{2.49}$$

$Straight\ line\ equation\ between\ the\ nearesst\ repeater\ and\ the\ gateway$

$$y = ax + b \tag{2.50}$$

$$a = \frac{y^{NE}_{r1} - y^1_1}{x^{NE}_{r1} - x^1_1} \tag{2.51}$$

$$b = y^1_1 - ax^1_1 = y^{NE}_{r1} - ax^{NE}_{r1} \tag{2.52}$$

$Finding\ the\ intersection\ points\ (x^{NE}_{gr1}, y^{NE}_{gr1})\ and\ (x^{NE}_{gr2}, y^{NE}_{gr2})\ between\ the\ straight\ line\ quation$
$and\ the\ range\ circles\ equations\ of\ the\ gateway\ and\ the\ nearest\ repaeter, respectively$

$$(x - x^{NE}_{r1})^2 + (y - y^{NE}_{r1})^2 = \left(r_{rp}\right)^2, (x - x^1_1)^2 + (y - y^1_1)^2 = (r_1)^2 \tag{2.53}$$

$$where\ x^1_1 < x^{NE}_{gr1} < x^{NE}_{r1}\ , x^1_1 < x^{NE}_{gr2} < x^{NE}_{r1} \tag{2.54}$$

$$and\ y^1_1 < y^{NE}_{gr1} < y^{NE}_{r1}\ , y^1_1 < y^{NE}_{gr2} < y^{NE}_{r1} \tag{2.55}$$

$$\Theta_{NE} = \tan^{-1}\frac{y^{NE}_{gr2} - y^{NE}_{gr1}}{x^{NE}_{gr2} - x^{NE}_{gr1}} \tag{2.56}$$

$$d^{\min 1}_{r,1}(NE) - r_{rp} - r_1 = \sqrt{\left(\left|x^{NE}_{gr2} - x^{NE}_{gr1}\right|\right)^2 + \left(\left|y^{NE}_{gr2} - y^{NE}_{gr1}\right|\right)^2} \tag{2.57}$$

$$xy_{\mathrm{grNE}\left(1\times N_{rp,g}(NE)\right)} = \left[(x^{NE}_{gr1}, y^{NE}_{gr1}), (x^{NE}_{gr1} + r_{rp}\cos\Theta_{NE}\ , y^{NE}_{gr1} + r_{rp}\sin\Theta_{NE}), (x^{NE}_{gr1} + 2r_{rp}\cos\Theta_{NE}\ , y^{NE}_{gr1} + 2r_{rp}\sin\Theta_{NE}), (x^{NE}_{gr1} + 3r_{rp}\cos\Theta_{NE}\ , y^{NE}_{gr1} + 3r_{rp}\sin\Theta_{NE}), \dots\dots\dots\dots, (x^{NE}_{gr1} + \left(N_{rp,g}(NE) - 2\right)r_{rp}\cos\Theta_{NE}, y^{NE}_{gr1} + \left(N_{rp,g}(NE) - 2\right)r_{rp}\sin\Theta_{NE}), (x^{NE}_{gr2}, y^{NE}_{gr2})\right] \tag{2.58}$$

<u>Case 2: Northwestern field quarter with maximum number of field devices out of the gateway effective range</u>

$$If\ M_1{}'(1) = N\left(L_j{}'^{NW}(1)\right) \longrightarrow\ (x_m^1 = x_m + x_{m+}), (y_m^1 = y_m + y_{m-})\ for\ each\ S_m\ \epsilon\ S_m^{out}(NW) \tag{2.59}$$

$$A_{out}^1(NW) = \left(x_m^{1\,max}(NW) - x_m^{1\,min}(NW)\right) \times \left(y_m^{1\,max}(NW) - y_m^{1\,min}(NW)\right) \tag{2.60}$$

$$No.of\ required\ repeaters\ N_{rp}(NW) = \left|\frac{A_{out}^1(NW)}{\pi\,(r_{rp})^2}\right| \tag{2.61}$$

$$R_{xNW} = \left|\frac{x_m^{1\,max}(NW) - x_m^{1\,min}(NW)}{2r_{rp}}\right| \tag{2.62}$$

$$R_{yNW} = \left|\frac{y_m^{1\,max}(NW) - y_m^{1\,min}(NW)}{2r_{rp}}\right| \tag{2.63}$$

$$No.of\ required\ repeaters\ \ N_{rp}(NW) = R_{xNW} \times R_{yNW} \tag{2.64}$$

$$x_r^{nx}(NW) = x_m^{1\,min}(NW) + r_{rp}(2n_x - 1)\ where\ n_x\ \epsilon\ \{1,2,3 \ldots\ldots,\ R_{xNW}\} \tag{2.65}$$

$$y_r^{ny}(NW) = y_m^{1\,min}(NW) + r_{rp}\left(2n_y - 1\right)\ where\ n_y\ \epsilon\ \left\{1,2,3 \ldots\ldots,\ R_{yNW}\right\} \tag{2.66}$$

$$xy_{\mathrm{rNW}(R_{xNW} \times R_{yNW})} = \begin{bmatrix} (x_{r1}^{NW},\ y_{r1}^{NW}) & (x_{r1}^{NW},\ y_{r2}^{NW}) & (x_{r1}^{NW},\ y_{r3}^{NW}) & \ldots & (x_{r1}^{NW},\ y_{rR_{yNE}}^{NW}) \\ (x_{r2}^{NW},\ y_{r1}^{NW}) & (x_{r2}^{NW},\ y_{r2}^{NW}) & (x_{r2}^{NW},\ y_{r3}^{NW}) & \ldots & (x_{r2}^{NE},\ y_{rR_{yNW}}^{NW}) \\ \vdots & \vdots & \vdots & \ldots & \vdots \\ \vdots & \vdots & \vdots & \ldots & \vdots \\ (x_{rR_{xNW}}^{NW},\ y_{r1}^{NW}) & (x_{rR_{xNW}}^{NW},\ y_{r2}^{NW}) & \ldots & \ldots & (x_{rR_{xNE}}^{NE},\ y_{rR_{yNW}}^{NW}) \end{bmatrix} \tag{2.67}$$

$$xy^i_{r\mathrm{NW}(R_{xNW} \times R_{yNW})} =$$

$$\begin{bmatrix} \sqrt{(|x_i - x_{r1}^{NW}|)^2 + (|y_i - y_{r1}^{NW}|)^2} & \sqrt{(|x_i - x_{r1}^{NW}|)^2 + (|y_i - y_{r2}^{NW}|)^2} & \ldots & \sqrt{(|x_i - x_{r1}^{NW}|)^2 + \left(\left|y_i - y_{rR_{yNW}}^{NW}\right|\right)^2} \\ \sqrt{(|x_i - x_{r2}^{NW}|)^2 + (|y_i - y_{r1}^{NW}|)^2} & \sqrt{(|x_i - x_{r2}^{NW}|)^2 + (|y_i - y_{r2}^{NW}|)^2} & \ldots & \sqrt{(|x_i - x_{r2}^{NW}|)^2 + \left(\left|y_i - y_{rR_{yNW}}^{NW}\right|\right)^2} \\ \vdots & \vdots & \ldots & \vdots \\ \vdots & \vdots & \ldots & \vdots \\ \sqrt{\left(\left|x_i - x_{rR_{xNW}}^{NW}\right|\right)^2 + (|y_i - y_{r1}^{NW}|)^2} & \sqrt{\left(\left|x_i - x_{rR_{xNW}}^{NW}\right|\right)^2 + (|y_i - y_{r2}^{NW}|)^2} & \ldots & \sqrt{\left(\left|x_i - x_{rR_{xNE}}^{NW}\right|\right)^2 + \left(\left|y_i - y_{rR_{yNE}}^{NW}\right|\right)^2} \end{bmatrix}$$

$$where\ S_i\ \epsilon\ S_m^{out}(NW) \tag{2.68}$$

$$For\ a\ repeater\ coordinates\ of\ \left(x_r^{nx}(NW), y_r^{ny}(NW)\right), if\ d_{rf} < d_{rf}^{min}\ , the\ point\ will\ be\ excluded \tag{2.69}$$

$$d_{r,1}^{\min 1}(NW) = \sqrt{(|x_{r1}^{NW} - x_1^1|)^2 + (|y_{r1}^{NW} - y_1^1|)^2} \tag{2.70}$$

$$if\ d_{r,1}^{\min 1}(NW) > r_{rp} + r_1 \tag{2.71}$$

$$N_{rp,g}(NW) = \left|\frac{d_{r,1}^{\min 1}(NW) - r_{rp} - r_1}{r_{rp}}\right| + 1 \tag{2.72}$$

Straight line equation between the nearesst repeater and the gateway

$$y = ax + b \tag{2.73}$$

$$a = \frac{y_{r1}^{NW} - y_1^1}{x_{r1}^{NW} - x_1^1} \tag{2.74}$$

$$b = y_1^1 - a x_1^1 = y_{r1}^{NW} - a x_{r1}^{NW} \tag{2.75}$$

$Finding\ \ the\ intersection\ points\ (x_{gr1}^{NW}, y_{gr1}^{NW})\ and\ \ (x_{gr2}^{NW}, y_{gr2}^{NW})\ \ between\ the\ straight\ line\ quation$
$and\ the\ range\ circles\ equations\ of\ the\ gateway\ and\ the\ nearest\ repaeter, respectively$

$$(x - x_{r1}^{NW})^2 + (y - y_{r1}^{NW})^2 = \left(r_{rp}\right)^2, (x - x_1^1)^2 + (y - y_1^1)^2 = (r_1)^2 \tag{2.76}$$

$$where\ \ x_1^1 > \ x_{gr1}^{NW} < x_{r1}^{NW}\ , x_1^1 > \ x_{gr2}^{NW} < x_{r1}^{NW} \tag{2.77}$$

$$and\ \ y_1^1 < \ y_{gr1}^{NW} < y_{r1}^{NW}\ , y_1^1 < \ y_{gr2}^{NW} < y_{r1}^{NW} \tag{2.78}$$

$$\theta_{NW} = \tan^{-1} \frac{y_{gr2}^{NW} - y_{gr1}^{NW}}{x_{gr2}^{NW} - x_{gr1}^{NW}} \tag{2.79}$$

$$d_{r,1}^{\min 1}(NW) - r_{rp} - r_1 = \sqrt{\left(\left|x_{gr2}^{NW} - x_{gr1}^{NW}\right|\right)^2 + \left(\left|y_{gr2}^{NW} - y_{gr1}^{NW}\right|\right)^2} \tag{2.80}$$

$$xy_{\mathrm{grNW}\left(1 \times N_{rp,g}(NW)\right)} = \left[(x_{gr1}^{NW}, y_{gr1}^{NW}), (x_{gr1}^{NW} - r_{rp}\cos\theta_{NW}\ , y_{gr1}^{NW} + r_{rp}\sin\theta_{NW}), (x_{gr1}^{NW} - 2r_{rp}\cos\theta_{NW}\ ,\ y_{gr1}^{NW} + 2r_{rp}\sin\theta_{NW}), (x_{gr1}^{NW} - 3r_{rp}\cos\theta_{NW}\ ,\ y_{gr1}^{NW} + 3r_{rp}\sin\theta_{NW}), \dots\dots\dots\dots, (x_{gr1}^{NW} - \left(N_{rp,g}(NW) - 2\right)r_{rp}\cos\theta_{NW}, y_{gr1}^{NW} + \left(N_{rp,g}(NW) - 2\right)r_{rp}\sin\theta_{NW}), (x_{gr2}^{NW},\ y_{gr2}^{NW})\right] \tag{2.81}$$

<u>Case 3: Southeastern field quarter with maximum number of field devices out of the gateway effective range</u>

$$If\ M_1{}'(1) = N\left(L_j{}'^{SE}(1)\right) \longrightarrow\ (x_m^1 = x_m + x_{m-}), (y_m^1 = y_m + y_{m+})\ for\ each\ S_m \in S_m^{out}(SE) \tag{2.82}$$

$$A_{out}^1(SE) = \left(x_m^{1\,max}(SE) - x_m^{1\,min}(SE)\right) \times \left(y_m^{1\,max}(SE) - y_m^{1\,min}(SE)\right) \tag{2.83}$$

$$No.of\ required\ repeaters\ N_{rp}(SE) = \left|\frac{A_{out}^1(SE)}{\pi\left(r_{rp}\right)^2}\right| \tag{2.84}$$

$$R_{xSE} = \left|\frac{x_m^{1\,max}(SE) - x_m^{1\,min}(SE)}{2r_{rp}}\right| \tag{2.85}$$

$$R_{ySE} = \left|\frac{y_m^{1\,max}(SE) - y_m^{1\,min}(SE)}{2r_{rp}}\right| \tag{2.86}$$

$$No.of\ required\ repeaters\ \ N_{rp}(SE) = R_{xSE} \times R_{ySE} \tag{2.87}$$

$$x_r^{nx}(SE) = \ x_m^{1\,min}(SE) + r_{rp}(2n_x - 1)\ where\ n_x \in \{1,2,3 \dots\dots,\ R_{xSE}\} \tag{2.88}$$

$$y_r^{ny}(SE) = \ y_m^{1\,min}(SE) + r_{rp}\left(2n_y - 1\right)\ where\ n_y \in \left\{1,2,3 \dots\dots,\ R_{ySE}\right\} \tag{2.89}$$

$$xy_{\mathrm{rSE}(R_{xSE} \times R_{ySE})} = \begin{bmatrix} (x_{r1}^{SE},\ y_{r1}^{SE}) & (x_{r1}^{SE},\ y_{r2}^{SE}) & (x_{r1}^{SE},\ y_{r3}^{SE}) & \dots & (x_{r1}^{SE},\ y_{rR_{ySE}}^{SE}) \\ (x_{r2}^{SE},\ y_{r1}^{SE}) & (x_{r2}^{SE},\ y_{r2}^{SE}) & (x_{r2}^{SE},\ y_{r3}^{SE}) & \dots & (x_{r2}^{SE},\ y_{rR_{ySE}}^{SE}) \\ \vdots & \vdots & \vdots & \dots & \vdots \\ \vdots & \vdots & \vdots & \dots & \vdots \\ (x_{rR_{xSE}}^{SE},\ y_{r1}^{SE}) & (x_{rR_{xSE}}^{SE},\ y_{r2}^{SE}) & \dots & \dots & (x_{rR_{xSE}}^{SE},\ y_{rR_{ySE}}^{SE}) \end{bmatrix} \tag{2.90}$$

$$xy^{i}_{r\mathrm{SE}(R_{xSE}\times R_{ySE})} =$$

$$\begin{bmatrix} \sqrt{(|x_i - x^{SE}_{r1}|)^2 + (|y_i - y^{SE}_{r1}|)^2} & \sqrt{(|x_i - x^{SE}_{r1}|)^2 + (|y_i - y^{SE}_{r2}|)^2} & \cdots & \sqrt{(|x_i - x^{SE}_{r1}|)^2 + (|y_i - y^{SE}_{rR_{ySE}}|)^2} \\ \sqrt{(|x_i - x^{SE}_{r2}|)^2 + (|y_i - y^{SE}_{r1}|)^2} & \sqrt{(|x_i - x^{SE}_{r2}|)^2 + (|y_i - y^{SE}_{r2}|)^2} & \cdots & \sqrt{(|x_i - x^{SE}_{r2}|)^2 + (|y_i - y^{SE}_{rR_{ySE}}|)^2} \\ \vdots & \vdots & \cdots & \vdots \\ \vdots & \vdots & \cdots & \vdots \\ \sqrt{(|x_i - x^{SE}_{rR_{xSE}}|)^2 + (|y_i - y^{SE}_{r1}|)^2} & \sqrt{(|x_i - x^{SE}_{rR_{xSE}}|)^2 + (|y_i - y^{SE}_{r2}|)^2} & \cdots & \sqrt{(|x_i - x^{SE}_{rR_{xSE}}|)^2 + (|y_i - y^{SE}_{rR_{ySE}}|)^2} \end{bmatrix}$$

$$where\ S_i \in S^{out}_m(SE) \tag{2.91}$$

$$For\ a\ repeater\ coordinates\ of\ \left(x^{nx}_r(SE), y^{ny}_r(SE)\right), if\ d_{rf} < d^{min}_{rf}\ , the\ point\ will\ be\ excluded \tag{2.92}$$

$$d^{\min 1}_{r,1}(SE) = \sqrt{(|x^{SE}_{r1} - x^1_1|)^2 + (|y^{SE}_{r1} - y^1_1|)^2} \tag{2.93}$$

$$if\ d^{\min 1}_{r,1}(SE) > r_{rp} + r_1 \tag{2.94}$$

$$N_{rp,g}(SE) = |\frac{d^{\min 1}_{r,1}(SE) - r_{rp} - r_1}{r_{rp}}| + 1 \tag{2.95}$$

$$Straight\ line\ equation\ between\ the\ nearesst\ repeater\ and\ the\ gateway$$

$$y = ax + b \tag{2.96}$$

$$a = \frac{y^{SE}_{r1} - y^1_1}{x^{SE}_{r1} - x^1_1} \tag{2.97}$$

$$b = y^1_1 - ax^1_1 = y^{SE}_{r1} - ax^{SE}_{r1} \tag{2.98}$$

Finding the intersection points $(x^{SE}_{gr1}, y^{SE}_{gr1})$ *and* $(x^{SE}_{gr2}, y^{SE}_{gr2})$ *between the straight line quation and the range circles equations of the gateway and the nearest repaeter, respectively*

$$(x - x^{SE}_{r1})^2 + (y - y^{SE}_{r1})^2 = \left(r_{rp}\right)^2, (x - x^1_1)^2 + (y - y^1_1)^2 = (r_1)^2 \tag{2.99}$$

$$where\ x^1_1 < x^{SE}_{gr1} < x^{SE}_{r1}\ , x^1_1 < x^{SE}_{gr2} < x^{SE}_{r1} \tag{2.100}$$

$$and\ y^1_1 > y^{SE}_{gr1} < y^{SE}_{r1}\ , y^1_1 > y^{SE}_{gr2} < y^{SE}_{r1} \tag{2.101}$$

$$\Theta_{SE} = \tan^{-1}\frac{y^{SE}_{gr2} - y^{SE}_{gr1}}{x^{SE}_{gr2} - x^{SE}_{gr1}} \tag{2.102}$$

$$d^{\min 1}_{r,1}(SE) - r_{rp} - r_1 = \sqrt{\left(|x^{SE}_{gr2} - x^{SE}_{gr1}|\right)^2 + \left(|y^{SE}_{gr2} - y^{SE}_{gr1}|\right)^2} \tag{2.103}$$

$$xy_{\mathrm{grSE}\left(1\times N_{rp,g}(SE)\right)} = \left[(x^{SE}_{gr1}, y^{SE}_{gr1}), (x^{SE}_{gr1} + r_{rp}\cos\Theta_{SE}\ , y^{SE}_{gr1} - r_{rp}\sin\Theta_{SE}), (x^{SE}_{gr1} + 2r_{rp}\cos\Theta_{SE}\ , y^{SE}_{gr1} - 2r_{rp}\sin\Theta_{SE}), (x^{SE}_{gr1} + 3r_{rp}\cos\Theta_{SE}\ , y^{SE}_{gr1} - 3r_{rp}\sin\Theta_{SE}), \ldots\ldots\ldots\ldots, (x^{SE}_{gr1} + \left(N_{rp,g}(SE) - 2\right)r_{rp}\cos\Theta_{SE}, y^{SE}_{gr1} - \left(N_{rp,g}(SE) - 2\right)r_{rp}\sin\Theta_{SE}), (x^{SE}_{gr2}, y^{SE}_{gr2})\right] \tag{2.104}$$

<u>Case 4: Southwestern field quarter with maximum number of field devices out of the gateway effective range</u>

$$If\ M_1{}'(1) = N\left(L_j{}'^{SW}(1)\right) \longrightarrow\ (x_m^1 =\ x_m +\ x_{m+}),(y_m^1 =\ y_m +\ y_{m+})\ for\ each\ S_m\ \epsilon\ S_m^{out}(SW) \tag{2.105}$$

$$A_{out}^1(SW)\ =\ \left(x_m^{1\,max}(SW) -\ x_m^{1\,min}(SW)\right) \times\ \left(y_m^{1\,max}(SW) -\ y_m^{1\,min}(SW)\right) \tag{2.106}$$

$$No.of\ required\ repeaters\ N_{rp}(SE) = \left|\frac{A_{out}^1(SW)}{\pi\,(r_{rp})^2}\right| \tag{2.107}$$

$$R_{xSW}\ =\ \left|\frac{x_m^{1\,max}(SW) -\ x_m^{1\,min}(SW)}{2r_{rp}}\right| \tag{2.108}$$

$$R_{ySW}\ =\ \left|\frac{y_m^{1\,max}(SW) -\ y_m^{1\,min}(SW)}{2r_{rp}}\right| \tag{2.109}$$

$$No.of\ required\ repeaters\ \ N_{rp}(SW) =\ R_{xSW}\ \times\ R_{ySW} \tag{2.110}$$

$$x_r^{nx}(SW) =\ \ x_m^{1\,min}(SW) + r_{rp}(2n_x - 1)\ where\ n_x\ \epsilon\ \{1,2,3\ \ldots\ldots\ ,\ R_{xSW}\} \tag{2.111}$$

$$y_r^{ny}(SW) =\ \ y_m^{1\,min}(SW) + r_{rp}\left(2n_y - 1\right)\ where\ n_y\ \epsilon\ \left\{1,2,3\ \ldots\ldots\ ,\ R_{ySW}\right\} \tag{2.112}$$

$$xy_{\mathrm{rSW}(R_{xSW} \times R_{ySW})} = \begin{bmatrix} (x_{r1}^{SW},\ y_{r1}^{SW}) & (x_{r1}^{SW},\ y_{r2}^{SW}) & (x_{r1}^{SW},\ y_{r3}^{SW}) & \cdots & (x_{r1}^{SW},\ y_{rR_{ySW}}^{SW}) \\ (x_{r2}^{SW},\ y_{r1}^{SW}) & (x_{r2}^{SW},\ y_{r2}^{SW}) & (x_{r2}^{SW},\ y_{r3}^{SW}) & \cdots & (x_{r2}^{SW},\ y_{rR_{ySW}}^{SW}) \\ \vdots & \vdots & \vdots & \cdots & \vdots \\ \vdots & \vdots & \vdots & \cdots & \vdots \\ (x_{rR_{xSW}}^{SW},\ y_{r1}^{SW}) & (x_{rR_{xSW}}^{SW},\ y_{r2}^{SW}) & \cdots & \cdots & (x_{rR_{xSW}}^{SW},\ y_{rR_{ySW}}^{SW}) \end{bmatrix} \tag{2.113}$$

$$xy_{r\mathrm{SW}(R_{xSW} \times R_{ySW})}^i = \begin{bmatrix} \sqrt{(|x_i - x_{r1}^{SW}|)^2 + (|y_i - y_{r1}^{SW}|)^2} & \sqrt{(|x_i - x_{r1}^{SW}|)^2 + (|y_i - y_{r2}^{SW}|)^2} & \cdots & \sqrt{(|x_i - x_{r1}^{SW}|)^2 + \left(\left|y_i - y_{rR_{ySW}}^{SW}\right|\right)^2} \\ \sqrt{(|x_i - x_{r2}^{SW}|)^2 + (|y_i - y_{r1}^{SW}|)^2} & \sqrt{(|x_i - x_{r2}^{SW}|)^2 + (|y_i - y_{r2}^{SW}|)^2} & \cdots & \sqrt{(|x_i - x_{r2}^{SW}|)^2 + \left(\left|y_i - y_{rR_{ySW}}^{SW}\right|\right)^2} \\ \vdots & \vdots & \cdots & \vdots \\ \vdots & \vdots & \cdots & \vdots \\ \sqrt{(|x_i - x_{rR_{xSW}}^{SW}|)^2 + (|y_i - y_{r1}^{SW}|)^2} & \sqrt{(|x_i - x_{rR_{xSW}}^{SW}|)^2 + (|y_i - y_{r2}^{SW}|)^2} & \cdots & \sqrt{(|x_i - x_{rR_{xSW}}^{SW}|)^2 + \left(\left|y_i - y_{rR_{ySW}}^{SW}\right|\right)^2} \end{bmatrix}$$

$$where\ S_i\ \epsilon\ S_m^{out}(SW) \tag{2.114}$$

$$For\ a\ repeater\ coordinates\ of\ \left(x_r^{nx}(SW), y_r^{ny}(SE)\right), if\ d_{rf} <\ d_{rf}^{min}\ , the\ point\ will\ be\ excluded \tag{2.115}$$

$$d_{r,1}^{\min 1}(SW) =\ \sqrt{(|x_{r1}^{SE} - x_1^1|)^2 + (|y_{r1}^{SE} - y_1^1|)^2} \tag{2.116}$$

$$if\ d_{r,1}^{\min 1}(SW) >\ r_{rp} +\ r_1 \tag{2.117}$$

$$N_{rp,g}(SW) = \left|\frac{d_{r,1}^{\min 1}(SW) - r_{rp} - r_1}{r_{rp}}\right| + 1 \tag{2.118}$$

Straight line equation between the nearesst repeater and the gateway

$$y = ax + b \tag{2.119}$$

$$a = \frac{y_{r1}^{SW} - y_1^1}{x_{r1}^{SW} - x_1^1} \tag{2.120}$$

$$b = y_1^1 - ax_1^1 = y_{r1}^{SW} - ax_{r1}^{SW} \tag{2.121}$$

$Finding\ \ the\ intersection\ points\ (x_{gr1}^{SW}, y_{gr1}^{SW})\ and\ \ (x_{gr2}^{SW}, y_{gr2}^{SW})\ \ between\ the\ straight\ line\ quation$
$and\ the\ range\ circles\ equations\ of\ the\ gateway\ and\ the\ nearest\ repaeter, respectively$

$$(x - x_{r1}^{SW})^2 + (y - y_{r1}^{SW})^2 = \left(r_{rp}\right)^2, (x - x_1^1)^2 + (y - y_1^1)^2 = (r_1)^2 \tag{2.122}$$

$$where\ \ x_1^1 > \ x_{gr1}^{SW} < x_{r1}^{SW}\ , x_1^1 > \ x_{gr2}^{SW} < x_{r1}^{SW} \tag{2.123}$$

$$and\ \ y_1^1 > \ y_{gr1}^{SW} < y_{r1}^{SW}\ , y_1^1 > \ y_{gr2}^{SW} < y_{r1}^{SW} \tag{2.124}$$

$$\Theta_{SE} = \tan^{-1} \frac{y_{gr2}^{SW} - y_{gr1}^{SW}}{x_{gr2}^{SW} - x_{gr1}^{SW}} \tag{2.125}$$

$$d_{r,1}^{\min 1}(SW) - r_{rp} - r_1 = \sqrt{\left(\left|x_{gr2}^{SW} - x_{gr1}^{SW}\right|\right)^2 + \left(\left|y_{gr2}^{SW} - y_{gr1}^{SW}\right|\right)^2} \tag{2.126}$$

$$xy_{\mathrm{grSW}\left(1 \times N_{rp,g}(SW)\right)} = \left[(x_{gr1}^{SW}, y_{gr1}^{SW}), (x_{gr1}^{SW} - r_{rp}\cos\Theta_{SW}\ , y_{gr1}^{SW} - r_{rp}\sin\Theta_{SW}), (x_{gr1}^{SW} - 2r_{rp}\cos\Theta_{SW}\ ,\ y_{gr1}^{SW} - 2r_{rp}\sin\Theta_{SW}), (x_{gr1}^{SW} - 3r_{rp}\cos\Theta_{SW}\ ,\ y_{gr1}^{SW} - 3r_{rp}\sin\Theta_{SW}), \dots\dots\dots\dots, (x_{gr1}^{SW} - \left(N_{rp,g}(SW) - 2\right)r_{rp}\cos\Theta_{SW}, y_{gr1}^{SW} - \left(N_{rp,g}(SW) - 2\right)r_{rp}\sin\Theta_{SW}), (x_{gr2}^{SW},\ y_{gr2}^{SW})\right] \tag{2.127}$$

$$d_j{}^1(1) = \{d_{2,1}{}^1, d_{3,1}{}^1, d_{4,1}{}^1, d_{5,1}{}^1, \dots\dots\dots\dots\dots, d_{n,1}{}^1\} \tag{2.128}$$

$$d_j{}^1(1) = d_{j(NE)}{}^1(1) \cup d_{j(NW)}{}^1(1) \cup d_{j(SE)}{}^1(1) \cup d_{j(SW)}{}^1(1) \tag{2.129}$$

$$d_j{}^{1\,out}(1) = d_{j(NE)}{}^{1\,out}(1) \cup d_{j(NW)}{}^{1\,out}(1) \cup d_{j(SE)}{}^{1\,out}(1) \cup d_{j(SW)}{}^{1\,out}(1) \tag{2.130}$$

$$d_j{}^{1\,in}(1) = d_{j(NE)}{}^{1\,in}(1) \cup d_{j(NW)}{}^{1\,in}(1) \cup d_{j(SE)}{}^{1\,in}(1) \cup d_{j(SW)}{}^{1\,in}(1) \tag{2.131}$$

$$d_j{}^1(1) = d_j{}^{1\,in}(1) \cup d_j{}^{1\,out}(1) \tag{2.132}$$

$$S_m^{out \to in}(NE) = L_j{}'^{NE}(1) \text{ - } L_j{}'^{NE}(1) \cap L_j{}^{1\,\prime NE}(1)$$

$For\ the\ gateway, N(L_j^{1'}(1))\ and\ \ N\left(L_j{}'(1)\right)\ , there\ will\ be\ 3\ options:$

$$\begin{gathered} N(L_j^{1'}(1)) = \ N\left(L_j{}'(1)\right) \longrightarrow movement\ from\ field\ devices\ and\ gateway\ towards\ each\ other \\ equations\ (35) and\ (36) \\ N(L_j^{1'}(1))\ <\ N\left(L_j{}'(1)\right) \longrightarrow movement\ from\ field\ devices\ and\ gateway\ towards\ each\ other \\ equations\ (35) and\ (36) \\ N(L_j^{1'}(1)) > \ N\left(L_j{}'(1)\right) \longrightarrow movement\ from\ field\ devices\ towards\ gateway\ and\ from\ the \\ gateway\ to\ the\ field\ devices\ with\ h_x\ and\ h_y\ \ increment\ factors\ where\ h_x\ and\ h_y\ \ are\ less \\ than\ one, till\ N(L_j^{1'}(1)) = \ \ \&N\left(L_j{}'(1)\right)\ or\ N(L_j^{1'}(1))\ <\ N\left(L_j{}'(1)\right) \end{gathered} \tag{2.133}$$

$The\ 2nd\ round\ of\ movement\ will\ be\ the\ movement\ of\ the\ field\ devices\ with\ the$

$$2nd\ maximum\ number\ of\ field\ devices\ out\ of\ range\ of\ the\ gateway\ towards\ the\ gateway\ or\ towards\ the\ other\ two\ quarters.$$

Table 2.3- Illustration for the various possibilities of number of field devices outside the effective range of the gateway sorted from maximum to minimum at the northeastern, northwestern, southeastern and southwestern field quarters

No.	Possibility of $M_1{}'$
1	$M_1{}' = \left[N\left(L_j{}'^{NE}(1)\right),\ N\left(L_j{}'^{NW}(1)\right),\ N\left(L_j{}'^{SE}(1)\right),\ N\left(L_j{}'^{SW}(1)\right)\right]$
2	$M_1{}' = \left[N\left(L_j{}'^{NE}(1)\right),\ N\left(L_j{}'^{NW}(1)\right),\ N\left(L_j{}'^{SW}(1)\right),\ N\left(L_j{}'^{SE}(1)\right)\right]$
3	$M_1{}' = \left[N\left(L_j{}'^{NE}(1)\right),\ N\left(L_j{}'^{SE}(1)\right),\ N\left(L_j{}'^{NW}(1)\right),\ N\left(L_j{}'^{SE}(1)\right)\right]$
4	$M_1{}' = \left[N\left(L_j{}'^{NE}(1)\right),\ N\left(L_j{}'^{SE}(1)\right),\ N\left(L_j{}'^{SW}(1)\right),\ N\left(L_j{}'^{NW}(1)\right)\right]$
5	$M_1{}' = \left[N\left(L_j{}'^{NE}(1)\right),\ N\left(L_j{}'^{SW}(1)\right),\ N\left(L_j{}'^{NW}(1)\right),\ N\left(L_j{}'^{SE}(1)\right)\right]$
6	$M_1{}' = \left[N\left(L_j{}'^{NE}(1)\right),\ N\left(L_j{}'^{SW}(1)\right),\ N\left(L_j{}'^{SE}(1)\right),\ N\left(L_j{}'^{NW}(1)\right)\right]$
7	$M_1{}' = \left[N\left(L_j{}'^{NW}(1)\right),\ N\left(L_j{}'^{NE}(1)\right),\ N\left(L_j{}'^{SE}(1)\right),\ N\left(L_j{}'^{SW}(1)\right)\right]$
8	$M_1{}' = \left[N\left(L_j{}'^{NW}(1)\right),\ N\left(L_j{}'^{NE}(1)\right),\ N\left(L_j{}'^{SW}(1)\right),\ N\left(L_j{}'^{SE}(1)\right)\right]$
9	$M_1{}' = \left[N\left(L_j{}'^{NW}(1)\right),\ N\left(L_j{}'^{SE}(1)\right),\ N\left(L_j{}'^{SW}(1)\right),\ N\left(L_j{}'^{NE}(1)\right)\right]$
10	$M_1{}' = \left[N\left(L_j{}'^{NW}(1)\right),\ N\left(L_j{}'^{SE}(1)\right),\ N\left(L_j{}'^{NE}(1)\right),\ N\left(L_j{}'^{SW}(1)\right)\right]$
11	$M_1{}' = \left[N\left(L_j{}'^{NW}(1)\right),\ N\left(L_j{}'^{SW}(1)\right),\ N\left(L_j{}'^{NE}(1)\right),\ N\left(L_j{}'^{SE}(1)\right)\right]$
12	$M_1{}' = \left[N\left(L_j{}'^{NW}(1)\right),\ N\left(L_j{}'^{SW}(1)\right),\ N\left(L_j{}'^{SE}(1)\right),\ N\left(L_j{}'^{NE}(1)\right)\right]$
13	$M_1{}' = \left[N\left(L_j{}'^{SE}(1)\right),\ N\left(L_j{}'^{SW}(1)\right),\ N\left(L_j{}'^{NE}(1)\right),\ N\left(L_j{}'^{NW}(1)\right)\right]$
14	$M_1{}' = \left[N\left(L_j{}'^{SE}(1)\right),\ N\left(L_j{}'^{SW}(1)\right),\ N\left(L_j{}'^{NW}(1)\right),\ N\left(L_j{}'^{NE}(1)\right)\right]$
15	$M_1{}' = \left[N\left(L_j{}'^{SE}(1)\right),\ N\left(L_j{}'^{NW}(1)\right),\ N\left(L_j{}'^{NE}(1)\right),\ N\left(L_j{}'^{SW}(1)\right)\right]$
16	$M_1{}' = \left[N\left(L_j{}'^{SE}(1)\right),\ N\left(L_j{}'^{NW}(1)\right),\ N\left(L_j{}'^{SW}(1)\right),\ N\left(L_j{}'^{NE}(1)\right)\right]$
17	$M_1{}' = \left[N\left(L_j{}'^{SE}(1)\right),\ N\left(L_j{}'^{NE}(1)\right),\ N\left(L_j{}'^{NW}(1)\right),\ N\left(L_j{}'^{SW}(1)\right)\right]$
18	$M_1{}' = \left[N\left(L_j{}'^{SE}(1)\right),\ N\left(L_j{}'^{NE}(1)\right),\ N\left(L_j{}'^{SW}(1)\right),\ N\left(L_j{}'^{NW}(1)\right)\right]$
19	$M_1{}' = \left[N\left(L_j{}'^{SW}(1)\right),\ N\left(L_j{}'^{NE}(1)\right),\ N\left(L_j{}'^{NW}(1)\right),\ N\left(L_j{}'^{SE}(1)\right)\right]$
20	$M_1{}' = \left[N\left(L_j{}'^{SW}(1)\right),\ N\left(L_j{}'^{NE}(1)\right),\ N\left(L_j{}'^{SE}(1)\right),\ N\left(L_j{}'^{NW}(1)\right)\right]$
21	$M_1{}' = \left[N\left(L_j{}'^{SW}(1)\right),\ N\left(L_j{}'^{NW}(1)\right),\ N\left(L_j{}'^{SE}(1)\right),\ N\left(L_j{}'^{NE}(1)\right)\right]$
22	$M_1{}' = \left[N\left(L_j{}'^{SW}(1)\right),\ N\left(L_j{}'^{NW}(1)\right),\ N\left(L_j{}'^{NE}(1)\right),\ N\left(L_j{}'^{SE}(1)\right)\right]$
23	$M_1{}' = \left[N\left(L_j{}'^{SW}(1)\right),\ N\left(L_j{}'^{SE}(1)\right),\ N\left(L_j{}'^{NE}(1)\right),\ N\left(L_j{}'^{NW}(1)\right)\right]$
24	$M_1{}' = \left[N\left(L_j{}'^{SW}(1)\right),\ N\left(L_j{}'^{SE}(1)\right),\ N\left(L_j{}'^{NW}(1)\right),\ N\left(L_j{}'^{SE}(1)\right)\right]$

The Second Round

$$\sum d_{2nd} = \min\{\sum d_g^2 \ ,\sum d_{d1}^2 \ ,\sum d_{d2}^2 \ ,\sum d^1\} \qquad (2.134)$$

$$N_1^2(V) = \min\{N_1(V_g^2)\ , N_1(V_{d1}^2)\ , N_1(V_{d2}^2)\ , N_1(V^1)\} \qquad (2.135)$$

Table 2.4- Illustration for the various possibilities of minimum average total mutual distances in matrix d and total number of out of range conditions in matrix V for probable relocation of the second group of field devices to the direction of the gateway, the first neighbor group of field devices and the second neighbor group of field devices

No.	$\boldsymbol{N_1^2(V)}$	$\sum \boldsymbol{d_{2nd}}$	Relocating Decision
1	$N_1(V_g^2)$	$\sum d_g^2$	Towards the gateway
2	$N_1(V_g^2)$	$\sum d_{d1}^2$	Towards the gateway
3	$N_1(V_g^2)$	$\sum d_{d2}^2$	Towards the gateway
4	$N_1(V_{d1}^2)$	$\sum d_{d1}^2$	Towards the 1st group of field devices
5	$N_1(V_{d1}^2)$	$\sum d_g^2$	Towards the 1st group of field devices
6	$N_1(V_{d1}^2)$	$\sum d_{d2}^2$	Towards the 1st group of field devices
7	$N_1(V_{d2}^2)$	$\sum d_g^2$	Towards the 2nd group of field devices
8	$N_1(V_{d2}^2)$	$\sum d_{d1}^2$	Towards the 2nd group of field devices
9	$N_1(V_{d2}^2)$	$\sum d_{d2}^2$	Towards the 2nd group of field devices
10	$N_1(V^1)$	$\sum d^1$	Towards the gateway
11	$N_1(V^1)$	$\sum d_g^2$	Towards the gateway
12	$N_1(V^1)$	$\sum d_{d1}^2$	Towards the 1st group of field devices
13	$N_1(V^1)$	$\sum d_{d2}^2$	Towards the 2nd group of field devices
14	$N_1(V_g^2)$	$\sum d^1$	Towards the gateway
15	$N_1(V_{d1}^2)$	$\sum d^1$	Towards the 1st group of field devices
16	$N_1(V_{d2}^2)$	$\sum d^1$	Towards the 2nd group of field devices

The Third Round

$$\sum d_{3rd} = \min\{\sum d_g^3 \ ,\sum d_{d1}^3 \ ,\sum d_{d2}^3 \ ,\sum d^2\} \qquad (2.136)$$

$$N_1^3(V) = \min\{N_1(V_g^3)\ , N_1(V_{d1}^3)\ , N_1(V_{d2}^3)\ , N_1(V^2)\} \qquad (2.137)$$

Table 2.5- Illustration for the various possibilities of minimum average total mutual distances in matrix d and total number of out of range conditions in matrix V for probable relocation of the third group of field devices to the direction of the gateway, the first neighbor group of field devices and the second neighbor group of field devices

No.	$\boldsymbol{N_1^3(V)}$	$\sum \boldsymbol{d_{3rd}}$	Relocating Decision
1	$N_1(V_g^3)$	$\sum d_g^3$	Towards the gateway
2	$N_1(V_g^3)$	$\sum d_{d1}^3$	Towards the gateway
3	$N_1(V_g^3)$	$\sum d_{d2}^3$	Towards the gateway

4	$N_1(V_{d1}^3)$	$\sum d_{d1}^3$	Towards the 1st group of field devices
5	$N_1(V_{d1}^3)$	$\sum d_g^3$	Towards the 1st group of field devices
6	$N_1(V_{d1}^3)$	$\sum d_{d2}^3$	Towards the 1st group of field devices
7	$N_1(V_{d2}^3)$	$\sum d_g^3$	Towards the 2nd group of field devices
8	$N_1(V_{d2}^3)$	$\sum d_{d1}^3$	Towards the 2nd group of field devices
9	$N_1(V_{d2}^3)$	$\sum d_{d2}^3$	Towards the 2nd group of field devices
10	$N_1(V^2)$	$\sum d^2$	Towards the gateway
11	$N_1(V^2)$	$\sum d_g^3$	Towards the gateway
12	$N_1(V^2)$	$\sum d_{d1}^3$	Towards the 1st group of field devices
13	$N_1(V^2)$	$\sum d_{d2}^3$	Towards the 2nd group of field devices
14	$N_1(V_g^3)$	$\sum d^2$	Towards the gateway
15	$N_1(V_{d1}^3)$	$\sum d^2$	Towards the 1st group of field devices
16	$N_1(V_{d2}^3)$	$\sum d^2$	Towards the 2nd group of field devices

The Fourth Round

$$\sum d_{4th} = \min\{\sum d_g^4 \ ,\sum d_{d1}^4 \ ,\sum d_{d2}^4 \ ,\sum d^3\} \qquad (2.138)$$

$$N_1^4(V) = \min\{N_1(V_g^4)\ ,N_1(V_{d1}^4)\ ,N_1(V_{d2}^4)\ ,N_1(V^3)\} \qquad (2.139)$$

Table 2.6- Illustration for the various possibilities of minimum average total mutual distances in matrix d and total number of out of range conditions in matrix V for probable relocation of the fourth group of field devices to the direction of the gateway, the first neighbor group of field devices and the second neighbor group of field devices.

No.	$\boldsymbol{N_1^4(V)}$	$\boldsymbol{\sum d_{4th}}$	Relocating Decision
1	$N_1(V_g^4)$	$\sum d_g^4$	Towards the gateway
2	$N_1(V_g^4)$	$\sum d_{d1}^4$	Towards the gateway
3	$N_1(V_g^4)$	$\sum d_{d2}^4$	Towards the gateway
4	$N_1(V_{d1}^4)$	$\sum d_{d1}^4$	Towards the 1st group of field devices
5	$N_1(V_{d1}^4)$	$\sum d_g^4$	Towards the 1st group of field devices
6	$N_1(V_{d1}^4)$	$\sum d_{d2}^2$	Towards the 1st group of field devices
7	$N_1(V_{d2}^4)$	$\sum d_g^4$	Towards the 2nd group of field devices
8	$N_1(V_{d2}^4)$	$\sum d_{d1}^4$	Towards the 2nd group of field devices
9	$N_1(V_{d2}^4)$	$\sum d_{d2}^4$	Towards the 2nd group of field devices
10	$N_1(V^3)$	$\sum d^3$	Towards the gateway
11	$N_1(V^3)$	$\sum d_g^4$	Towards the gateway
12	$N_1(V^3)$	$\sum d_{d1}^4$	Towards the 1st group of field devices
13	$N_1(V^3)$	$\sum d_{d2}^4$	Towards the 2nd group of field devices
14	$N_1(V_g^4)$	$\sum d^3$	Towards the gateway

15	$N_1(V_{d1}^4)$	$\sum d^3$	Towards the 1st group of field devices
16	$N_1(V_{d2}^4)$	$\sum d^3$	Towards the 2nd group of field devices

Adding Neighbor Repeaters:

$$K_j''(n) = [K_{m1}(n), \dots \dots \dots \dots \dots \dots \dots, K_{mk}(n)] \tag{2.140}$$

$$L_j''(n) = [L_{t1}(n), \dots \dots \dots \dots \dots \dots \dots, L_{tk}(n)] \tag{2.141}$$

$$Where \begin{cases} j \neq 1 \\ j \neq n \\ K_j(i) \neq 0 \\ \{t1, \dots, tk\} \subset \{1,2,3, \dots \dots, n-1, n+1, \dots, \dots, nr\} \\ \{m1, \dots, mk\} \subset \{1,2,3, \dots \dots, n-1, n+1, \dots, \dots, nr\} \\ \min\left(d_j{}^{out}(n)\right) = d_{t1,n} \; or \; d_{n,t1} \\ \min\left(d_j{}^{in}(n)\right) = d_{m1,n} \; or \; d_{n,m1} \\ \max\left(d_j{}^{out}(n)\right) = d_{tk,n} \; or \; d_{n,tk} \\ \max\left(d_j{}^{out}(n)\right) = d_{mk,n} \; or \; d_{n,mk} \end{cases} \tag{2.142}$$

$$Straight\ line\ equation\ between\ the\ field\ device\ and\ the\ fth\ out\ of\ range\ device$$

$$y = ax + b \tag{2.143}$$

$$a = \frac{y_q^f - y_n}{x_q^f - x_n} \tag{2.144}$$

$$NB_{rp}^n = NB_{min} - N\left(K_j''(i)\right) \tag{2.145}$$

$$b = y_n - ax_n = y_q^f - ax_q^f \; where \; q \in \{t1, \dots, tk\} \; and \; f = 1{:}\, NB_{rp}^n \tag{2.146}$$

$$Finding\ \ the\ intersection\ points\ (x_{rq,f}^{1n}, y_{rq,f}^{1n}), (x_{rq,f}^{2n}, y_{rq,f}^{2n})\ \ between\ the\ straight\ line$$
$$and\ the\ range\ circles\ of\ the\ field\ device\ (n)\ and\ \ the\ field\ device\ at\ \left(x_q^f, y_q^f\right), respetively$$

$$(x - x_n)^2 + (y - y_n)^2 = (r_n)^2 \tag{2.147}$$

$$\left(x - x_q^f\right)^2 + \left(y - y_q^f\right)^2 = (r_n)^2 \tag{2.148}$$

$$d_q^n = \sqrt{\left(\left|x_{rq,f}^{2n} - x_{rq,f}^{1n}\right|\right)^2 + \left(\left|y_{rq,f}^{2n} - y_{rq,f}^{1n}\right|\right)^2} \tag{2.149}$$

$$If\ d_q^n < \left(2r_{rp}\right), the\ repeater\ will\ be\ installed\ at\ a\ distance\ \left(\frac{d_q^n}{2}\right)\ d_{rf}^{min} \tag{2.150}$$

$$If\ d_q^n > (2r_{rp}) \begin{cases} d_q^{n''} = d_q^n - \left(\left\lfloor \frac{d_q^n}{2r_{rp}} \right\rfloor\right)(2r_{rp}) \\ Repeater\ can\ be\ installed\ at\ distances\ \frac{d_q^{n''}}{3}, \frac{2d_q^{n''}}{3}\ and\ d_q^{n''}\ from\ (x_{rq,f}^{1n}, y_{rq,f}^{1n}) \\ where\ d_{rf}^{min}\ is\ not\ exceeded \end{cases} \quad (2.151)$$

$The\ equation\ of\ the\ fth\ repeater\ for\ the\ field\ device\ (n)\ near\ the\ device\ q$

$$(x - x_{rq,f}^n)^2 + (y - y_{rq,f}^n)^2 = (r_{rp})^2 \quad (2.152)$$

$After\ each\ addition\ of\ a\ new\ repeater, nr\ will\ be\ incremented\ by\ 1\ and\ array\ K_J''(n)\ will\ be\ recalculated$

$$K_J''(i,p) = The\ sorting\ index\ of\ the\ repeater\ p\ in\ the\ array\ K_J''(i)\ where\ i \in \{2,\ldots,n\}\ \&\ p \in \{1,\ldots,nr\} \quad (2.153)$$
$$K_J''(i,p) = 0\ if\ field\ device\ i\ and\ repeater\ p\ are\ not\ neighbour\ devices$$

Optimization of Overall Number of Repeaters:

$$W_{\mathrm{i,p}\ (\mathrm{n}-1)\times nr'} = \begin{bmatrix} K_J''(2,1) & K_J''(2,2) & K_J''(2,3) & K_J''(2,4) & K_J''(2,5) & \ldots & \ldots & K_J''(2,nr') \\ K_J''(3,1) & K_J''(3,2) & K_J''(3,3) & K_J''(3,4) & K_J''(3,5) & \ldots & \ldots & K_J''(3,nr') \\ K_J''(4,1) & K_J''(4,2) & K_J''(4,3) & K_J''(4,4) & K_J''(4,5) & \ldots & \ldots & K_J''(4,nr') \\ K_J''(5,1) & K_J''(5,2) & K_J''(5,3) & K_J''(5,4) & K_J''(5,5) & \ldots & \ldots & K_J''(5,nr') \\ K_J''(6,1) & K_J''(6,2) & K_J''(6,3) & K_J''(6,4) & K_J''(6,5) & \ldots & \ldots & K_J''(6,nr') \\ \vdots & \vdots & \vdots & \vdots & \vdots & \vdots & \vdots & \vdots \\ \vdots & \vdots & \vdots & \vdots & \vdots & \vdots & \vdots & \vdots \\ K_J''(n,1) & K_J''(n,2) & K_J''(n,3) & K_J''(n,4) & K_J''(n,5) & \ldots & \ldots & K_J''(n,nr') \end{bmatrix} \quad (2.154)$$

$$K_J''(i,RP)\ For\ a\ specific\ repeater\ RP \in \{1,2,3,\ldots,\ldots,\ nr'\} \quad (2.155)$$

$$W_{\mathrm{i},RP} = [K_J''(2,RP), K_J''(3,RP), K_J''(4,RP), K_J''(5,RP), K_J''(6,RP), \ldots, \ldots, K_J''(n,RP)] \quad (2.156)$$

$$W'_{\mathrm{i},RP} = [K_J''(2,RP), K_J''(3,RP), K_J''(4,RP), K_J''(5,RP), K_J''(6,RP), \ldots, \ldots, K_J''(n,RP)] \quad (2.157)$$

$$where\ K_J''(i,RP) \neq 0$$

$$W''_{\mathrm{i},RP} = W'_{\mathrm{i},RP} \cap \{1,2,\ldots,NB_{min}\} \quad (2.158)$$

$The\ repeater\ (RP)\ will\ be\ eliminated\ from\ the\ network\ if\ W''_{\mathrm{i},RP} = \{\ \}, otherwise\ it\ will\ be\ approved$

$to\ be\ among\ the\ final\ number\ of\ repeaters\ to\ reinforce\ the\ network$

MRFDD Method:

$$R_x^f = \left\lfloor \frac{x_f}{r_{rp}\ (1 + k_f)} \right\rfloor \quad (2.159)$$

$$R_y^f = \left\lfloor \frac{y_f}{r_{rp}\ (1 + k_f)} \right\rfloor \quad (2.160)$$

$where\ k_f\ is\ an\ area\ intefernce\ coefficient\ for\ the\ range\ circles\ of\ vales\ from\ 0.5\ to\ 0.9$

$$x_r^f(n_{xf}) = \left(\frac{r_{rp}}{2}\right)(1 + k_f)(2n_{xf} - 1)\ where\ n_{xf} \epsilon \{1,2,3 \ldots\ldots, R_x^f\} \tag{2.161}$$

$$x_r^f(n_{xf}) = k_f'(2n_{xf} - 1)\ where\ n_{xf} \epsilon \{1,2,3 \ldots\ldots, R_x^f\} \tag{2.162}$$

$$x_r^{f-}(n_{xf}) = x_r^f(n_{xf}) - k_f' \tag{2.163}$$

$$x_r^{f+}(n_{xf}) = x_r^f(n_{xf}) + k_f' \tag{2.164}$$

$$y_r^f(n_{yf}) = \left(\frac{r_{rp}}{2}\right)(1 + k_f)(2n_{yf} - 1)\ where\ n_{yf} \epsilon \{1,2,3 \ldots\ldots, R_y^f\} \tag{2.165}$$

$$y_r^f(n_{yf}) = k_f'(2n_{yf} - 1)\ where\ n_{yf} \epsilon \{1,2,3 \ldots\ldots, R_y^f\} \tag{2.166}$$

$$y_r^{f-}(n_{yf}) = y_r^f(n_{yf}) - k_f' \tag{2.167}$$

$$y_r^{f+}(n_{yf}) = y_r^f(n_{yf}) + k_f' \tag{2.168}$$

$$xy_{r\ (R_x^f \times R_y^f)}^f = \begin{bmatrix} (x_{r1}^f,\ y_{r1}^f) & (x_{r1}^f,\ y_{r2}^f) & (x_{r1}^f,\ y_{r3}^f) & \ldots & (x_{r1}^f,\ y_{rR_y^f}^f) \\ (x_{r2}^f,\ y_{r1}^f) & (x_{r2}^f,\ y_{r2}^f) & (x_{r2}^f,\ y_{r3}^f) & \ldots & (x_{r2}^f,\ y_{rR_y^f}^f) \\ \vdots & \vdots & \vdots & \ldots & \vdots \\ \vdots & \vdots & \vdots & \ldots & \vdots \\ (x_{rR_x^f}^f,\ y_{r1}^f) & (x_{rR_x^f}^f,\ y_{r2}^f) & \ldots & \ldots & (x_{rR_x^f}^f,\ y_{rR_y^f}^f) \end{bmatrix} \tag{2.169}$$

$For\ each\ single\ point\ identified\ by\ a\ single\ pair\ \left(x_r^f(n_{xf}), y_r^f(n_{yf})\right), the\ matrix\ xy_{2\times n}^{(n_{xf},n_{yf})}$
$will\ be\ formed\ to\ discover\ if\ there\ is\ at\ least\ a\ single\ field\ device\ located\ inside\ the$
$the\ rectangle\ formed\ by\ the\ points\ x_r^{f-}(n_{xf}), x_r^{f+}(n_{xf}), y_r^{f-}(n_{yf}), y_r^{f+}(n_{yf})$

$$xy_{2\times n}^{(n_{xf},n_{yf})} = \begin{bmatrix} \frac{x_1 - x_r^{f-}(n_{xf})}{x_r^{f+}(n_{xf}) - x_1} & \frac{x_2 - x_r^{f-}(n_{xf})}{x_r^{f+}(n_{xf}) - x_2} & \frac{x_3 - x_r^{f-}(n_{xf})}{x_r^{f+}(n_{xf}) - x_3} & \frac{x_4 - x_r^{f-}(n_{xf})}{x_r^{f+}(n_{xf}) - x_4} & \ldots & \ldots & \ldots & \frac{x_n - x_r^{f-}(n_{xf})}{x_r^{f+}(n_{xf}) - x_n} \\ \frac{y_1 - y_r^{f-}(n_{yf})}{y_r^{f+}(n_{yf}) - y_1} & \frac{y_2 - y_r^{f-}(n_{yf})}{y_r^{f+}(n_{yf}) - y_2} & \frac{y_3 - y_r^{f-}(n_{yf})}{y_r^{f+}(n_{yf}) - y_3} & \frac{y_4 - y_r^{f-}(n_{yf})}{y_r^{f+}(n_{yf}) - y_4} & \ldots & \ldots & \ldots & \frac{y_n - y_r^{f-}(n_{yf})}{y_r^{f+}(n_{yf}) - y_n} \end{bmatrix} \tag{2.170}$$

$If\ xy_{1,i}^{(n_{xf},n_{yf})} > 0\ \&\ xy_{2,i}^{(n_{xf},n_{yf})} > 0, then\ the\ field\ device\ of\ the\ index\ (i)\ is\ located\ inside$
$the\ rectangle\ formed\ by\ the\ points\ x_r^{f-}(n_{xf}), x_r^{f+}(n_{xf}), y_r^{f-}(n_{yf}), y_r^{f+}(n_{yf})\ and\ there\ will\ be$
$, otherwise\ the\ field\ device\ of\ the\ index\ (i)\ is\ located\ outside\ that\ rectangle$

$$S_i^{(n_{xf},n_{yf})} = [S_1^{(n_{xf},n_{yf})}, S_2^{(n_{xf},n_{yf})}, S_3^{(n_{xf},n_{yf})}, S_4^{(n_{xf},n_{yf})}, S_5^{(n_{xf},n_{yf})}, \ldots, \ldots, S_n^{(n_{xf},n_{yf})}] \tag{2.171}$$

$$For\ i = 1{:}n, If\ xy_{1,i}^{(n_{xf},n_{yf})} > 0\ \&\ xy_{2,i}^{(n_{xf},n_{yf})} > 0, then\ S_i^{(n_{xf},n_{yf})} = 1, otherwise\ S_i^{(n_{xf},n_{yf})} = 0 \tag{2.172}$$

$Only\ if\ S_i^{(n_{xf},n_{yf})} = \{\ \}, a\ repeater\ will\ be\ installed\ at\ inside\ \left(x_r^f(n_{xf}), y_r^f(n_{yf})\right)$
$the\ rectangle\ formed\ by\ the\ points\ x_r^{f-}(n_{xf}), x_r^{f+}(n_{xf}), y_r^{f-}(n_{yf}), y_r^{f+}(n_{yf})$

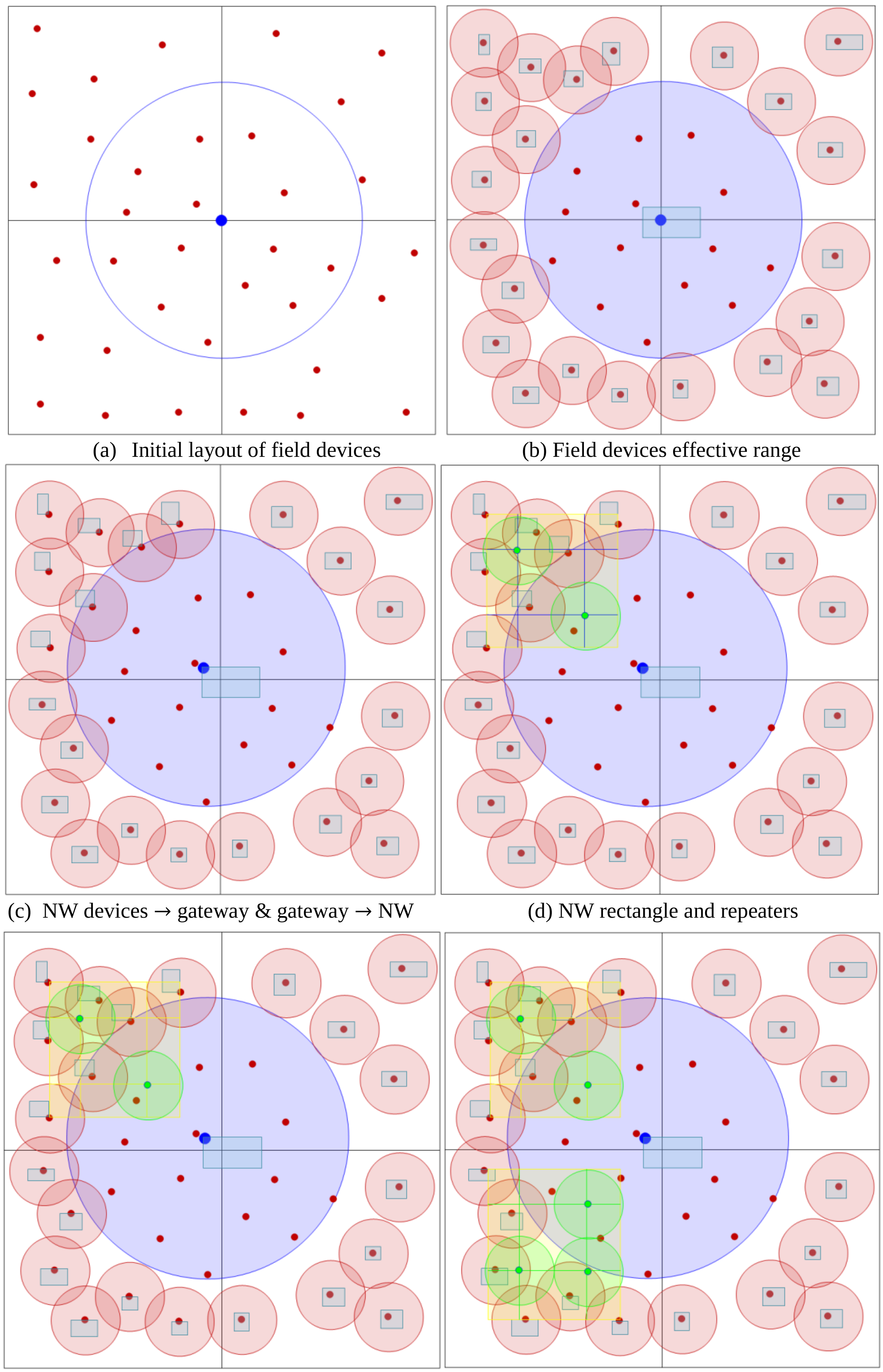

(a) Initial layout of field devices
(b) Field devices effective range
(c) NW devices → gateway & gateway → NW
(d) NW rectangle and repeaters
(e) SW devices → NW quarter
(f) SW rectangle and repeaters

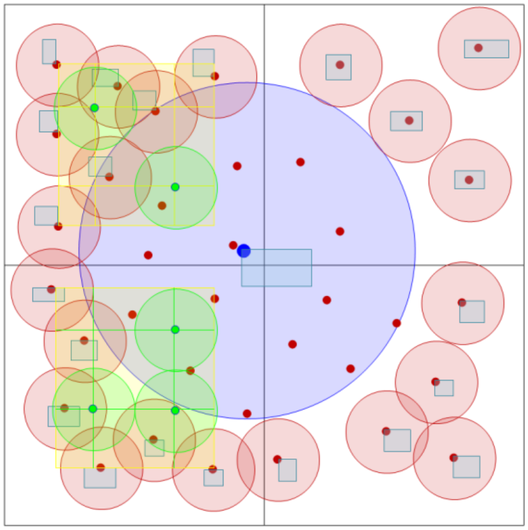

(g) SE devices towards gateway

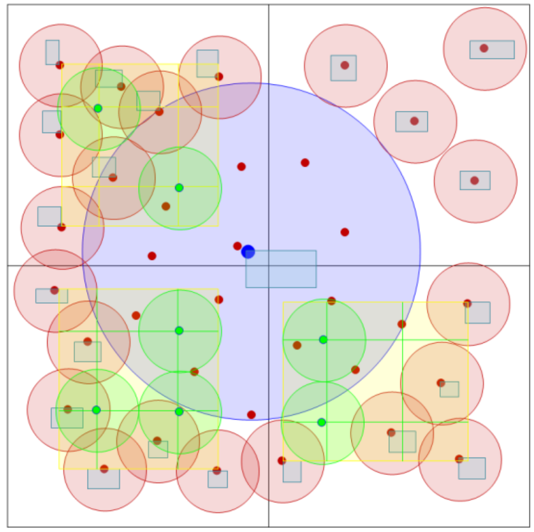

(h) SE rectangle and repeaters

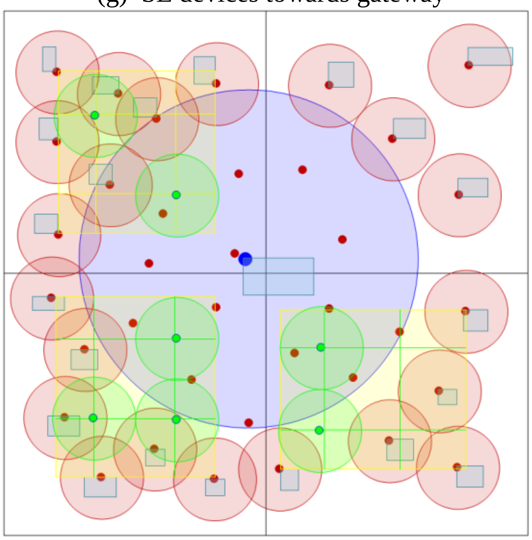

(i) NE devices towards gateway

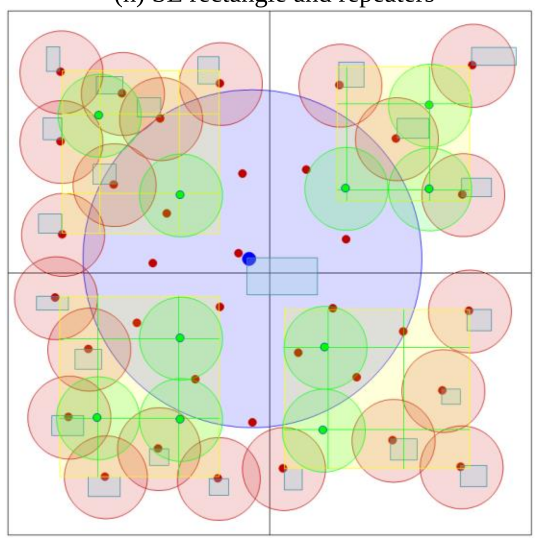

(j) NE rectangle and repeaters

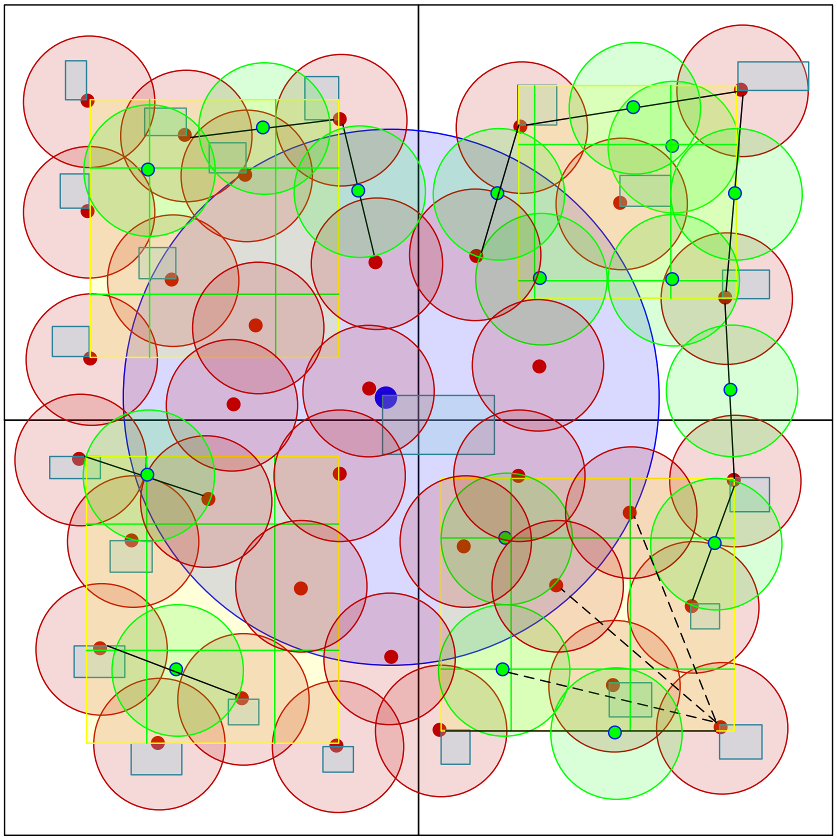

(k) Adding neighbor repeaters at Midway between devices and optimization

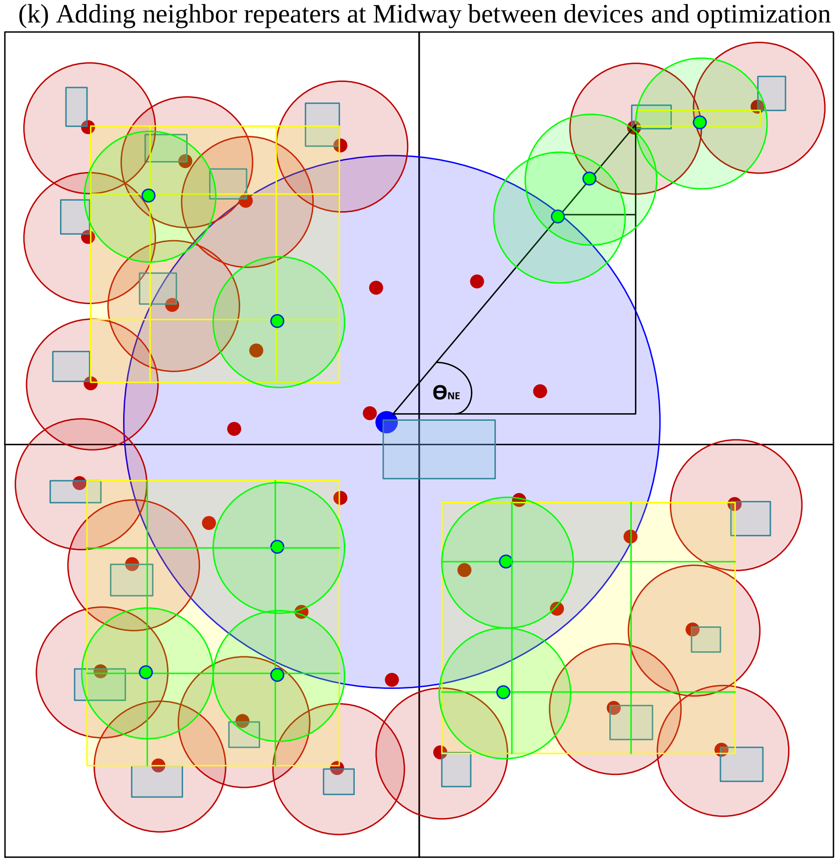

(l) Adding repeaters to approach distant isolated devices to the gateway

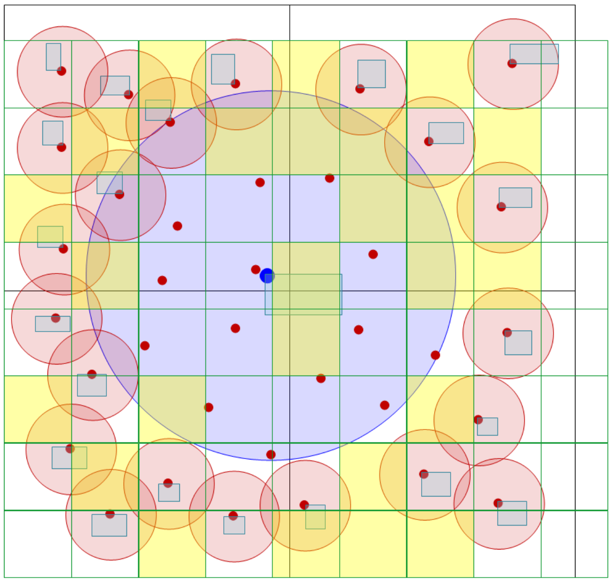

(m) Indicating the MRFDD method empty cells

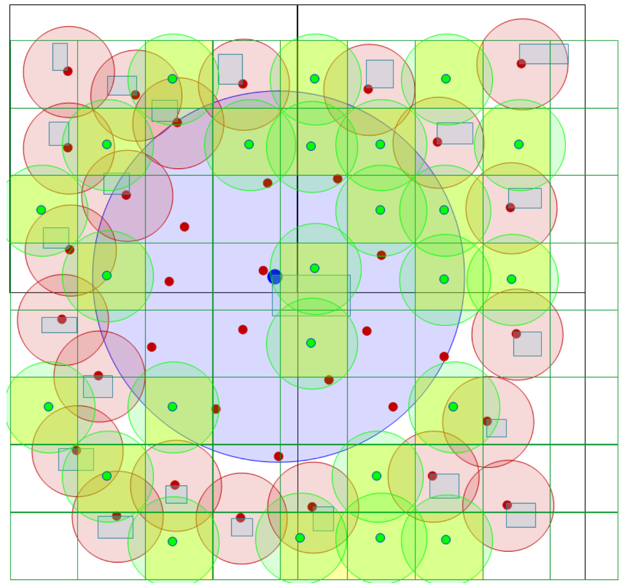

(n) Installing repeaters at the MRFDD method empty cells

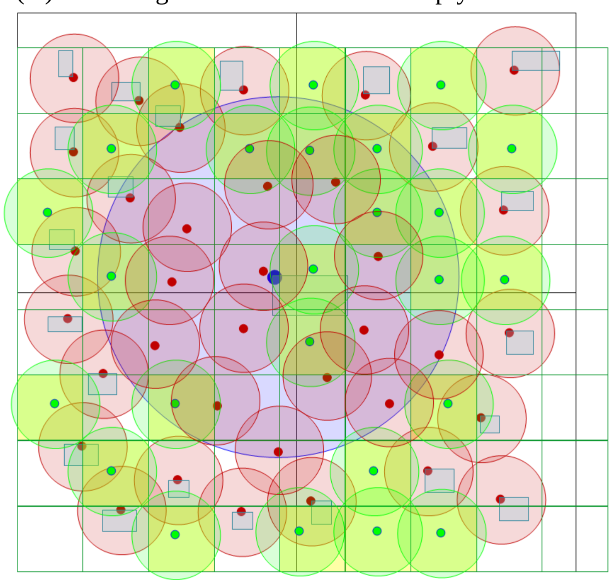

(o) Preparing for checking the neighbor devices

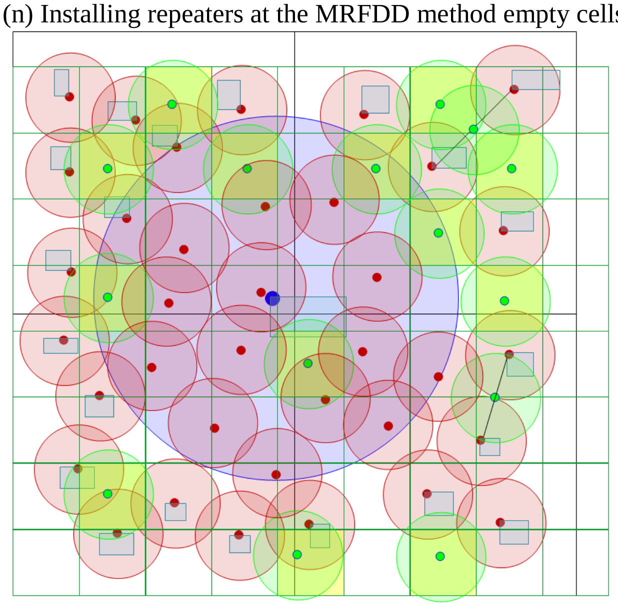

(p) Installing neighbor repeaters and optimization

Figure 2.3- Step by step illustration for both examples to implement the NRR and MRFDD methods in addition to adding neighbor devices and optimization of total number of repeaters

- $\boldsymbol{d}_{\mathbf{n}\times\mathbf{n}}$: Matrix of all the mutual distances between devices from 1 to n
- $\frac{\boldsymbol{C}_{\mathbf{n/2}\times\mathbf{n-1}}}{\boldsymbol{n\ even}}$: Reduced matrix for $d_{\mathrm{n}\times\mathrm{n}}$, where n is an even value.
- $\frac{\boldsymbol{C}_{\mathbf{n-1/2}\times\mathbf{n}}}{\boldsymbol{n\ odd}}$: Reduced matrix for $d_{\mathrm{n}\times\mathrm{n}}$, where n is an odd value.
- $\frac{R_{\mathrm{n/2}\times\mathrm{n-1}}}{n\ even}$ and $\frac{R_{\mathrm{n-1/2}\times\mathrm{n}}}{n\ odd}$: Matrices where $R_{i,j}$ = 1 if devices (i) and (j) are out of range.
- $\frac{V_{\mathrm{n/2}\times\mathrm{n-1}}}{n\ even}$ and $\frac{V_{\mathrm{n-1/2}\times\mathrm{n}}}{n\ odd}$: Matrices where $V_{i,j}$ = 1 if devices (i) and (j) are in range.

- $xy_{2\times n}$: Matrix referring to the Cartesian Coordinates of all the field devices from 1 (the gateway) to n.

- $\Delta xy_{4\times n}$: Matrix including the margins of mobility for all the field devices in the positive and negative directions of (x) and (y).

- S_i : An array of all field devices
- $S_m(NE), S_m(NW), S_m(SE), S_m(SW)$: An array of all field devices located at the northeastern, northwestern, southeastern and southwestern divisions of the field, respectively.
- x_f : width of the field , y_f : length of the field
- $K_j(i)$: An array including the indices (j)s of the field devices located in the effective range of the field device (i).
- $K_j'(i)$: An array including the indices (j)s of the field devices located out of the effective range of the field device (i), where $j \neq 1$ & $i \neq j$ & $K_j(i) \neq 0$ & $\{n1, n11\} \subset \{1,2,3, \dots \dots, n\}$.
- $L_j(i)$: An array including the indices (j)s of the field devices located out of the effective range of the field device (i).
- $L_j'(i)$: An array including the indices (j)s of the field devices located out of the effective range of the field device (i), where $j \neq 1$ & $i \neq j$ & $L_j(i) \neq 0$ & $\{n1, n11\} \subset \{1,2,3, \dots \dots, n\}$.
- $L_j'^{NE}(1)$: An array including the indices (j)s of the field devices located out of the effective range of the gateway located at the northeastern division of the field, where $j \neq 1$ & $i \neq j$ & $L_j(i) \neq 0$ & $\{n2, n22\} \subset \{1,2,3, \dots \dots, n\}$.
- $L_j'^{NW}(1)$: An array including the indices (j)s of the field devices located out of the effective range of the gateway located at the northwestern division of the field, where $j \neq 1$ & $i \neq j$ & $L_j(i) \neq 0$ & $\{n3, n33\} \subset \{1,2,3, \dots \dots, n\}$.
- $L_j'^{SE}(1)$: An array including the indices (j)s of the field devices located out of the effective range of the gateway located at the southeastern division of the field, where $j \neq 1$ & $i \neq j$ & $L_j(i) \neq 0$ & $\{n4, n44\} \subset \{1,2,3, \dots \dots, n\}$.
- $L_j'^{SE}(1)$: An array including the indices (j)s of the field devices located out of the effective range of the gateway located at the southwestern division of the field, where $j \neq 1$ & $i \neq j$ & $L_j(i) \neq 0$ & $\{n5, n55\} \subset \{1,2,3, \dots \dots, n\}$.
- M_1 : an array including the number of elements at each of the $L_j'^{NE}(1), L_j'^{NW}(1), L_j'^{SE}(1), L_j'^{SW}(1)$ arrays.
- M_1': an array including the number of elements at each of the $L_j'^{NE}(1), L_j'^{NW}(1), L_j'^{SE}(1), L_j'^{SW}(1)$ arrays, sorted from the array with the maximum number of elements to the array with the minimum number of elements.
- x_1^1, y_1^1 : Cartesian coordinates after relocation of the gateway at the first round.
- h_x, h_y : The increments by which the gateway will be relocated from minimum to maximum values of mobility margins.
- x_m^1, y_m^1 : Cartesian coordinates after relocation of field devices out of the effective range of the gateway at a specific quarter after the first round.
- $x_m^{1\,max}(NE)$: The maximum coordinate of x for the devices out of the effective range of the gateway located at the northeastern division after the first round relocation.
- $x_m^{1\,min}(NE)$: The minimum coordinate of x for the devices out of the effective range of the gateway located at the northeastern division after the first round relocation.
- $y_m^{1\,max}(NE)$: The maximum coordinate of y for the devices out of the effective range of the gateway located at the northeastern division after the first round relocation.
- $y_m^{1\,min}(NE)$: The minimum coordinate of y for the devices out of the effective range of the gateway located at the northeastern division after the first round relocation….
- $x_m^{1\,max}(NW)$: The maximum coordinate of x for the devices out of the effective range of the gateway located at the northwestern division after the first round relocation.
- $x_m^{1\,min}(NW)$: The minimum coordinate of x for the devices out of the effective range of the gateway located at the northwestern division after the first round relocation.
- $y_m^{1\,max}(NW)$: The maximum coordinate of y for the devices out of the effective range of the gateway located at the northwestern division after the first round relocation.
- $y_m^{1\,min}(NW)$: The minimum coordinate of y for the devices out of the effective range of the gateway located at the northwestern division after the first round relocation.

- $x_m^{1\,max}(SE)$: The maximum coordinate of x for the devices out of the effective range of the gateway located at the southeastern division after the first round relocation.
- $x_m^{1\,min}(SE)$: The minimum coordinate of x for the devices out of the effective range of the gateway located at the southeastern division after the first round relocation.
- $y_m^{1\,max}(SE)$: The maximum coordinate of y for the devices out of the effective range of the gateway located at the southeastern division after the first round relocation.
- $y_m^{1\,min}(SE)$: The minimum coordinate of y for the devices out of the effective range of the gateway located at the southeastern division after the first round relocation.
- $x_m^{1\,max}(SW)$: The maximum coordinate of x for the devices out of the effective range of the gateway located at the southwestern division after the first round relocation.
- $x_m^{1\,min}(SW)$: The minimum coordinate of x for the devices out of the effective range of the gateway located at the southwestern division after the first round relocation.
- $y_m^{1\,max}(SW)$: The maximum coordinate of y for the devices out of the effective range of the gateway located at the southwestern division after the first round relocation.
- $y_m^{1\,min}(SW)$: The minimum coordinate of y for the devices out of the effective range of the gateway located at the southwestern division after the first round relocation.
- $A_{out}^1(NE), A_{out}^1(NW), A_{out}^1(SE), A_{out}^1(SW)$: The area of the rectangular inside which the repeaters will be installed for the field devices out of the gateway effective range at the northeastern, the northwestern, the southeastern and the southwestern quarters of the field during the 1st round.
- $R_{xNE}, R_{xNW}, R_{xSE}, R_{xSE}$ and R_{xSW}: The number of divisions at the x direction of the rectangular at which repeaters will be installed for the field devices out of the gateway effective range at the northeastern, the northwestern, the southeastern and the southwestern quarters of the field during the 1st round.
- $R_{yNE}, R_{yNW}, R_{ySE}, R_{ySE}$ and R_{ySW}: The number of divisions at the y direction of the rectangular at which repeaters will be installed for the field devices out of the gateway effective range at the northeastern, the northwestern, the southeastern and the southwestern quarters of the field during the 1st round.
- $N_{rp}(NE), N_{rp}(NW), N_{rp}(SE), N_{rp}(SW)$: Number of repeaters that will be installed inside the rectangular for the field devices out of the gateway effective range at the northeastern, the northwestern, the southeastern and the southwestern quarters of the field during the 1st round.
- $xy_{\mathrm{rNE}(R_{xNE}\times R_{yNE})}, xy_{\mathrm{rNW}(R_{xNW}\times R_{yNW})}, xy_{\mathrm{rSE}(R_{xSE}\times R_{ySE})}, xy_{\mathrm{rSW}(R_{xSW}\times R_{ySW})}$: Matrices for the coordinates of the repeaters that will be installed inside the rectangular for the field devices out of the gateway effective range at the northeastern, the northwestern, the southeastern and the southwestern quarters of the field during the 1st round, respectively.
- $d_{r,1}^{\min 1}(NE), d_{r,1}^{\min 1}(NW), d_{r,1}^{\min 1}(SE), d_{r,1}^{\min 1}(SW)$: The distance between the gateway and the nearest repeater at the northeastern, the northwestern, the southeastern and the southwestern quarters of the field during the 1st round, respectively.
- $N_{rp,g}(NE), N_{rp,g}(NW), N_{rp,g}(SE), N_{rp,g}(SW)$: Number of the required repeaters to connect between the gateway effective range circle and the nearest repeater at a distant rectangle at the northeastern, the northwestern, the southeastern and the southwestern quarters of the field during the 1st round, respectively.
- $\Theta_{NE}, \Theta_{NW}, \Theta_{SE}, \Theta_{SW}$: The inclination angle of the line between the gateway and the nearest repeater at the northeastern, the northwestern, the southeastern and the southwestern quarters of the field during the 1st round, respectively.
- $xy_{\mathrm{grNE}\left(1\times N_{rp,g}(NE)\right)}, xy_{\mathrm{grNE}\left(1\times N_{rp,g}(NE)\right)}, xy_{\mathrm{grNE}\left(1\times N_{rp,g}(NE)\right)}, xy_{\mathrm{grNE}\left(1\times N_{rp,g}(NE)\right)}$: Arrays for the Cartesian coordinated at which repeaters will be additionally installed to connect between the gateway and a distant group of field devices at the northeastern, the northwestern, the southeastern and the southwestern quarters of the field during the 1st round, respectively.
- $\sum d_{2nd}$: the minimum value of the sum of the average distances at the matrix (d) resulting from the relocation of the second group of field devices at the second round towards the gateway and also towards the other neighbor two groups of field devices.
- $\sum d_g^2$ $,\sum d_{d1}^2$ $,\sum d_{d2}^2$ $,\sum d^1$: The average value of the sum of distances at the matrix (d) resulting from the relocation of the second group of field devices at the second round towards the gateway and also towards the other neighbor two groups of field devices, in addition to the average value of the sum of distances at the matrix (d) directly after finishing the first round.

- $N_1^2(V)$: The minimum value of the overall number of ones at the matrix (V) calculated after the relocation of the second group of field devices at the second round towards the gateway and also towards the other neighbor two groups of field devices.
- $N_1(V_g^2)$, $N_1(V_{d1}^2)$, $N_1(V_{d2}^2)$, $N_1(V^1)$: The overall number of ones at the matrix (V) calculated after the relocation of the second group of field devices at the second round towards the gateway and also towards the other neighbor two groups of field devices. in addition to the average value of the sum of distances at the matrix (d) directly after finishing the first round.
- $\sum d_{3rd}$: the minimum value of the sum of the average distances at the matrix (d) resulting from the relocation of the third group of field devices at the third round towards the gateway and also towards the other neighbor two groups of field devices.
- $\sum d_g^3$,$\sum d_{d1}^3$,$\sum d_{d2}^3$,$\sum d^2$: The average value of the sum of distances at the matrix (d) resulting from the relocation of the third group of field devices at the third round towards the gateway and also towards the other neighbor two groups of field devices, in addition to the average value of the sum of distances at the matrix (d) directly after finishing the second round.
- $N_1^3(V)$: The minimum value of the overall number of ones at the matrix (V) calculated after the relocation of the third group of field devices at the third round towards the gateway and also towards the other neighbor two groups of field devices.
- $N_1(V_g^3)$, $N_1(V_{d1}^3)$, $N_1(V_{d2}^3)$, $N_1(V^2)$: The overall number of ones at the matrix (V) calculated after the relocation of the third group of field devices at the third round towards the gateway and also towards the other neighbor two groups of field devices. in addition to the average value of the sum of distances at the matrix (d) directly after finishing the second round.
- $\sum d_{4th}$: the minimum value of the sum of the average distances at the matrix (d) resulting from the relocation of the fourth group of field devices at the fourth round towards the gateway and also towards the other neighbor two groups of field devices.
- $\sum d_g^4$,$\sum d_{d1}^4$,$\sum d_{d2}^4$,$\sum d^3$: The average value of the sum of distances at the matrix (d) resulting from the relocation of the fourth group of field devices at the fourth round towards the gateway and also towards the other neighbor two groups of field devices, in addition to the average value of the sum of distances at the matrix (d) directly after finishing the third round.
- $N_1^4(V)$: The minimum value of the overall number of ones at the matrix (V) calculated after the relocation of the fourth group of field devices at the fourth round towards the gateway and also towards the other neighbor two groups of field devices.
- $N_1(V_g^4)$, $N_1(V_{d1}^4)$, $N_1(V_{d2}^4)$, $N_1(V^3)$: The overall number of ones at the matrix (V) calculated after the relocation of the fourth group of field devices at the fourth round towards the gateway and also towards the other neighbor two groups of field devices. in addition to the average value of the sum of distances at the matrix (d) directly after finishing the third round.
- $K_J''(n)$: Array of the indices of the field devices located inside the effective range of the field device (n).
- $L_J''(n)$: Array of the indices of the field devices located outside the effective range of the field device (n).
- NB_{min}: The minimum required number of neighbor devices to each field device.
- NB_{rp}^n: The additional needed neighbor devices for the field device (n).
- $K_J''(i,p)$: The sorting index of the repeater p in the array $K_J''(i)$ where $i \in \{2, \dots, n\}$ & $p \in \{1, \dots, nr\}$.
- $W_{\mathrm{i,p}\ (\mathrm{n}-1)\times nr'}$: The optimization matrix to rectify the overall number of repeaters to a final optimal number.

2.6 Wireless HART Application on Commercial Ships

2.6.1 Tank Level Measurement System on Bulk Carriers

In [44], the research has provided a detailed description for the possibility of using wireless HART level transmitters on commercial ships through analyzing a wireless HART network dedicated to measuring the sea water levels in ballast water tanks. The research recommended the use of wireless HART radar transmitters for top side tanks and wireless HART pressure transmitters for double bottom tanks. The analysis in the research was based on adopting three effective ranges for the field devices and the gateway (30 meters, 76 meters and 152 meters) corresponding to three levels (high, medium and low) of infrastructural obstacles that might disrupt the propagation of the RF waves [44,68]. The research analysis was carried out for a tank level measurement system on a bulk carrier ship, taking into account that three values of field devices and gateway effective range were assumed to be applied at three operational statuses for the ship:

1. The ship is at sailing condition (effective range = 152 meters) (Figure 2.4-a)
2. The ship is at loading/ discharging condition using the ship cargo cranes (effective range = 76 meters) (Figure 2.4-b).
3. The ship is at loading/ discharging condition using the port cranes (effective range = 30 meters) (Figure 2.4-c).

For both cases of 30 meters and 76 meters, the research has recommended the use of wireless HART adapters and repeaters for the purpose of reinforcing the network at specific locations where RSSI levels are expected.

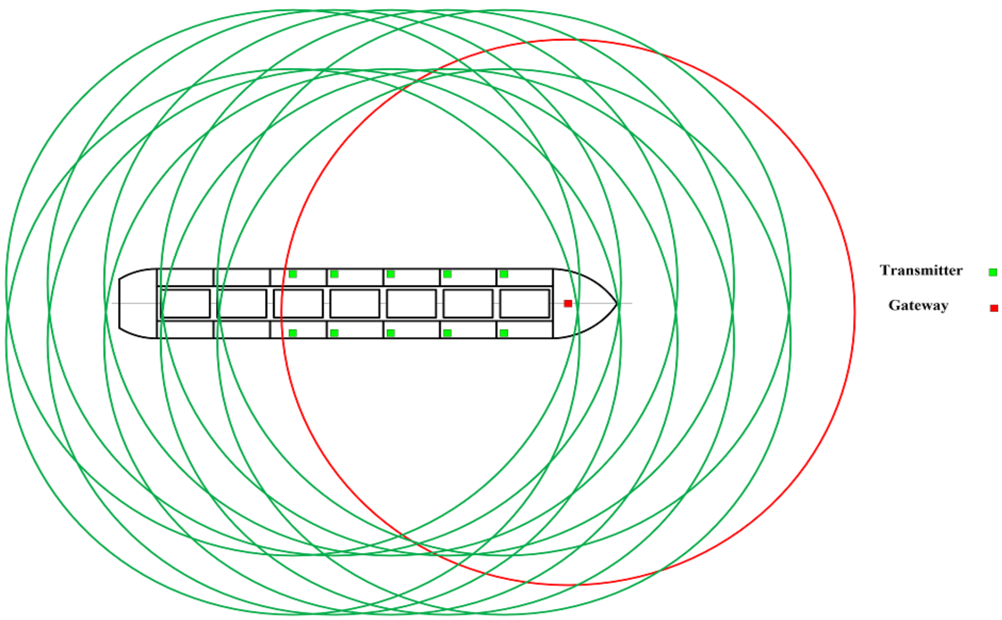

(a)

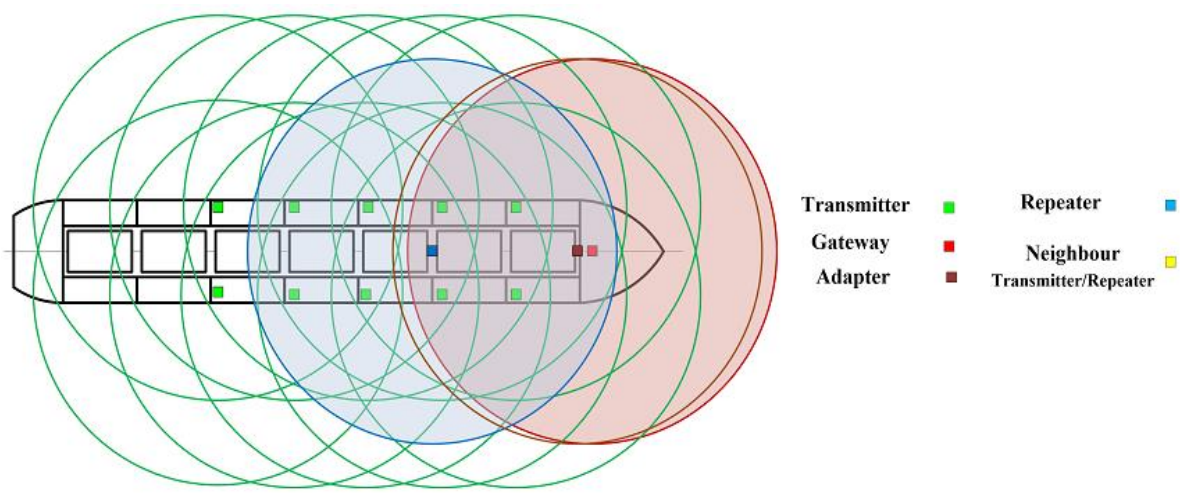

(b)

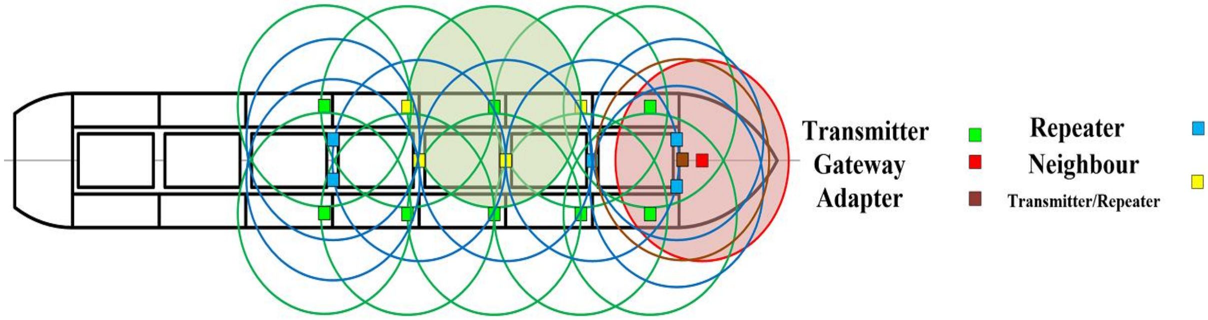

(c)

Figure 2.4- Wireless HART network planning example applied at sea water ballast tanks on a bulk carrier ship with respect to three recommended effective ranges correspondent to three levels of infrastructural density according to the Emerson wireless HART network planning guide.

2.6.2 Monitoring of Most Important Systems in Engine Room (ER)

In order to provide more detailed maritime engineering application for wireless HART protocol in accordance with the proposed mathematical model for the reinforcement of wireless HART networks, an analysis was carried out for the case of adopting wireless HART technology in measurement and control systems centralized at the engine room. This analysis will be based on the following hypotheses:

- It is more efficient from an economical point of view not to dedicate an independent wireless HART field device for each single measured quantity.
- It is recommended to adopt the idea of using wireless HART adapters which are capable of collecting the measurement data from multiple 4-20 mA (Classical or HART supported transmitters) such as the Bullet wireless HART adapter and send it wirelessly to the gateway. The measuring 4-20 mA conventional as well as HART-based transmitters are connected together with the adapter in a multidrop communication loop through a single twisted pair of wires. The Bullet wireless HART Pepperl+Fuchs adapter can communicate simultaneously with up to 8x(4-20mA) transmitters [44,69], while the Emerson THUM wireless HART adapter can communicate only with 1x(4-20mA) transmitters [44,70].
- From a perspective related to cost effectiveness, the application of wireless HART protocol in engine room is recommended to include only 4-20 mA analogue signals from analogue transmitters. For the ON/OFF state changing switches such as temperature and pressure switches, it is possible only to integrate such signals into a wireless HART network, only if the switch was a binary HART supported switch. The price of the binary HART supported state changing quantity measuring switches, is extremely higher than the price of the classical pressure and temperature switches. For such binary signals, it is recommended to collect them in groups and to be forwarded to the host controller using general use wireless technologies such as Wi-Fi.
- Due to safety operational considerations related to the high level of operational and environmental hazards on commercial ships, the wireless HART protocol will be implemented in a functionally safe configuration in conjunction with cabling as two mediums (cabling will be the main medium, while wireless HART will be the backup medium) dedicated to data transaction in the most important measurement / control systems aboard the ship.

- The Bullet wireless HART adapter is deployed to undertake the task of collecting the measurement data from up ton of 8 field devices in a functionally safe configuration. The output 4-20 mA current signal from the field device measuring a specific quantity, will be fed as an input signal to a 4-20 mA signal splitter. The first output signal of the splitter will be sent to the host controller through cabling as a medium for data transaction. The second output of the signal splitter will be connected in parallel with the outputs of the remaining seven signal that will form a multidrop communication loop with the Bullet wireless HART adapter [44,69].

Table (2.7) provides a detailed description for the monitored signals and their corresponding measurement/control shipboard systems. Figure (2.5-a) illustrates the proposed layout for the Bullet adapters (connected to different systems) as well as the gateway. Figure (2.5-b) illustrates the proposed locations for added repeaters to reinforce the wireless HART network according to the MRFDD method.

Table 2.7- Illustration for the most important analogue input signals at shipboard measurement and control systems centralized at the engine room, in addition to the required wireless HART Bullet adapters required to integrate these signals into a wireless HART network.

No.	System	Signals and Adapters
1.	Main Engine Safety and Control System (ME)	**Adapter 1 (8 signals):** • 8 Jacket cooling water temperature transmitters PT100. **Adapter 2 (8 signals):** • 8 Exhaust temperature transmitters thermocouples. **Adapter 3 (8 signals):** • 8 Cylindrical oil temperature transmitters PT100. **Adapter 4 (8 signals):** • 8 Oil mist detectors. **Adapter 5 (8 signals):** • High fresh water cooling temperature inlet • Low lubrication oil pressure inlet • Turbo charger exhaust gas inlet temperature • Turbo charger exhaust gas outlet temperature • FO inlet pressure • FO inlet temperature. • Starting Air inlet pressure • Control Air inlet pressure.
2.	No.1 Auxiliary Engine AE/1	**Adapter 6 (8 signals):** • 8 Jacket cooling water temperature transmitters PT100. **Adapter 7 (8 signals):** • 8 Exhaust temperature transmitters thermocouples. **Adapter 8 (8 signals):** • 8 Oil mist detectors. **Adapter 9 (8 signals):** • High fresh water cooling temperature inlet • Low lubrication oil pressure inlet • Turbo charger exhaust gas inlet temperature • Turbo charger exhaust gas outlet temperature • FO inlet pressure • No.1 Winding temperature. • No.2 Winding temperature.

		• No. 3 Winding temperature
3.	No.1 Auxiliary Engine AE/2	**Adapter 10 (8 signals):** • 8 Jacket cooling water temperature transmitters PT100. **Adapter 11 (8 signals):** • 8 Exhaust temperature transmitters thermocouples. **Adapter 12 (8 signals):** • 8 Oil mist detectors. **Adapter 13 (8 signals):** • High fresh water cooling temperature inlet • Low lubrication oil pressure inlet • Turbo charger exhaust gas inlet temperature • Turbo charger exhaust gas outlet temperature • FO inlet pressure • No.1 Winding temperature. • No.2 Winding temperature. • No. 3 Winding temperature.
4.	No.1 Auxiliary Engine AE/3	**Adapter 14 (8 signals):** • 8 Jacket cooling water temperature transmitters PT100. **Adapter 15 (8 signals):** • 8 Exhaust temperature transmitters thermocouples. **Adapter 16 (8 signals):** • 8 Oil mist detectors. **Adapter 17 (8 signals):** • High fresh water cooling temperature inlet • Low lubrication oil pressure inlet • Turbo charger exhaust gas inlet temperature • Turbo charger exhaust gas outlet temperature • FO inlet pressure • No.1 Winding temperature. • No.2 Winding temperature. • No. 3 Winding temperature.
5.	Air Conditioning and Refrigerating Plant	**Adapter 18 (8 signals):** • No.1 AC compressor High gas refrigerant pressure • No.1 AC compressor low liquid refrigerant pressure • No.2 AC compressor High gas refrigerant pressure • No.2 AC compressor low liquid refrigerant pressure • Cooling Sea Water inlet pressure • No. 1 AC compressor oil temperature. • No. 2 AC compressor oil temperature. **Adapter 19 (8 signals):** • No.1 refrigerating compressor High gas refrigerant pressure • No.1 refrigerating compressor low liquid refrigerant pressure • No.2 refrigerating compressor High gas refrigerant pressure • No.2 refrigerating compressor low liquid refrigerant pressure • Cooling Sea Water inlet pressure. • No. 1 refrigerating compressor oil temperature • No. 2 refrigerating compressor oil temperature.
6.	Steering Gear and Autopilot System	**Adapter 20 (2 signals):** • No.1 steering gear rudder angle feedback unit (1 signal).

		• No.2 steering gear rudder angle feedback unit (1 signal).
6.	Tank level Measurement System	**Adapter 20 (2 signals):** • Starboard side Fresh Water Tank (1 signal). • Port side Fresh Water Tank (1 signal).
7.	Diesel Oil, Fuel Oil and Lubrication Oil purifiers	**Adapter 21 & Adapter 22 (15 signals):** • Inlet flow meter (3 signals). • Outlet Pressure transmitter (3 signals). • Outlet Temperature transmitter (3 signals). • Rotational separation speed rpm (3 signals).. • Unbalance sensor check (3 signals).
	Tank level Measurement System	**Adapter 22 (1 signals):** • Fuel oil settling tank (1 signal).
	Tank level Measurement System	**Adapter 23 (3 signals):** • Fuel oil service tank (1 signal). • Diesel oil settling tank (1 signal). • Diesel oil service tank (1 signal).
	Ballast Water Treatment System (BWTS)	**Adapter 23 (4 signals):** • Ballast water inlet Flow meter (1 signal). • Ballast water inlet Pressure transmitter (1 signal). • Ballast water inlet Temperature transmitter (1 signal). • UV lamp intensity (1 signal).
	Fuel Oil Conditioning System	**Adapter 24 (8 signals):** • FO Flow transmitter (1 signal). • FO pressure transmitter 1 (1 signal). • FO pressure transmitter 2 (1 signal). • FO temperature transmitter 1 (1 signal). • FO temperature transmitter 2 (1 signal). • FO Viscosity sensor 1 (1 signal). • FO Viscosity sensor 2 (1 signal). • FO Viscosity signal from PCB (1 signal).
	Air Compressing System	**Adapter 25 (4 signals):** • Air temperature by compressor 1 (1 signal). • Air temperature by compressor 2 (1 signal). • Air pressure inside the first bottle (1 signal). • Air pressure inside the second bottle (1 signal).
	Tank level Measurement System	**Adapter 25 (3 signals):** • FO storage tank (1 signal). • DO storage tank (1 signal). • LO storage tank (1 signal).
7.	Composite Boiler	**Adapter 26 (8 signals):** • Water level transmitter (1 signal). • Output steam pressure (1 signal). • Burner FO pressure (1 signal). • Burner FO temperature (1 signal). • Exhaust gas temperature transmitter (1 signal).

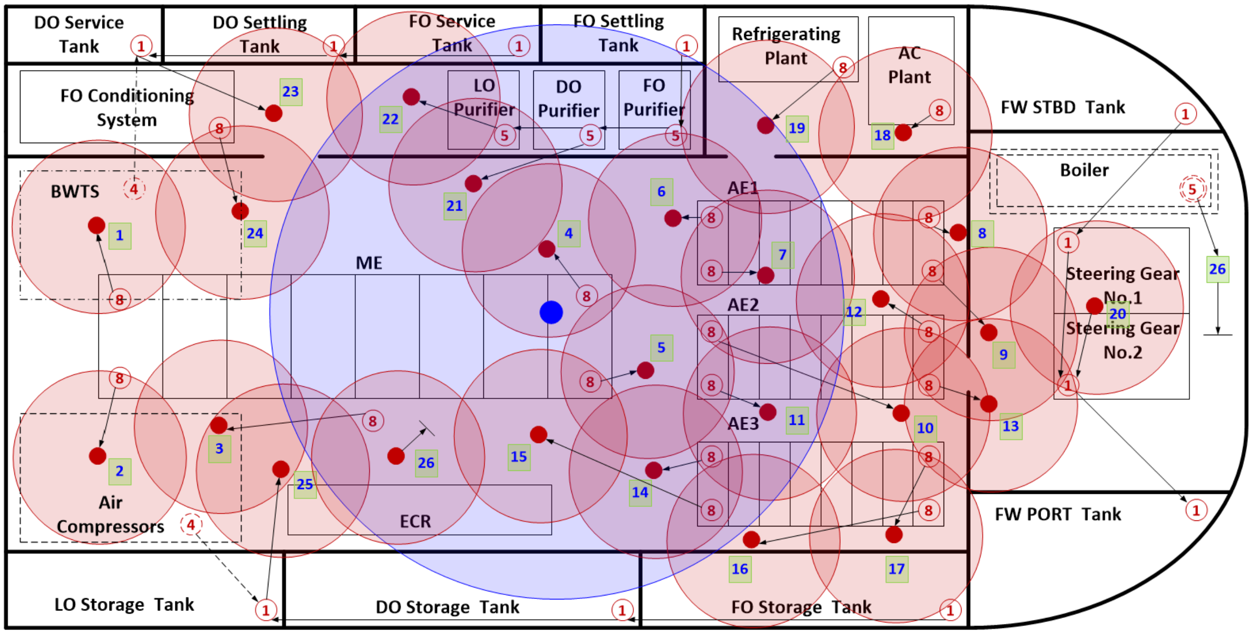
DO Service Tank
DO Settling Tank
FO Service Tank
FO Settling Tank
Refrigerating Plant
AC Plant
FO Conditioning System
LO Purifier
DO Purifier
FO Purifier
FW STBD Tank
BWTS
ME
AE1
AE2
AE3
Boiler
Steering Gear No.1
Steering Gear No.2
Air Compressors
ECR
FW PORT Tank
LO Storage Tank
DO Storage Tank
FO Storage Tank

(a)

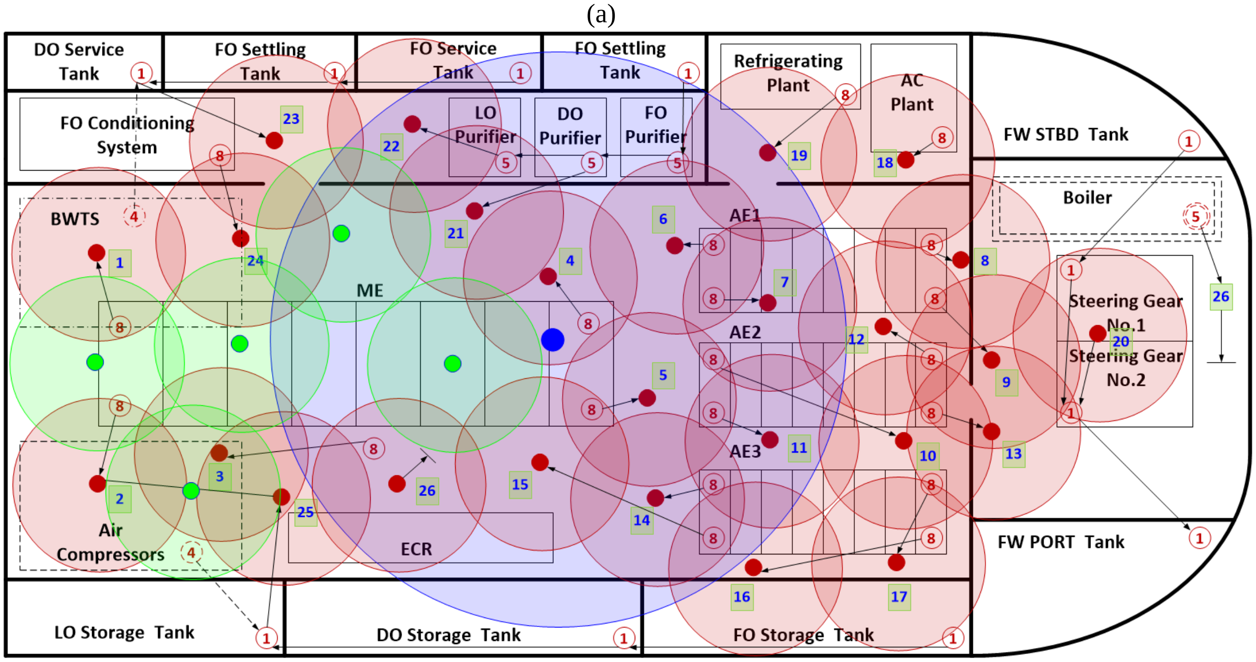
DO Service Tank
FO Settling Tank
FO Service Tank
FO Settling Tank
Refrigerating Plant
AC Plant
FO Conditioning System
LO Purifier
DO Purifier
FO Purifier
FW STBD Tank
BWTS
ME
AE1
AE2
AE3
Boiler
Steering Gear No.1
Steering Gear No.2
Air Compressors
ECR
FW PORT Tank
LO Storage Tank
DO Storage Tank
FO Storage Tank

(b)

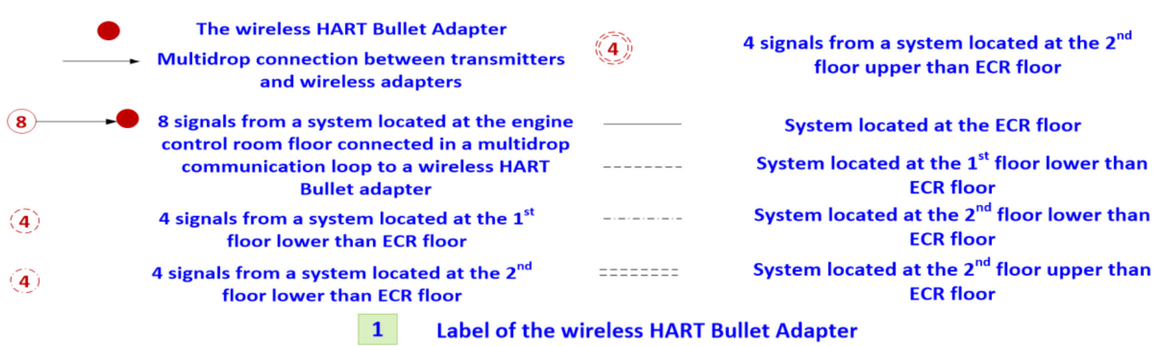
The wireless HART Bullet Adapter
Multidrop connection between transmitters and wireless adapters
8 signals from a system located at the engine control room floor connected in a multidrop communication loop to a wireless HART Bullet adapter
4 signals from a system located at the 1st floor lower than ECR floor
4 signals from a system located at the 2nd floor lower than ECR floor
4 signals from a system located at the 2nd floor upper than ECR floor
System located at the ECR floor
System located at the 1st floor lower than ECR floor
System located at the 2nd floor lower than ECR floor
System located at the 2nd floor upper than ECR floor
Label of the wireless HART Bullet Adapter

Figure 2.5- At (a) Illustration for the locations of the most important shipboard measurement and control systems on a small container ship, in addition to the recommended positions for the wireless HART Bullet adapters which will collect the data from the analogue transmitters through multidrop communication loops. At (b), the MRFDD method was applied to reinforce the planned wireless HART network so that any possible instability of the RF waves propagation due to the high density of the ship's hull metallic infrastructure.

3. General Use Wireless Technologies (Wi-Fi)

3.1 Laboratory Stand

As a technology of lower cost as well as lower security and encryption levels, Wi-Fi technology can be deployed as a data transaction medium in marine measurement and control systems as an alternative for more expensive wireless technologies which are solely dedicated to industrial automation (wireless HART and ISA100.11a) or as a coexistent technology [71-74] with them. In [75], the research has introduced a laboratory stand at which Wi-Fi general use technology will be used as data transaction medium in a configuration aimed to:

1- Collect the measurement data from multiple 4-20 mA analogue transducers.
2- Authenticate the reception of the transmitted data to the host controller.
3- Verification of the measured data through coexistence with Wireless HART protocol.

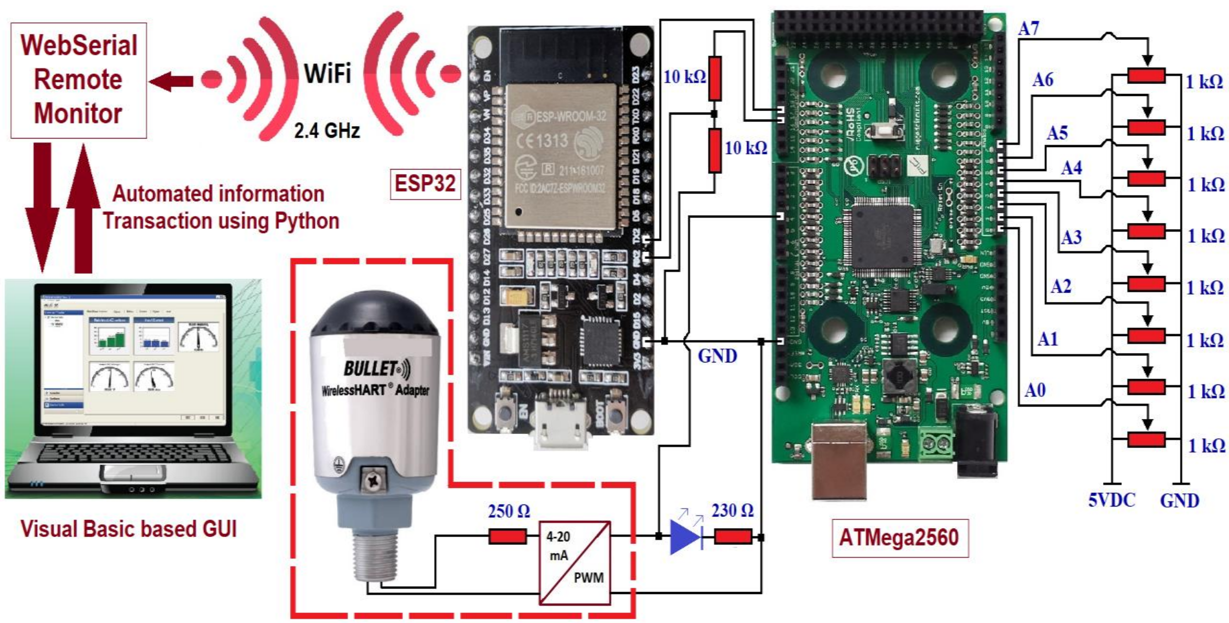

Figure 3.1- Connection diagram for the laboratory stand

Main components of the laboratory stand (Figure 3.1) are an Arduino MEGA 2560 controller [76], an ESP32 controller [77-81] and a Bullet wireless HART adapter. Measurement data will be collected at the Arduino MEGA 2560 controller through 8 simulated analogue inputs of 1-5 VDC. The analogue standard of 1-5 VDC is the corresponding DC voltage standard to the 4-20 mA analogue DC current standard, as the 4-20 mA measurements loop current is usually converted into 1-5 VDC voltage signal through a 250 ohms load resistance. The ESP32 controller can tolerate analogue input of a maximum voltage of 3.3 VDC, while Arduino MEGA 2560 controller can receive up to 5 VDC analogue input signal. Therefore, it is more recommended to convert the 4-20 mA measurement current signals into 1-5 VDC signal and connect them to the Arduino controller, as the wider span of the 1-5 VDC range than the 0-3.3 VDC, will lead to higher accuracy level processing the measurement data. On the other hand, the non-zero lower range limit of the 1-5 VDC analogue standard will facilitate the process of signal conversion from 4-20 mA into 1-5 VDC, in addition to preserving one of the main advantages of the 4-20 mA analogue standard, which is the possibility to detect any possible failure at 4-20 mA current loop that might lead to a zero (less than 1 VDC) lower range limit value.

The collected measurement date at the Arduino controller will be forwarded to the ESP-32 controller using serial communication. The exact configuration to perform serial communication between the Arduino and the ESP32 controller was explained elaborately at [75]. The ESP32 controller will forward the measurement data to the host controller using Wi-Fi. The host controller will collect the forwarded measurement data from the ESP32 controller through using the remote serial monitor WebSerial [82-84].

WebSerial [82-84] is a Serial monitor for ESP8266 and ESP32 microcontrollers that can be accessed remotely via a web browser. Webpage is stored in program memory of the microcontroller. In order to set up the ESP32 controller to perform WiFi communication with the webserial websocket, firstly, the following libraries should be included in the code; *WiFi.h*, *ESPAsyncWebServer.h*, *WebSerial.h* and *AsyncTCP.h* [83,84].

A python software at the host controller will process the received data and respond with sending feedback authenticating messages to the ESP32 controller which will forward these authenticating messages to the Arduino controller. The Bullet wireless HART adapter will be connected to one of the Arduino controller analogue outputs in a multidrop communication loop. This analogue output will be corresponding to the reading from one of the 8 analogue inputs. According to a specific timing pattern, the Arduino controller will toggle between the eight analogue inputs, so that one of them will be passed as an analogue output to be integrated with the wireless HART adapter in a multidrop communication loop [85-87].

The purpose of connecting the wireless HART adapter only with a single analogue output from the Arduino controller, is to achieve the following possible goals:

- If splitters were applied to the input measured signals with their first outputs applied to the analogue input ports of the Arduino controller and their second outputs are connected in a multidrop configuration with the wireless HART Bullet adapter, it will be possible to apply some sort of verification process to the measured data as well as the output signal. Such a verification can be carried out through comparison between two groups of data transmitted wirelessly and simultaneously to the control station side. The first group includes the eight measured data altogether through Wi-Fi to the host controller (1st outputs of splitters), while the second group includes the measured signals connected in a multidrop connection with the Bullet wireless HART adapter to the Asset Management System AMS (2nd outputs of splitters). Using software tools, the comparison between the two groups of data will definitely result in a measurement/control system with higher accuracy levels and less corrupted data.
- The connection of the single analogue output port of the Arduino controller to the wireless HART Bullet adapter in series with a 4-20 mA actuator, allows for performing possible control tasks locally without any supervision from the host controller side. Additionally, it will be possible to monitor the actuator control signal wirelessly using both wireless HART and Wi-Fi. Such a configuration will facilitate the process of calibration and current compensation through comparison between the output actuator current that should be generated (sent through Wi-Fi to the host controller) and the actual current flowing through the actuator (sent through wireless HART to the AMS). Accordingly, not only the positioning feedback signal will be scanned by the host controller (naturally, through cabling) but also, the control signal itself,

which will consequently result in more efficient undertaken procedure during maintenance or troubleshooting, as in most of the marine monitoring system only the feedback positioning signal is detected not the control signal.

In order to render a more profound perception for such a point, the following example for a control process in a maritime engineering application will be discussed. Assuming that there was one conditioning unit for fuel oil on a commercial ship. The unit has the following transducers:

1- Inlet temperature transmitter.
2- Outlet pressure transmitter.
3- Outlet temperature transmitter.
4- Water level transmitter.
5- Inlet pressure transmitter.
6- Heating steam pressure transmitter.
7- FO viscosity sensor.

The data received from the previous transducers will be processed by the Arduino controller to generate the output signal to an actuator mounted at the steam line to be opened with a percentage from 0% to 100%. This control signal will be also forwarded to the AMS system through the wireless HART adapter (connected in series with the actuator at the analogue output port of the Arduino controller). Such an example for a possible use for the laboratory stand is a clear demonstration for the coexistence between the Wi-Fi general use wireless technology and the wireless HART protocol as a wireless technology dedicated to industrial automation.

As was previously mentioned, the laboratory stand is based on using timing patterns in order to carry out the process of authentication for the transmitted measurement data. The research in [75] has extensively differentiated between two programming techniques to generate these timing patterns. One technique is recommended, while the other is not recommended. Table (3.1) illustrates a summarized comparison between the two discussed programming techniques. Figures (3.2) and (3.3) illustrate the block diagrams of the not recommended techniques to execute timing patterns while performing simultaneous wireless and serial communication tasks.

Table 3.1- Illustration for the recommended as well as the advised against programming techniques for timing patterns

Technique	Specification	Explanation
Not Recommended	Based on: • *delay()* function [87-90]. • Built-in timers [91,92]. • Interrupt subroutines [93,94]	• An increased number of messages waiting at the serial buffer (Overloading the serial buffer). • Increases the complexity of the code as well as the latency of the system. • Timer subroutines stops the execution of the program, which leads to the disconnection of the Wi-Fi network generated by the ESP32 controller and crashing the Python program at the host controller
Recommended	Based on: • *millis()* function [95].	• More accurate time intervals without leading to the crash of the programs being executed neither at any of the controllers (Arduino or ESP32) nor at the host controller (Python program).

The research in [75] has highlighted some of the important functions used by the code at both controllers (Arduino and ESP32) in addition to the Python code used to provide an automated response by the WebSerial remote serial monitor at the host controller. In Table (3.2), a brief description is rendered for each of these functions.

Regarding the format by which serial communication between the ATMEGA2560 (Arduino controller) and the ESP32 controllers will take place, it will take the form of a single string variable containing all the measured data from all sensors. This string variable will be sent wirelessly to the WebSerial websocket. A Python program at the host controller station will save the received data string into a text file. Through using text manipulation in python, the last part of the string will be detected. Through manipulating the last part of the received string, authentication of the received information will be achieved. The last part of the received string will include two letters (T) and (F). (T) refers to the information sent to the WebSerial remote monitor from the controllers' side, while (F) refers to the information sent from the WebSerial remote monitor to the controllers side [75]. Table (3.3) illustrated how authentication process is achieved through the significance of the digits detected following both the letters T and F. Figure (3.4) illustrates the Graphical User Interface (GUI) of the system where the measured reading from each transmitter will be extracted from the stored information in the text file through using text manipulation in visual basic 6. Additionally, the visual basic GUI will display from which simulated sensor the data will be passed to the analogue output after being authenticated. The displayed readings from the simulated sensors are mapped from the (0-255) range to the (1-5 VDC) range [75].

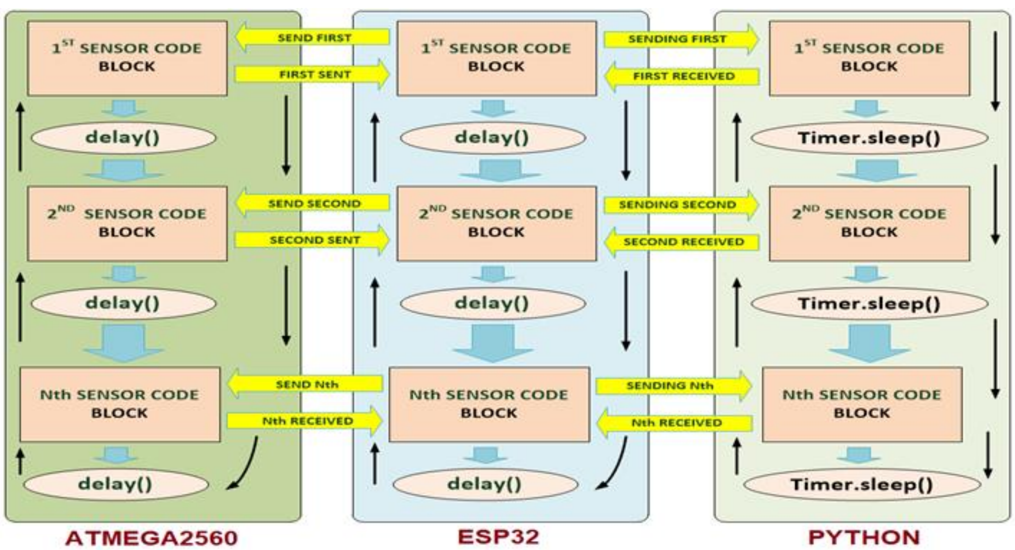

Figure 3.2 - Non-recommended Programming Technique based on using delay() function and multiple Authentication messages.

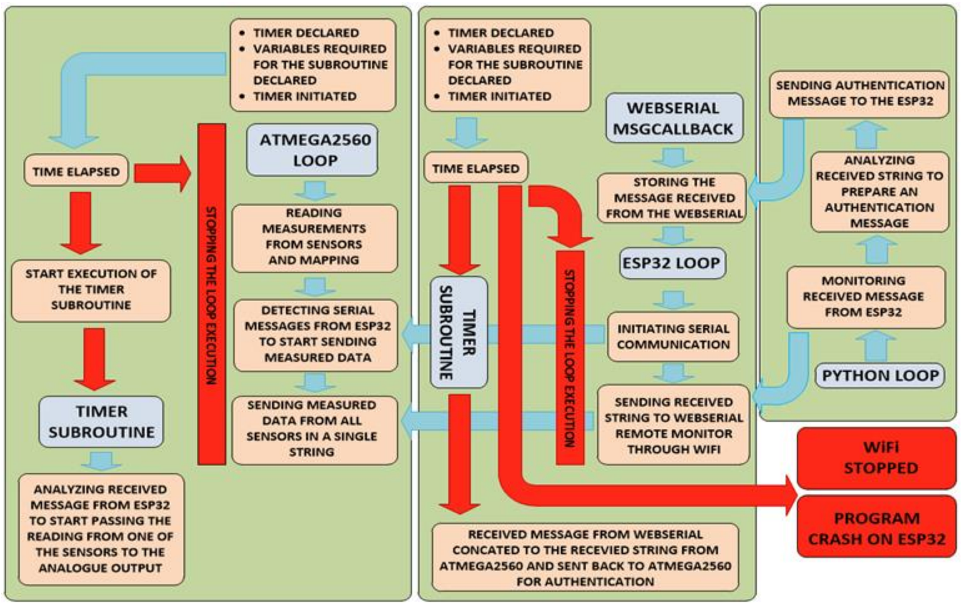

Figure 3.3 – Non-recommended Programming Technique based on using built-in timers and their interrupts subroutines.

Table 3.2 – Most important functions used during the programming of the laboratory stand

Function	Location	Description
Serial.begin(9600)	Arduino	Set up the serial port connection with the PC
Serial2.begin(9600)	Arduino	Set up the serial port connection with the ESP32
Serial.begin(115200)	ESP32	Set up the serial port connection with the PC
Serial2.begin(9600, SERIAL_8N1, RXD2, TXD2)	ESP32	Set up the serial port connection with Arduino
WiFi.softAP(ssid, password)	ESP32	Set up the Wi-Fi mode of operation as an access point
webserial.begin(&server)	ESP32	Starting the webserial remote monitor at the http server
webserial.msgCallback(recvMsg)	ESP32	Starting the webserial msgCallback function
Server.begin()	ESP32	Satrting the webserver at port 80
disconnect()	ESP32	Disconnect the Wi-Fi generated by the ESP32 in case a serial information was detected at the serial buffer of the ESP32's second serial buffer (*Serial2.available > 0*)
reconnect()	ESP32	Reconnect the Wi-Fi generated by the ESP32 when the ESP32 controller was about to send data to the WebSerial websocket
async with websockets.connect(url) as ws	Python	Command used to connect to the websocket URL

await ws.recv()	Python	Command used to receive data from the URL into a string variable
await ws.send ()	Python	Command used to send data from a string variable to the websocket

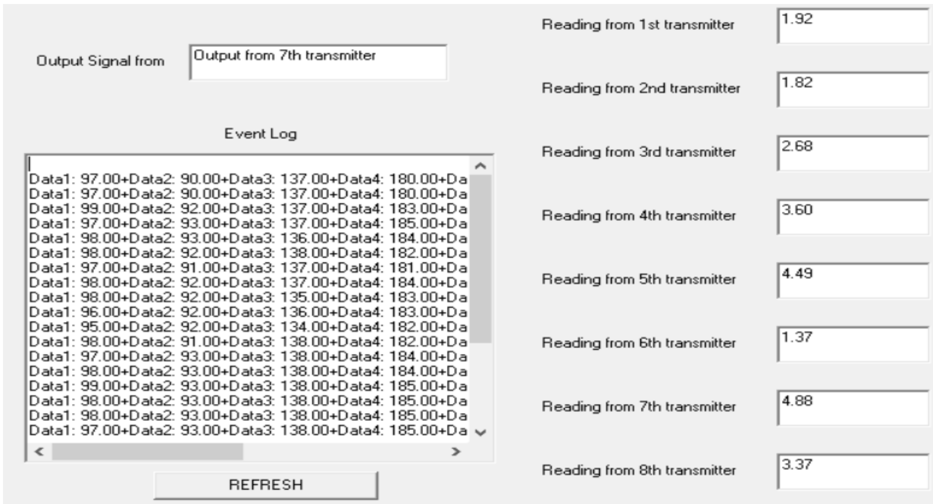

Figure 3.4 – GUI for authenticated data transaction at the laboratory stand

Table 3.3 – Examples for authentication messages and their significance.

Message	Previous Analogue Output	Current Analogue Output	Significance
T01F	Null	Passed from 1st sensor	Controllers informs WebSerial that Analogue output started to be passed from 1st sensor
TF01	Null	Passed from 1st sensor	WebSerial confirms that analogue output is correspondent to the reading of the 1st sensor
T01F01	Passed from 1st sensor	Passed from 1st sensor	Outputting from 1st sensor till timer toggles the output
T02F01	Passed from 1st sensor	Passed from 2nd sensor	Controllers informs WebSerial that Analogue output started to be passed from 2nd sensor
T01F02	Passed from 1st sensor	Passed from 2nd sensor	WebSerial confirms that analogue output is correspondent to the reading of the 2nd sensor
T02F02	Passed from 2nd sensor	Passed from 2nd sensor	Outputting from 2nd sensor till timer toggles the output
T03F02	Passed from 2nd sensor	Passed from 3rd sensor	Controllers informs WebSerial that Analogue output started to be passed from 3rd sensor

T02F03	Passed from 2^{nd} sensor	Passed from 3^{rd} sensor	WebSerial confirms that analogue output is correspondent to the reading of the 3^{rd} sensor
T03F03	Passed from 3^{rd} sensor	Passed from 3^{rd} sensor	Outputting from 3^{rd} sensor till timer toggles the output
T01F08	Passed from 8^{th} sensor	Passed from 1^{st} sensor	Controllers informs WebSerial that Analogue output started to be passed from 8^{th} sensor
T08F01	Passed from 8^{th} sensor	Passed from 1^{st} sensor	WebSerial confirms that analogue output is correspondent to the reading of the 8^{th} sensor
T08F08	Passed from 8^{th} sensor	Passed from 8^{th} sensor	Outputting from 8^{th} sensor till timer toggles the output

3.2 ESP-WebSerial Limited Range

Figure (3.5) illustrates the limited range (without using external antennas at the ESP32 unit) of the laboratory stand corresponding to various distances from the host controller. This problem can be overcome by considering the option of collaboration between the ESP-WebSerial and the ESP-NOW protocol. The obtained RSSI levels of -35,-57 and -74 dbm was measured at distances of 1,6 and 12 meters of separation between the host controller located inside a room, while the multiple sensors station is located outside the room. This configuration was selected to simulate the host controller located inside a control room, while the measurement data are collected at the plant outside the control room and forwarded wirelessly to the host controller similar to the situation on most of the commercial ships.

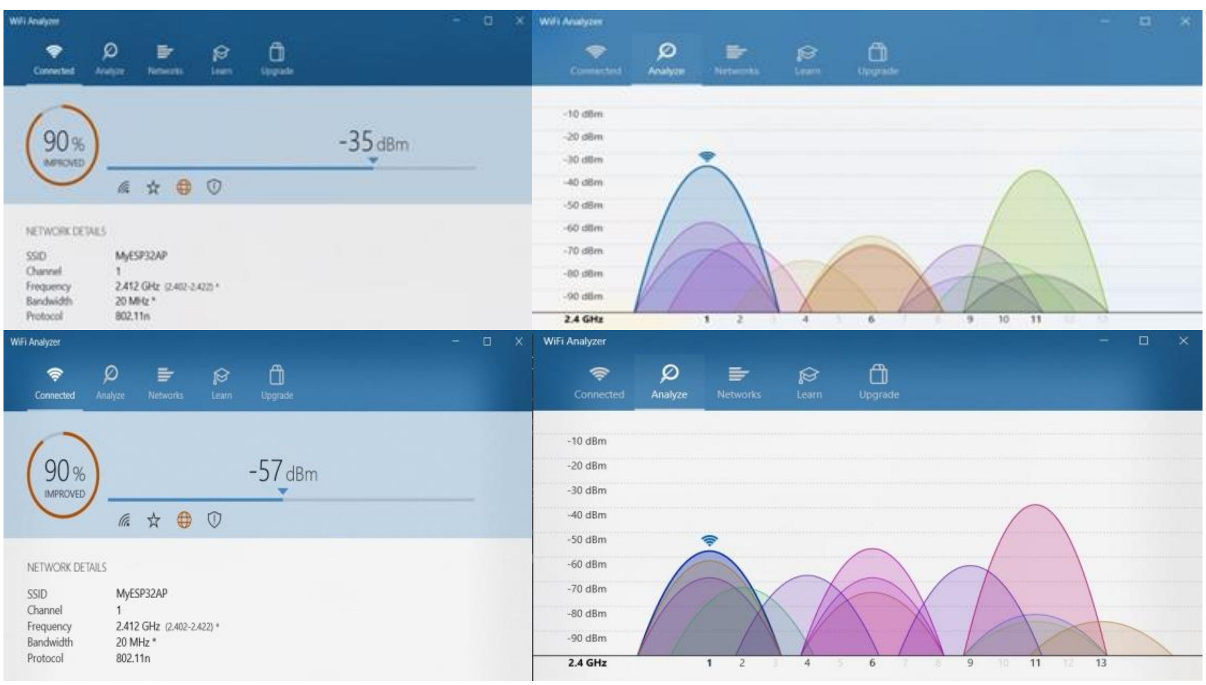

Figure 3.5- Decreased (RSSI) Levels of -35,-57 and -74 dbm corresponding to distances of 1, 6 and 12 meters from Host Controller, respectively.

3.2.1 Problem Characterization

In order to characterize the relation between RSSI levels and the distance from the host controller to the ESP32 access point included in the laboratory stand at specific indoor as well as outdoor sites, five sites were taken into account. The indoor sites are located at the Faculty of Electrical Engineering in Gdynia Maritime University, while the outdoor sites are located at the neighborhood of the university building [97]:

1. Straight corridor (indoor site, length: 75 meters) (Figure 3.6-a).
2. Straight corridor (indoor site, length: 50 meters) (Figure 3.6-a).
3. Straight long passage (outdoor site, length: 180 meters) (Figure 3.6-b).
4. Parking site, shopping stores and fuel station (outdoor site) (Figure 3.6-c).
5. Straight corridor at the upper floor from the location of the host controller (indoor site, length: 50 meters) (Figure 3.6-d).

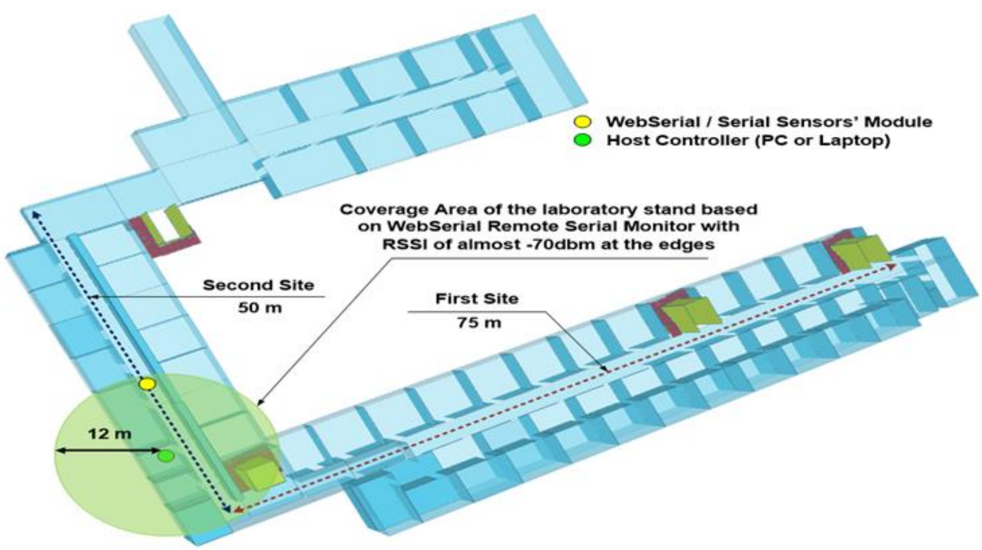

(a) Limited range of WebSerial based Laboratory stand, 1st and 2nd sites used to derive and verify equation(3.1)

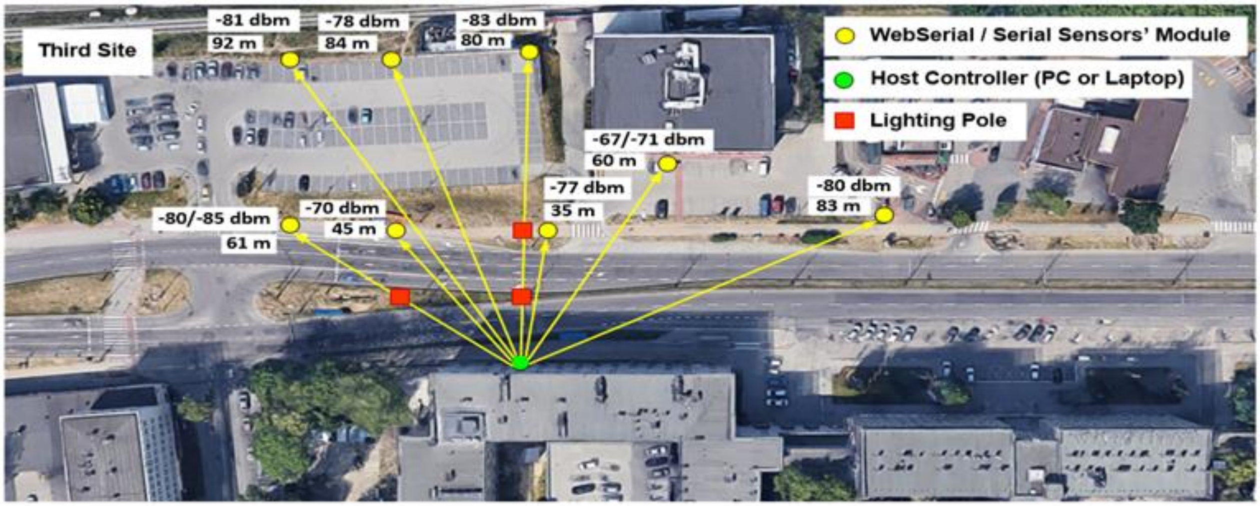

(b) RSSI measured at points deflected from LOS (3rd site).

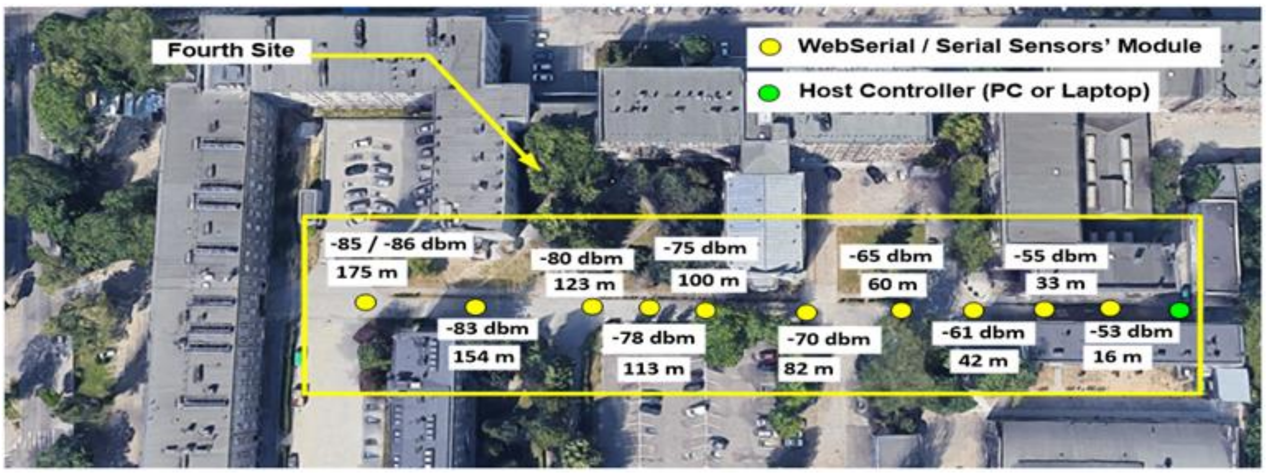

(c) RSSI measured at points on the straight LOS (4th site)

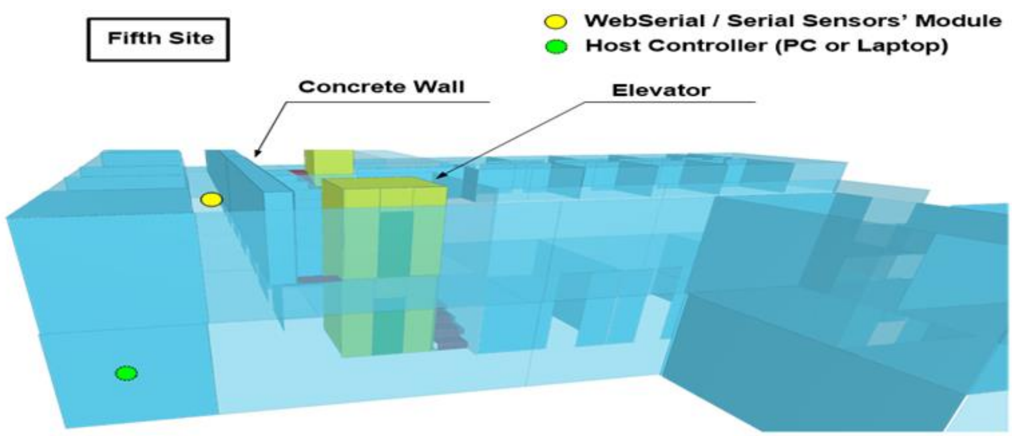

(d) Fifth site

Figure 3.6 - Five indoor/outdoor sites used for experimental analysis of ESP32 Wi-Fi range

Summary for the results of detecting the RSSI levels at the five sites [97]:

- Equation (3.1) was derived from the obtained average RSSI readings with respect to the distance between the host controller and the sensors' module only at the 1^{st} site using Matlab curve fitting tool (Figure 3.7-a).
- RSSI measurements at the second site were used to verify if the equation (3.1) is applicable or not (Measurements at the 2^{nd} site were used to validate the equation derived by measurements at the 1^{st} site).
- Equation (3.2) was derived from the RSSI readings taken in the third outdoor site (Figure 3.7-b).
- The recommended RSSI level should not be less than - 60 dbm [44]. Consequently and based on the obtained results from equations (3.1) and (3.2), the RSSI level of – 60 dbm is correspondent to a distance (from the host controller to the ESP32 unit) of 20 meters or 40 meters for indoor and outdoor applications, respectively (Figure 3.7-c).
- 20 meters and 40 meters are the maximum recommended distances between ESP32 WiFi access point (without external antenna) and the host controller at a straight LOS without obstacles for indoor and outdoor applications, respectively.
- RSSI values measured at both of the fourth and the fifth sites were recorded to indicate some assumed points that were intended to be covered in an assumed wireless WiFi instrumentation network (based on only ESP32 WebSerial), and were not covered due to the low RSSI levels at such points.

$$RSSI_{indoor}\ (dbm) = k_{i1} d^4 + k_{i2} d^3 + k_{i3} d^2 + k_{i4}\ d + k_{i5} \quad (3.1)$$

$$RSSI_{outdoor}\ (dbm) = k_{o1} d^3 + k_{o2} d^2 + k_{o3} d + k_{o4} \quad (3.2)$$

Where k_{i1} = 9.95e-06 dbm/m^4, k_{i2} = -0.001587 dbm/m^3, k_{i3} = 0.0894 dbm/m^2, k_{i4} = -2.282 dbm/m, k_{i5} = -38.76 dbm

k_{o1} = -5.9e-06 dbm/m^3, k_{o2} = 0.002781 dbm/m^2, k_{o3} = -0.5587 dbm/m, k_{o4}= -41.23 dbm and d is the distance from the host controller to the sensors module in meters.

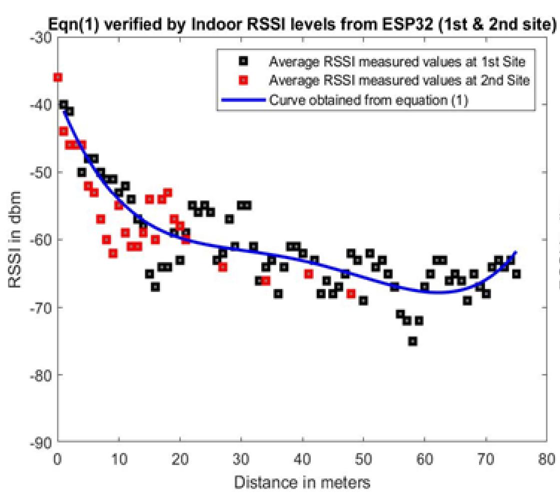

(a)

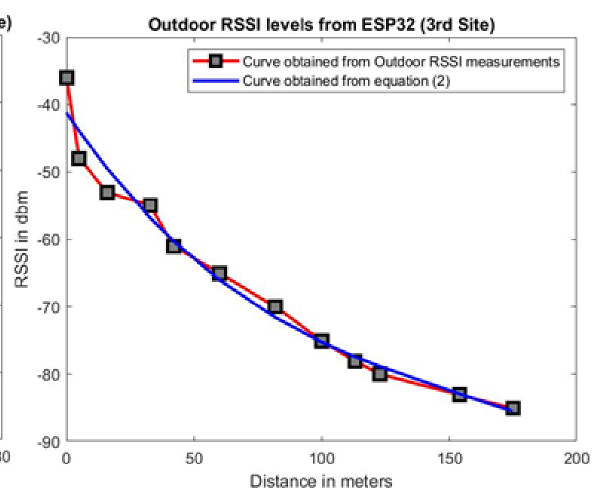

(b)

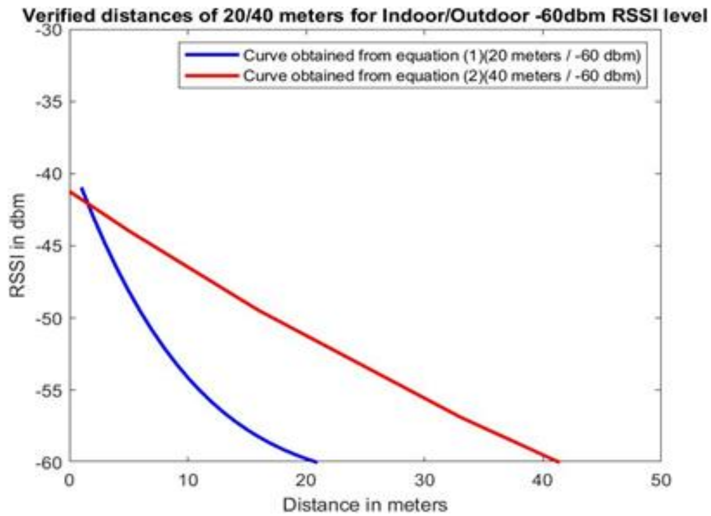

(c)

Figure 3.7 - Curves obtained from RSSI measurement with respect to distance at 1st, 2nd and 3rd sites and curves obtained from equations (3.1) and (3.2)

3.3 ESP-NOW PROTOCOL

Table 3.4 illustrates a brief description for the ESP-NOW protocol

Table 3.4 – Most important features of the ESP-NOW protocol

Specifications	Wi-Fi wireless communication protocol developed by Espressif in order to perform wireless low power and quick communication tasks based on transaction of messages with a maximum size of 250 bytes between ESP32 and ESP8266 units only through the knowledge of their MAC addresses. [98-103]
Security & Encryption	• ESP-NOW protocol also allows for encrypted data transaction in order to increase the security level of wireless communication. • Counter Mode with Cipher Block Chaining Message Authentication Code Protocol (CCMP) is used by ESP-NOW to execute encrypted data transaction. • CCMP protocol is mainly based on using a Primary Master Key PMK and several Local Master Keys LMK for the purpose of identifying the devices allowed to communicate with. • The AES 128 algorithm is used to set up both master keys [98-103]
Important Considerations	The following considerations should be taken into account when performing such a type of communication: • Using Wi-Fi mode as an access point and independent station *WiFi.mode(WIFI_AP_STA);* • Considering possible change of the Wi-Fi Communication channel. [98-103]
Setups	1. Single master and multiple slaves (one to many) . 2. Single slave and multiple masters (many to one). 3. Simplex, half duplex or full duplex communication. [98-103]

Important Functions	• *esp_now_send()*: Dedicated to sending data by using ESP-NOW protocol. This function requires three parameters, which are the MAC address of the ESP32 receiver unit, pointer to the variable holding the data which will be sent and length of such a data. This function returns multiple responses, however the most important of them is ESP_OK which indicates that the sent data has been successfully delivered to the receiving unit. • *esp_now_register_send_cb:* This function registers a callback function triggered upon sending data from the ESP32 unit using ESP-NOW. This callback function detects the status of the enumeration esp_now_send_status_t. If the status of that enumerator was ESP_NOW_SEND_SUCCESS, it means that data has been delivered successfully to the receiver, however if its status was ESP_NOW_SEND_FAIL, it means that data was not successfully delivered to the receiver (Authentication). [98-103]

3.4 Proposed Configurations for Improved Range Capabilities

Table 3.5 summarizes the most important features of the suggested configurations to expand the ESP32 based Wi-Fi network coverage area. Figure 3.8 illustrates the functionality techniques adopted by each configuration. Figure 3.9 demonstrates the improved range at the five test sites.

Table 3.5 – Proposed configurations to deploy additional ESP32 controllers as wireless switches to expand the generated Wi-Fi network coverage area

1st Configuration (Figure 3.8-a)	• Based on using only two ESP32 controllers [97]. • The first controller (located at sensors' module) will collect the measured data by the sensors through serial communication with the Arduino controller and send it wirelessly using ESP-NOW protocol to the second controller [97]. • The second controller (located near host controller) will be as independent WiFi station communicating with the first controller to collect the measured data using ESP-NOW protocol and send the collected data to the host controller through using WebSerial remote serial monitor [97]. • Both controllers should be located on the same straight LOS, otherwise a communication failure is highly probable to occur [97].
2nd Configuration (Figure 3.8-b)	• An upgraded version of the first configuration, at which additional ESP32 unit/units will be added to the network to perform as wireless switches at points where communication failure is expected due to low RSSI values detected during the planning phase [97]. • Adopts two simultaneous setups for executing communication tasks: 1. Many to one (messages from other ESP32 units to the ESP32 switch). 2. One to many (messages from the ESP32 switch to the other ESP32 units). • In order to ensure stable reliable communication in such a case, the ESP32 switch will be programmed to separate between both types of communication with break time intervals, which means that the ESP32 switch will perform two way half duplex communication [97].

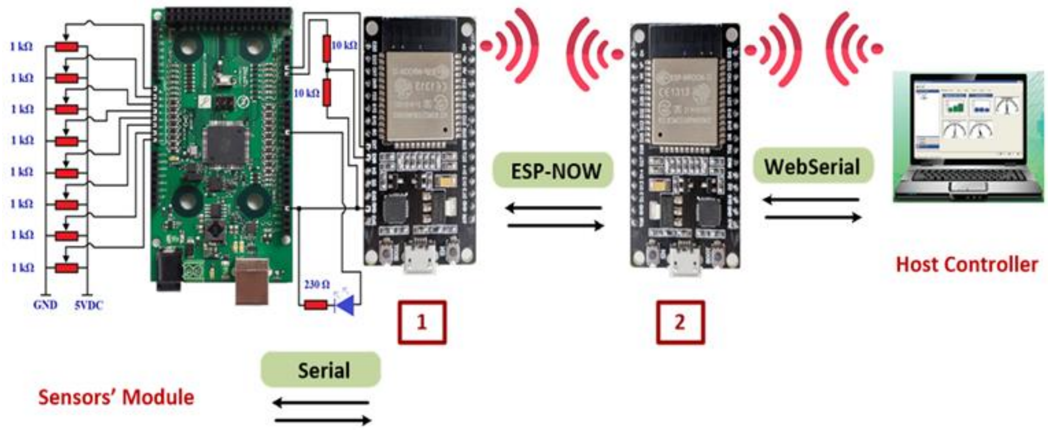

(a) 1st Proposed Configuration

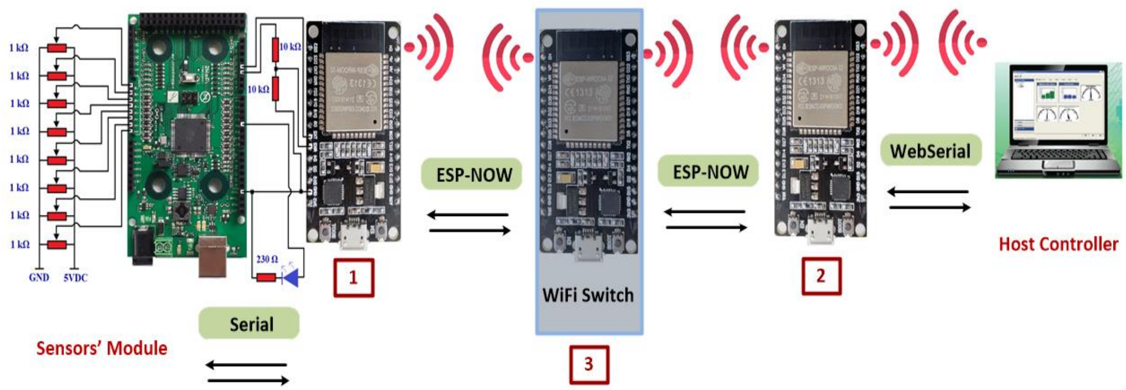

(b) 2nd Proposed Configuration

Figure 3.8 - Proposed solution to increase the range and coverage area of ESP32 WiFi based network. Numbers 1,2 and 3 refer to ESP32 units at sensors' module, host controller and in the middle (Performing as a switch) respectively.

Table 3.6 – Reasons making the 2nd configuration a better choice

Why the 2nd configuration is more recommended than the 1st configuration?
• It provides a longer range as well as a wider coverage for Wi-Fi communication in a specific area [97]. • It allows for the possibility of adding more ESP32 units to perform as switches in the designated area with a very simple program uploaded to these units without the need for conducting major changes at the program uploaded to both ESP32 units communicating with the sensors or with the host controller [97]. • Adding more ESP32 units to the network allows for increased reliability due to the increased number of possible links for information transaction between the sensors' module and the host controller [97]. • Adopting the second configuration gives the opportunity for expanding the wireless instrumentation network, through upgrading the assigned task to the ESP32 units performing as switches to perform as routers collecting measurement data from additional newly installed sensors modules located in a close range to it [97].

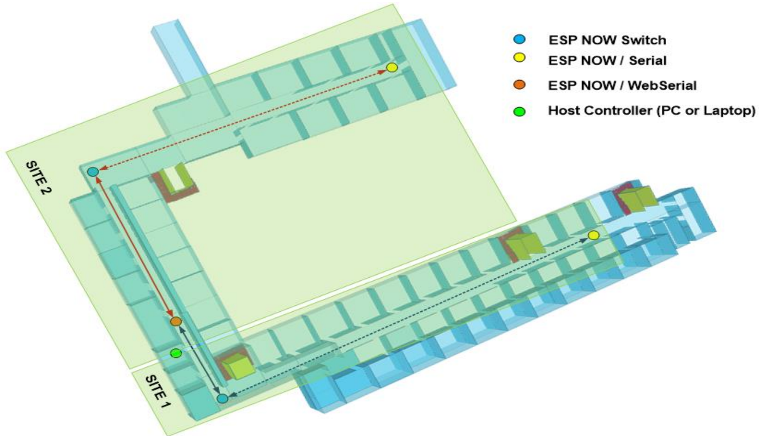

(a) 1st and 2nd Indoor Sites (improved range)

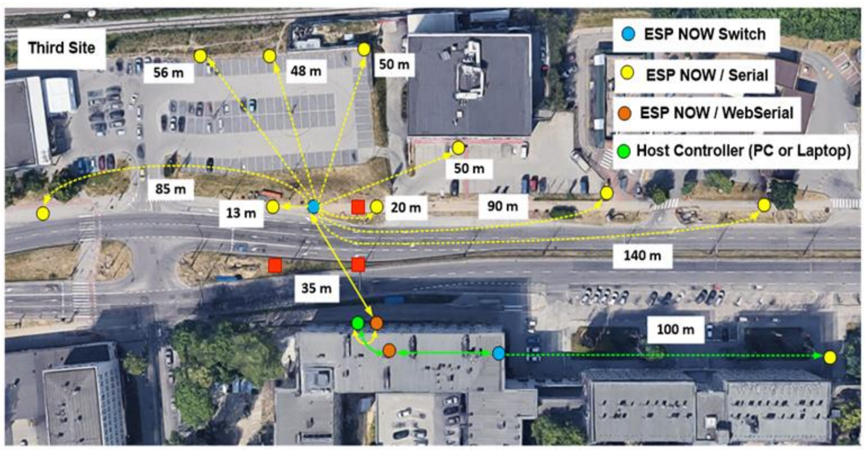

(b) 3rd Outdoor Site (improved range)

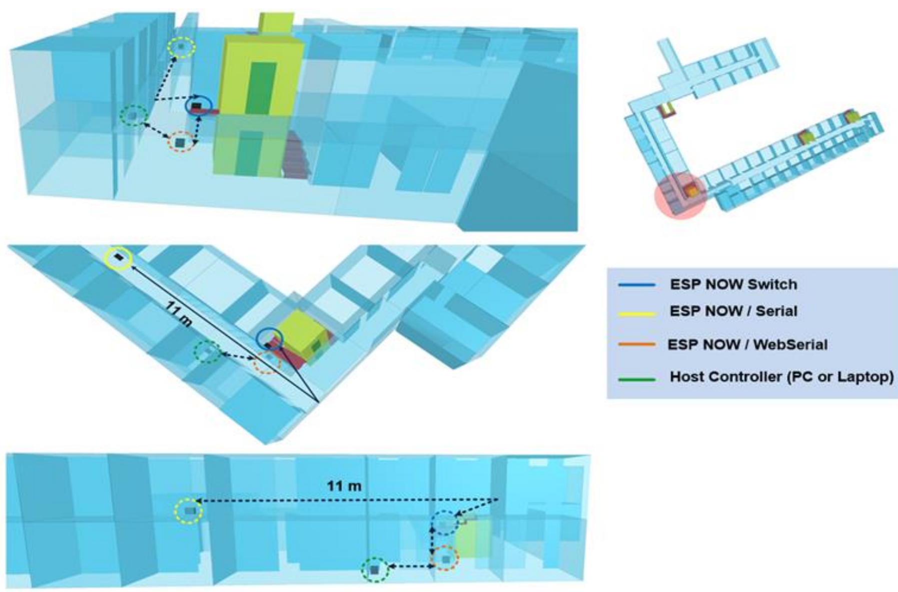

(c) 5th Outdoor Site (improved range)

Figure 3.9 - Increased range and coverage area of ESP32 Wi-Fi based network due to application of 2nd Configuration

3.5 Application of ESP32 Based Wi-Fi on Commercial Ships

In order to consider the possible applications for the ESP32 based Wi-Fi in maritime engineering applications, the following aspects should be taken into account:

1. Unlike wireless HART protocol, the use of ESP32 based Wi-Fi as a medium for measurement /control data transaction can be applied on small as well as large scales. In other words, the ESP32 based Wi-Fi can be dedicated to data transaction in one or two systems, the same as being used for multiple or all systems in a specific maritime engineering application such as commercial ships. On the contrary, in wireless HART Protocol, it is highly recommended to build a large network of wireless HART field devices supporting each other as neighbor devices in order to maintain high levels of reliability and robustness.

2. Unlike wireless HART protocol, the ESP32 based Wi-Fi identically provides an equal level of cost effectivity and economic efficiency, while processing measurement/control data from sensors based on different types of analogue standards the same as sensors based on binary ON-OFF switching standards without any imposed restrictions. In wireless HART protocol, higher levels of cost effectivity is provided while processing data from sensors based on analogue standards than the provided economic efficiency while processing data from sensors based on on/off state changing standards as the cost of a single wireless HART analogue transmitter is extremely high in comparison with the cost of the ESP32 controller of few US dollars. Moreover, it does not make any sense to afford an expensive wireless HART binary transmitter to detect the data from a limited number (two or three) classical pressure or temperature switches, as the binary wireless HART binary transmitter will not even replace the ON-OFF state changing switches, it will simply collaborate with them.

3. The only advantage that can be provided by wireless HART protocol is the high level of security and data encryption during the execution of wireless data transaction. The ESP32 based Wi-Fi can execute encrypted as well as unencrypted wireless data transaction, particularly when ESP-NOW protocol is adopted in order to ensure improved range capabilities.

4. In ESP-NOW protocol, the maximum permissible ESP32 devices is 20 devices for unencrypted data transaction and 17 devices for encrypted data transaction. This aspect should be considered carefully if it was intended to depend on the ESP32 based Wi-Fi as a medium for data transaction on a large scale from many control and measurement systems.

5. Based on the elaborately described laboratory stand and its expected use for processing measurement/control data through the two previously explained configurations, an additional host controller should be utilized if the total number of the ESP32 devices, is expected to exceed the maximum permissible number of field devices in large scale applications. The added host controllers can be separated physically (through using another PC) or virtually (through using virtual operating systems or added software tools) from the first host controller.

If multiple host controllers are planned to be implemented at the ESP32 based Wi-Fi instrumentation network, it is highly recommended that these host controllers are linked in a configuration that can be treated as a master-slave configuration. The role of the slave host controller is to receive the measurement data wirelessly from the ESP32 controller through the WebSerial remote the serial monitor, while the role of master host controller will be to process the data collected from all the slave host controllers and forward to the GUI of the large scale plant. The master host controller also will be as the backup host controller for any of the slave host controllers in case of any possible failure.

6. In light of the previously introduced laboratory stand and the related proposed configurations for range improvement capabilities, it is recommended to position the Arduino controller to which multiple sensors are connected, at the center of the plant section, only if the connected sensors are not located in a confined part of such a plant section, but fairly distributed at its area.

7. The use of Arduino controller is recommended at the laboratory stand, only when processing data from multiple analogue transmitters based on analogue standards such as the 4-20 mA analogue standard, which is preferably converted into 1-5 VDC signal for accuracy considerations, as the Arduino controller can tolerate voltage slightly more than 5 VDC. In case of processing data collected from ON-OFF state changing switches, it is recommended to connect these signals directly to the ESP32 controller without the necessity of utilizing the Arduino controller, because in such a case, the state of the binary switch can be rendered accurately with the 3 VDC level adopted by the ESP32 controller.

8. ESP32/1 is the ESP32 controller unit at which Webserial communication tasks are being executed simultaneously with the ESP-NOW data exchange with the other ESP32 devices in the instrumentation network.

9. ESP32/0 is the ESP32 controller unit at which only ESP-NOW data exchange is executed with the other ESP32 devices in the instrumentation network

10. ESP32/2 is the ESP32 controller unit at which serial communication with the Arduino controller is taking place simultaneously with the ESP-NOW data exchange with the other ESP32 devices in the instrumentation network.

3.5.1 Large Scale Application on a Commercial Container Ship (Planning Example).

Inside the engine room of a container ship, Figure (3.10-a) illustrates the obtained RSSI values for an ESP32 based Wi-Fi network at specific locations near specific systems, from which the measurement data are planned to be transmitted wirelessly to the host controller located at the control room based on the previously described laboratory stand and the related configurations for range enhancement at the upgraded version of the stand. The purpose of conducting such a measurement is to identify the best location at which the ESP32/1 will be positioned. As shown in figure (3.10-b), the best location for such a purpose is the one at which the obtained RSSI reading is - 37 dbm with respect to the location of the host controller inside the engine control room (ECR).

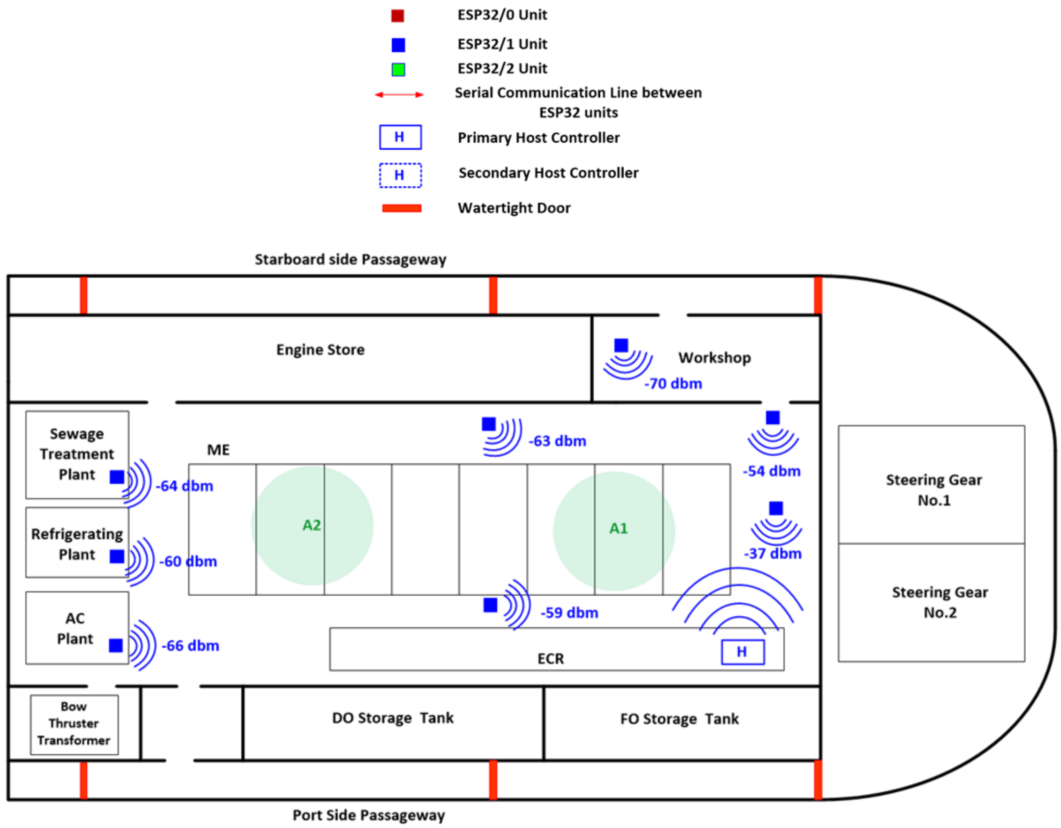

(a) Measured RSSI levels at various locations in engine room with the host controller at the engine control room

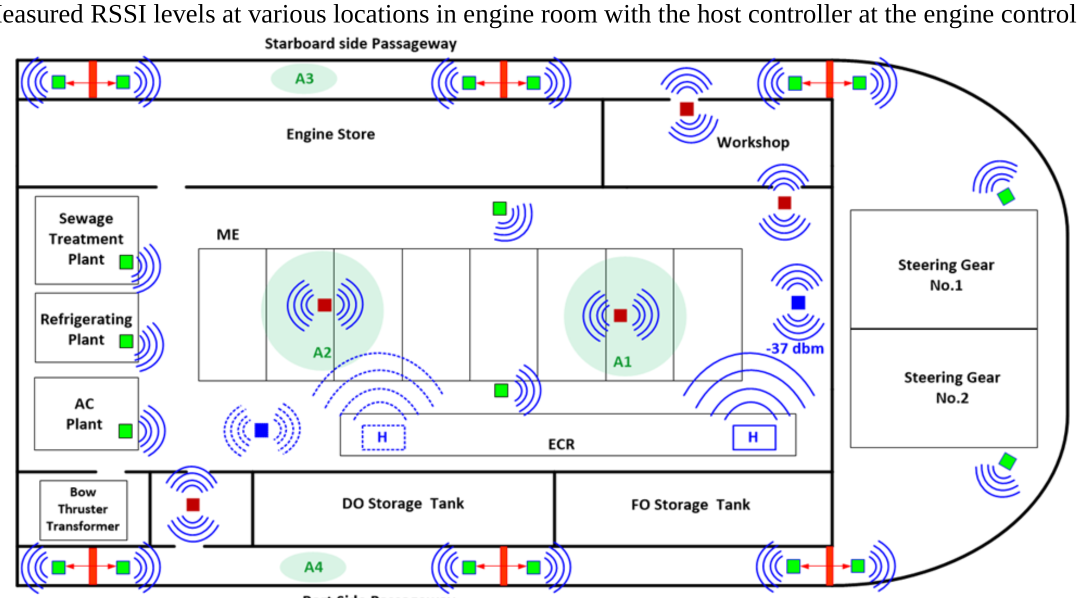

(b) Distribution of the ESP32/0, ESP32/1 and ESP32/2 units to collect data from various systems at the ER

Figure 3.10 – Large scale planning example for the application of the ESP32 based Wi-Fi in engine room (ER)

After indicating the position of the ESP32/1 controller and in accordance with the locations of the systems from which measurement data will be collected, areas A1 and A2 are indicated as possible locations for ESP32/0 controller (switches) in order to facilitate the communication between various ESP32/2 controllers at different sides of the engine room. Additionally, ESP32/0 units will be also installed at some specific locations at close proximity to both entrances of the passageways (At the workshop and the bow thruster transformer unit) for the purpose of collecting the different types of measured data at the passageways. The passageways are two long passages at both sides of any container ships extending from the ship's stern to the ship's front. The basic purpose of the passageways is to give an easy access for the cargo holds with the loaded containers inside it. The passageways are divided into sections separated by watertight doors. Watertight doors are heavy metallic doors the purpose of which is to isolate specific sections of the ship in case of emergency situations leading to water immersion inside these sections. In order to transmit the measurement data wirelessly along the passageway, the watertight doors are expected to be an obstacle disrupting the uniform propagation of the RF waves. The RSSI values were measured before a closed watertight door from an ESP32 positioned after the watertight door. The detected RSSI level in such a case was in the range between - 59 and - 63 dbm which is not a very high level, however successful wireless communication can still be maintained in such a range. This measurement was applied on a watertight aged door the service lifetime of which is almost 20 years, with an insulating rubber material that might have never been overhauled or replaced. Therefore, a future research is planned to be carried out on different types of watertight doors with different ages of service lifetimes in order to identify the exact possibility of RF waves propagation through secured watertight doors. In this example, it will be possible to execute Wi-Fi based communication tasks through watertight doors with low RSSI values. In case of lack of such a possibility on another ship or in other operational conditions, serial communication will be the only solution to overcome such a choking point during wireless communication along the passage way. This can be achieved using a short serial link of single twisted pair cable connected between the two ESP32 controllers located before and after the closed watertight door. The most important signals that can be collected from the passageways are:

- Cargo hold bilge level switches.
- Cargo hold Fans operational condition (On-Off-Overload).
- Sea water ballast tanks analogue transmitters.

3.5.2 Small Scale Application on a Ship (Fire Alarm Planning Example).

Fire alarm system is one of the most important safety systems in any facility. According to the International Convention of Safety of Life at Sea (SOLAS), many regulations were issued by the International Maritime Organization (IMO) for the aim of defining the minimal compulsory requirements needed for the components of the fire detection and prevention systems in order to be approved for installation aboard various types of commercial ships. Fire detection equipment are extensively deployed all over any commercial ship in locations such as engine room, accommodation, forward as well as AFT stations and cargo crane funnels. For the purpose of analyzing the possibility of using the ESP32 based Wi-Fi in fire detection system at the ship's accommodation, the RSSI levels were measured at several floors of the ship's accommodation with respect to the host controller planned to be installed at the upper deck in the cargo office, which is the most convenient location for the host controller from a point of view affiliated to the possibility of establishing a reliable interconnection between multiple sections included in a single shipboard system (one section located most probably spread at the engine room, while the other sections are laid out at either the accommodation or on deck). Examples for such systems are:

1. Valve remote control system
   - Engine room section.
   - Main deck section.
2. Tank level measurement system
   - Engine room section.
   - Main deck section.
3. Ballast water treatment system (BWTS)
   - Engine room section.
   - Cargo room operational panel section.
4. Fire detection and alarm system
   - Main engine section.
   - Ship's accommodation section.
   - Forward and AFT stations sections.

Accordingly, the selection of the cargo office as a location for the host controller, will consequently allow for facilitated integration between the accommodation section and the main engine section of the fire alarm and detection system (if desired in the future). Due to the excessive presence of high density metallic infrastructure inside the accommodation with narrow spaces between such infrastructural obstacles, the entrance of the cargo room is the best position at which the highest RSSI levels was obtained (-48 dbm to - 35 dbm). Therefore, the ESP32/1 unit (communicating with the host controller through the WebSerial remote serial monitor) is recommended to be mounted at the entrance of the cargo control room.

Each floor at the ship's accommodation usually includes two manual call points and two optical smoke detectors as fire detection devices. The application of using the ESP32 based Wi-Fi for data transaction at accommodation fire alarm section, can be based on adopting the first or second configuration for range enhancement. As the stairs area at the accommodation can be considered as an area of relatively low density of metallic infrastructure, then, the ESP32/2 units can be mounted at the area of the stairs funnel. The number of the required ESP32/2 units can be determined according to the selected number of signals from each floor to be processed by a single ESP32/2 unit. The higher was the number of ESP32/2 units, the more stable was the process of wireless communication between the ESP32/1 units, the ESP32/2 units and the host controller. Figure 3.11- a and b illustrate two options for the connection of the fire detection devices with the ESP32/2 units. The first option is to allocate a single ESP32/2 unit to process four fire detection signals from each floor (Figure 3.11- a). The second option is to allocate a single ESP32/2 unit to process 8 fire detection signals from each two floors (Figure 3.11- b).

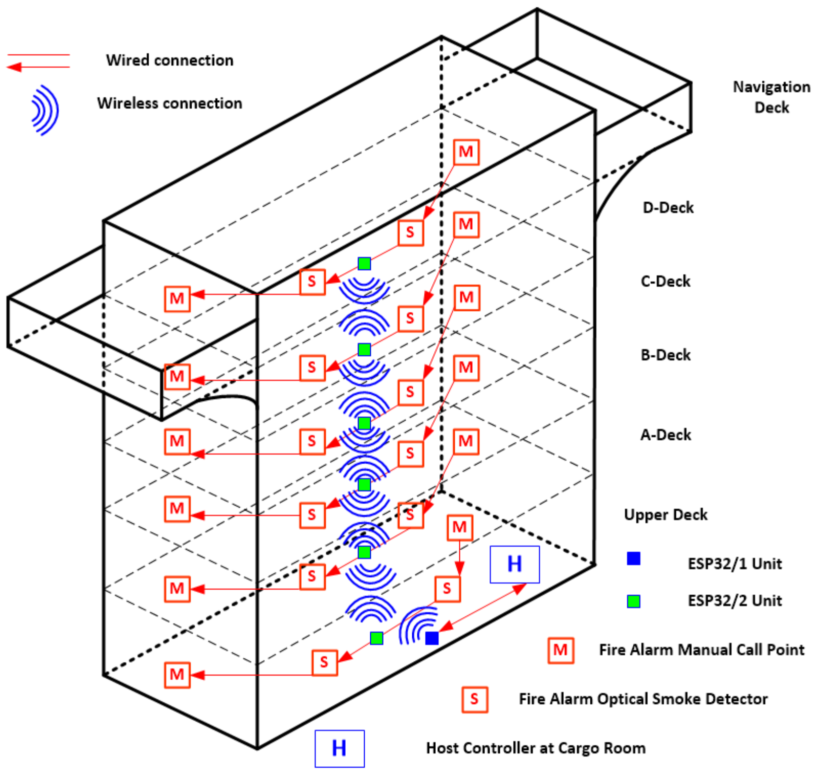

(a) ESP32/2 units collecting data from optical smoke detectors and manual call points at each floor

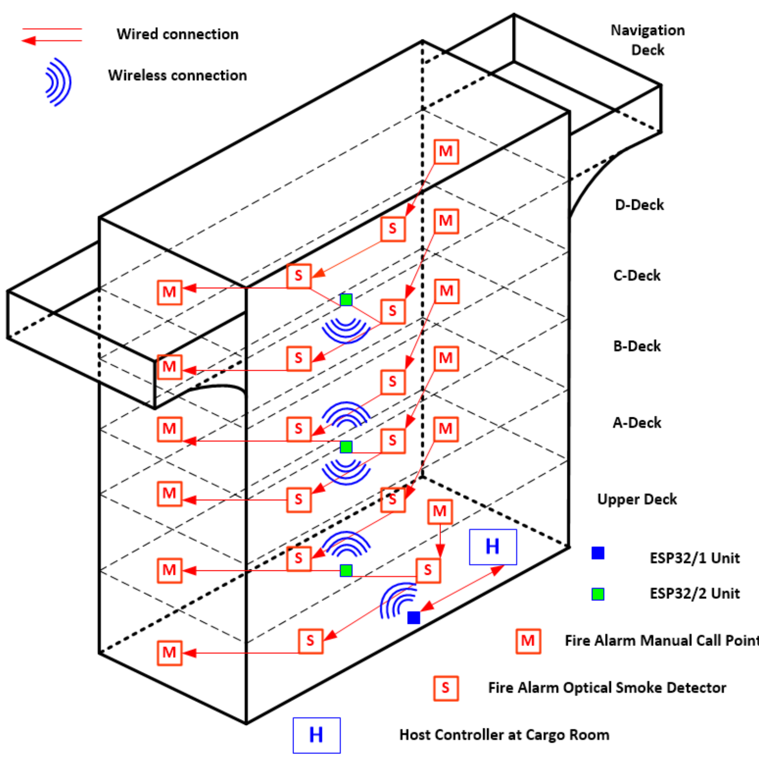

(b) ESP32/2 units collecting data from optical smoke detectors and manual call points at each two floors

Figure 3.11 – Small scale planning example for the application of ESP32 based Wi-Fi in fire detection and alarm system inside the accommodation

3.5.3 Cargo Cranes Wireless Safety and Performance System (Small Scale Total Realization)

The research in [15] has discussed the subject of total realization of a wireless system dedicated to cargo cranes safety and performance monitoring on a container ship. The system is based on the described laboratory stand in this doctoral study in accordance with the proposed configurations for range expansion. Adopting the ESP32 based Wi-Fi as a cost effective medium for measurement data transaction at the discussed system has resulted in increased levels of operational safety at marine cargo cranes through the implementation of both principles of functional safety and predictive maintenance (PdM). Figure 3.13 demonstrates the GUI of the system. Table 3.7 illustrates the processed signals by the system and the purpose of monitoring each of them. Table 3.8 illustrates the operational ranges as well as the alarm ranges of each of the monitored and processed signals. The system is based on using:

- Two ESP32/2 units located at the top of the cargo cranes (ESP32 No.1 and ESP32 No.2 at Figure 3.14)
- Two ESP32/0 units located at starboard and port sides of the navigational bridge (ESP32 No.4 and ESP32 No.5 at Figure 3.14).
- One ESP32/1 unit located at the bridge center (ESP32 No.3 at Figure 3.14)

Table 3.7 – Description for the most important parameters monitored by the developed Wi-Fi based wireless system dedicated to marine cargo cranes

No.	Signal	Description
1	Fire alarm	Through a loop consisting of two manual call points and two optical smoke detectors (Figure 3.12), the system will provide the possibility of wireless detection of any expected fire incidents that might be caused by: • Possible contact between hydraulic oil splashes and hot surfaces. • Possible electrical sparks at the area of the three phases 440 VAC supplying voltage slip-rings.
2	Hydraulic oil level	Each cargo electrohydraulic crane has its own storage tank of hydraulic oil. The level of the hydraulic oil inside the tank should be in its normal range in order to maintain smooth pumping provided by the crane feed pump.
3	Brake valve status	• Each crane has three brake valves for three types of movements provided by three different hydraulic motors. These movements are luffing, slewing and hoisting. • Hoisting is most important type of movement as it handles the greatest portion of the weight of the object loaded or discharged by the crane. • When the brake valve is energized, the brakes are released. • When the brake valve is de-energized, the brakes are activated.
4	Hydraulic oil feed pressure	The oil pressure provided by the crane feed pump should be within the normal operational range so that this feed pressure would be adequate for providing smooth operation of the hydraulic motors

		(providing the required and speed and torque) required for the three types of movement (slewing, luffing and hoisting).
5	Hydraulic oil feed temperature	• The temperature of the pumped hydraulic oil during operation should be kept within operational permissible range, otherwise increased temperature of the pumped hydraulic oil might lead to the change of the hydraulic oil dynamic viscosity which will consequently result in hydraulic failures. • On the other hand, very low temperature levels leads to very low output pressure from the feed pump, which consequently leads to an operational failure.
6	Hoisting joystick output voltage	Detecting the hoisting operator lever is very important to evaluate the condition of its potentiometers and replace them in case of any observed abnormalities so that any possible crane stoppage can be avoided.
7	Hoisting load pressure	• The load pressure is the hydraulic oil pressure proportional to the weight being handled by the crane. • If the load pressure will be higher than a specific value, the hoisting hydraulic motor will shift from operating with high speed to operating with lower speed as more torque will be required to handle loads of heavier weights.
8	Listing angle	The listing angle is the angle that the ship swerves from its rolling axis either to starboard side or to the port side.

Table 3.8 - Critical values for the parameters of cargo crane monitored by the developed Wi-Fi based wireless system. Default state refers to the parameter state when the crane is not in operational state. Operational state refers to the parameter state when the crane is handling cargo (Loading / Discharging).

No.	Parameter	Default State	Operational State
1	Fire Alarm	Normal	Alarm
2	Brake Valve Status	De-energized Engaged Idle	Energized Disengaged In operation
3	Hydraulic Oil Tank Level	Normal	Low (Alarm)
4	Operator Joystick Output Voltage	6 VDC (Neutral)	(0-6 VDC) (Lowering) (6-12 VDC) (Hoisting)
5	Hydraulic Oil Feed Pressure	0 bar (Idle)	(20 – 40 bar)(Normal) (< 20 bar)(Alarm) (> 40 bar)(Alarm)
6	Hydraulic Oil Temperature	Ambient Temp. (Idle)	(< 60° C)(Normal) (> 60° C)(Alarm)
7	Hoisting Load Pressure	0 bar (Idle)	(< 200 bar)(High Speed) (> 200 bar)(Low speed)
8	Listing Angle	Ideal State (Should be 0°)	Operational State (< 4° Normal) (> 4° Alarm)

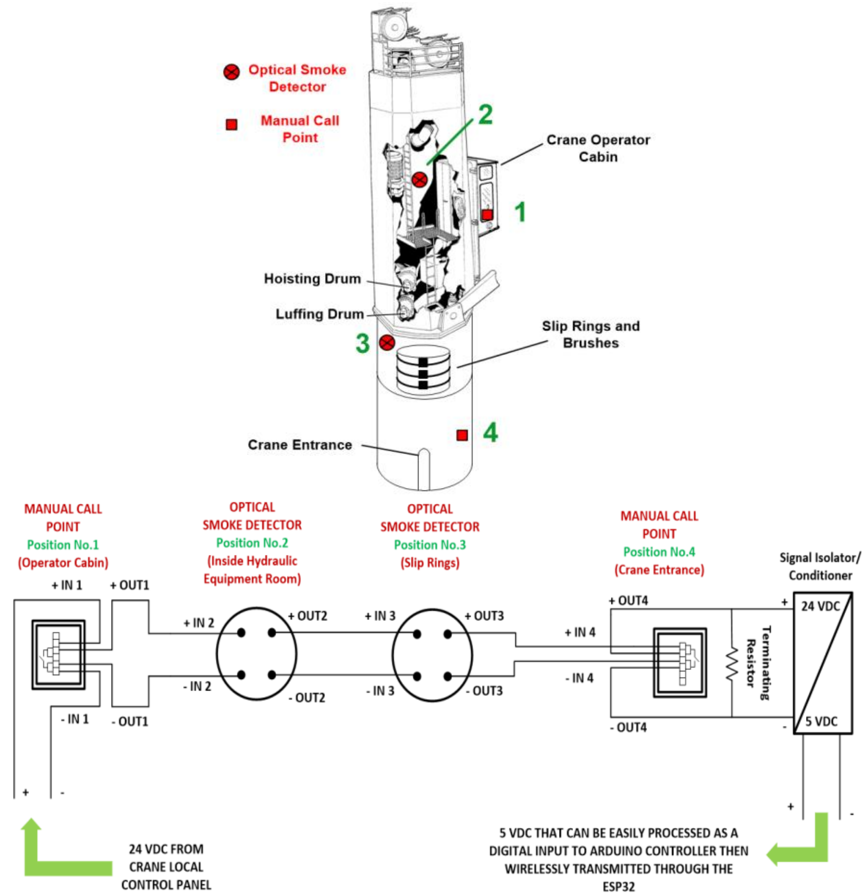

Figure 3.12 – Location and connection diagram of the fire detection sensors (optical smoke detectors and manual call points)

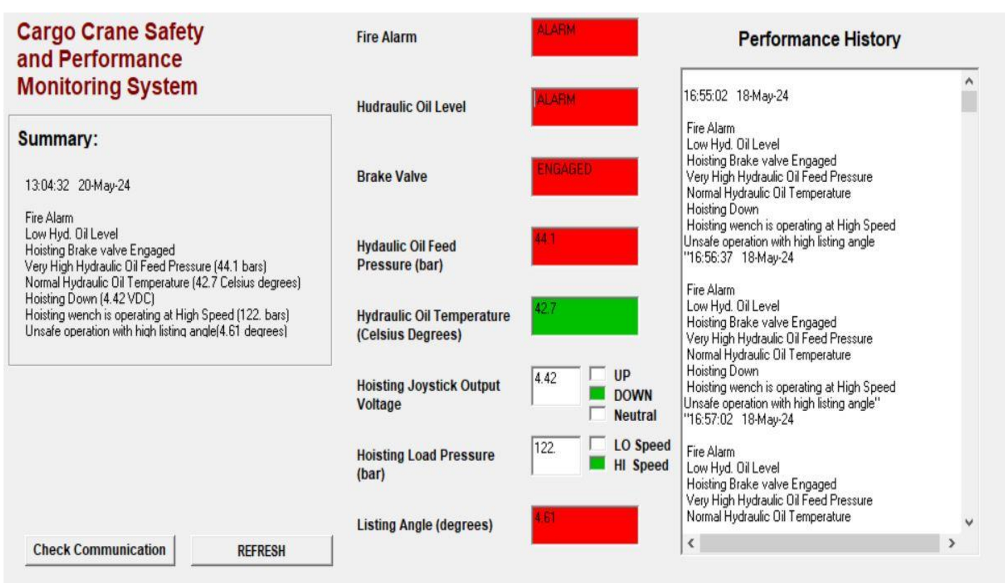

Figure 3.13 - Demonstration of the System GUI (Graphical User Interface) during operation

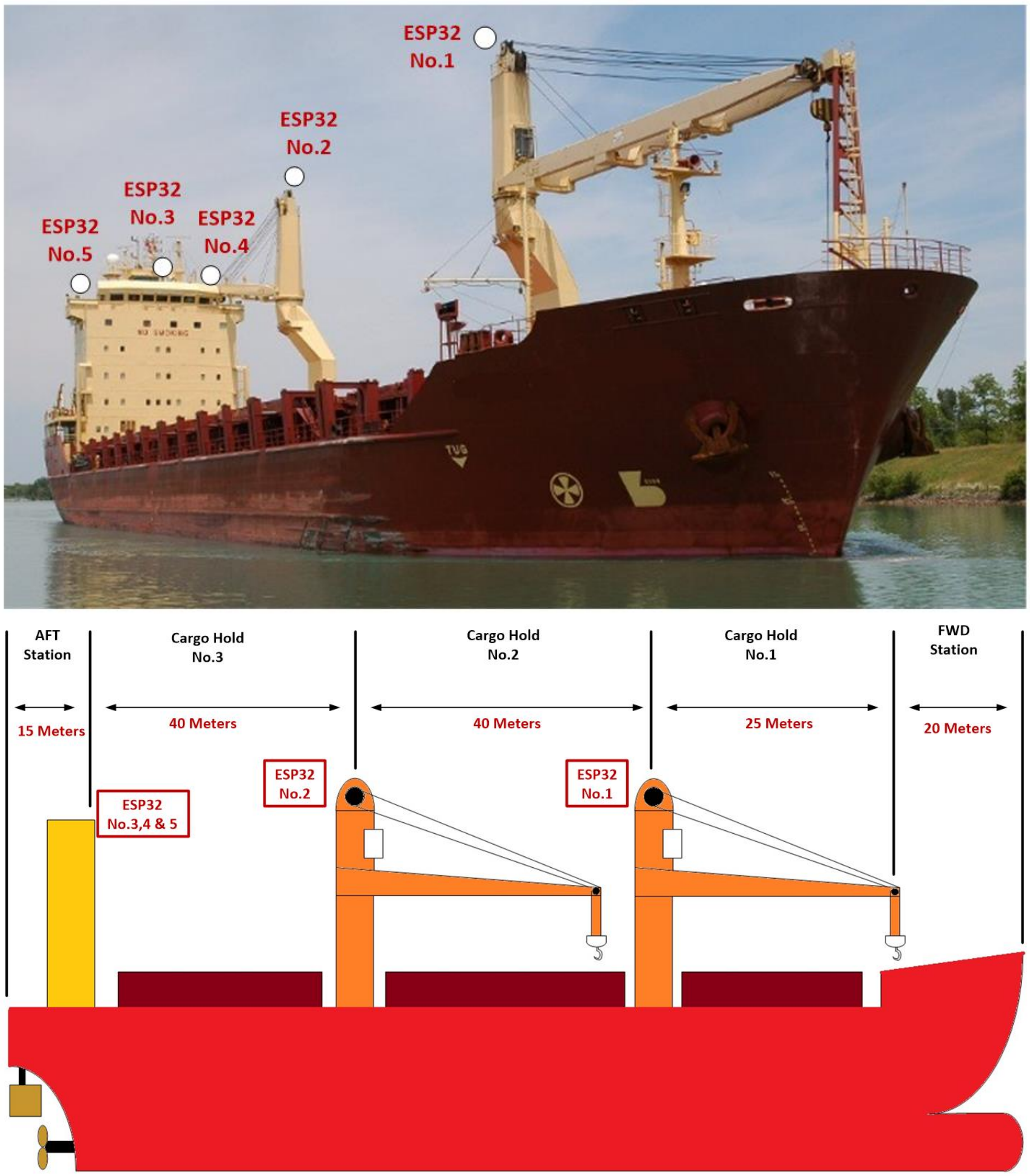

Figure 3.14 - Illustration for the locations of the required ESP32 modules for the developed wireless system, in addition to an approximate dimensional drawing for the ship.

3.5.3.1 Cost Analysis

The research in [15] has highlighted two possible recommended cabling options and advised against one cabling option in marine engineering applications. The specifications of each of these options are illustrated in Table 3.9. The options at the table are sorted from the best to the worst. In Table 3.10 and Figure 3.15, an illustration is provided for the required cost to apply the 1st cabling option through utilizing different types of cables through estimating the cost needed for each type of cables and the final average cost of all types. Similarly, the same analysis was carried out and demonstrated at Table 3.11 and Figure 3.16 for the application of the 2nd cabling option at the discussed cargo crane system.

In order to demonstrate the cost efficiency of the developed wireless system from a perspective related to the comparative analysis of the selected cabling options (1st and 2nd options), the total cost required to implement the Wi-Fi wireless data transaction medium should be calculated. The developed wireless system is based on using five ESP32 modules. The cost of each of these modules is almost 10 $ at the local market, which means that the overall cost to implement the Wi-Fi wireless data transaction medium is 50 $. Accordingly, the cost saving efficiency can be calculated as follows for both the 1st and 2nd cabling options.

Cost saving efficiency = [1 – (Wi-Fi implementation cost / Average Cabling Cost)] × 100 (3.3)

Cost saving efficiency (1st cabling option) = [1 – (50 / 4933)] × 100 = 98.986 %
Cost saving efficiency (2nd cabling option) = [1 – (50 / 2181.86)] × 100 = 97.7 %

Table 3.9 – Recommended and advised against cabling options in shipboard systems

Option	Description
1st Cabling Option ***(Highly Recommended)***	• Using single cable of two twisted pairs for each of the 8 variables, which means that the total number of cables will be 8 cables. The spare capacity in such a case will be 100%, as each signal will be transmitted through a twisted pair of wires, while the remaining twisted pair in the same cable will be treated as a spare pair in case of any future failure for the used twisted pair. • The replacement of the whole cable will be the only choice in case of any possible failure if the cable included only a single twisted pair of wires (3rd cabling option).
2nd Cabling Option ***(Recommended)***	• Using a single cable with (1.5 n) twisted pairs where (n) is the number of the processed signals,. The spare capacity in such a case will be 50%. • For the discussed cargo cranes wireless performance and safety system, 8 twisted pairs will be used for the whole 8 scanned variables and 4 twisted pairs reserved as spare wires in case of any failure for the already in service pairs. Total number of twisted pairs will be 12. • The selected 50% spare capacity was assumed here as a moderate alternative to calculate the cabling cost with taking a moderate risk of a maximum pair failure probability of 50% of the used pairs
3rd Cabling Option <u>**Most Popular**</u> ***(Advised against)***	• Using a single twisted pair cable or multiple twisted pair cable with a total number of twisted pairs equal to the exact number of the processed signals (n) with 0% spare capacity. For • In such a case, any expected future failure will mean only the overall replacement of the cable. • For the discussed cargo cranes wireless performance and safety system, 8 twisted pairs the whole required number of twisted pairs. • Cables replacement in maritime engineering applications is a time as well as effort and cost consuming processes especially

	for systems located on main deck and monitored in engine room, as the cables dedicated to such systems are extended in steel pipes on main deck, which is extremely hard to access, particularly on rather old ships where such pipes are negatively affected by ageing and high levels of salinity and corrosion

Table 3.10 - Instrumentation cables that might be used in cabling process in case 1st option was taken into account.

No.	Material , No. of Pairs, Shielding, Vmax	AWG/Wire Diameter mm	Price for 200 meters
1	PLTC, Overall Shield, 300V 2 Pairs	20 / 0.812	2,519.04 $
2	PLTC, Individual & Overall Shield, 300V 2 Pairs	18 / 1.024	2,991.36 $
3	PLTC, Individual & Overall Shield, 300V 2 Pairs	16 / 1.291	4,040.96 $
4	XLP/CPE, Individual & Overall Shield, UL Type TC, 600V 2 Pairs	16 / 1.291	7,189.76 $
5	TC-ER, Individual & Overall Shield, 600V 2 Pairs	18 / 1.024	3,201.28 $
6	TC-ER, Individual & Overall Shield, 600V 2 Pairs	16 / 1.291	4,670.72 $
7	FR-EPR/CPE, Individual & Overall Shield, UL Type TC, 600V 2 Pairs	16 / 1.291	10,338.56 $

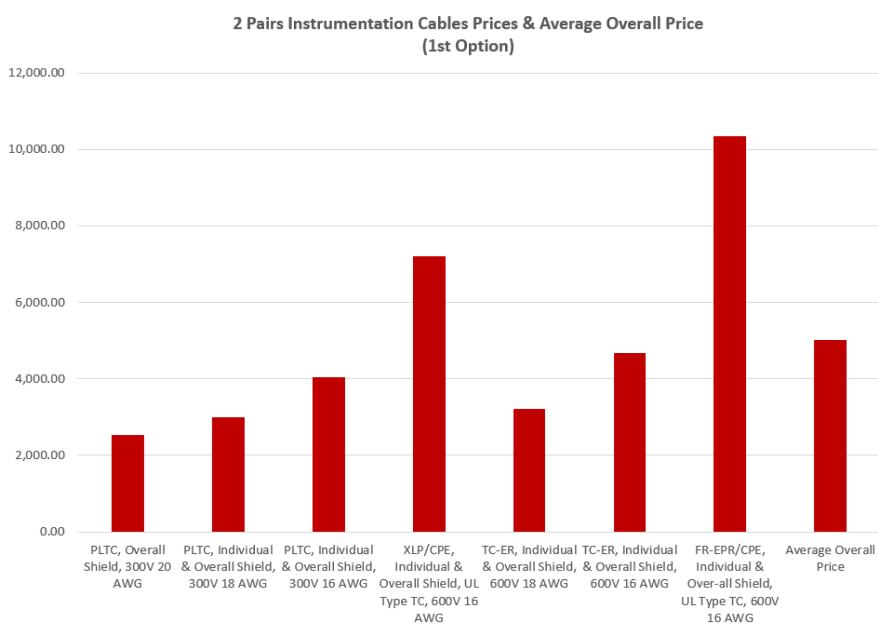

Figure 3.15 - Illustration for the prices of the 7 types of the two pairs instrumentation cables indicated in table 2 with an average overall price of almost 4933 $

Table 3.11 - Instrumentation cables that might be used in cabling process in case 2nd option was taken into account

No.	Material , No. of Pairs, Shielding, Vmax	AWG/Wire Diameter mm	Price for 200 meters
1	PLTC, Individual & Overall Shield, 300V 12 Pairs	20 / 0.812	1804 $
2	PLTC, Individual & Overall Shield, 300V 12 Pairs	18 / 1.024	2184.48 $
3	TC-ER, Individual & Overall Shield, 600V 12 Pairs	16 / 1.291	3,312.8 $
4	TC-ER, Individual & Overall Shield, 600V 12 Pairs	14 / 1.628	3,608 $

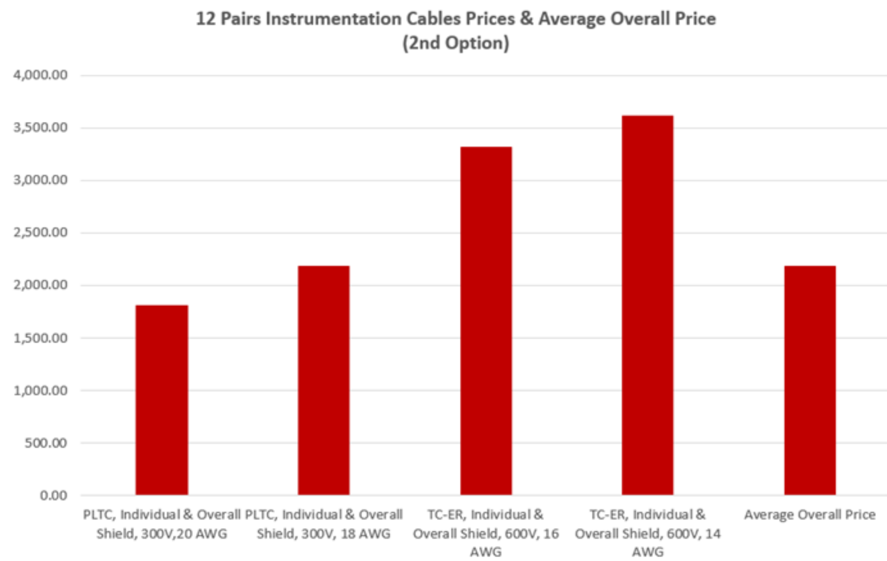

Figure 3.16 - Illustration for the prices of the 4 types of the twelve pairs instrumentation cables indicated in table 3 with an average overall price of almost 2181.86 $

3.5.3.2 Functionally Safe Configuration

The principle of functional safety is basically based on pairing the components included in any measurement system so that any component can be taken over by its functional pair in case of failure. For example, in a simple 4-20 mA measurement current loop, in order to implement the principle of functional safety partially from a perspective linked to the multichannel concept, the developed wireless proposed system will adopt an additional wireless channel for measurement data transaction, which will function as a backup channel for the cabling channel at the original system (Figure 3.17) based on classical control/measurement techniques. This redundant decomposition for the data transaction medium, is a basic requirement for the application of functional safety principle. Table (3.12) demonstrates four cases for implementing the concept of redundant decomposition for data transaction channels according to the obtained results from cost analysis of the two recommended cabling options at the cargo crane wireless performance and safety monitoring system [104-106]. Based on the same concept rendered by equation (3.3), the cost saving efficiency was calculated for the two analyzed choices to implement the functional safety principal partially through using two data transaction channels through depending on either two cabling channels (1st choice) or one cabling channel and one wireless Wi-Fi channel (2nd choice). Both choices will be applied for both of the 1st and the 2nd cabling options. The results of the conducted calculations has shown an achieved cost saving efficiencies of 49.493 % and 48.854 % for the 1st and the 2nd cabling options by embracing the second choice of using an additional Wi-Fi wireless redundant back up channel for the main cabling channel.

Cost saving efficiency (1st Case, 2nd Case) (1st cabling option) =

$$[1 - (4983\ \$ / 9866\ \$)] \times 100 = 49.493\ \%$$

Cost saving efficiency (3rd Case, 4th Case) (2nd cabling option) =

$$[1 - (2231.86\ \$ / 4363.72\ \$)] \times 100 = 48.854\ \%$$

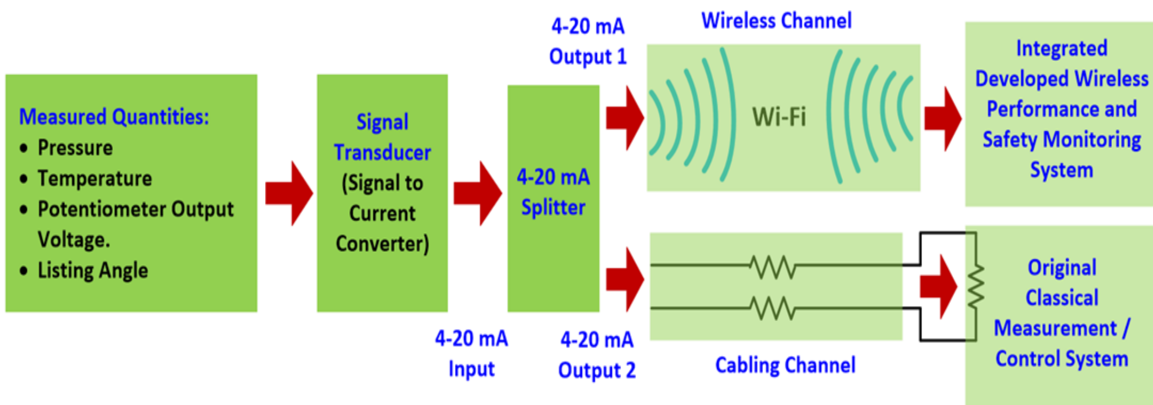

Figure 3.17 - Illustration for the partial implementation of the functional safety principle through the redundant decomposition of the channel through which measurement / control data are exchanged, into two channels. The first channel is Wi-Fi wireless based, while the second is based on conventional cabling (Multichannel Architecture).

Table 3.12 – Description and cost of implementing various cases for redundant decomposition of data transaction medium in functional safety (using additional cabling channel or wireless channel to be paired with the main channel)

Cases	Description	Required Cost
Case 1	Two cabling channels (1st cabling option)	2×4933 $ = 9866 $
Case 2	One Cabling channel + One Wi-Fi wireless channel (1st cabling option) (100% spare capacity)	50$ + 4933 $ = 4983 $
Case 3	Two cabling channels (2nd cabling option)	2×2181.86 $ = 4363.72 $
Case 4	One Cabling channel + One Wi-Fi wireless channel (2nd cabling option) (50% spare capacity)	50$ + 2181.86 $ = 2231.86 $

3.5.3.3 Predictive Maintenance PdM Application (Hydraulic oil dynamic viscosity)

PdM has basically evolved after the emergence of industry 4.0 (I4.0). Machine learning (ML) and Deep Learning (DL) are considered as approaches to guarantee the successful implementation of PdM. Internet of Things IoT can be considered as a tool facilitating the functionality of these approaches with lower costs and better efficiency. An example for PdM, is to create algorithms or mathematical models comparing between historical and recent data collected by specific sensors. This technique is called Supervised Learning (ML method) . Another example for PdM, is to carry out analysis for data sequences collected over specific consistent periods of time. This technique is called Time Series analysis (DL method). Alarm IDs and their timestamps included in event data logs are very important tool to apply both of machine learning and deep learning [107,108].

The major purpose of predictive maintenance at the developed wireless safety and performance system for marine cargo cranes is to provide a means of early detection for future failures through a performance monitoring log illustrating the changes in some critically important parameters over an unlimited period of time during cargo crane operation. By additional software tools, charts can be built for the collected stored data at the performance monitoring log. Based on these charts, maintenance plans will be modified to eliminate minor uncritical failures before it becomes major and critical. This will consequently result in less down time during crane failures. With such an effective maintenance plan based on reliable measurement data stored at the performance monitoring log, the lifetime of the marine cargo crane critical equipment will be extended which will lead to less need for repetitive replacement of spare parts. The less will be the demand for spare parts, the more will be the economic efficiency of the ship's cargo crane, and also the more will be the economical profit achieved by the ship owner.

The PdM application is dedicated to monitor the changes at the cargo crane hydraulic oil dynamic viscosity values which are calculated and stored at the wireless system performance log at the host controller. The hydraulic oil dynamic viscosity values will be calculated through the Vogel equation (Figure 3.18) using the monitored values for the most important two monitored parameters; the hydraulic oil feed pressure and the hydraulic oil temperature [15,109,110]. The calculated dynamic viscosity values will be compared with the obtained dynamic viscosity values from the charts provided by the hydraulic oil supplier or the cargo crane manufacturer. The following mathematical model is dedicated to analyze the differences between the reference and the calculated values of the dynamic viscosity at specific working hours. Such differences might be a reflection of possible hydraulic equipment failure or an indication for a serious deterioration at the hydraulic oil condition and a change in its properties.

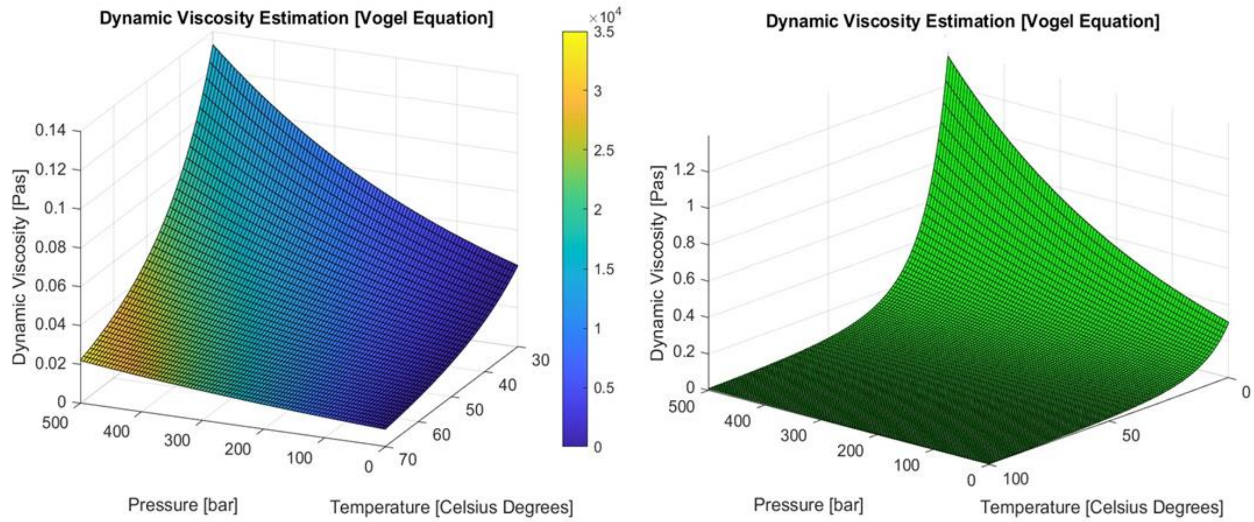

Figure 3.18 - . Example for Hydraulic Oil Dynamic Viscosity Estimation Charts that can be provided by the hydraulic oil supplier or the cargo crane manufacturer. Dynamic viscosity (μ) is measured in (Pas). Pressure is measured (p) in (bar). Temperature (T) is measured in °C [15].

$$\mu(p,T) = ae^{\left[\frac{b}{(T+273.15)-c}\right]}e^{\left[\frac{p}{a_1+a_2T}\right]} \tag{3.4}$$

$$p(n) = [p_1, p_2, p_3, p_4, p_5, \dots \dots \dots \dots, p_n] \tag{3.5}$$

$$T(n) = [T_1, T_2, T_3, T_4, T_5, \dots \dots \dots \dots, T_n] \tag{3.6}$$

$$\mu_c(n) = [\mu_{c_1}, \mu_{c_2}, \mu_{c_3}, \mu_{c_4}, \mu_{c_5}, \dots \dots \dots \dots, \mu_{c_n}] \tag{3.7}$$

$$\mu_r(n) = [\mu_{r_1}, \mu_{r_2}, \mu_{r_3}, \mu_{r_4}, \mu_{r_5}, \dots \dots \dots \dots, \mu_{r_n}] \tag{3.8}$$

$$\Delta\mu(j) = |\ \mu_c(j) - \ \mu_r(j)\ |\ where\ j = 1{:}\,n \tag{3.9}$$

$$A(n) = [\Delta\mu(1), \Delta\mu(2), \Delta\mu(3), \Delta\mu(4), \Delta\mu(5), \dots \dots \dots \dots, \Delta\mu(n)] \tag{3.10}$$

$$A(j) = \begin{cases} j & if\ \Delta\mu(j) > \Delta\mu_{CRITICAL} \quad where\ j = 1{:}\,n \\ 0 & if\ \Delta\mu(j) < \Delta\mu_{CRITICAL} \quad where\ j = 1{:}\,n \end{cases} \tag{3.11}$$

$$A(n_r) = [A_1, A_2, A_3, A_4, A_5, \dots \dots \dots \dots, A_{n_r}]$$

$$B_{\mathrm{nr \times nr}} = \begin{bmatrix} A_{1,1} & A_{1,2} & A_{1,3} & A_{1,4} & A_{1,5} & \dots \dots \dots & \dots \dots \dots & A_{1,nr} \\ A_{2,1} & A_{2,2} & A_{2,3} & A_{2,4} & A_{2,5} & \dots \dots \dots & \dots \dots \dots & A_{2,nr} \\ A_{3,1} & A_{3,2} & A_{3,3} & A_{3,4} & A_{3,5} & \dots \dots \dots & \dots \dots \dots & A_{3,nr} \\ A_{4,1} & A_{4,2} & A_{4,3} & A_{4,4} & A_{4,5} & \dots \dots \dots & \dots \dots \dots & A_{4,nr} \\ A_{5,1} & A_{5,2} & A_{5,3} & A_{5,4} & A_{5,5} & \dots \dots \dots & \dots \dots \dots & A_{5,nr} \\ \vdots & \vdots & \vdots & \vdots & \vdots & \vdots & \vdots & \vdots \\ \vdots & \vdots & \vdots & \vdots & \vdots & \vdots & \vdots & \vdots \\ A_{nr,1} & A_{nr,2} & A_{nr,3} & A_{nr,4} & A_{nr,5} & \dots & A_{nr,nr-1} & A_{nr,nr} \end{bmatrix} \tag{3.12}$$

$$B_{\mathrm{nr}\times\mathrm{nr}} = \begin{bmatrix} 0 & 0 & 0 & 0 & 0 & \dots\dots\dots & \dots\dots\dots & 0 \\ A_{2,1} & 0 & 0 & 0 & 0 & \dots\dots\dots & \dots\dots\dots & 0 \\ A_{3,1} & A_{3,2} & 0 & 0 & 0 & \dots\dots\dots & \dots\dots\dots & 0 \\ A_{4,1} & A_{4,2} & A_{4,3} & 0 & 0 & \dots\dots\dots & \dots\dots\dots & 0 \\ A_{5,1} & A_{5,2} & A_{5,3} & A_{5,4} & 0 & \dots\dots\dots & \dots\dots\dots & 0 \\ \vdots & \vdots & \vdots & \vdots & \vdots & \ddots & \vdots & \vdots \\ \vdots & \vdots & \vdots & \vdots & \vdots & \vdots & \ddots & \vdots \\ A_{nr,1} & A_{nr,2} & A_{nr,3} & A_{nr,4} & A_{nr,5} & \dots & A_{nr,nr-1} & 0 \end{bmatrix} \tag{3.13}$$

$$d_1 = [A_{2,1}, A_{3,2}, A_{4,3}, A_{5,4}, A_{6,5}, \dots\dots\dots\dots, A_{nr,nr-1}],\ h_1 = nr-1 \tag{3.14}$$

$$d_2 = [A_{3,1}, A_{4,2}, A_{5,3}, A_{6,4}, A_{7,5}, \dots\dots\dots\dots, A_{nr,nr-2}], h_2 = nr-2 \tag{3.15}$$

$$d_3 = \{A_{4,1}, A_{5,2}, A_{6,3}, A_{7,4}, A_{8,5}, \dots\dots\dots\dots, A_{nr,nr-3}\}, h_3 = nr-3 \tag{3.16}$$

$$d_4 = [A_{5,1}, A_{6,2}, A_{7,3}, A_{8,4}, A_{9,5}, \dots\dots\dots\dots, A_{nr,nr-4}], h_3 = nr-4 \tag{3.17}$$

$$d_5 = [A_{6,1}, A_{7,2}, A_{8,3}, A_{9,4}, A_{10,5}, \dots\dots\dots\dots, A_{nr,nr-5}], h_3 = nr-5 \tag{3.18}$$

$$\vdots$$

$$d_{nr-2} = \{A_{nr-1,1}, A_{nr,2}\}, h_{nr-2} = 2 \tag{3.19}$$

$$d_x = \{A_{nr,1}\}, h_x = 1 \ where\ x = nr-1 \tag{3.20}$$

$$\frac{C_{\mathrm{nr}/2\times\mathrm{nr}-1}}{nr\ even} = \begin{bmatrix} C_{1,1} & C_{1,2} & C_{1,3} & C_{1,4} & C_{1,5} & \dots\dots\dots & \dots\dots\dots & C_{1,nr-1} \\ C_{2,1} & C_{2,2} & C_{2,3} & C_{2,4} & C_{2,5} & \dots\dots\dots & \dots\dots\dots & C_{2,nr-1} \\ C_{3,1} & C_{3,2} & C_{3,3} & C_{3,4} & C_{3,5} & \dots\dots\dots & \dots\dots\dots & C_{3,nr-1} \\ \vdots & \vdots & \vdots & \vdots & \vdots & \vdots & \vdots & \vdots \\ C_{\frac{nr}{2},1} & C_{\frac{nr}{2},2} & C_{\frac{nr}{2},3} & C_{\frac{nr}{2},4} & C_{\frac{nr}{2},5} & \dots & C_{\frac{nr}{2},nr-2} & C_{\frac{nr}{2},nr-1} \end{bmatrix} \tag{3.21}$$

$$\frac{C_{\mathrm{nr}/2\times\mathrm{nr}-1}}{nr\ even} =$$

$$\begin{bmatrix} A_{2,1} & A_{3,2} & A_{4,3} & A_{5,4} & A_{6,5} & \dots\dots\dots & \dots\dots\dots & \dots\dots\dots & \dots\dots\dots & A_{nr,nr-1} \\ A_{3,1} & A_{4,2} & A_{5,3} & A_{6,4} & A_{7,5} & \dots\dots\dots & \dots\dots\dots & \dots\dots\dots & A_{nr,nr-2} & A_{4,1} \\ A_{5,2} & A_{6,3} & A_{7,4} & A_{8,5} & A_{9,6} & \dots\dots\dots & A_{nr,nr-3} & A_{5,1} & A_{6,2} & A_{7,3} \\ \vdots & \vdots & \vdots & \vdots & \vdots & \vdots & \vdots & \vdots & \vdots & \vdots \\ \dots\dots\dots & \dots\dots\dots & \dots\dots\dots & \dots\dots\dots & \dots\dots\dots & A_{nr-1,2} & A_{nr,3} & A_{nr-1,1} & A_{nr,2} & A_{nr,1} \end{bmatrix} \tag{3.22}$$

$$\frac{C_{\mathrm{nr}-1/2\times\mathrm{nr}}}{nr\ odd} = \begin{bmatrix} C_{1,1} & C_{1,2} & C_{1,3} & C_{1,4} & C_{1,5} & \dots\dots\dots & \dots\dots\dots & C_{1,nr} \\ C_{2,1} & C_{2,2} & C_{2,3} & C_{2,4} & C_{2,5} & \dots\dots\dots & \dots\dots\dots & C_{2,nr} \\ C_{3,1} & C_{3,2} & C_{3,3} & C_{3,4} & C_{3,5} & \dots\dots\dots & \dots\dots\dots & C_{3,nr} \\ \vdots & \vdots & \vdots & \vdots & \vdots & \vdots & \vdots & \vdots \\ C_{\frac{nr-1}{2},1} & C_{\frac{nr-1}{2},2} & C_{\frac{nr-1}{2},3} & C_{\frac{nr-1}{2},4} & C_{\frac{nr-1}{2},5} & \dots & C_{\frac{nr-1}{2},nr-1} & C_{\frac{nr-1}{2},nr} \end{bmatrix} \tag{3.23}$$

$$\frac{C_{\mathrm{nr}-1/2\,\times\,\mathrm{nr}}}{nr\ odd} =$$

$$\begin{bmatrix} A_{2,1} & A_{3,2} & A_{4,3} & A_{5,4} & A_{6,5} & \dots\dots\dots & \dots\dots\dots & \dots\dots\dots & A_{nr,nr-1} & A_{3,1} \\ A_{4,2} & A_{5,3} & A_{6,4} & A_{7,5} & A_{8,6} & \dots\dots\dots & A_{nr,nr-2} & A_{4,1} & A_{5,2} & A_{6,3} \\ A_{7,4} & A_{6,3} & \dots\dots\dots & A_{nr,nr-3} & A_{5,1} & A_{6,2} & A_{7,3} & A_{8,4} & A_{9,5} & A_{10,6} \\ \vdots & \vdots & \vdots & \vdots & \vdots & \vdots & \vdots & \vdots & \vdots & \vdots \\ \dots\dots\dots & \dots\dots\dots & \dots\dots\dots & \dots\dots\dots & \dots\dots\dots & A_{nr-1,2} & A_{nr,3} & A_{nr-1,1} & A_{nr,2} & A_{nr,1} \end{bmatrix} \tag{3.24}$$

$$C_{u,v} = A_{w,y}\ where\ u = 1{:}\,k\ , v = 1{:}\,l$$

$$S = (u-1)l + v \tag{3.25}$$

$$\sum_{x=1}^{x=g-1} h_x \ < \ S \ \le \ \sum_{x=1}^{x=g} h_x \ \ where\ g \in d_g \tag{3.26}$$

$$h_g = nr - g \tag{3.27}$$

$$h_x = 1\ where\ x = nr - 1 \tag{3.28}$$

$$f = \ \sum_{x=1}^{x=g} h_x - S \tag{3.29}$$

$$y = h_g - f \tag{3.30}$$

$$w = y + g \tag{3.31}$$

Example 1:

$$A(6) = \{2,3,4,5,7,10\}\ where\ nr = 6$$

$$B_{6\times6} = \begin{bmatrix} 0 & 0 & 0 & 0 & 0 & 0 \\ 1 & 0 & 0 & 0 & 0 & 0 \\ 2 & 1 & 0 & 0 & 0 & 0 \\ 3 & 2 & 1 & 0 & 0 & 0 \\ 5 & 4 & 3 & 2 & 0 & 0 \\ 8 & 7 & 6 & 5 & 3 & 0 \end{bmatrix}$$

$$C_{3\times5} \ = \begin{bmatrix} C_{1,1} = A_{2,1} = 1 & C_{1,2} = A_{3,2} = 1 & C_{1,3} = A_{4,3} = 1 & C_{1,4} = A_{5,4} = 2 & C_{1,5} = A_{6,5} = 3 \\ C_{2,1} = A_{3,1} = 2 & C_{2,2} = A_{4,2} = 2 & C_{2,3} = A_{5,3} = 3 & C_{2,4} = A_{6,4} = 5 & C_{2,5} = A_{4,1} = 3 \\ C_{3,1} = A_{5,2} = 4 & C_{3,2} = A_{6,3} = 6 & C_{3,3} = A_{5,1} = 5 & C_{3,4} = A_{6,2} = 7 & C_{3,5} = A_{6,1} = 8 \end{bmatrix}$$

$$C_{3\times5} \ = \begin{bmatrix} \mathbf{1} & \mathbf{1} & \mathbf{1} & 2 & 3 \\ 2 & 2 & 3 & 5 & 3 \\ 4 & 6 & 5 & 7 & 8 \end{bmatrix}$$

Example 2:

$$A(7) = \{1,2,3,4,5,7,10\}\ where\ nr = 7$$

$$B_{7\times7} = \begin{bmatrix} 0 & 0 & 0 & 0 & 0 & 0 & 0 \\ 1 & 0 & 0 & 0 & 0 & 0 & 0 \\ 2 & 1 & 0 & 0 & 0 & 0 & 0 \\ 3 & 2 & 1 & 0 & 0 & 0 & 0 \\ 4 & 3 & 2 & 1 & 0 & 0 & 0 \\ 6 & 5 & 4 & 3 & 2 & 0 & 0 \\ 9 & 8 & 7 & 6 & 5 & 3 & 0 \end{bmatrix}$$

$$C_{3\times7} = \begin{bmatrix} C_{1,1} = A_{2,1} = 1 & C_{1,2} = A_{3,2} = 1 & C_{1,3} = A_{4,3} = 1 & C_{1,4} = A_{5,4} = 1 & C_{1,5} = A_{6,5} = 2 & C_{1,6} = A_{6,5} = 3 & C_{1,7} = A_{3,1} = 2 \\ C_{2,1} = A_{4,2} = 2 & C_{2,2} = A_{5,3} = 2 & C_{2,3} = A_{6,4} = 3 & C_{2,4} = A_{7,5} = 5 & C_{2,5} = A_{4,1} = 3 & C_{2,6} = A_{5,2} = 3 & C_{2,7} = A_{6,3} = 4 \\ C_{3,1} = A_{7,4} = 6 & C_{3,2} = A_{5,1} = 4 & C_{3,3} = A_{6,2} = 5 & C_{3,4} = A_{7,3} = 7 & C_{3,5} = A_{6,1} = 6 & C_{3,6} = A_{7,2} = 8 & C_{3,7} = A_{7,1} = 9 \end{bmatrix}$$

$$C_{3\times7} = \begin{bmatrix} \mathbf{1} & \mathbf{1} & \mathbf{1} & \mathbf{1} & 2 & 3 & 2 \\ 2 & 2 & 3 & 5 & 3 & 3 & 4 \\ 6 & 4 & 5 & 7 & 6 & 8 & 9 \end{bmatrix}$$

Table 3.13 – Most important symbols utilized at the PdM mathematical model and their significance

No.	Symbol	Explanation
1	a1, a2, b & c	Constants of Vogel equation, the values of which are dependent on the nature of the analyzed hydraulic oil
2	n	Number of elapsed working hours for which dynamic viscosity will be scanned
3	$p(n)$	Array of collected averaged values of hydraulic oil feed pressure for (n) working hours
4	$T(n)$	Array of collected averaged values of hydraulic oil temperature for (n) working hours
5	$\mu_c(n)$	Calculated values of hydraulic oil dynamic viscosity using corresponding pressure and temperature values at p(n) and T(n) for (n) working hours
6	$\mu_r(n)$	Values of hydraulic oil dynamic viscosity using corresponding pressure and temperature values at p(n) and T(n) for (n) working hours from the charts rendered by the hydraulic oil supplier or the crane manufacturer
7	$\Delta\mu(n)$	the deviation values between corresponding values of calculated hydraulic oil dynamic viscosity values at $\mu_c(n)$. and reference chart hydraulic oil dynamic viscosity values at $\mu_r(n)$
8	$\Delta\mu_{CRITICAL}$	the critical deviation value between dynamic viscosity value obtained through calculation and dynamic viscosity value obtained from the supplier or manufacturer charts
9	$A(n_r)$	Array indicating the working hours at which $\Delta\mu(n)$ has exceeded the critical deviation value $\Delta\mu_{CRITICAL}$
10	B	Matrix B will be constructed to provide a pattern for the repetition of $\Delta\mu(n)$ values which exceeded $\Delta\mu_{CRITICAL}$, as each element of the matrix $A_{w,y}$ will represent the difference Between $A_{nr}(w)$ and $A_{nr}(y)$ where the deviation between the calculated dynamic viscosity value and reference value from the supplier charts was greater than $\Delta\mu_{CRITICAL}$ for working hours w and y

11	C	Reduced matrix of (B) where main diagonal elements as well as elements located above the main diagonal, will be eliminated. Main diagonal element of B will be eliminated as they will be equal to zero. Since elements located at the upper half of matrix B will have the same absolute values as those located at the lower half, they will be also eliminated. The size of matrix C will be $C_{\mathrm{nr}/2\,\times\,\mathrm{nr}-1}$ for n_r even values, while it will be $C_{\mathrm{nr}-1/2\,\times\,\mathrm{nr}}$ for n_r odd values. Each element of the C matrix $C_{\mathrm{u}\,\times\,\mathrm{v}}$ will be equal to a corresponding element $A_{\mathrm{w}\,\times\,\mathrm{y}}$

Example 1 illustrates the case for obtained 6 (n_r is even) working hours when $\Delta\mu$ was greater than $\Delta\mu_{CRITICAL}$, while Example 2 illustrates the case for obtained 7 (n_r is odd) working hours when $\Delta\mu$ was greater than $\Delta\mu_{CRITICAL}$. The first row of the C matrix is the most important as it reflects the repetition pattern for the working hours at which $\Delta\mu$ was greater than $\Delta\mu_{CRITICAL}$. At the 1st example, the first row of the C matrix was (1,1,1,2,3), which indicates that $\Delta\mu$ was greater than $\Delta\mu_{CRITICAL}$ for 3 successive hours (1,1,1), then it returned to normality where $\Delta\mu$ was less than $\Delta\mu_{CRITICAL}$ only for one working hour then it jumped back again to be greater than $\Delta\mu_{CRITICAL}$ after 2 hours (from 5th to 7th working hours) since the last deviation (1,2), then it came back to normality for two hours, then it jumped back to a level greater than $\Delta\mu_{CRITICAL}$ after 3 hours (from 7th to 10th working hours) from the last deviation (2,3) [15].

At the 2nd example [15], the first row of the C matrix contained (1,1,1,1,2,3), which indicates that $\Delta\mu$ was greater than $\Delta\mu_{CRITICAL}$ for 4 successive hours (1,1,1,1), then it returned to normality where $\Delta\mu$ was less than $\Delta\mu_{CRITICAL}$ only for one working hour then it jumped back again to be greater than $\Delta\mu_{CRITICAL}$ after 2 hours (from 5th to 7th working hours) since the last deviation (1,2), then it came back to normality for two hours, then it jumped back to a level greater than $\Delta\mu_{CRITICAL}$ after 3 (from 7th to 10th working hours) hours from the last deviation (2,3).

At the 1st example, the number of elements included in matrices B and C are 36 and 15 respectively. Similarly, the number of elements included in matrices B and C are 49 and 21 respectively at the 2nd example. Accordingly, it can be easily noticed that adopting such a technique of forming reduced size matrix C to store the time span between the working hours at which $\Delta\mu$ was greater than $\Delta\mu_{CRITICAL}$, will lead to constructing databases of less size than it would been if only the B matrix was used [15].

4. Discussion

This doctoral study has analyzed the different possibilities of enhancing the reliability as well as the stability levels at maritime measurement and control systems which are mostly based on conventional measurement and control techniques adopting classical binary/analogue standards. The main goal of the study is to conduct such enhancement mainly through considering the use of wireless technology as a collaborative medium of data transaction at marine measurement and control systems. The word "collaborative" here refers to the necessity of coexistence and cooperation between the wireless technology and cabling as two mediums of data transaction at upgraded measurement/control systems embracing either wireless technology simultaneously with conventional binary/analogue standards or wireless technology simultaneously with wired smart sensors based on HART or FF protocols, for instance. Additionally, the word " collaborative" also refers to the use of wireless technology as a medium for data transaction through the concurrent utilization of two types of wireless technologies; these dedicated to industrial automation and those general use wireless technologies.
Accordingly, the study has initially analyzed some of the negative effects associated with cabling at marine conventional measurement/control systems in conjunction with the influence induced by extreme marine environmental conditions. In light of the most important conclusions rendered by other researchers in previous literature, the study has highlighted the effect of temperature and humidity on twisted pair cable (as a major component of cabling-based measurement/control systems) dielectric properties:

- Changing the dielectric constant of the cable due to thermal variations.
- Increasing the partial discharge inception voltage PDIV due to increased levels of absolute and relative humidity.

Similarly, this doctoral dissertation has elaborately depicted the effect of salt water on twisted pair cables in maritime engineering applications in light of a research which analyzed the same concept at control and measurement systems involved at traction applications. Based on the results obtained by such a research [14], the doctoral study has related these results to the expected similar effect at tank level measurement system on commercial ships where 4-20 mA pressure transmitters with cables of lengths up to 30 meters, are immersed in salt sea water. Increased mutual capacitance as well as coupling capacitance are the major detected influences when twisted pair cables are immersed in salt water for long periods of time. The increased values of such capacitance will consequently lead to:

- Increased induced current due to capacitive coupling.
- Increased dielectric permittivity, decreased characteristic impedance, increased reflection coefficient, increased power loss and decreased return loss of the twisted pair cable

4-20 mA analogue standard is the most popular analogue standard in conventional measurement/control systems. It is also the only standard which coexists with the smart sensing HART protocol. Most of the recently produced 4-20 mA analogue transmitters are HART supported transmitters. Therefore, this doctoral study has necessarily presented a Simulink model demonstrating the various preventive measures that can be carried out to eliminate the effect of common mode noise as well as coupled noise in 4-20 mA measurement current loops in a tank level measurement system on a commercial ship. This Simulink model was demonstrated in light of the most popular cabling techniques in marine engineering applications where multiple junction boxes are used in remotely distant locations to collect the measurement data from several similar distant locations and forward the overall gathered measurement data to the host controller. The

Simulink model has highlighted the use of low pass filters to eliminate coupled noise signals and also the use of instrumentation amplifiers to eliminate common mode noise signals.

Wired HART protocol can be considered the most popular cabling-based smart sensing protocol in maritime measurement and control systems. The major advantages of HART protocol from a perspective related to the principle of coexistence are:

- HART protocol basic principle of operation is based on the collaboration with the 4-20 mA analogue standard through the superimposition of digital diagnostic information on the analogue current signal.
- HART protocol can be easily upgraded to wireless technology by using wireless HART adapters collecting measurement data from multiple 4-20 mA analogue transmitters.

The research in [1] has provided an analysis for simulating some of the possible environmental effects on a 4-20 mA smart HART measurement current loop based on using a HART temperature transducer. The results obtained from such an analysis can be summarized as follows:

- HART protocol is more sensitive to vibration associated with high levels of humidity than the classical 4-20 mA analogue standard.
- It is highly recommended that the 4-20 mA current loop should be power supplied through an insulation transformer in order to minimize the possibilities of ground loops occurrence, which will lead to quicker failure of the HART 4-20 mA measurement loop than the classical 4-20 mA current loop.

Foundation Fieldbus protocol is a digital communication protocol based on which many smart field devices are built. Unlike HART protocol which is a hybrid analogue-digital protocol, Foundation Fieldbus protocol is a totally digital protocol at which measurement/control data are collected through using a Manchester coded 31.25 kbps signal.

The research in [32] has discussed the recommended techniques to eliminate the effect of additive white Gaussian noise signals on the Foundation Fieldbus Manchester coded signal. Through using simulation models on matlab as well as Simulink, the research has primarily introduced a new technique which can be adopted to eliminate the effect of white Gaussian noise on the FF signal during demodulation process. The technique is based on the calculation of the average wave energy at specific periods of time every 8 microseconds and comparison between the average wave energy calculated each 32 microseconds seconds periods of time within the 8 microseconds wave cycle of the Manchester coded signal.

The possible deployment of FF protocol in maritime engineering applications has been discussed in [18] through an example simulating the use of FF level transmitters in tank level measurement system on a bulk carrier commercial ship, particularly at sea water ballast tanks. In order to avoid the negative effect of immersing pressure transmitters in sea water, the simulation model has recommended the use of FF radar transmitters at tanks such as ballast sea water top side tanks. The research has discussed the possibility of using one non-intrinsically safe model and five intrinsically safe models in order to apply the FF protocol. A comparative analysis was carried out for the results obtained from the simulation of both the non-intrinsically safe model as well as the five intrinsically safe models. The research has particularly highlighted the non-linear polynomial behavior of the field barrier and the segment protectors at the HPTC intrinsically safe model. Additionally, the comparative analysis between the various FF models, has resulted in interesting conclusions related to the highest required number of segments, maximum allowable spur length in the discussed FF models.

Obviously, it can be observed that this doctoral study has dedicated its primary part to discuss wired instrumentation for the purpose of formulating the base, on which a general strategy can be constructed in order to improve the performance and also increase the reliability level in conventional marine measurement/control systems. The upgraded conventional marine measurement/control systems of higher quality, can be considered as the catalyst for implementing the principle of coexistence with wireless technology in a functionally safe configuration performing highly reliable monitoring tasks in general and control tasks in particular.

The second section of this doctoral study is dedicated to explore the extent to which wireless technology can be used as a medium for data transaction in marine measurement and control systems. This doctoral study has concentrated on the wireless HART protocol and Wi-Fi as two wireless technologies that can be deployed in marine engineering applications; one technology which is purely dedicated to industrial automation (Wireless HART), while the other one which is dedicated to general use applications (Wi-Fi). A brief explanation was given for the wireless HART protocol at the beginning from a point of view related to the practical considerations affiliated to the application of the wireless protocol. Among such considerations were the rule of minimum three, the rule of minimum 5, the rule of percentage and the rule of minimum distance, which were introduced by the Emerson wireless HART guide for networking planning. These rules aimed simply to increase the number of field devices within the effective range of the gateway as well as increasing the number of neighbor devices for each field device so that higher levels of reliability, stability and robustness can be maintained at the wireless HART network. The guide has advised for taking these rules into account, however it didn’t render the precise exact mechanism through which these rules can be applied. On the other hand, the network planning guide didn't take into account a very important factor that might induce its negative impact on the wireless HART network performance. This factor is the ageing of the various components of the network such as the gateway and the field devices. The research in [44] has highlighted such a negative impact for the gateway as well as field devices. According to the results of the research, field devices were still able to communicate with the gateway at a power supply level of 5 VDC. Indeed, the gateway was able to receive all the variables from the wireless HART field devices at such a voltage level, however a decreased power supply level to the field device (similar to the effect of battery ageing) will necessarily affect the range of the field device (a detailed research will be conducted to discuss such an issue in the near future).

According to such considerations, it would have been worthy to develop an algorithm dedicated to the application of the rules recommended by the Emerson network planning guide, and also dedicated to network reinforcement. Based on such an algorithm, software tools can be created to achieve the same goal of applying these rules, which is ensuring as many links as possible between the field devices and the gateway, and also between the field devices themselves. Therefore, this doctoral study has presented a mathematical model performing such a task. At this mathematical model, the following assumptions were taken into account:

- Gateway is centralized at the field including the field devices.
- Gateway has a margin of mobility higher than the field devices margin of mobility due to the limitation imposed by the P/I structure for the positions of specific points on specific pipes to measure specific variables, where field devices are planned to be mounted.

- Increasing the number of field devices located within the effective range of the gateway is a goal of higher priority than the goal of increasing the number of neighbor devices for each field device.

Based on the previous four assumptions, the mathematical model has adopted a relocation technique to reduce the distances between the field devices and the gateway as well as between the field devices themselves. This technique is based on:

- Dividing the field into four equal quarters (northeastern, northwestern, southeastern and southwestern) with the gateway centralized in it.
- (1st Round) Relocating the gateway to the direction of the quarter at which are located the maximum number of field devices out of the gateway effective range.
- (1st Round) After relocating the gateway towards an out of range specific group of field devices, the same group of field devices will be relocated towards the gateway, and thus minimum possible distances between the gateway and such a group of field devices will be guaranteed.
- (2nd, 3rd and 4th Rounds)Following to the 1^{st} round of relocation, processing will be launched for the second quarter which includes the second maximum number of field devices outside the gateway. There will be three options for relocation for the field devices at this quarter. First option is to be relocated towards the gateway, while the second and third options will be the relocation of the field devices into such a quarter towards of the two neighbor quarters. The mathematical model will execute a decision making process based on the resulted overall average distances between the field devices (matrix d) as well as the resulted overall out of range cases (matrix V). According to the results obtained from such a decision making process, relocation will be applied on the field devices inside the second quarter which are positioned outside the gateway effective range. Similarly, relocation will take place for the field devices outside the effective range of the gateway inside the third and the fourth quarters.
- After completion of the relocation process, there will be a need to install repeaters at specific locations which were not reinforced by the process of relocation. The mathematical model has introduced two general methods to install repeaters into the field and an additional one method dedicated to the purpose of linking between a relatively distant group of field devices and the gateway. NRR and MRFDD are the two general methods dedicated to installing repeaters to reinforce the network. NRR method is based on creating the network reinforcement rectangle at the area of the out of range field devices and installing repeaters inside it. The MRFDD method is based on dividing the whole fields into square cells of a specific accuracy (mostly 1.5 times the radius of the repeater circle of effective range). The minimum field device density inside each of these cells, should be at least one field device per cell. If not, a repeater will be installed into such a cell. The third method to install repeaters is based on creating a line between the gateway and the nearest field device among a group of distant field devices outside the effective range of the gateway. The created line will be divided into sections at which repeaters will be installed to link between this group of distant devices and the gateway.
- Once the repeater installation process is completed, the mathematical model will commence the process of checking the neighbor devices for each field device. The field devices are indexed from 1 to (n) according to their proximity to the gateway, as the field device (n) is the furthest field device from the gateway. The process of checking the number of neighbor devices will be applied on all field devices from the field device (n) to the field device (2) except the field device (1), which is the gateway. Repeaters will be installed at a midway between the field device and the nearest out of range field device case the distance between

both devices was less than twice the radius of the field device effective range, otherwise the neighbor repeater will be installed closer to the analyzed field device.
- After checking number of neighbor devices for each field device, the mathematical model will start the process of optimization at which it will exclude the unneeded repeaters as neighbor devices or as linking devices with distant group of field devices.

Two illustrative examples were presented at this doctoral dissertation for applying both of the proposed general methods to reinforce the wireless HART network with repeaters. The comparative analysis for those examples has revealed the following conclusions characterizing both methods:
- The MRFDD method requires less computational energy than the NRR method.
- The MRFDD method is more suitable for fields with high infrastructural density than the NRR method, as the MRFDD method covers the whole field, while the NRR method covers only the area out of the gateway effective range.
- The MRFDD method facilitates the process of checking neighbor devices.
- The application of both methods has eventually resulted in almost a similar final number of added repeaters after the optimization phase.

As the main goal of this doctoral study is to evaluate the possibility of applying the wireless technology in maritime engineering applications, the discussion has provided two planning examples for the application of wireless HART protocol on commercial ships. The first example was dedicated to partial integration of wireless HART protocol with a conventional tank level measurement system on a bulk carrier ship for the purpose of measuring sea water levels in sea water ballast tanks. This example was discussed elaborately in [44] and briefly discussed in this doctoral dissertation. The second example was dedicated to the application of wireless HART protocol inside the engine room in light of the proposed mathematical model for network reinforcement. The following conclusions can be derived from the analysis of both examples:
- In order to achieve an acceptable economic efficiency, the use of wireless HART transmitters should be restricted to applications at which measuring points are remotely separated by relatively uniform long distances (water ballast tanks). The research in [44] has highlighted the result of better obtained RSSI levels where wireless HART transmitters are uniformly distant from each other.
- The maximum possible expected cost effectivity can be obtained through the use of wireless HART adapters which can collect the measurement data from multiple 4-20 mA analogue HART transmitters. The Pepperl+Fuchs Bullet adapter is a good example for such devices collecting data from up to 8 analogue transmitters.
- The wireless HART protocol is recommended to process only analogue input signals from 4-20 mA analogue transmitters. It is highly not recommended to utilize the wireless HART binary transmitters to process signals from on-off binary switches. The choice of such transmitters is totally an inefficient option from an economical point of view, that's why, it is recommended to depend on general use wireless technologies such as Wi-Fi if on-off binary cabling-based signals were intended to be processed wirelessly.
- If the wireless HART protocol is intended to be used at systems widely distributed all over the ship, it is recommended to have two gateways, one is located on deck (at bridge navigation deck or at forward station) and another one at the engine room outside the engine control room. Both gateways will be connected to the AMS through Ethernet.

After exploring the different possibilities of applying wireless HART protocol at maritime engineering applications as a wireless technology dedicated to industrial automation, the analysis at this doctoral dissertation went on to investigate the different possibilities of deploying Wi-Fi as a general use wireless technology at shipboard measurement/control systems from a point of view affiliated to the collaboration with Internet of Things (IoT) in marine applications [111]. The research has specifically focused on the ESP32 controller as an efficient tool through which Wi-Fi based wireless communication tasks can be executed. Accordingly, the ESP32 controller was the backbone of the laboratory stand introduced in [75] in order to perform authenticated data transmission from multiple sensors in conjunction with the Arduino controller. Authenticated communication at the introduced laboratory stand was performed through the use of the WebSerial monitor automated by a Python based software tool in order to generate short notifications from the host controller to the sensors' station confirming the reception of the measurement data. On the other hand, the research in [75] has highlighted some of the programming techniques that should be avoided as well as some of the recommended programming techniques if serial communication and Wi-Fi based wireless communication tasks were planned to be performed simultaneously by the ESP32 controller.

The way in which the laboratory stand was configured, allows for:

- Measurement data collection from multiple sensors.
- Authenticating the reception of the data by the host controller.
- Carrying out Wi-Fi based communication tasks at low power consumption levels. The average power consumption levels of an ESP32-S3-WROOM1 module in deep sleep mode and active mode, are 25.85 µW and 78.32 mW respectively, while the current consumption levels in both modes, are 81.4 µA and 23.88 mA, respectively [15,112].
- Coexistence between Wi-Fi and wireless HART as the collected data can be forwarded to the host controller (through Wi-Fi) and also forwarded to the wireless HART asset management system AMS (through wireless HART adapter), which is a functional safe configuration independent of cabling, as it adopts two mediums for data transaction (Wi-Fi and Wireless HART). If such a configuration was intended to be integrated with a conventional cabling-based control system, there will be three mediums for data transaction at the system (cabling, Wi-Fi and Wireless HART).
- Assuming the case that the collected signals are treated as input signals for a local control system including an actuator, it will be possible to monitor the actuator control signal and not only the feedback signal.

The limited coverage area is the major drawback of the laboratory stand first version where only one ESP32 unit was used to collect the measurement data forwarded serially from the Arduino controller and send it wirelessly to the WebSerial remote serial monitor. Therefore, the research in [97] has introduced a specific technique to expand the coverage area of the laboratory stand. This technique is based on adding ESP32 wireless switches at locations where RSSI levels are expected. Based on the ESP-NOW protocol, these switches are ought to exchange short messages between the ESP32 unit connected to the sensors' module and the ESP32 switches in order to pass the measurement data from the sensors module to the host controller and also it will pass the authentication feedback messages from the host controller to the sensors module.

The research in [97] has similarly investigated the maximum allowable distances at which the ESP32 controller will be able to execute successful Wi-Fi communication tasks at RSSI levels not less than - 60 dbm for indoor as well as outdoor applications. The results of the research has shown that such distances are 20 meters and 40 meters for indoor and outdoor allocations respectively.

Based on the second version of the laboratory stand (upgraded with ESP-NOW based switches), this doctoral dissertation has explored the possible application of the ESP32 based Wi-Fi in maritime engineering applications such as shipboard systems on commercial ships. The study has rendered one large scale planning example (inside the engine room) as well as one small scale planning example (fire alarm inside the accommodation) for the deployment of the ESP32 based Wi-Fi technology in marine engineering. Both examples took into account the measured RSSI levels at different locations of the ship, which were measured during existence aboard the vessel.

At the first example dedicated to the engine room, ESP32 wireless switches were proposed to be mounted at specific locations in engine room. At the same example, this doctoral study has highlighted the impairing effect of the watertight doors into the passage ways of container ships, as an obstacle that might disrupt the uniform propagation of the RF waves. In order to overcome such a problem, the analysis in this dissertation has proposed to establish a serial connection between the ESP32 switches located at both sides of the watertight door (more detailed analysis will be conducted in the near future for such a subject).

The second example (fire alarm inside the accommodation) has discussed the possible use of the upgraded version of the laboratory stand for the purpose of implementing a fire detection system inside the ship's accommodation. The example has emphasized the possibility of having the ESP32/1 unit located outside the cargo office, while the host controller located inside the cargo office. Each floor in the accommodation usually includes two optical smoke detectors and two manual call points. These equipment will be connected to an ESP32/2 unit which can be dedicated to only one floor or two floors. It is recommended to allocate a single ESP32/2 unit for a not more than two floors in order to ensure higher stability levels at the Wi-Fi based wireless network through the reinforcing impact by the added ESP32/2 units.

The research in [15] has introduced the complete implementation of a proposed wireless performance and safety monitoring system dedicated to marine cargo cranes on container ships. The developed system is based on the upgraded version of the laboratory stand using ESP32 switches to expand the coverage area of the system. Such a system is intended to integrate with an already installed conventional control system for the marine cargo cranes through coexisting with the conventional crane cabling-based control system in order to overcome a specific drawback that existed at the wired control system. This drawback was the absence of monitoring signals dedicated to the crane most important parameters interconnected with the ship's central alarm monitoring system. In order to implement a cabling-based similar system, it will be a time as well as finance and effort consuming process due to the difficulty imposed by adding cables extending from the cranes' locations on deck to the alarm monitoring system in engine room through aged corroded pipes on a relatively old ship. Accordingly, it was much easier as well as more economically efficient option to execute such a task through an ESP32 based Wi-Fi system adopting the upgraded version of the laboratory stand.

Through the monitored parameters by the crane, performance logs are constructed in order to create database for the collected data, based on which predictive maintenance models can be built. The research in [15] has illustrated an application for the implementation of predictive maintenance principle PdM. The model was aimed to monitor the changes in the cargo crane hydraulic oil dynamic viscosity through the comparison between the dynamic viscosity calculated values by the Vogel equation (based on the monitored values of hydraulic oil feed pressure and temperature) and the dynamic viscosity values obtained from the hydraulic oil charts provided by the crane manufacturer or the hydraulic oil supplier [15,109,110]. The PdM model has detected the repetition rate for the working hours, at which the difference between the calculated and reference values of dynamic viscosity was greater than a critical value. Such patterns can be exploited by the maintenance engineer to detect any possible change at the hydraulic oil properties, which is the main goal of applying the predictive PdM principle through preventing failures before its expected occurrence.

In addition to the predictive maintenance principle, the functional safety principle was also implemented by the proposed wireless system if it was assumed that the same parameters monitored by the system, were monitored by the ship's central alarm monitoring system through cabling. In such a case, the data transaction task of the system would have been executed through using two mediums (cabling and Wi-Fi), which is a partial implementation for the principal of functional safety through the redundant decomposition of the data transaction channel.

Additionally, it can be easily noticed that the use of the ESP32 based Wi-Fi technologies (WebSerial and ESP-NOW) has allowed for the implementation of the PdM and functional safety principles in a cost effective manner. The cost analysis rendered in [15] has thoroughly analyzed such an aspect through the comparison between the required cost for two cabling options and the required cost for five ESP32 units, which are the backbone of the proposed wireless monitoring system of the cargo cranes. The analysis revealed that the proposed wireless monitoring system has achieved cost savings efficiencies of 98.986% and 97.7% for the first and second cabling options respectively.

Moreover, the research in [15] has spotted the light on another criteria according to which the shipboard measurement/ control systems can be classified from a point of view affiliated to the possibility of deploying various wireless technologies dedicated to monitoring purposes. Based on such criteria, the shipboard measurement/control systems can be classified as follows:

1. Systems which are active only during sailing (main engine and bow thruster during maneuvering).
2. Systems which are active only during ship's existence in port (cargo cranes and hatch covers hydraulic units).
3. Systems which are continuously active regardless of ship's location (diesel generators, firefighting and detection systems, ballast water treatment system, tank level measurement system and others).

Generally, the overall sailing periods are longer than the periods of ship's existence in ports, except for some rare cases particularly at smaller size ships. Therefore, shipboard systems which are only active during ship's existence in ports, have less working hours than shipboard systems which are only active during sailing. Accordingly, it is much more easier to implement a wireless monitoring process for such systems from a perspective related to the expected life time of the used equipment, power consumption and longer periods of inactivity that can be dedicated to periodic maintenance or upgrading the system. On the other hand, it should be taken into account that systems which are continuously active during sailing and also in port, are the most critical shipboard systems, especially diesel generators and electrical power generation units. Consequently, the implementation of wireless monitoring process for such systems, mandates more careful selective requirements during the planning phase of implementing such a process. Robustness, rigid structure and being less affected by vibration, are examples for such selective requirements, especially when choosing the wireless modules based on which the wireless monitoring process will be constructed.

Through an experimental research conducted in [15,113], authors have reached a certain conclusion that path loss of RF wave propagation increases at higher vibration levels. The research was carried out on different types of antennas at RF frequencies of 2.7 GHz and 4.8 GHz. These RF frequencies are located in a very close proximity to the ISM band Wi-Fi frequencies of 2.4 GHz and 5 GHz, that's why, wireless measurement systems based on using Wi-Fi modules, might suffer a similar effect at higher vibration levels. Due to such a drawback, authors had the following recommendations to avoid the negative influence on RF waves propagation:

- Avoiding antennas installations at positions with accelerated vibration.
- Utilizing directional or beamforming antennas and avoiding omnidirectional antennas.
- At high vibration levels, it would be favorable to adopt the 5 GHz ISM Wi-Fi frequency band.

Accordingly, It would be valuable to consider embracing such recommendations in order to avoid reduced path loss levels if Wi-Fi technology was utilized for measurement data transaction in maritime engineering applications, particularly at those systems which are continuously active regardless of the ship’s location and those which are active only during sailing, as both categories are subjected to higher vibration levels than systems which are only active during ship’s existence in port [15].

Conclusions

To a specific extent, the formulated theses of this doctoral dissertation were successfully validated through a built up strategy aimed to deploy the selected wireless technologies as integrative collaborative data transaction mediums with cabling. The supporting pillars of such a strategy are the procured major obtained results from the executed experimental, simulation-based and real-time analysis. The outcome of such analysis can be summarized as follows:

- Measurement and control systems at marine engineering applications based on cabling (particularly twisted pair cables) are negatively affected by high levels of temperature, humidity and salinity associated with maritime environment. In light of the conclusions obtained at related previous literature, this doctoral study has spotted the light on the increased mutual and coupling capacitances of the twisted pair cable due to the impact of immersion in salt water (similar to shipboard tank level measurement system). This dissertation has mathematically illustrated the increased current induced by capacitive coupling, the increased dielectric permittivity, the decreased characteristic impedance, the increased reflection coefficient, the increased power loss and the decreased return loss of the twisted pair cable. Additionally, the study has demonstrated the change of the twisted pair cable dielectric constant due to thermal variations as well as the increased partial discharge inception voltages PDIV induced by high levels of absolute/relative humidity.

- This doctoral study has recommended for adopting two cabling options at marine engineering applications in order to ensure wires spare capacities of 100% and 50% for the first and the second cabling options, respectively. Similarly, the study has advised against using cabling options of 0% wires spare capacity.

- High levels of humidity, corrosion associated with simultaneous high vibration levels (exactly similar to the effect of vibration at junction boxes located on deck, at passageways or in void spaces as examples for locations of high humidity and corrosion levels on any commercial ship) leads to failure of the 4-20 mA HART current loop, as the current in the loop will jump to the high alarm level (23 mA) or will decay to the low alarm level (3.78 mA). Such an effect was not detected at the classical 4-20 mA measurement current loop, which means that HART 4-20 mA hybrid analogue-digital standard is more vulnerable to the effect of humidity and vibration than the classical 4-20 mA analogue standard.

- The effect of additive white Gaussian noise on the 31.25 kbps H1 bus at FF smart sensors, can be eliminated through using Kalman filters or through comparison between the calculated average wave energies every 8 microseconds within a single wave cycle of 32 microseconds, identifying the locations of maximum and minimum average wave energies.

- The simulated application of the FF protocol (one non-intrinsically safe model and five intrinsically safe models including entity model, FISCO, FNICO, HPTC and DART) on a shipboard system such as tank level measurement system, has revealed the nonlinear polynomial behavior of voltage and current values at field barriers and segment protectors in the HPTC intrinsically safe model. The case study based simulation example has also revealed the independency of the maximum allowable spur length on the number of field devices at FISCO, FNICO and entity intrinsically safe models.

- The best option for the deployment of wireless technologies in marine engineering applications, is to coexist either with conventional measurement/control systems based on classical analogue standards such as 4-20 mA current loop or with measurement/control systems based on smart sensors adopting digital communication protocols such as HART and Foundation Fieldbus.

- The deployment of wireless technology as a medium for data transaction on shipboard systems can be implemented through adopting either wireless technologies purely dedicated to industrial automation such as wireless HART or general use wireless technologies such as Wi-Fi or through simultaneous utilization of both of them.

- The main advantage of wireless HART protocol over Wi-Fi is the higher level of security and encryption adopted at the wireless HART mesh network.

- The advantages of using Wi-Fi technology over using the wireless HART protocol are the simplicity as well as the flexibility of implementation and maintenance, in addition to the capability of processing all types of measurement/control signals such as on/off state changing switches (pressure, temperature and flow switches) and analogue transmitters such as (temperature, pressure and flow transmitters).

- Wireless HART protocol is recommended to process only analogue input signals in order to achieve optimal level of economic efficiency.

- After specific period of service time, it is necessary to reinforce the wireless HART mesh network deployed abroad a maritime facility with repeaters due to factors mainly affiliated to ageing such as the decay of the supplied voltage by the batteries to the field devices, in addition to possible deterioration of field devices and gateway antennas at rough weather conditions.

- MRFDD and NRR are two developed methods that were introduced by this doctoral study for the purpose of adding repeaters to the wireless HART network according to precise steps that were described by a detailed mathematical model dedicated to increasing the field devices inside the effective range of the gateway (1st priority) and also increasing the number of neighbor devices for each field device (2nd priority). Software tools dedicated to the same purpose (based on the mathematical model) are planned to be presented in a recent future study.

- Wireless HART adapters collecting measurement data from more than a single transmitter such as the BULLET wireless HART adapter, are recommended to be utilized in maritime engineering applications to form multidrop communication loops collecting data from multiple analogue wired transmitters at shipboard systems where measuring points are centralized in specific smaller areas (measurement/control systems centralized in engine room).

- For shipboard systems widely spread over larger areas, Wireless HART transmitters are advised to be deployed at such shipboard systems where measuring points are remotely separated by long distances and long cabling installations are needed from the sensors' locations to the host controller (Tank level measurement system).

- The advantage of data authentication was appended to the list of advantages of adopting Wi-Fi as a wireless medium for data transaction through the use of the ESP32 based laboratory stand presented in this study as a measurement data collection station exchanging data wirelessly (using Wi-Fi) with the host controller.

- The simultaneous engagement of the ESP-NOW based wireless switches with the WebSerial remote serial monitor, has overcome the drawback of the limited range of the ESP32 based laboratory stand adopting solely the WebSerial remote serial monitor.

- The maximum permissible straight LOS (line of sight) distances between the ESP32 controller and the host controller are 20 meters and 40 meters for indoor and outdoor applications, respectively.

- The upgraded version of the laboratory stand (using simultaneously the WebSerial and ESP-NOW protocols), has rendered improved range capabilities through adopting two configurations. The first configuration is recommended for relatively clear straight line of sight (LOS) applications, while the second configuration is recommended for applications with higher density of infrastructural obstacles.

- As a potential application resulting from exploring the major capabilities of both technologies (wireless HART and ESP32 based Wi-Fi), the data transaction medium at a specific shipboard measurement/control system can be tripled through the coexistence between cabling, wireless HART protocol and ESP32 based Wi-Fi in a functional safe cost effective configuration minimizing the probability of data transaction failure and facilitating the process of fault detection during troubleshooting.

- The principle of predictive maintenance can be implemented in an economically efficient manner through the deployment of the ESP32 based Wi-Fi as a medium dedicated to authenticated transaction of measurement data. An example for such a case was provided in this doctoral dissertation to detect the critical changes in the values of the hydraulic oil dynamic viscosity in a marine cargo crane at specific working hours based on the collected and stored parameters in a performance log created by a software tool processing the selected measured major quantities though a multiple-sensors station based on the upgraded version of the laboratory stand.

- Ultimately, this doctoral dissertation has defined the required outlines to construct a strategy based on which wireless technologies such as wireless HART protocol and Wi-Fi, can be deployed at marine engineering applications. This strategy is based on the collaboration between both wireless technologies, coexisting with conventional measurement/control systems (based on analogue standards such as 4-20 mA) as well as smart sensing based systems (HART and FF) . The study explored the different possibilities for reinforcing wireless HART mesh networks through a mathematical model dedicated to such a purpose in addition to exploring some selected capabilities of the IoT based Wi-Fi networks. The analysis at the dissertation has also illustrated detailed planning examples to deploy both technologies in shipboard measurement/control systems, in addition to the complete realization of deploying IoT based Wi-Fi technology on a container ship dedicated to cargo cranes in a configuration that allowed for the economical efficient implementation of important principles such as predictive maintenance (PdM) and functional safety. The aspect of functionally safe coexistence allows for performing not only monitoring tasks but also control tasks. From a similar perspective adopting the idea of collaboration between general use wireless technologies and industrial automation based wireless technologies, Bluetooth Low Energy BLE and ISA100.11A will be elaborately analyzed in a near future research from a point of view affiliated to their possible applications in maritime engineering applications.

Bibliography:

1. Abotaleb M., Mindykowski J., Dudojc B., Masnicki R.; Digital Communication Links Cooperating with the Analog 4-20 mA Standard for Marine Applications, *Bulletin of the Polytechnic Institute of Iași. Electrical Engineering, Power Engineering, Electronics Section, 67, pp. 21-44,* **2021**; https://doi.org/10.2478/bipie-2021-0002
2. Solas V., Efendioglu H.S., Colak B., Garip M.; Research on the Influence of Mechanical Vibration on Radio Wave Propagation, *IV International Electromagnetic Compatibility Conference (EMC Turkiye)* **2017**; http://dx.doi.org/10.1109/EMCT.2017.8090354
3. Min B., Yang N.H.W., Palermo S.; 10 Gb/s adaptive receive-side near-end and far-end crosstalk cancellation circuitry, *IEEE 57th International Midwest Symposium on Circuits and Systems (MWSCAS)* **2014**, ISSN: 1548-3746, e-ISSN: 1558-3899; https://doi.org/10.1109/MWSCAS.2014.6908356
4. Pignari S.A., Spadacini G.; Influence of twist-pitch random non-uniformity on the radiated immunity of twisted-wire pairs, *URSI General Assembly and Scientific Symposium* **2011**, Istanbul, Turkey https://doi.org/10.1109/URSIGASS.2011.6050751
5. Baghdadi B., Abdelber B., Reineix A., Dafif O., Slimani H.; Experimental study of the behaviour of the crosstalk of shielded or untwisted-pair cables in high frequency, *Serbian Journal of Electrical Engineering* **2019**, 16(3), pp. 311-324; http://dx.doi.org/10.2298/SJEE1903311B
6. Payne B.; Skin Effect, Proximity Effect and the Resistance of Circular and Rectangular Conductors; **2021**.
7. Al-Asadi M., Duffy A., Hodge K.G., Willis A.J.; Twisted Pair Cable Design Analysis and Simulation, *International Wire and Cable Symposium* **2000**, 49.
8. Akinnuoye S.F., Sasse H., Cave P., Prescott S., Duffy A.; Long-term Effect of Thermal Variation on the Performance of Ethernet Cabling Dielectrics., *School of Engineering and Sustainable Development De Montfort University, Leicester, LE1 9BH, United Kingdom*, **2019**.
9. Akinnuoye S.F., Long-term Effects of Thermal Variation on the Performance of Balanced Twisted Pair Cabling. PhD of Philosophy; School of Engineering and Sustainable Development, Faculty of Computing, Engineering & Media (CEM), Institute of Engineering Sciences, Centre for Electronic and Communications Engineering, De Montfort University, United Kingdom, 29.10.2019.
10. Ji Y., Giangrande P., Zhao W., Madonna V., Zhang H., Jing L., Galea M.; Investigation on Combined Effect of Humidity–Temperature on Partial Discharge through Dielectric Performance Evaluation, *IET Science, Measurement and Technology* **2022**, 17(1), pp. 37-46; https://doi.org/10.1049/smt2.12128
11. Khouildi E., Attia R., Cherni R.; Investigating Thermal Effect on a Cross Linked Polyethylene Power Cable, *Indonesian Journal of Electrical Engineering and Computer Science* **2017**, 5(1), pp. 33-40; http://doi.org/10.11591/ijeecs.v5.i1.pp33-40
12. Geng P., Song J., Tian M., Lei Z., Du Y.; Influence of thermal ageing on AC leakage current in XLPE insulation, *AIP Advances 8, 025115*, **2019,** https://doi.org/10.1063/1.5017297 .
13. Ge X., Fan F., Given M.J., Stewart B.G.; XLPE Cable Insulation Resistance Modelling under Annealing and Thermal Ageing Effects, *IEEE Conference on Electrical Insulation and Dielectric Phenomena (CEIDP)*, **2023,** https://doi.org/10.1109/CEIDP51414.2023.10410560 .
14. Grzechca D., Zielinski D., Filipowski W.; What Is the Effect of Outer Jacket Degradation on the Communication Parameters? A Case Study of the Twisted Pair Cable Applied in the Railway Industry, *Energies, 14(972),* **2021,** https://doi.org/10.3390/en14040972 .
15. Abotaleb M., Mindykowski J.; Enhancement of Operational Safety in Marine Cargo Cranes on a Container Ship Through the Application of Authenticated Wi-Fi Based Wireless Data Transmission from Multiple Sensors, *Sensors, 24(21), 6977,* **2024,** https://doi.org/10.3390/s24216799 .
16. Dudojc B., Mindykowski J., Analysis of selected properties of measurement channels used in hazardous areas of ships, *IEEE Instrumentation and Measurement Technology Conference, Brussels, Belgium*, **1996**, IMTC Proceedings, volume II, 826-831.
17. Dudojc B., Mindykowski J., Checking current analog measurement channels, *Proc. of the IMEKO TC-4 Conference, Vienna*, **2000**, 175-180.
18. Abotaleb M., Mindykowski J., Dudojc B., Masnicki R..; Case-Study-Based Overview of Methods and Technical Solutions of Analog and Digital Transmission in Measurement and Control Ship Systems, *Sensors, 22(18), 6931,* **2022,** https://doi.org/10.3390/s22186931 .
19. Liptak B.G, Instrument Engineers' Handbook, Process and Control Optimization Volume II , 4th Edition, International Society of Automation, CRC Press Taylor and Francis Group © **2006**, pp.561-574, pp. 690-692, pp. 780-784.

20. Liptak B.G., Halit E., Instrument Engineers' Handbook, Process Software and Digital Networks Volume III, 4th Edition, International Society of Automation, CRC Press Taylor and Francis Group © **2012**, pp. 578-635.
21. Mackay S., Wright E., Park J., Practical Data Communications for Instrumentation and Control, 1st edition, 11 June **2003**, pp. 3-67, pp. 205-238, pp. 240-287.
22. Mehta B. R., Reddy Y. J., Industrial Process Automation Systems Design and Implementation, Butterworth-Heinemann is an imprint of Elsevier, Copyright © **2015** Elsevier Inc. pp. 16-20, pp. 306-339, pp. 365-415.
23. Frantloviu M. P., Jovanov V.J., and Miljkoviü B. LJ., Intelligent Industrial Transmitters of Pressure and Other Process Parameters, Telfor Journal, Vol. 1, No. 2, **2009**.
24. Berge J., Introduction to Fieldbuses for Process Control. Copyright © **2002** ISA — The Instrumentation, Systems, and Automation Society, ISA.
25. Sen, S.K. Highway Addressable Remote Transducer (HART). In Fieldbus and Networking in Process Automation, 1st ed., CRC Press: Boca Raton, FL, USA, **2014**; pp. 93–108.
26. Barreira, J.M.D.; Postolache, O.; Girao, P.S. HART Protocol Analyser Based in LabVIEW. In Proceedings of the IEEE International Workshop on Intelligent Data Acquisition and Advanced Computing Systems: Technology and Applications, Lviv, Ukraine, 8–10 September **2003**.
27. Emerson Automation Solutions. Rosemount 3051S Series Scalable Pressure, Flow, and Level Solution with HART Protocol, Reference Manual 00809-0100-4801, Rev HA; Emerson Automation Solutions: Chanhassen, MN, USA, **2024**.
28. Verhappen, I., Pereira, A.; Foundation Fieldbus, 4th ed.; International Society of Automation: Eindhoven, Netherlands, **2012**; pp. 1–38.
29. Tooley M.; Plant and Process Engineering 360, 1st ed.; Newnes: Oxford, UK, **2009**; pp. 176–180.
30. Mehta B.R., Reddy Y.J.; Applying Foundation Fieldbus, 3rd ed.; International Society of Automation: Durham, NC, USA, **2016**; pp. 21–55, pp. 114–129.
31. Sen S.K.; Foundation Fieldbus, In Fieldbus and Networking in Process Automation, 1st ed.; CRC Press: Boca Raton, FL, USA, **2014**; pp. 109–146.
32. Abotaleb M., Mindykowski J., Dudojc B., Masnicki R..; Simulation of Foundation Fieldbus Manchester Coded 31.25 kbps H1 Bus Using MATLAB and Simulink, *Scientific Journal of Gdynia. Maritime University, 123,* **2022,** pp. 18-31; https://www.doi.org/10.26408/123.02 .
33. Emerson Automation Solutions. Rosemount 3051 Pressure Transmitter with Foundation Fieldbus Protocol, Reference Manual 00809-0100-4774, Rev DA; Emerson Automation Solutions: Chanhassen, MN, USA, **2020**; pp. 93–103.
34. Sen S.K., Intrinsically Safe Fieldbus Systems. In Fieldbus and Networking in Process Automation, 1st ed.; CRC Press: Boca Raton, FL, USA, **2014**, pp. 245–258.
35. Beck A., Hennecke, A.; Intrinsically Safe Fieldbus in Hazardous Areas; Pepperl + Fuchs GmbH: Mannheim, Germany, **2008**; pp. 1–12.
36. Eaton Electric Limited. MTL5000 Range Isolating Interface Units, Instruction Manual, MTL Fieldbus Networks; Eaton Electric Limited: Luton, UK, **2016**; pp. 25-32.
37. Kegel G., Kessler M., Rogoll G.; FISCO-Model versus Conventional Intrinsic Safety Evaluation in Fieldbus Technology; Foundation Fieldbus End User Council Australia Inc.: Perth, Australia, **2001**; pp. 1–10.
38. Eaton Electric Limited. FISCO Intrinsically Safe Fieldbus Systems, Application Note AN9026; Eaton Electric Limited: Luton, UK, **2005**; pp. 1–24.
39. Eaton Electric Limited. FNICO Non-Incendive Fieldbus System, Application Note AN9027 Rev.5; Eaton Electric Limited: Luton, UK, **2016**; pp. 1–36.
40. Saward P.; Fieldbus Non-Incendive Concept Takes FISCO into Zone 2 and Division 2 Hazardous Areas; Foundation Fieldbus End Users Council Australia Inc.: Berth, Australia, **2003**, pp.1–10.
41. Schuessler B.; The High Power Trunk Alternative to FISCO and FNICO; Pepperl + Fuchs GmbH: Mannheim, Germany, **2007**; pp. 1–8.
42. Klatt T.; DART—The Future of Explosion Protection Technology; Pepperl-Fuchs, Mannheim, Germany, IChemE : **2009**.
43. ARC Advisory Group. DART Ushers in the Next Generation of Intrinsic Safety; ARC Advisory Group: Dedham, Massachusetts, USA, **2011**; pp. 1–12.
44. Abotaleb M., Mindykowski J., Dudojc B., Masnicki R.; Towards Reliability and Safety Improvement of Measurement and Control Processes on Ships: Implementation of Wireless HART Protocol, *Bulletin of the*

Polytechnic Institute of Iași. Electrical Engineering, Power Engineering, Electronics Section,68, pp. 17-48, **2022**; https://doi.org/10.2478/bipie-2022-0002

45. Chen D., Nixon M., Aloysius M.; Wireless HART Real Time Mesh Network for Industrial Automation, Springer Science Business Media **2010**, New York, USA, 5-12, 19-48, 89-111, 138-151, https://link.springer.com/book/ 10.1007/978-1-4419-6047-4
46. Hassan S.M., Rosdiazli I., Bingi K., Chung T.D., Saad N.; Application of Wireless Technology for Control: A WirelessHART Perspective, *Procedia Computer Science, 105*, **2017**, pp. 220-247; https://doi.org/10.1016/j.procs.2017.01.217
47. Kim A.N., Hekland F., Petersen S., Doyle P., *When HART Goes Wireless: Understanding and Implementing the WirelessHART Standard*, IEEE International Conference on Emerging Technologies and Factory Automation, Hamburg, Germany, **2008**; https://doi.org/10.1109/etfa.2008.4638503
48. Sen, S.K. Wireless HART. In Fieldbus and Networking in Process Automation, 1st ed.; CRC Press: Boca Raton, FL, USA, **2014**; pp. 315–354.
49. Biasi, M.D. Implementation of a WirelessHART Simulator and Its Use in Studying Packet Loss Compensation in Networked Control. Master's Thesis, KTH Royal Institute of Technology, Stockholm, Sweden, February **2008**.
50. Dust Networks, Inc. Technical Overview of Time Synchronized Mesh Protocol (TSMP); Document Number: 025-0003-01; Dust Networks, Inc.: Milpitas, CA, USA, **2006**.
51. Deshmukh S., Bhosle U., *Performance Evaluation of Spread Spectrum System Using Different Modulation Schemes*, International Conference on Computational Modeling and Security (CMS 2016)), Procedia Computer Science 85 **(2016**) 176-182, http://dx.doi.org/10.1016/j.procs.2016.05.207
52. Kochanska, I.; Schmidt, J.H. Simulation of Direct-Sequence Spread Spectrum Data Transmission System for Reliable Underwater Acoustic Communications. Vib. Phys. Syst. **2019**, 30, 1–8.
53. Motlagh, N.H. Frequency Hopping Spread Spectrum: An Effective Way to Improve Wireless Communication Performance. In Advanced Trends in Wireless Communications; IntechOpen Limited, London, UK, **2011** . https://doi.org/10.5772/15482.
54. Ullah, S.; Shen, B.; Islam, S.M.R.; Khan, P.; Saleem, S.; Kwak, K.S. A Study of MAC Protocols for WBANs. Sensors **2010**, 10, 128–145. https://doi.org/10.3390/s100100128.
55. Amara, Y.; Beghdad, R. Improving the Collision Avoidance of the CSMA/CA Medium Access Control Protocol. WSEAS Trans. Comput. **2004**, 3, 1331–1336.
56. Ho, T.S.; Chen, K.S. Performance analysis of IEEE 802.11 CSMA/CA medium access control protocol. In Proceedings of the PIMRC'96—7th International Symposium on Personal, Indoor, and Mobile Communications, Taipei, Taiwan, 18 October **1996**.
57. Bhattacharjee S., May **2021**, *Introduction to Global Maritime Distress Safety System (GMDSS) – What You Must Know*, https://www.marineinsight.com/marine-navigation/introduction-gmdss-global-maritime-distress-safety-system/
58. Bhattacharjee S., March **2021**, *Marine Radars and Their Use in the Shipping Industry* https://www.marineinsight.com/marine-navigation/marine-radars-and-their-use-in-the-shipping-industry/
59. Ghorbanzadeh M., Visotsky E., Yang W., Moorut P., Clancy C., *Radar In-Band and Out-of-Band Interference into LTE Macro and Small Cell Uplinks in the 3.5 GHz Band*, **2015**, DOI: 10.1109/WCNC.2015.7127746.
60. Gummadi R., Wetherrall D., Greenstein B., Seshan S., *Understanding and Mitigating the Impact of RF Interference on 802.11 Networks*, Conference on Applications, Technologies, Architectures, and Protocols for Computer Communications, **2007**, 385-396, https://doi.org/10.1145/1282427.1282424.
61. Ferrara N.g., Bhuiyan M.Z.H., Soderholm S., Ruotsalainen L., *A New Implementation of Narrowband Interference Detection, Characterization, and Mitigation Technique for a Software-defined Multi-GNSS Receiver*, GPS Solutions, **2018,** https://doi.org/10.1007/s10291-018-0769-z
62. Umar R., Ibrahim Z.O., Mokhtar W.Z.A.W., Sabri N.,H., *Radio frequency interference: The study of rain effect on radio signal attenuation;* Malaysian Journal of Analytical Sciences; ISSN 1394-2506; Worldcat; v. 19(5); p. 1093-1098, **2015**.

63. Amajama J., *Impact of Weather Components on (UHF) Radio Signal*, International Journal of Engineering Research and General Science Volume 4, Issue 3, ISSN 2091-2730, **2016**, https://www.academia.edu/28948219/Impact_of_Weather_ Components_on_UHF_Radio_Signal
64. Chilo J., Karlsson C., Angskog P., Stenumgaard P., *EMI disruptive effect on wireless industrial communication systems in a paper plant*, IEEE International Symposium on Electromagnetic Compatibility, Austin, TX, USA, **2009**, DOI: 10.1109/ISEMC.2009.5284581
65. Gaj P., Mackowski M., *Electromagnetic compatibility issues in hybrid wired and wireless industrial networks*, PLoS One. **2020**; 15(5): e0232405, https://doi.org/10.1371/journal.pone.0232405
66. Daiya V., Ebenezer J., Murty S.A.V.S., Raj B., *Experimental analysis of RSSI for distance and position estimation*, International Conference on Recent Trends in Information Technology (ICRTIT), Chennai, India, **2011**, http://dx.doi.org/10.1109/ICRTIT.2011.5972367
67. Dong Q., Dargie W., *Evaluation of the reliability of RSSI for indoor localization*, International Conference on Wireless Communications in Underground and Confined Areas, **2012**, https://doi.org/10.1109/ICWCUCA.2012.6402492
68. Emerson Process Management, System Engineering Guidelines IEC 62591 Wireless HART, February - **2016** Revision 04, https://www.emerson.com /documents/automation/engineering-guide-system-engineering-guidelines-iec-62591-wirelesshart-en-79900.pdf
69. WHA-BLT-F9D0-N-A0 Pepperl+Fuchs Wireless HART Adapter Manual, TDOCT-4909-ENG-09/**2015**, https://www.pepperl-fuchs.com/global/en/classid_pa.htm?view=productdetails&prodid=90287#product
70. Emerson™ Wireless 775 THUM™ Adapter, Reference Manual 00809-0100-4075, Rev CD July **2017**, https://www.emerson.com/documents/automation/manual-smart-wireless-thum-adapter-en-87168.pdf
71. Al Kala, M.O., Seidman, S., Quang, J., 2018, *An outlook on wireless coexistence with focus on medical devices*, IEEE Electromagnetic Compatibility Magazine, vol. 7, Issue. 3, pp. 60–64, DOI: 10.1109/MEMC.2018.8479340.
72. Yang D., Youzhi X., Gidlund M., *Wireless coexistence between IEEE 802.11- and IEEE 802.15.4-based networks: A survey*, IEEE International Conference on Distributed Computing in Sensor Systems Workshops (DCOSSW), Santa Barbara, CA, USA, **2010**, http://dx.doi.org/10.1155/2011/912152
73. Gomaa, R., *Coexistence Study of 2.4 GHZ Wireless Technologies for Nuclear and Radiological Applications*, International Journal of Engineering Research & Technology (IJERT), **2020**, vol. 9, Issue. 8, DOI : 10.17577/IJERTV9IS080344.
74. LaSorte, N.J., Seidman, S., Quang, J., *Experimental Method for Evaluating Wireless Coexistence of Wi-Fi Medical Devices*, Biomedical Instrumentation and Technology, **2016**, vol. 50(s6), pp. 18–25, DOI: 10.2345/0899-8205-50.s6.18.
75. Abotaleb, M. *Authenticated WiFi-Based Wireless Data Transmission from Multiple Sensors Through a Laboratory Stand Based on Collaboration Between ATMEGA2560 and ESP32 Microcontrollers.* Scientific Journal of Gdynia Maritime University **2023**, 127, pp. 27-41; https://www.doi.org/10.26408/127.03.
76. Arduino, 2023, Arduino® MEGA 2560 Rev3Product Refrence Manual, SKU: A00067, (03.02.2025), https://fiona.dmcs.pl/~cmaj/SM_2st/Arduino-mega2560_R3-datasheet.pdf
77. ESP32 Technical Reference Manual Version 5.3, **2025**, Copyright © 2025 Espressif Systems (Shanghai) Co., Ltd. All rights reserved. www.espressif, https://fiona.dmcs.pl/~cmaj/SM_2st/Arduino-mega2560_R3-datasheet.pdf
78. Babiuch M., Foltynek p., Smutny P.; *Using the ESP32 Microcontroller for Data Processing*. 20th International Carpathian Control Conference (ICCC), **2019**, https://doi.org/10.1109/CarpathianCC.2019.87659443.
79. Hercog, D., Lehrer, T., Truntic, M., Tezak O.; *Design and Implementation of ESP32-Based IoT Devices*, Sensors, **2023**, 23(15), DOI: 10.2345/0899-8205-50.s6.18.
80. Hercog, D., Lehrer, T., Truntic, M., Tezak O.; *Matter Protocol Integration Using Espressif's Solutions to Achieve Smart Home Interoperability*, Electronics, **2024**, 13(11), https://doi.org/10.3390/electronics13112217
81. Onggo, L., Wibowo, S., Ainul R.D.; *Revolutionizing Classroom Attendance: A Wireless Smart System Using ESP-NOW Protocol*, Electronics, **2024**, 13(11), https://doi.org/10.3390/electronics13112217

82. Sharma, A., **2021**, *WebSerial: Remote Serial Monitor for ESP8266 and ESP32*, (04.02.2025), https://github.com/ayushsharma82/WebSerial.
83. Randomnerdtutorials, August 2021, *ESP32 WebSerial: Web-based Remote Serial Monitor*, (04.02.2025), https://randomnerdtutorials.com/esp32-webserial-library/
84. Techtutorialsx, **2022,** *ESP32: WebSerial console over Soft AP*, (04.02.2025), https://techtutorialsx.com/2021/07/23/esp32-webserial-console-over-soft-ap/
85. DelCastillo, G., **2021**, *Python Websocket Server*, (04.02.2025), https://github.com/ParametricCamp/TutorialFiles/tree/master/Misc/WebSockets
86. Solomon, B., **2019**, *ESP32: Async IO in Python: A Complete Walkthrough*, (04.02.2025), https://realpython.com/async-io-python/
87. *Websockets*, (04.02.2025), https://websockets.readthedocs.io/en/stable/
88. Santos, R., **2015,** *Why You Shouldn't Always Use the Arduino Delay Function*, (04.02.2025), https://randomnerdtutorials.com/why-you-shouldnt-always-use-the-Arduino-delay-function/
89. Arduino Forum, **2017**, *Why is using delay Bad?*, (04.02.2025), https://forum.Arduino.cc/t/why-is-using-delay-bad/465334/1
90. Cura, M., G., Boot & Work Corp. S.L., **2020**, *Industrial Arduino Millis () vs Delay ()*, (04.02.2025), https://www.industrialshields.com/blog/Arduino-industrial-1/post/industrial-Arduino-millis-vs-delay-248
91. Liang, O., **2013**, *Arduino Timer and Interrupt Tutorial*, (04.02.2025), https://oscarliang.com/Arduino-timer-and-interrupt- tutorial /#:~:text=On%20the%20Arduino%20Mega%20we,and%2013%3A%20controlled%20by%20Timer0
92. Toptechboy, **2018**, *Lesson 30: Advanced Software Interrupt Techniques for Reading Serial Data with Arduino*, (04.02.2025), https://toptechboy.com/lesson-30-advanced-software-interrupt-techniques-for-reading-serial-data-with-Arduino/
93. Stoffregen, P., **2015**, *TimerOne Modified Library*, (04.02.2025), https://github.com/PaulStoffregen/TimerOne
94. Joseph J., **2022**, *ESP32 Timers & Timer Interrupts*, (04.02.2025), https://circuitdigest.com/microcontroller-projects/esp32-timers-and-timer-interrupts
95. Arduino References, **2022**, *Time Function millis()*, (04.02.2025), https://reference.Arduino.cc/reference/en/language/functions/time/millis/
96. Arduino References, 2021, *Datatypes: Stringobject String()*, (04.02.2025), https://www.Arduino.cc/reference/en/language/variables/data-types/stringobject/
97. Abotaleb M., *Improved Performance of Wi-Fi Based Communication with Multiple Sensors Through Collaboration Between the WebSerial Remote Serial Monitor and ESP-NOW Protocol*. Scientific Journal of Gdynia Maritime University **2023**, 127, pp. 42-56; https://www.doi.org/10.26408/127.04.
98. Randomnerdtutorials, April **2020**, *ESP-NOW with ESP32: Send Data to Multiple Boards (one-to-many)*, (04.02.2025), https://randomnerdtutorials.com/esp-now-one-to-many-esp32-esp8266/
99. Randomnerdtutorials, April **2020**, *ESP-NOW with ESP32: Receive Data from Multiple Boards (many-to-one)*, (04.02.2025), https://randomnerdtutorials.com/esp-now-many-to-one-esp32/
100. Randomnerdtutorials, August **2021**, *ESP32 WebSerial: Web-based Remote Serial Monitor*, (04.02.2025), https://randomnerdtutorials.com/esp32-webserial-library/
101. Randomnerdtutorials, January **2020**, *Getting Started with ESP-NOW (ESP32 with Arduino IDE)*, (04.02.2025), https://randomnerdtutorials.com/esp-now-esp32-Arduino-ide/
102. Randomnerdtutorials, January **2020**, *ESP-NOW Two-Way Communication Between ESP32 Boards*, (04.02.2025), https://randomnerdtutorials.com/esp-now-two-way-communication-esp32/
103. Randomnerdtutorials, May **2020**, *ESP32: ESP-NOW Web Server Sensor Dashboard (ESP-NOW + Wi-Fi)*, (04.02.2025), https://randomnerdtutorials.com/esp32-esp-now-wi-fi-web-server/
104. Frigerio, A., *Functional-safety analysis of ASIL decomposition for redundant automotive systems*. PhD Thesis, Eindhoven University of Technology, Eindhoven-Netherlands, 21.04.2022. pp. 28–33.
105. Piesik E., Śliwiński M., Subramanian N., Zalewski J., *Concept of Multifactor Method and Non-Functional Requirements Solution to Increase Resilience through Functional Safety with Cybersecurity Analysis*.

Eksploatacja i Niezawodnosc – Maintenance and Reliability **2024** 26(3):189454), 26(3) ; http://doi.org/10.17531/ein/189454.
106. Hanselaar C., Silvas E., Terechko A., Heemels W.P.M.H., *The Safety Shell: An Architecture to Handle Functional Insufficiencies in Automated Driving*. IEEE Transactions on Intelligent Transportation Systems **2024** 25(7), pp. 7522–7540; https://doi.org/10.1109/TITS.2024.3352829
107. Abdelillah F.M., Hamour N., Ouchani S., Benselimane S.M., *Predictive Maintenance Approaches in Industry 4.0: A Systematic Literature Review*. IEEE International Conference on Enabling Technologies: Infrastructure for Collaborative Enterprises (WETICE), Paris, France **2023**, pp. 1-6; https://doi.org/10.1016/j.cie.2020.106889
108. Coanda P., Avram M., Constantin V., *A state of the art of predictive maintenance techniques*. IOPConference Series: Materials Science and Engineering, **2020**; doi: 10.1088/1757-899X/997/1/012039
109. Knezevic D., Savic V., *Mathematical Modelling of Changing of Dynamic Viscosity, as a Function of Temperature and Pressure of Mineral Oils for Hydraulic Systems*. Facta Universitatis: Mechanical Engineering , **2006**; 4(1), pp. 27-34.
110. Bair S., Michael P., *Modelling The Pressure and Temperature Dependence of Viscosity and Volume for Hydraulic Fluids*. International Journal of Fluid Power 11, **2010**; No.2, pp. 37-42.
111. Xu G., Shi Y., Sun X., Shen W., *Internet of Things in Marine Environment Monitoring: A Review*, Sensors **2019**, 19, 1711; doi:10.3390/s19071711
112. ESP-IDF Programming Guide: Current Consumption Measurement of Modules. Available online: https://docs.espressif.com/projects/esp-idf/en/stable/esp32/api-guides/current-consumption-measurement-modules.html (10.02.2025).
113. Feng Z., Jinglu S., Minchago H., Peiyan Z., Guoliang S., Rui J., Jianwei L., Shuqiang J., Fanyang C., *Research on the Influence of Mechanical Vibration on Radio Wave Propagation*, IEEE Access, **2023**, 11, pp. 111936 - 111943; https://doi.org/10.1109/ACCESS.2023.3320584